Investigate measures to minimize the effect of operations of Anderson Ranch Dam on the South Fork Boise River between Anderson Ranch and Arrowrock Reservoirs

---

Reported to:	US Bureau of Reclamation
USBR Project #:	Rl2APJ 1025
Reported type:	Final Report
Report Date:	December 31, 2017
Prepared by:	Rohan Benjankar, Mohammad Mehdi Sohrabi, Daniele Tonina
	Center for Ecohydraulics Research,
	University Of Idaho,
	Boise, ID

List of Content

LIST OF CONTENT **I**

LIST OF FIGURES **IX**

LIST OF TABLES **XVIII**

1 EXECUTIVE ABSTRACT **1**

2 INTRODUCTION **4**

2.1 PROJECT OBJECTIVES AND TASKS 4

2.2 STUDY AREA 7

2.2.1 Hydrology *8*

2.2.2 Basin climate *9*

2.2.3 Basin geology *9*

2.3 DATA AVAILABLE AND REQUIREMENT 9

2.3.1 Watershed topographical data *10*

2.3.2 Channel bathymetry and adjacent topography *11*

2.3.2.1 Topographic data quality analysis 11

2.3.3 Hydrological data *13*

2.3.4 Climate and meteorology data *15*

2.3.5 Climatic scenarios selection *15*

3 HYDRAULIC AND HYDROLOGICAL MODEL SELECTION **18**

3.1 HYDROLOGICAL MODEL SELECTION 18

3.1.1 Comparison of hydrologic models 18

3.1.1.1 Variable Infiltration Capacity (VIC): 18

3.1.1.2 Hydrologic Simulation Program FORTRAN (HSPF): 19

3.1.1.3 MIKE SHE: 19

3.1.1.4 Penn State Integrated Hydrologic modeling system (PIHM): 20

3.2 HYDRAULIC MODELING TEST FOR THE SFBR 20

4 STREAM TEMPERATURE ESTIMATION 27

4.1 INTRODUCTION 27

4.2 STUDY AREA AND DATA 29

4.3 METHOD 33

4.3.1 Data collection 33

4.3.2 Model development 34

4.3.3 Model evaluation 37

4.3.4 Stream temperature prediction for Tributaries without observed stream temperature: 38

4.3.5 Role of discharge 38

4.3.6 Effect of inclusion of the autoregressive component 39

4.3.7 Historical reconstruction 39

4.3.8 Comparison to the Modified Mohseni Model 39

4.4 RESULTS 40

4.4.1 Model evaluation 40

4.4.2 Stream temperature prediction 42

4.4.3 Role of discharge 44

4.4.4 Effect of inclusion of the autoregressive component 46

4.4.5 Historical reconstruction 47

4.4.6 Comparison to the modified Mohseni model 48

4.5 DISCUSSION 49

4.6 CONCLUSIONS 53

5 HYDROLOGICAL MODEL 54

5.1 INTRODUCTION 54

5.2 METHOD 55

5.2.1 Description of snow Model: ISNOBAL 55

5.2.2 Forcing data and spatial distribution method 56

5.2.3 Pre-calibration analyses 59

5.2.4 PIHM inputs 65

5.2.5 Sensitivity analyses 68

5.2.6 Initial calibration and evaluation of the model 68

5.2.7 Final calibration and evaluation of the model 68

5.3 RESULT AND DISCUSSION 70

5.3.1 Sensitivity analysis 70

5.3.2 Initial calibration and evaluation of the model 72

5.3.3 Final calibration and evaluation of the model 74

5.4 CONCLUSION 79

6 ONE-DIMENSIONAL HYDRAULIC MODEL 80

6.1 INTRODUCTION 80

6.2 METHOD 81

6.2.1 1D hydraulic model development 81

6.2.2 River Network 82

6.2.3 Channel cross-section 82

6.2.4 Upstream and downstream boundary conditions 83

6.2.5 Tributary inflows 83

6.2.6 Mass balance analysis of discharge within the study reach 84

6.2.7 Boundary resistance 87

6.2.8 Stream temperature model development 88

6.2.9 Hydraulic model calibration and validation 90

6.2.10 Stream temperature model calibration 92

6.3 CALIBRATION RESULT AND DISCUSSION 92

6.3.1 Hydraulic model 92

6.3.2 Stream temperature model 96

7 TWO-DIMENSIONAL HYDRAULIC MODEL 100

7.1 INTRODUCTION 100

7.2 METHODOLOGY 103

7.2.1 2D hydraulic model setup 103

7.2.2 2D hydraulic model calibration 105

7.3 CALIBRATION RESULT AND DISCUSSION 106

8 FISH HABITAT MODEL 109

8.1 INTRODUCTION 109

8.2 METHODOLOGY 111

8.2.1 Preference curves 112

8.2.2 Fish habitat model development 114

8.2.3 Habitat function of discharge 115

8.2.4 Habitat time series 115

8.2.5 Habitat prediction 116

8.3 RESULTS: 116

8.3.1 Hydraulics 116

8.3.2 Habitat 118

8.3.3 Temperature effect *118*

8.3.4 Spatial habitat shift *119*

8.4 DISCUSSIONS 120

8.5 CONCLUSIONS 123

9 IMPACTS OF DAM MANAGEMENT ON AQUATIC HABITAT 124

9.1 INTRODUCTION 124

9.2 METHODOLOGY 125

9.2.1 Climatic conditions *125*

9.2.2 Impacts of dam management *126*

9.3 RESULTS AND DISCUSSIONS 127

9.3.1 Dam impacts *130*

9.3.1.1 Habitat 130

9.3.1.2 Spatial habitat shift 133

9.3.2 Can dam management offset degraded habitat? *135*

9.4 CONCLUSIONS 136

10 ANALYSIS OF STRANDING POOL FORMATION 138

10.1 INTRODUCTION 138

10.2 METHODOLOGY 138

10.3 RESULTS AND DISCUSSION 139

10.3.1 Probabilities stranding pool formation 142

10.3.2 Flow recession rates 143

10.4 CONCLUSION 143

11 HYPORHEIC FLUX MODEL 144

11.1 INTRODUCTION 144

11.2 METHODS 144

11.3 TEMPERATURE PROBES DESIGN 145

11.4 TEMPERATURE PROBES INSTALLATION 146

11.5 FIELD STUDY SITE 149

11.6 CONCLUSION 152

12 APPENDIX A: MAPPING OF SUCCESSFUL COTTONWOOD RECRUITMENT AND PLANTATION IN THE SOUTH FORK BOISE RIVER 153

12.1 INTRODUCTION 153

13 METHODOLOGY 153

13.1 STUDY AREA 153

13.2 REQUIREMENT FOR SUCCESSFUL NATURAL COTTONWOOD RECRUITMENT 154

13.3 SURVEY OF COTTONWOOD RECRUITMENT SITES 155

13.4 2D HYDRAULIC AND COTTONWOOD MODEL 156

13.5 PREDICTION OF AREAS FOR SEEDLING PLANTATION 157

13.6 RESULT AND DISCUSSION 158

13.6.1 Survey of cottonwood recruitment sites..... 158

13.6.2 Simulated favorable areas for cottonwood seedling plantation..... 158

14 CONCLUSIONS 163

15 REFERENCES 164

List of Figures

Figure 2.1: South Fork Boise River (SF Boise River) basin and study area 7

Figure 2.2: South Fork Boise River basin and nearby weather stations. 10

Figure 2.3: LiDAR (green circles) and University of Idaho survey points (purple triangles) within ground survey perimeter (red pollygon) depicting one of the four areas used to calculate deviation between the two survey methods. 12

Figure 2.4: Elevation of UI (University of Idaho) and LiDAR surveyed random points plotted against X-coordinates for the four locations: Power house, Anderson Dam gauge, Cow Creek and Danskin Bridge. 13

Figure 2.5: Hydrograph (Featherville gauge station) categorized for wet (a), average (b) and dry (c) years. 17

Figure 3.1: Simulated water surface elevations (WSE) with 1D and 2D hydraulic models in South Fork Boise River for low and high discharge scenarios. A 0 chainage in the figure is a first point where WSE is compared, not a beginning of the study reach. WSEs were just compared at the locations where we assumed there is no boundary effects (upstream and boundary). 21

Figure 3.2: Spatially distributed flow depth and velocity distribution for reach of the South Fork Boise River. Sub-figure numbers are: a. depth for high discharge (HQ), b. velocity for HQ, c. depth for low discharge (LQ), and d. velocity for LQ 22

Figure 3.3: Spatially distributed flow depth, velocity and habitat suitability distribution for straight reach of the South Fork Boise River. Sub-figure numbers are: a. depth for high discharge (HQ), b. velocity for HQ, c. depth for low discharge (LQ), and d. velocity for LQ, e. combined cell suitability index (CSI) form 1D model for HQ, f. combined CSI form 2D model for HQ, g. combined (CSI) form 1D model for LQ, f. combined CSI form 2D model for LQ. 23

Figure 3.4: Spatially distributed habitat suitability distribution for meander reach in the South Fork Boise River. Sub-figure numbers are: a. combined cell suitability index (CSI) from 1D model for high discharge (HQ), b. combined CSI form 2D model for HQ, c. combined (CSI) form 1D model for low discharge (LQ), and d. combined CSI form 2D model for LQ. 25

Figure 4.1. Study area and spatial distribution of the metrological, hydrological and temperature gauge stations. 30

Figure 4.2. Location of weather and stream temperature stations at eight different climate regions in United States. 31

Figure 4.3. Linear and non-linear relationship between daily stream water and air temperatures at station T10. 34

Figure 4.4. One-day and seven-day lagged autocorrelation of daily stream water temperature at station CT7. 35

Figure 4.5: Observed stream water temperature at Dixie, Cow, Granite and Pierce creeks. 38

Figure 4.6. RMSE and NSC, including both calibration and validation periods, of Ta model. ... 41

Figure 4.7. Simulated and observed daily stream water temperatures and discharge at CT2 (a) and CT6 (b) stations. 42

Figure 4.8. Average RMSE of Ta model for each month. 42

Figure 4.9: RMSE and NSC at four stations at Boise River Basin. 43

Figure 4.10: Predicted water stream temperature at Pierce Creek by using posterior distributions calculated from Dixie Creek. 44

Figure 4.11. Changes in the RMSE of SWTM by adding discharge. 45

Figure 4.12. Changes in the RMSE of SWTM by adding discharge as a predictor at a monthly scale..... 45

Figure 4.13. Time series of simulated and observed daily stream water temperatures at CT5 (the top figure) and T7 (the bottom figure) stations, respectively. 46

Figure 4.14. Effect of disregarding autoregressive component at T22 (the top figure) and CT7 (the bottom figure). Red line indicates estimated stream water temperatures from Ta model. Green line shows estimated stream water temperatures from Ta model without autoregressive component..... 47

Figure 4.15. Hindcast of daily stream water temperature (Ta-Q model) for the period with different hydrological conditions from the calibration period at station D2. The top figure indicates calibration period (average year) and the bottom figure shows validation period (wet year). 48

Figure 4.16. Comparison of daily stream water temperature predicted with the modified Mohseni and SWTM..... 49

Figure 4.17. Comparison between generated daily stream temperatures from SWTM and the modified Mohseni model at CT5, a snow dominated basin..... 49

Figure 5.1: Spatial distribution of weather and SNOTEL sites (full circle). 57

Figure 5.2: Comparison of spatially averaged melt and discharge at Featherville and Dixie gauge stations. 61

Figure 5.3: Melt partitioned with elevation and aspect bands. Note that Avg Melt shows spatially average melt over the watershed. The first letter of aspect-elevation name indicates the aspect band and letter "e" followed by a number the elevation band. For instance, S-e1 indicates melt in southern aspect and first elevation band..... 63

Figure 5.4: Spatial distribution of SWI for the April and May peak discharges over SFB watershed. 64

Figure 5.5: Generated river elements and meshes for the sub-basins of Pierce, Dixie, and South Fork of Boise River upstream of the Featherville gauge. 66

Figure 5.6: Groundwater initial water table elevation for PIHM at Featherville..... 67

Figure 5.7: River elements and mesh cells for upstream of Anderson Ranch Dam. 69

Figure 5.8: Sensitivity analysis results for soil vertical hydraulic conductivity (sV), macro-pore vertical hydraulic conductivity (mV), porosity (p) and Beta. Simulated Q is discharge simulation without any change in calibration factors. Letters H and L show increase and decrease in a parameter, respectively..... 71

Figure 5.9: Comparison between simulated and measured discharges at Featherville, Dixie and Pierce gauge stations..... 73

Figure 5.10: Simulated and observed stream flow at Featherville..... 75

Figure 5.11: Simulated and observed stream flow at Anderson. 77

Figure 5.12: Simulated and observed streamflow at Dixie (the left graph) and Pierce (the right graph) for wy2013..... 78

Figure 5.13: Correlation between measured stream flow of Pierce and Featherville for wy2013. 79

Figure 6.1: Gauge stations within Boise River Basin and transducers location to measure stages and water temperatures. 85

Figure 6.2: Regression equations developed by correlating discharges of Fall, Dixie and Pierce creeks to Mores Creek (a, b, c). Measured and predicted discharges from regression

equation based correlation between Dixie and Mores Creeks at the Pierce Creek and weighted-area approach (d)..... 86

Figure 6.3: Measured and estimated discharges at the Neal Bridge gauge station..... 87

Figure 6.4: Measured and simulated water surface elevation for low flow (8.5 m^3/s)..... 93

Figure 6.5: Measured and simulated water surface elevation for medium flow (45.6 m3/s)..... 93

Figure 6.6: Simulated and observed WSE at the Cow Creek Bridge..... 95

Figure 6.7: Simulated and observed WSE at the Private Bridge..... 95

Figure 6.8: Simulated and observed WSE at the Canyon section..... 96

Figure 6.9: Observed and simulated temperatures at the Cow Creek Bridge..... 97

Figure 6.10: Observed and simulated temperatures at the Danskin Bridge..... 97

Figure 6.11: Observed and simulated temperatures at the Private Bridge..... 98

Figure 6.12: Observed and simulated temperatures at the Canyon section..... 98

Figure 7.1: Upper and lower 2D model extents, water surface elevation and velocity measured locations along the channel..... 104

Figure 7.2: Difference between measured and predicted water surface elevations for discharges of 8.5 (left) and 45.6 m^3/s (right). +ve and –ve values indicate higher and lower measured values, respectively..... 106

Figure 7.3: Simulated and predicted velocity for discharge 8.5 m^3/s at Cow Creek and Private Bridge, respectively. The progressive distance is from the right to left bank..... 107

Figure 8.1: Temperature preference curve and green diamonds represents measured water temperatures at fish locations (left).Water depth and velocity preference curves for Bull

Trout rearing habitat, red squares and blue triangles are measured depths and velocities at fish locations (right). 113

Figure 8.2: Maximum daily temperature from upstream (XS3300) to downstream (XS24000) for the entire simulated water year (WY 2013) 113

Figure 8.3: Observed fish distribution over spatially distributed habitat quality 114

Figure 8.4: Box plots for minimum (5%), first quartile (25%), median (50%), third quartile (75%) and maximum (95%) of water depths (bottom) and velocities (top) for different discharges. Green line indicates inundated area (extent) for different discharges. 117

Figure 8.5: Spatial distribution of velocities and inundated areas for discharges 68 m^3/s (top panel) and 102 m^3/s (bottom panel). Red lines indicates bankfull channel boundary. 117

Figure 8.6: WUA and HSI quantified with water depth and velocity only (without temperature) as a function of discharges calculated for channel, off-channel and combined spatial extents. 118

Figure 8.7: Dam regulated and unregulated (natural) weighted usable area (WUA) (left). Temperature in legend indicates inclusion of water temperature for WUA calculation. ... 119

Figure 8.8: Spatial shift in high quality habitat for low (8 m3/s) and high flows (102 m3/s) (right). 120

Figure 8.9: Water temperature patterns for the water year 2013 for unregulated and regulated scenarios. 121

Figure 8.10: WUA and SI for Bull Trout (BT) and rainbow trout (RBT) rearing habitats as a function of discharges 122

Figure 9.1: Regulated, modified and unregulated hydrology and daily averaged water temperature at the Anderson Dam for a. dry (2007), b. average (2010), and c. wet (2006) climatic years 129

Figure 9.2: Total (channel and lateral channel) WUA with all three hydraulic variables water depth, velocity and temperature for regulated, modified and unregulated flows for a. dry (2007), b. average (2010), and c. wet (2006) climatic years. Hydraulic-quantified WUA is based on water depth and velocity only. 131

Figure 9.3: Channel and lateral channel WUA for regulated and unregulated flows for a. dry (2007), b. average (2010), and c. wet (2006) climatic years. 134

Figure 9.4: Spatially distributed habitat quality in main- and lateral-channel for a. 227, b. 142, c. 68, d. 45, and e. 17 m^3/s. Green line is boundary for bankfull extent..... 135

Figure 10.1: Preliminary map of model delineated stranding pools (green) for discharge 57 m^3/s and field surveyed stranding pools in 2012. 140

Figure 10.2: Model delineated number of stranding pools and area against discharge magnitude. 141

Figure 10.3: Spatially distributed stranding pools for a. 227*, b. 142*, c. 68, d. 57, and e. 17 m^3/s. *only pools more than 200 m^2 are shown. 141

Figure 10.4: a. stranding pool (area) formation when flows recede from high (e.g., 250 m^3/s) to base flow (8 m^3/s), b. frequency of days (%) that specific areas of stranding pool formation between regulated and unregulated scenarios for dry, average and wet climatic conditions, c., frequency of days for down ramping rate of <8.5, 8.5-17, and >17 m^3/s/day during flow <68 m^3/s and d. flow >68 m^3/s. 142

Figure 11.1: Left: South Fork Boise River study site showing the debris flow that added sediment to the channel, with approximate thermal scour/ deposition chain installation locations 1, 2, 3, 4. (Photo used with permission from the USDA, Boise National Forest); Middle: Field temperature probe; Right: Temperature probe installed with data logger. 148

Figure 11.2: Pre-flood (blue) and post-flood (red) grain size distribution at South Fork Boise River locations 1 and 2. Locations 3 and 4 did not experience significant change in grain

size distribution due to little scour or deposition and their grain size distribution remained similar to the pre-flood condition. 148

Figure 11.3: South Fork Boise River measured and calculated stream bed elevations at locations 1, 2, 3, and 4, plotted with the hydrograph released from Anderson Ranch Dam (secondary y-axis, blue line)..... 150

Figure 11.4: South Fork Boise River calculated sediment seepage velocities at field locations 1, 2, 3, and 4, plotted with the hydrograph released from Anderson Ranch Dam (secondary y-axis, blue line). Depth of temperature sensor increases with increasing sensor number 151

Figure 13.1**:** Required physical criteria for successful cottonwood requirement and typical hydrographs for pre-dam (unregulated) and post-dam (regulated) reaches (Benjankar et al., 2014a). Green line shows water surface optimal rate of change for cottonwood recruitment. 154

Figure 13.2: Example of field survey natural cottonwood recruitment area (a) and field surveyed cottonwood recruitment on a narrow band near channel (b and c)..... 156

Figure 13.3: Input physical variables and output from the cottonwood model. Figure is modified from Benjankar, et al. (Benjankar et al., 2014a)..... 157

Figure 13.4: Favorable areas for cottonwood plantation. 159

Figure 13.5: Detailed favorable areas (green) for cottonwood plantation at Site 1, downstream of Anderson Ranch Gauge Station (2790 m river distance from the Dam). Red triangles and yellow circles indicate river distance (m) from Anderson Ranch Dam and road distance based on Anderson Ranch Gauge Station, respectively..... 160

Figure 13.6: Detailed favorable areas (green) for cottonwood plantation at Site 2, downstream of Cow Creek Bridge (12990 m river distance from the Dam). Red triangles and yellow circles indicate river distance (m) from Anderson Ranch Dam and road distance based on Cow Creek Bridge, respectively..... 161

Figure 13.7: Detailed favorable areas (green) for cottonwood plantation at Site 2, downstream of Danskin Bridge (18690 m river distance from the Dam). Red triangles and yellow circles indicate river distance (m) from Anderson Ranch Dam and road distance based on Danskin Bridge, respectively. 162

List of Tables

Table 2.1: Area weighted mean difference in elevations between LiDAR and UI surveyed random points 13

Table 2.2: Basin area, 1.5-year Recurrence Interval (RI) flow, Yearly average flow of different tributaries between Anderson Dam and Little Rattlesnake Creek 14

Table 2.3: Existing USGS and new gauge stations where discharge, water surface and temperature measurements 15

Table 2.4: Recurrence interval (RI) floods based on frequency analysis for maximum and mean annual flow at USGS gauge 13186000 South Fork Boise River near Featherville, Idaho. .. 16

Table 2.5: Representative years for different climatic conditions 17

Table 3.1: Differences in flow depth and velocity for high (HQ) and low (LQ) discharges 23

Table 3.2: Differences in WUA, HHS from 1D and 2D models for high and low discharges (Q) and agreement between the maps using error matrix 26

Table 4.1. Detailed information of stream temperature stations 32

Table 4.2: Detailed information of water temperature gauge stations. 43

Table 5.1: Detailed information of the stations. 57

Table 5.2: Elevation bands 60

Table 5.3: Aspect bands 60

Table 5.4: NSC and PBIAS values 74

Table 5.5: NSC and PBIAS values for Featherville 76

Table 5.6: NSC and PBIAS values for Anderson. 76

Table 5.7: NSC and PBIAS values for wy2013 for Dixie and Pierce. 79

Table 6.1: Tributaries and their locations included in the MIKE11 model. 84

Table 6.2: The regression equation used to predict tributary discharges..... 85

Table 7.1: Root mean square error (RMSE) and average error (AE) for water surface elevation and velocity. +ve and –ve values indicate higher and lower measured values, respectively 107

Table 9.1: Hydrologic scenarios of dry, average and wet climatic conditions for habitat analysis. 126

1 EXECUTIVE ABSTRACT

Bottom-released Anderson Ranch Dam operations regulate the thermograph and hydrograph of the lower South Fork Boise River (SFBR), which is federally listed as Foraging, Migration, and Overwintering (FMO) critical habitat for adult and sub-adult Bull Trout (*Salvelinus confluentus*). The dam regulated hydrograph and thermograph may vary from the natural conditions and their effects on Bull Trout habitat and, in turn, on fish behavior is relatively unknown. To address this question, this project quantified and map the habitat distribution of Bull Trout as a function of Dam operation and compare them with the unregulated flows. This approached is based on the current knowledge that habitat conditions (e.g., stream flow, water temperature, physical habitat quality and quantity) are key indicators of fish abundance and productivity. The principle behind this approach is that if habitat is suitable, aquatic species would respond positively because habitat quality affects ecosystem function. Consequently, understanding the effects of water releases from Anderson Ranch Dam, tributary flows and stream water temperature on the SFBR thermal and hydraulic regimes will improve our understanding of habitat conditions and biological processes, specifically rearing and migratory cues of Bull Trout within the basin. We used rearing habitat quality for Bull Trout as a surrogate to study their biological processes and behavior because of the linkage between physical habitat quality and species use of the habitat.

To achieve the project's goal, we developed a set of numerical models, which include a watershed hydrologic model (ISNOBAL, a physical based distributed snowmelt model, coupled with the multi-scale hydrological model Penn State Integrated Hydrological Model, PIHM), one- and two-dimensional (1D and 2D) surface water hydraulic models (MIKE11 and MIKE21 DHI software), one-dimensional streamwise temperature model and an aquatic habitat model. The topographical data of the SFBR below Anderson Ranch Reservoir was collected in 2007 with the Experimental Advance Airborne Research Lidar, EAARL. This resulted in a high resolution digital elevation model, DEM, of the entire study reach. Hydrographs and thermographs measured at Anderson Ranch Dam outlet were used as upstream boundary conditions for the regulated cases, whereas hydrographs for unregulated scenarios were constructed from mass balance models within the reservoir and the thermograph from data recorded at the unregulated

South Fork Boise River upstream the reservoir at Featherville. Habitat quality was estimated within the range of discharges expected for both regulated and unregulated conditions. We also focused on the habitat condition under 3 climate years: wet, average and dry.

Our modeling results showed that regulated flows provide better good conditions year around for adult Bull Trout in the SFBR system regardless of climatic conditions. They also provided stable good habitat during the hot summer month when unregulated flow provided poor if not unusable habitat conditions in all climatic conditions because summer temperatures are higher than those preferred by Bull Trout. Water temperature caused degradation of habitat quantity and quality in summer and early fall months for the unregulated scenario. This condition is further exacerbated by low flows. In contrast, regulated flows maintain uniform habitat throughout the summer period for all three climatic conditions because Anderson Ranch Dam operations maintain water temperatures within the range of Bull Trout preference. This suggests that dam management has the potential to offset negative impacts on fish habitat quality from future climate variability effects especially during dry climatic years. This ameliorating effect lasts over a period of several consecutive dry years (at least 4 year from our historic data analysis). Our results showed that reduction of current minimum flow (8 m^3/s) could result in less habitat.

Our results revealed that lateral-channel habitats are important part of the SFBR ecosystem. They connect with the main stem during high flows. During high flows, high quality habitat shifts from the main-channel, where flow velocities would be outside the upper range used by Bull Trout and prey fish, to lateral-channels, consequently sustaining the high quality habitat during high flows specifically in average and wet climatic conditions. Our modeling did not account for series of hydrographs (sequence of dry years or wet years) but we modeled each climatic condition separately. Future studies should account for potential climatic scenarios time series based on climatic projections. This would allow quantifying the risk of climate change on the ecosystems due to succession of dry and wet years. Especially for investigating the impact of new dam operations.

Stranding pools analysis showed that large discharges (above bankfull, 68 m^3/s) have higher probability of developing stranding pools than small discharges. Probabilities of formation of stranding pools were higher for unregulated than for regulated flows for all climatic cases. Dam management lowers flow magnitude and in-turn reduces stage fluctuations via controlled ramping rates, which are similar to discharge changes in the unregulated scenarios, resulting in less potential of inducing stranding pools.

2 INTRODUCTION

2.1 *Project objectives and tasks*

Anderson Ranch Reservoir operations regulate the stream flow of the lower South Fork Boise River (SFBR) with bottom-released flows. The dam regulated hydrograph and water thermograph may vary from the natural conditions as in other systems such as in Kootenai River (Marotz et al., 2001) and the effect of the current water management operations on fish behavior is relatively unknown. Bull Trout (*Salvelinus confluentus*) a native fish species of the SFBR is listed as a threatened fish species under the Endangered Species Act. Bull Trout are known to use the SFBR for overwintering and rearing (Salow, 2005). The study area is federally listed as Bull Trout critical habitat and classified as Foraging, Migration, and Overwintering (FMO) habitat for adult and subadult Bull Trout. The authors recognize this classification; however, for the purpose of this report the study area will be referred to as rearing habitat for adult and subadult Bull Trout.

Habitat quality degradation has been identified as a main cause for the decline of fish populations (Levin and Schiewe, 2001) and it has been directly or indirectly linked to river flow alterations (Malcolm et al., 2012). Changes in flows from unregulated conditions affect egg development, migration pattern and habitat distribution. Imposed low flows due to dam operations may interrupt migration and reduce available good habitat quality distribution and size due to reduce water depths and velocities (Solomon and Sambrook, 2004). These observations have suggested that habitat conditions (e.g., stream flow, water temperature, physical habitat quality and quantity) are key indicators of fish abundance and productivity (Statzner et al., 1988). Current river restoration practices are mainly based on this principle that if habitat is suitable, aquatic species would respond positively because habitat quality affects ecosystem function (Ward et al., 2001). This understanding has led to the process of improving river habitat quality through changes in physical characteristics of streams and rivers to restore fish population and ecosystem function (Watters *et al.*, 2003; Palmer *et al.*, 2005).

Consequently, understanding the effects of water releases from Anderson Ranch Dam, of tributary flows and of water temperature on the SFBR thermal and hydraulic regimes may help

to improve our understanding of habitat conditions and biological processes, specifically rearing and migratory cues of Bull Trout within the basin. Therefore, the main objective of this study is to determine how Anderson Ranch Reservoir regulation could alter habitat quality and so behavior of Bull Trout in the South Fork Boise River between Anderson Ranch and Arrowrock reservoirs. We used rearing habitat quality for Bull Trout as a surrogate to study their biological processes and behavior because of the linkage between physical habitat quality and species use of the habitat (Statzner et al., 1988).

To achieve the project's goal, we developed a set of numerical models, which include a watershed hydrologic model, one- and two-dimensional (1D and 2D) surface water hydraulic models, one-dimensional streamwise temperature model and an aquatic habitat model that will help to understand current flow and temperature regime of the study area and impact on these variables from modified river (flow) management. The topographical data of the SFBR below Anderson Ranch Reservoir was collected in 2007 with the Experimental Advance Airborne Research Lidar, EAARL, sensor. The EAARL sensor is a narrow-beam in the green light wavelength lidar capable of surveying submerged terrestrial topography (McKean et al., 2009b).

The project is designed and led by the United States Bureau of Reclamation (Reclamation) and University of Idaho (UI). The project is funded by Reclamation and conducted in collaboration with several government and non-government entities including the Center for Ecohydraulic Research (CER), University of Idaho and United States Forest Services (USFS). The work under this contract, entitled "South Fork Boise River Hydrodynamic Modeling" is to develop a method that quantifies the status of channel physical processes after the operation of Anderson Ranch Dam and its impact on the fish habitat, biological processes and behavior specifically of Bull Trout in the South Fork Boise River (SFBR) between Anderson Ranch and Arrowrock Reservoirs.

The main objectives of the project are:

- Assess the available physical habitat (temperature, water depth, velocity) under a variety of flow conditions utilizing the Experimental Advance Airborne Research Lidar

(EAARL) derived bathymetry, hydraulic and temperature modeling tools, and habitat classifications.

- Assess the Bull Trout habitat use and biological processes based on the physical habitat under a variety of flow conditions in the SFBR, utilizing and hydraulic and temperature modeling tools and fish observation data.
- Use the above information to evaluate impact of the Anderson Ranch Dam in the SFBR below the dam.

The 1D and 2D hydraulic models simulated variables are used developed fish habitat model, which is validated with fish observed data and to predict potential stranding pools at different flow releases from Anderson Ranch Dam. Bull Trout habitats were then analyzed at different flow scenarios. The study site stretches from below Anderson Ranch Reservoir to the USGS SF Boise Neal Bridge gauge stations.

The following tasks have been selected to achieve the project goals:

Task 1: Database review and validation

Task 2: Develop mass balance model

Task 3: Develop rain run-off model (Hydrologic model)

Task 4: Develop and test hydraulic modeling of the SFBR

Task 5: Process and analyze EAARL data

Task 6: Classification and stratification of reaches for fish habitat

Task 7: Develop 1-dimensional (1D) hydrodynamic and temperature model

Task 8: Develop 2-dimensional (2D) hydraulic model

Task 9: Analyze 1D and 2D and fish habitat models for selected scenarios to quantify impacts of dam management on downstream aquatic habitat

Task 10: Hyporheic fluxes along the SFBR

Task 11: Communication/Reporting/Meetings

2.2 *Study area*

The study site is a 47 km long reach of the South Fork Boise River (SFBR) between Anderson Ranch and Arrowrock Dams (Figure 2.1). The SFBR watershed has an area of approximately 3,382 km^2 at the edge of the Sawtooth Mountain Range (DEQ 2008). Flow releases from Anderson Ranch Dam exert an important control on the flow discharge in the lower SFBR. The reach has an average width and slope of 41 m and 0.0043 m/m, respectively. It can be divided into two segments: an upper south more open canyon reach (here after upper reach) and a lower north narrower canyon reach (here after lower reach). The lower canyon reach extends for 19.2 km between Trail Creek and Neal Bridge. This reach is narrow with severely restricted access due to a nearly vertical 300 m canyon walls (Moore et al., 1979). The channel is narrow and the flow is swift with subdue pools in this reach, while substrate is dominated by boulder larger than 30.5 cm diameter (Wade et al., 1978). The upper open canyon reach is located between Anderson Ranch Dam and Trail Creek. The stream is generally broad, shallow, and characterized by riffles and runs. The substrate is dominated by gravel (0.2-6.4 cm), cobble (6.4-25.6 cm) and boulder (>25.6 cm) (Wade et al., 1978). The adjacent floodplain of this reach ranges from 30 to 200 m wider than the river channel, which is braided in several areas.

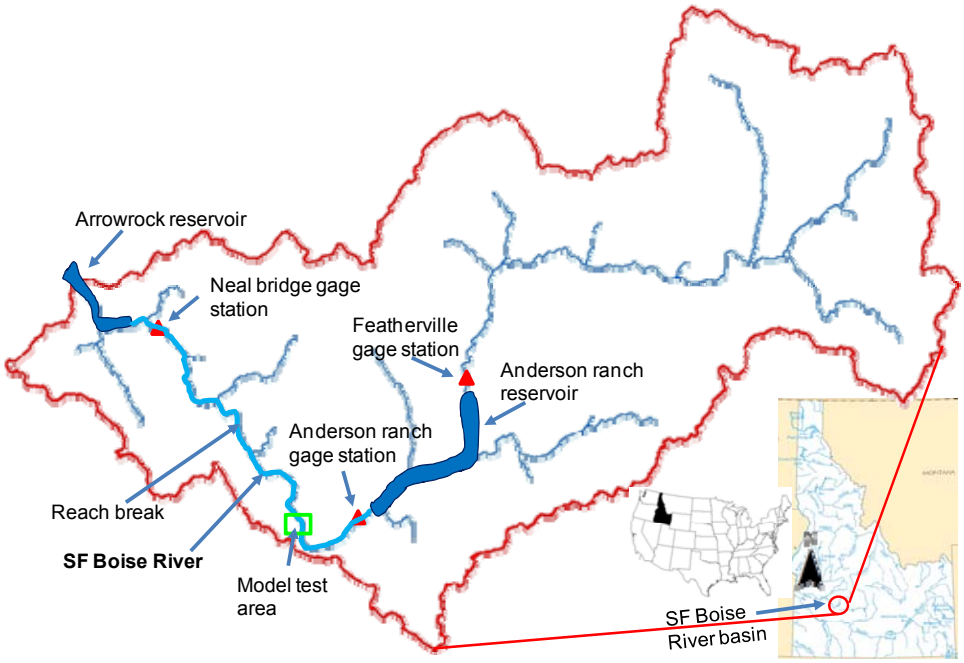

Figure 2.1: South Fork Boise River (SF Boise River) basin and study area

Stream discharges regulated by Anderson Ranch Dam, which is managed for irrigation, flood control and power production, vary between 8.5 and 200 m^3/s. The maximum flows occur in May during normal water years when the reservoir fills and spills may occur. However, spill has not occurred for a long time and it is avoided as much as possible to reduce Bull Trout entrainment. Flow is held between 45.5 and 51 m^3/s during the summer irrigation season, which runs from April 1 through September 1. Outside of irrigation season, flow is typically around 8.5 m^3/s.

We focus on habitat analysis in 23 km of upper open canyon reach, which has pools, riffles and runs with several braided sections and active side channels. Most of the side channels are ephemeral and connected with the main channel during high flows, but some of them are connected during winter flows. Furthermore, this is the section where Bull Trout are observed most of time during monitoring period.

2.2.1 Hydrology

The basin hydrologic regime is snowmelt dominated, with snowmelt runoff occurring from late March to May. However, snowpack accumulated in the higher part of the drainage generates peak flows, which begin in late April and may last until mid-June. The runoff periods are followed by warm and dry summers, which cause decreased stream flows. Occasional localized summer thunderstorms can result in flash floods within small drainage basins.

Different factors influence channel stability and flow regime such as significant fine sediment inputs, hydrologic modification, and catastrophic wildfire in the South Fork Boise River sub-basin. Land uses affect channel and flow stability including road construction, mining, logging, livestock grazing, recreation, and urban development. These processes result in pools or other depositional zones filled with sediment, sand bars and braided channel development, and channel scour and simplification. In general, logging and road construction can increase water runoff and sediment delivery to rivers and streams.

2.2.2 Basin climate

The South Fork Boise River watershed elevations vary between 975 and 3,000 m, consequently a wide range of air temperatures and precipitation rates characterize the SFBR watershed (DEQ, 2008). Weather station data, report that air temperatures may exceed 38°C during summer and -35°C during winter. The average annual precipitation ranges from 50.8 to 127 cm. Winter months are dominated by frequent heavy snowfall; but snow cover is generally dependent on the elevation. Most of the snowpack is usually melted by mid June in most of the watershed but this depends on winter snow accumulation and summer ambient air temperature (DEQ, 2008).

2.2.3 Basin geology

The South Fork Boise River sub-basin's geology is complex and is dominated by the Cretaceous Idaho Batholith and younger tertiary granitic intrusions. The area includes several major regional fault zones that formed the river canyons (Clayton, 1992). The watershed is subject to rapid erosion and mass wasting with both chemical and mechanical weathering processes that provide material for stream channels as well provide well-drained soils that enhance productivity for a forested ecosystem and commercial forest production. The watershed recently experienced catastrophic wildfire events and extreme weather conditions that contributed to blow-outs (DEQ, 2008). The SFBR stream channel morphology is also controlled by intermediate knick-points.

2.3 *Data available and requirement*

All data used in the project will be stored in a Reclamation database such as flows, temperature, water quality, channel bathymetry, fish tracking data, and other available pertinent information as determined by Reclamation after being reviewed by the University for quality control, completeness, and validation.

We reviewed, validated and collected the data required to accomplish the project goals including basin topography, Digital Elevation Model (DEM) for the channel, hydrology and,

climate and meteorological data. Basin topography and channel bathymetry were defined by a DEM, which describes the elevation of a specific point at the defined spatial resolution. We stored all GIS related data in projected horizontal coordinate system NAD_1983_UTM_Zone_11N in meter (m) and the vertical datum D_North_American_1983. The analysis results are reported in the international SI unit.

We collaborated with Reclamation, USFS, and Agricultural Research Service (ARS) regarding the data for the project, data collection, data quality, model selection (hydrologic) and analyzing EAARL surveyed DEM. Communication among collaborators and cooperating agencies were accomplished by teleconference and personnel meetings.

2.3.1 Watershed topographical data

The 10 by 10 m DEM data set (a series-level metadata record describing by14 DEM tiles) is available for Idaho, which is converted to the NAD83 datum by U.S. Geological Survey (USGS) from the 7.5-minute elevation data (http://insideidaho.org/) (Figure 2.2). The DEM of the watershed supported the hydrological modeling.

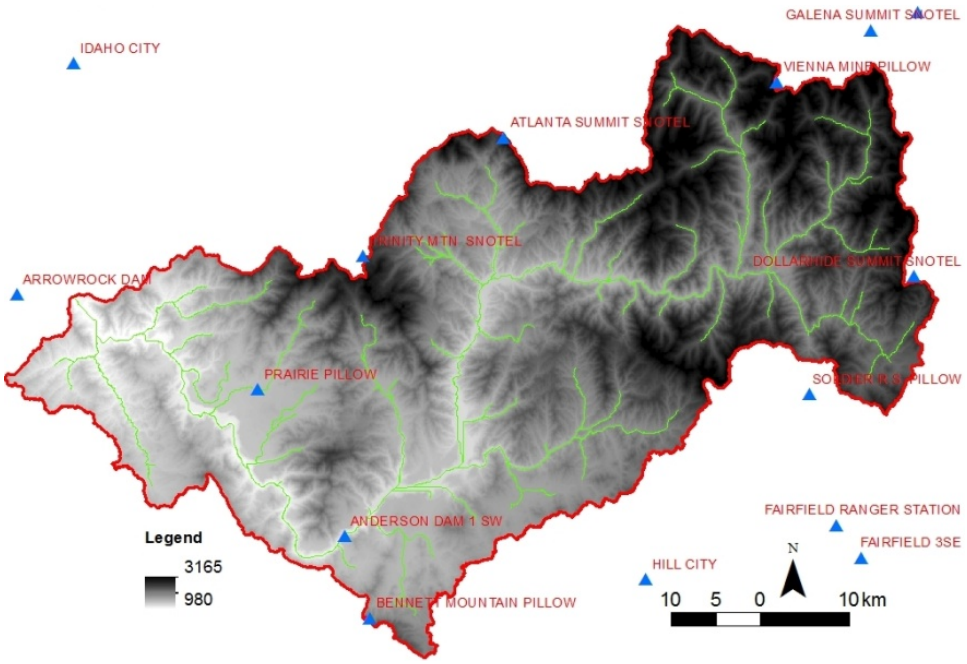

Figure 2.2: South Fork Boise River basin and nearby weather stations.

2.3.2 Channel bathymetry and adjacent topography

The channel bathymetry and adjacent topography for the SFBR is derived from the 2007 survey with the aquatic-terrestrial Experimental Advanced Airborne Research LiDAR (EAARL). The survey provides spatial and elevation data accurate on the order of centimeters (McKean et al., 2009a; McKean et al., 2009b). EAARL is a narrow beam laser able to collect both submerged bathymetry and terrestrial topography adjacent to the channel simultaneously. The EAARL system has a vertical root mean square error (RMSE) of approximately 0.1-0.15 m in point elevation measurements (McKean et al., 2009b). Tests show that this amount of uncertainty has small impact on the flow hydraulic distributions predicted with a two-dimensional model (McKean et al., 2009b). LiDAR point clouds are used to create a high-resolution 1m digital elevation model (DEM) to represent river bathymetry and adjacent topography.

2.3.2.1 Topographic data quality analysis

High-resolution bathymetric and topographic data of riverine and floodplain environments are important for fisheries and riparian ecosystem management. Thus, it is important to perform accuracy analysis of such data sets in order to determine uncertainties associated with it prior to application. As mentioned above, the channel bathymetry and adjacent topography was surveyed using EAARL technology. Skinner (2011) performed accuracy analysis of the EAARL data and found root mean square error (RMSE) ranging from 0.13 m to 0.35 m over flat areas and 0.25 m to 0.78 m in the stream hydrogeomorphic settings in Deadwood and South Fork Boise River based on comparison with field surveyed ground points.

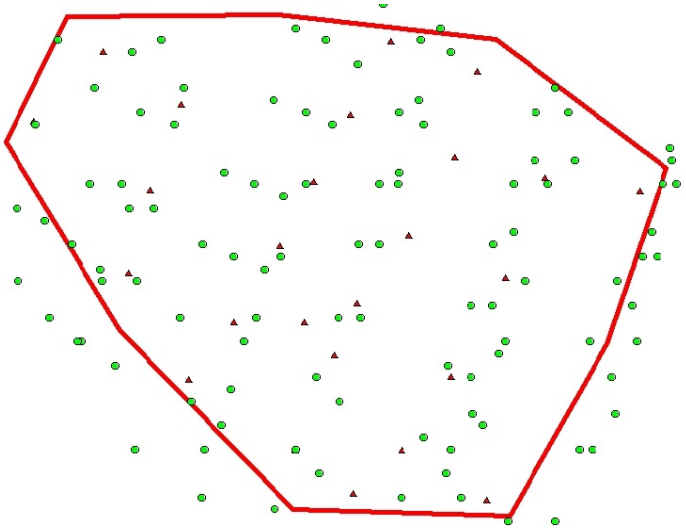

Figure 2.3: LiDAR (green circles) and University of Idaho survey points (purple triangles) within ground survey perimeter (red pollygon) depicting one of the four areas used to calculate deviation between the two survey methods.

We also conducted a ground survey (here after University of Idaho (UI) points) in the SFBR to estimate uncertainties in the elevation of EAARL surveyed topography. We surveyed 20-30 points over a flat ground near the road along the SFBR at four different locations, which are near the Power house, SFBR below Anderson Ranch gauge (USGS # 13190500), Cow Creek Bridge and Danskin Bridge. The points were surveyed using a survey grade, real-time kinematic global positioning system (RTK Leica-GPS System500). The RTK system provides an accuracy of centimeter horizontally and vertically (Jackson, 1999) and it was set to exclude any data collected outside of a desired accuracy limit, which was set at 0.05 m. Points from LiDAR and ground survey within the ground survey area are shown in Figure 2.3 and Figure 2.4. We calculated mean elevation of all the points inside the polygon (Figure 2.3) at all four areas (Figure 2.4) from each data set and subtract from one to another in order to calculate the deviation. Finally, we calculated area weighted mean difference from all four locations to estimate the variability (Table 2.1). The analysis estimated that the LiDAR surveyed elevations are 0.39 m on average lower than the UI ground surveyed elevations. This variability is close with one estimated by Skinner (2011). Nonetheless, uncertainties are not linear or consistent, but random and depend on locations of the study area.

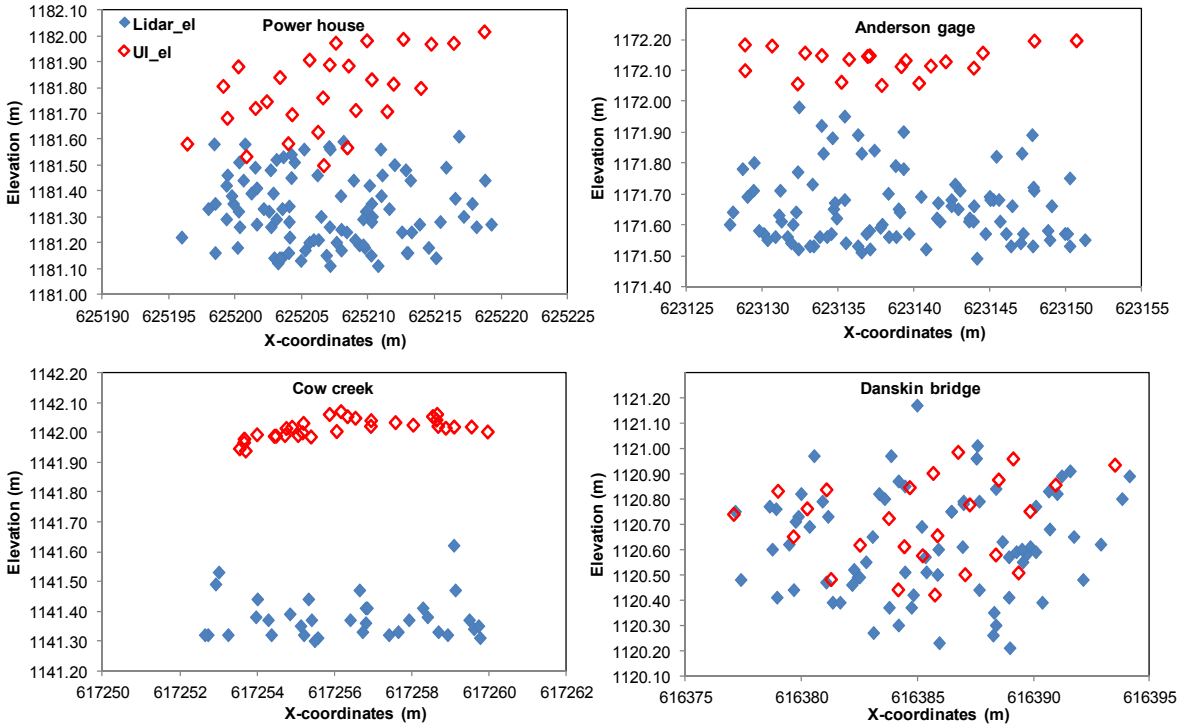

Figure 2.4: Elevation of UI (University of Idaho) and LiDAR surveyed random points plotted against X-coordinates for the four locations: Power house, Anderson Dam gauge, Cow Creek and Danskin Bridge.

Table 2.1: Area weighted mean difference in elevations between LiDAR and UI surveyed random points

Surveyed area	Sample		Mean Elevation		Different	Area weighted
	UI	Lidar	UI (m)	Lidar (m)	(m)	mean (m)
Power house	28	95	1181.78	1181.33	0.46	0.39
Anderson Gage	20	94	1172.13	1171.65	0.47	
Cow creek	31	35	1142.01	1141.38	0.63	
Danskin bridge	25	77	1120.71	1120.63	0.08	

2.3.3 Hydrological data

Main objective of this task is to evaluate the input discharges of the tributaries of the South Fork Boise River below Anderson Ranch Dam. These inputs are used as boundary condition of the hydraulic models. These inflow time series are developed from tributary streamflow measured at the gauge stations. A mass balance model is developed (Task 2) to analyze distribution of tributary flows (section 5.2.6). The time series of stream flow contributed by ungauged tributaries will be quantified with the hydrological model (Task 3). The tributary flow

information is also required to understand the relative influence of tributary discharges on reservoir releases.

The mass balance model of the SFBR system is developed based on stream temperature and flow data collected in the mainstem and tributaries downstream of the reservoir (section 5.2.6). It is useful to reconstruct historical as well as existing temperature and flow pattern of the system, to study trends. These data are used as boundary conditions for the hydraulic and temperature models.

Table 2.2: Basin area, 1.5-year Recurrence Interval (RI) flow, Yearly average flow of different tributaries between Anderson Dam and Little Rattlesnake Creek

No.	Creek Name	Side	$^{\varphi}$Area	$^{\beta}$Q1.5	$^{\theta}$Q	**R	CS	Rank	$^{\Delta}$R
1	Little Rattle snake	R	112	155	1.47	31	31	1	8.5
2	Smith	R	134	314	1.04	22	53	2	6.0
3	Rock	R	76	90.7	0.65	14	67	3	3.7
4	Dead Horse	R	13	-	0.30	6	73	4	1.7
5	Pierce	R	13	13.2	0.23	5	78	5	1.3
6	Big Fiddler	L	10	9.52	0.17	4	82	6	1.0
7	Granite	R	9	10	0.14	3	85	7	0.8
8	Dixies	L	26	17.4	0.13	3	88	8	0.8
	Long Gulch	R	25	-	0.14	3	91	9	0.8
9	Little Fiddler	L	2	1.6	0.07	1	92	10	0.4
10	Hell hole	L	2	1.21	0.06	1	94	11	0.3
11	Trial	L	7	4.75	0.05	1	95	12	0.3
12	Devils Hole	L	6	2.25	0.04	1	96	13	0.2
13	Bounds	L	3	2.25	0.04	1	96	14	0.2
14	Bock	L	10	7.94	0.04	1	97	15	0.2
15	Mennecke	L	10	8.41	0.03	1	98	16	0.2
16	Cayuse	L	9	5.64	0.02	1	98	17	0.1
17	Rough	L	5	4.36	0.02	1	99	18	0.1
18	Dive	R	3	0	0.02	0	99	19	0.1
19	Cow	L	7	5.18	0.02	0	100	20	0.1
	Main Stem Anderson Dam gage				**17.36**				
	Total tributary input*				**4.69**				

*Between Anderson dam and Little Rattle Snake Creek

**Ratio between yearly average tributary flow and total tributary input (%)

$^{\Delta}$Ratio between yearly average tributary flow and main stem flow at Anderson Ranch gage station(%)

^{R}Right side of tributary

^{L}Left side of tributary

$^{\varphi}$Watershed area (km^2)

$^{\beta}$1.5-Recuerence Interval (RI) flow based on USGS's stream stat (m^3/s)

$^{\theta}$Yearly average flow based on USGS's stream stat (m^3/s)

^{CS}Cumulative sum (%)

The hydrological analysis of tributaries was performed to estimate their contributions to the mainstem of South Fork Boise River (Figure 2.1). This analysis highlighted the need of additional gauge stations at different locations along the mainstem and at several tributaries to

collect temperature, discharge and stage measurements. These locations are selected based on their contribution, accessibility and importance for the project (Table 2.3). These are used to calibrate and validate the hydrodynamic (1D and 2D), temperature and hydrologic models.

Table 2.3: Existing USGS and new gauge stations where discharge, water surface and temperature measurements.

SN	Gage station	Measurment	Peroid	
	Main stem South Fork Boise			
1	* SF Boise River below Anderson Ranch Dam	T	-	-
2	$^{\varphi}$13190500 SF Boise River at Anderson Ranch Dam	Q+T	4/9/1943	12/5/2012
3	USGS 13190550 SF Boise River below Cow Creek	Q+WSE+T	-	-
4	$^{\Delta}$Private Bridge at Danskin Ranch Property	Q+WSE+T	-	-
5	$^{\Delta\theta}$Canyon reach	WSE+T	-	-
6	USGS 13192200 SF Boise River at Neal Bridge	Q+WSE+T	8/5/2012	11/6/2012
	Tributaries to South Fork Boise			
1	USGS 13190505 Dixie Creek	Q+WSE+T	10/27/2010	6/12/2012
2	USGS 13190548 Cow Creek	T	4/2/2010	12/1/2012
3	USGS 13190565 Pierce Creek	Q+WSE+T	4/20/2011	12/2/2012
4	USGS 13190560 Granite Creek	T	4/1/2010	12/1/2012
5	*USGS 13190570 Mennecke Creek	T	-	-
6	USGS 13190586 Rock Creek	T	5/14/2010	12/2/2012
7	USGS 13191500 Smith Creek		-	-

$^{\theta}$Location need to be decided based on accessbility
$^{\Delta}$waiting for the permission
* Temperature tidbits has been installed
^{WSE}Water surface elevation
$^{\varphi}$Temperature measurement may be available internally from USGS or USBR
^{WSE}Temperature ^{Q}Discharge

2.3.4 Climate and meteorology data

The hydrologic model (Task 3) of the basin was developed to predict ungauged tributaries flows and historic flow pattern of the basin. It was calibrated and validated with collected discharges from key tributaries of the SFBR. The development of the hydrological model requires basin topography (DEM), meteorological and climatologic information, which includes precipitation, air temperature, solar radiation, relative humidity, potential evapotranspiration (ET), dew-point temperature and wind speed and direction. The dataset of the weather stations located within or nearby the SF Boise basin were analyzed for data type and frequency to be used in the hydrological model (Figure 1.2).

2.3.5 Climatic scenarios selection

The hydrologic analysis is performed to select representative years for comparison between different functional scenarios. The representative years are selected on their characteristics as

typical wet, average and dry climatic years. The typical wet, average and dry years are identified based on annual natural flow characteristics of the basin. The natural flow characteristics are a surrogate for indication of annual climatic conditions. The selection of representative years utilizes unregulated flows measured at USGS gauge 13186000 SFBR near Featherville, ID, which is located at the upstream of the Anderson Ranch Reservoir. Frequency analysis is performed for the measured flows in order to estimate different recurrence interval (RI) floods (Table 2.4).

Table 2.4: Recurrence interval (RI) floods based on frequency analysis for maximum and mean annual flow at USGS gauge 13186000 South Fork Boise River near Featherville, Idaho.

Recurrence Interval (Year) (Probability)	Max annual flow (m^3/s)	Mean annual flow (m^3/s)
1 in 1.01	29	7
1 in 1.25	84	9
1 in 1.5	105	12
1 in 2	129	20
1 in 5	178	28
1 in 10	203	32
1 in 25	228	36
1 in 50	242	40
1 in 100	254	42
1 in 200	264	45

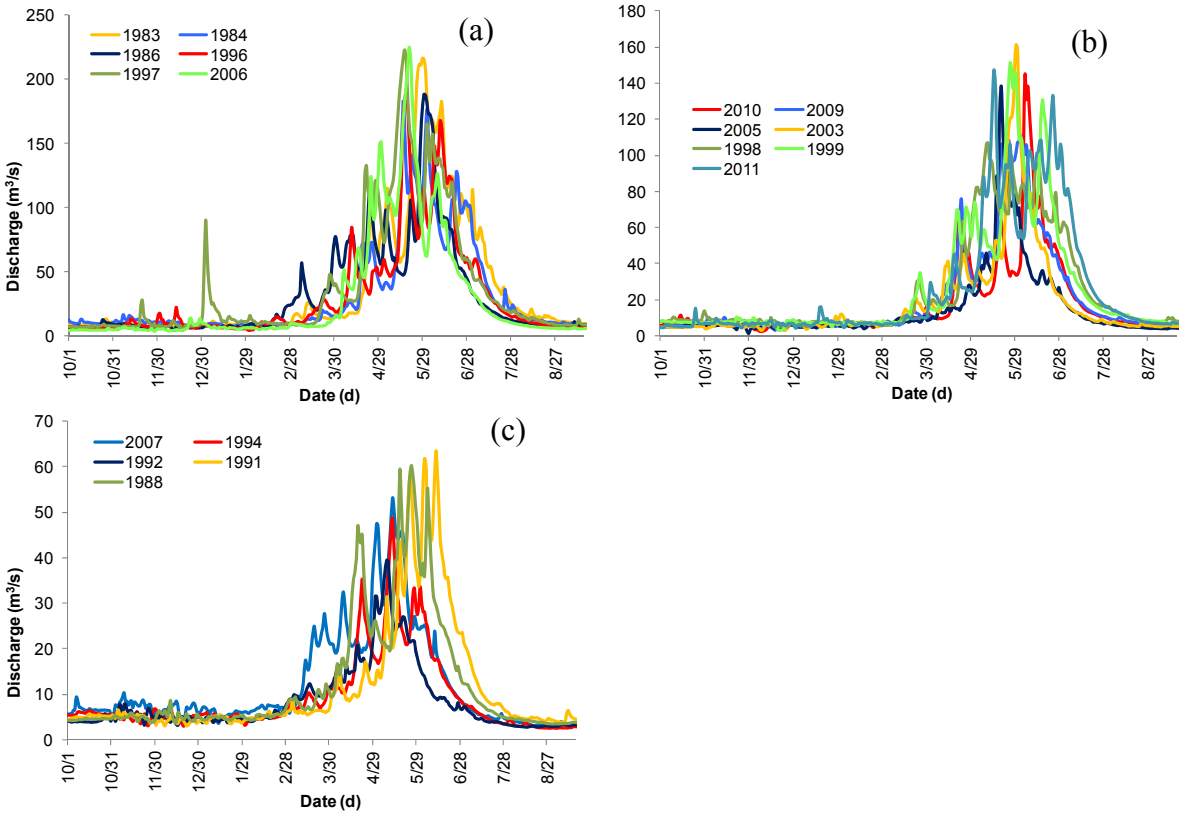

Figure 2.5: Hydrograph (Featherville gauge station) categorized for wet (a), average (b) and dry (c) years.

The annual maximum flow, mean flow and three drought indices (Sohrabi et al., 2015) are used to classify the climatic years. Each year between 1977 and 2012 is classified as dry, average or wet year based on flow magnitude of less than 1.5-year RI, between 1.5 and 5-year RI and greater than 5-year RI, respectively in both annual maximum and mean floods and based on drought indices (Sohrabi et al., 2015). Years of the same category (dry, average or wet) based on the flow and drought indices are then grouped into dry, average or wet year. Then the hydrograph shape is analyzed to detect any anomaly (Figure 2.5). Results show that water years 2006, 2010 and 2007 are good candidate as wet, average and dry years, respectively (Table 2.5).

Table 2.5: Representative years for different climatic conditions

SN.	Year	Annual flow		Recurrence Interval		Climatic condition
		Maximum	Mean	Maximum	Mean	
	-	m^3/s	m^3/s	Year	Year	-
1	2007	53	12	< 1.5	< 1.5	**Dry**
2	2010	144	17	1.5-5	1.5-5	**Average**
3	2006	225	28	10-25	5-10	**Wet**

3 HYDRAULIC AND HYDROLOGICAL MODEL SELECTION

3.1 *Hydrological model selection*

Hydrologic models have been developed since 1950's. With advancement in computer technology, hydrologic models account for complicated physical processes, including snowmelt, sublimation, and groundwater flows. Currently, several hydrologic models are available and they differ for how they approximate the physical domain and processes. In general, most hydrologic models represent part of the hydrologic cycle in a simplified way. For this representation, there are two types of hydrologic models: a) stochastic models, which are based on regression analysis of measured data to predict the system response from input parameters and b) physically-based models that simulate the hydrology of an area based on the physical processes including evapotranspiration, runoff and groundwater.

Because the South Fork Boise River basin is a mountainous basin, snow is a key factor for discharge estimation. Consequently, it is important to model snow pack accumulation and snowmelt processes accurately. A review of available hydrological models is presented below with the approach to estimate tributary's water temperatures.

3.1.1 Comparison of hydrologic models

The following section presents the outstanding characteristics of the most widely used hydrologic models:

3.1.1.1 Variable Infiltration Capacity (VIC):

The VIC is developed by Xu Liang (Liang et al., 1994) at the University of Washington.

- VIC is macro-scale hydrologic model
- The model is based on water and energy balance
- Snow modeling is based on energy balance
- Grid based hydrologic model

3.1.1.2 Hydrologic Simulation Program FORTRAN (HSPF):

HSPF model is developed by U.S. Environmental Protection Agency (USEPA). This software package simulates watershed hydrology and water quality. HSPF automatically gathers selected inputs by connecting to EPA website, so manipulation input data sets is challenging.

- HSPF divides basins to several sub-basins and simulates hydrologic parameters for each sub-basin (semi-lump model)
- Snow modeling is based on energy balance
- HSPF is able to estimate stream temperature
- It is challenging to change the input data or couple another model with this model

3.1.1.3 MIKE SHE:

Freeze and Harlan (1969) suggested the blue print for modeling the hydrologic cycle. A consortium of three European organizations has been developing the Système Hydrologique Européen (SHE), an integrated hydrological modeling system according to Freeze and Harlan's work since 1977. Danish Hydraulic Institute (DHI) has been developing MIKE SHE software since mid-1980s. Unlike the other widely used hydrologic models, MIKE SHE is a commercial software.

- Grid based hydrologic model
- Snow modeling is based on air temperature
- MIKE SHE has a coefficient to convert dry snow to wet snow to give proper lag time to snowmelt
- MIKE SHE considers sublimation from dry snow
- MIKE SHE considers the effect of rain on the snow

3.1.1.4 Penn State Integrated Hydrologic modeling system (PIHM):

The PIHM modeling system was initially developed under research grants to the Pennsylvania State University (Penn State) from NSF, NOAA, NASA and with continuing grants from NSF and EPA for community model development.

- PIHM divides basin to triangular cells (the area of triangles are defined by users) (unstructured mesh)
- PIHM is able to couple with ISNOBAL , which is a robust snow model
- ISNOBAL has been applied in a basin in Idaho by ARS Boise

ISNOBAL is a robust energy and mass-balance snow model. The model initially presented by Marks (1988). Garen and Marks (1996) applied an energy balance snow model in a large mountainous basin (Boise River basin). Since then, ISNOBAL has been applied for various basins in different states. Recently, Marks coupled ISNOBAL with PIHM for a basin in Idaho.

It is difficult to judge which hydrologic model is better or has better performance. However, according to the application purpose one can decide which hydrologic model is suitable. As aforementioned, a hydrologic model that accounts for accurate snow modeling is needed for the current project. Based on the applicability of all the hydrological models, PIHM can be a proper choice for the current project for the following reasons:

- PIHM can couple with a highly advanced snow model (ISNOBAL) by collaboration with Agricultural Research Service (ARS).
- The size (area) of mesh is adjustable based on the purpose of application, which can reduce the model computational time.

3.2 *Hydraulic modeling test for the SFBR*

The study for quantification of differences in hydraulic quantities between 1D and 2D hydraulic models are sparse as well as their effects on habitat modeling is unclear. Therefore, we used 1D and 2D model in one of the reaches (Figure 1.1) of the SFBR in order to estimate

difference in simulated hydraulic variables and their impact in habitat suitability analysis. Detail about model development and result interpretation can be found in Benjankar et al. (2014b). Here, we only present the main results, which help the selection of the appropriate approach between 1D and 2D for hydraulic modeling in the SFBR for habitat analysis. The Danish Hydraulic Institute (DHI) software MIKE 11 (1D) and MIKE 21 (2D) are used in this analysis.

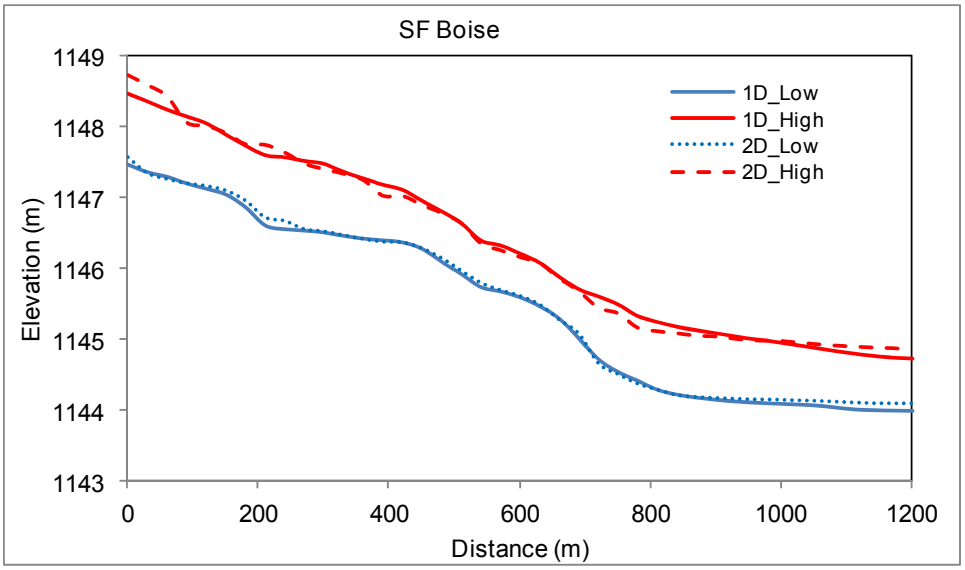

Figure 3.1: Simulated water surface elevations (WSE) with 1D and 2D hydraulic models in South Fork Boise River for low and high discharge scenarios. A 0 chainage in the figure is a first point where WSE is compared, not a beginning of the study reach. WSEs were just compared at the locations where we assumed there is no boundary effects (upstream and boundary).

The specific reach for 1D or 2D analysis is located in the upper reach of the SFBR about 10 km downstream from the Anderson Ranch Dam and is 1,350 m long (Figure 1.1). We divide the study reach into straight (Sinuosity Index<1.2) and meander (Sinuosity Index>1.2) reaches. We use 10.65 and 63.43 m^3/s flows as low and high discharges, respectively to simulate hydraulic variables (water depth and velocity) using 1D and 2D hydraulic models. The difference in water surface elevation (WSE) with 1D and 2D model (Figure 2.3) for low and high flows are 0.06 and 0.1 m, respectively.

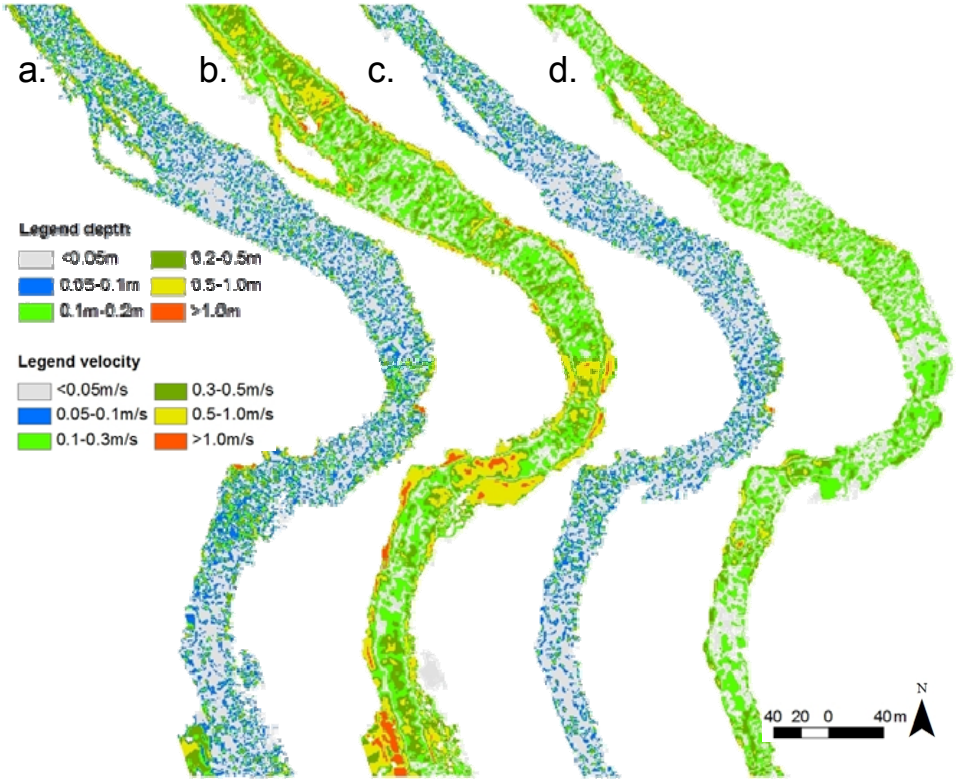

Figure 3.2: Spatially distributed flow depth and velocity distribution for reach of the South Fork Boise River. Sub-figure numbers are: a. depth for high discharge (HQ), b. velocity for HQ, c. depth for low discharge (LQ), and d. velocity for LQ

The differences in average bathymetric elevation between the 1D and 2D models are 0.19±0.21m and 0.13±0.20m for straight and meander reaches, respectively in the South Fork Boise River (Table 3.1). The differences in average depths are greater in the straight reach for both low (0.16±0.14m) and high (0.21±0.19m) discharge scenarios than in the meander reach (0.11±0.10m and 0.14±0.15m) for low and high discharge scenarios, respectively. The velocity trend is opposite from the depth where, average velocities are higher for meander reach than in the straight reach for both discharge scenarios (Figure 2.4, 2.5 and Table 3.1).

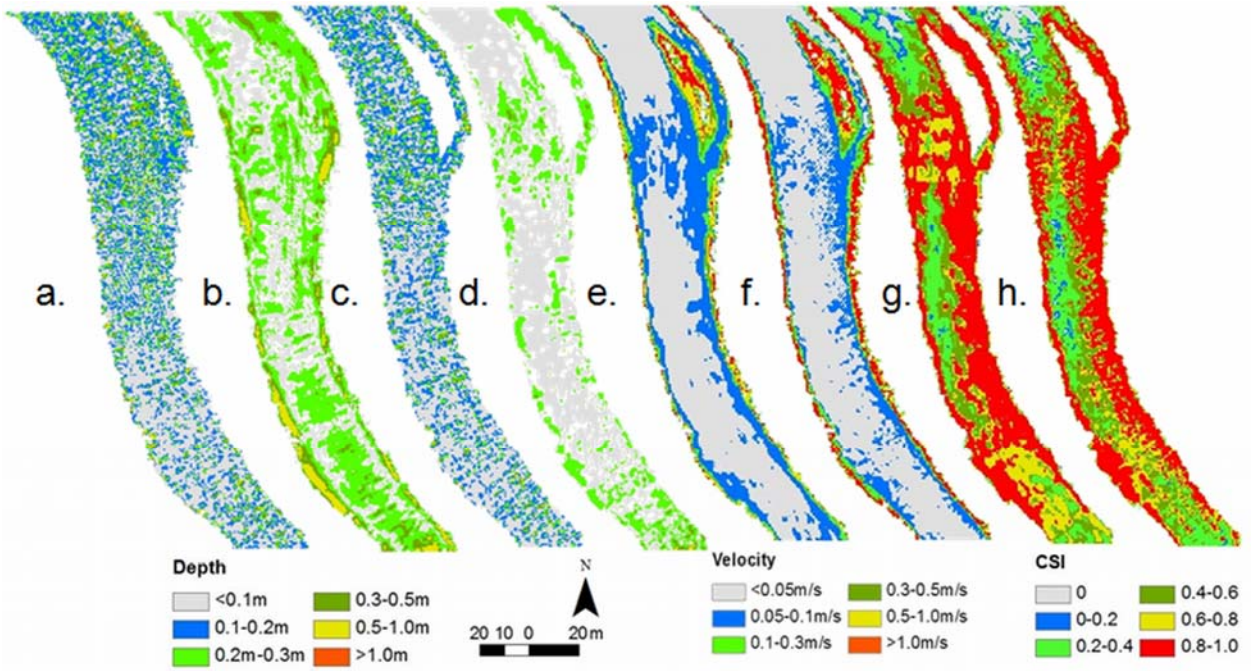

Figure 3.3: Spatially distributed flow depth, velocity and habitat suitability distribution for straight reach of the South Fork Boise River. Sub-figure numbers are: a. depth for high discharge (HQ), b. velocity for HQ, c. depth for low discharge (LQ), and d. velocity for LQ, e. combined cell suitability index (CSI) form 1D model for HQ, f. combined CSI form 2D model for HQ, g. combined (CSI) form 1D model for LQ, f. combined CSI form 2D model for LQ.

Average mean depth differences are more than 0.1 m but median depth difference are within the 0-0.1 m class. Generally, differences are noticeable near the edge of water in both discharge scenarios. This is likely due to the differences in channel topography represented in the 1D and 2D models, which causes different inundation area for the specific discharge. The difference in flow depths follows similar trend with the difference in bathymetry, where differences in depth are higher in the straight reach for both discharge scenarios. This may indicate that the difference in bathymetry between the 1D and the 2D models plays a major role in the depth differences.

Table 3.1: Differences in flow depth and velocity for high (HQ) and low (LQ) discharges

River	Reach	*SI	Bathymetry			LQ_depth				HQ_depth				LQ_velocity				HQ_velocity			
			Mean	SD	φMed	Mean	Δ	SD	φMed	Mean	Δ	SD	φMed	Mean	Δ	SD	φMed	Mean	Δ	SD	φMed
		-	m	m	m	m	%	m	m	m	%	m	m	m/s	%	m/s	m	m/s	%	m/s	m
SF Boise	St	1.04	0.19	0.21	0-0.1	0.16	26	0.14	0-0.1	0.21	19	0.19	0.1-0.2	0.07	14	0.07	0-0.05	0.17	16	0.16	0-0.05
	Md	1.28	0.13	0.20	0-0.1	0.11	17	0.10	0-0.1	0.14	13	0.15	0-0.1	0.17	33	0.14	0-0.05	0.34	32	0.30	0.1-0.3

*Sinousity Index LQLow discharge HQHigh discharge MdMeander reach StStraight reach

φMedian range is based on cumulative frequency (%), which is near to the 50 percentile

Velocity also follows similar trend with flow depth, where larger difference between 1D and 2D are observed near the edge of water (Figure 3.3 and Figure 3.4). This can be the result of combination of the channel geometry and the complex pattern of velocity distribution in the channel, which a 1D model is not able to handle. However, 2D model considers mass and momentum conservation in the transversal and longitudinal directions based on detailed channel geometry description (Kondolf et al., 2000), which is similar to natural flow phenomenon. A 2D model is capable of reproducing the smallest of 2D (natural) flow features, but bed geometry must be described precisely (Bovee, 1986; Kondolf et al., 2000). Hydraulic simulations of natural rivers with several large boulders can significantly affect predicted flow parameters velocity gradients and transverse flows. The model will not be able to simulate these phenomena when topographical features, such as cobbles and boulders, geometry is not incorporated into the hydraulic model (Crowder and Diplas, 2000; Crowder and Diplas, 2002).

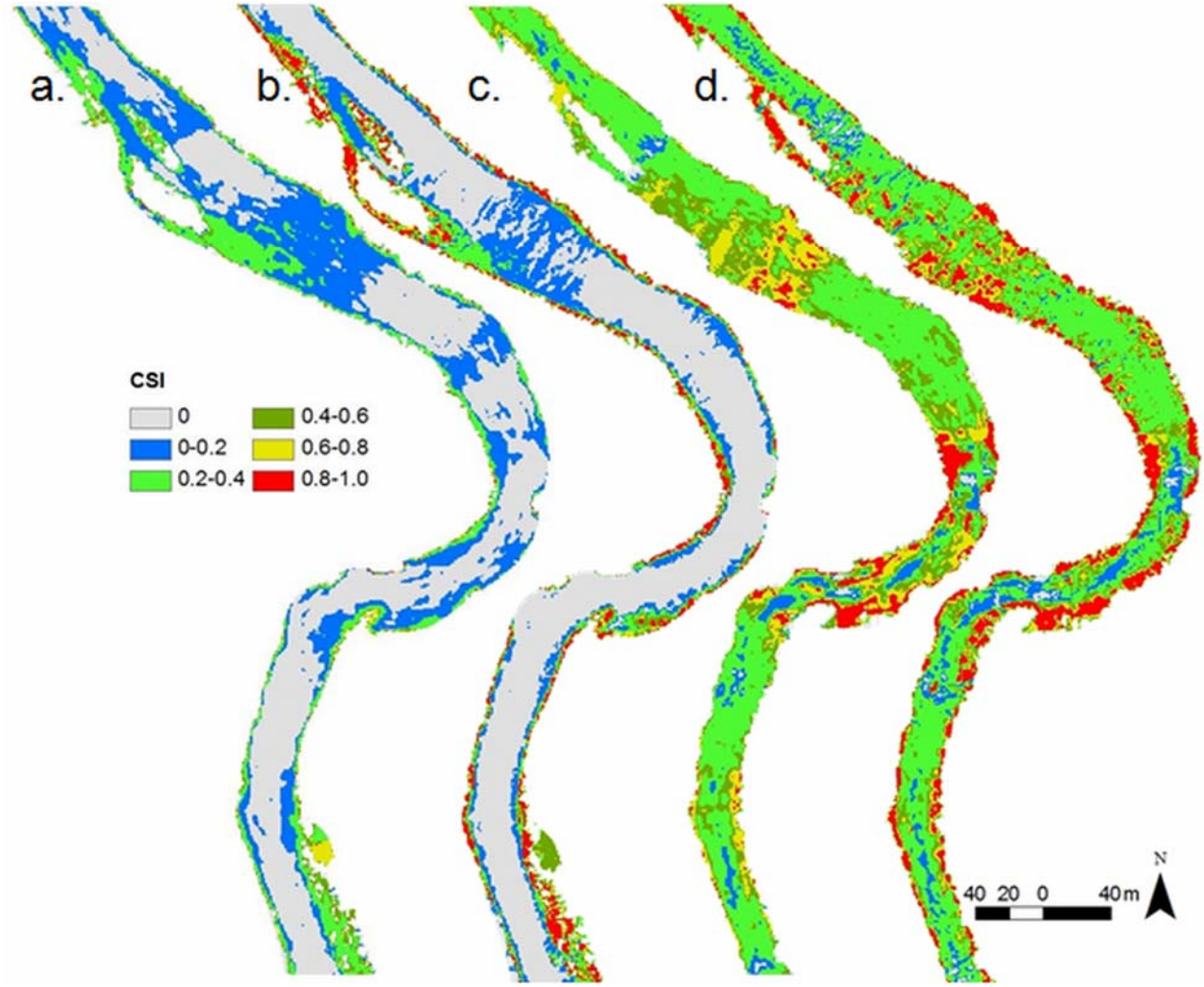

Figure 3.4: Spatially distributed habitat suitability distribution for meander reach in the South Fork Boise River. Sub-figure numbers are: a. combined cell suitability index (CSI) from 1D model for high discharge (HQ), b. combined CSI form 2D model for HQ, c. combined (CSI) form 1D model for low discharge (LQ), and d. combined CSI form 2D model for LQ.

Total WUAs are greater in 2D model in both straight (25%) and meander (42%) reaches than in 1D model for the high discharge in the South Fork Boise River (Figure 2.5, 2.6 and Table 3.2). Conversely, 1D model predicts higher WUA (4%) for the low discharge in the straight reach but lower WUA (7%) in the meander reach. The analysis of error matrix (Congalton and Green, 2008) shows that agreement (K) between two maps (1D and 2D models) are higher in straight reach (0.27) than in the meander reach (0.25) for the low discharge scenario (Figure 2.6), whereas overall accuracy (OA) trend is opposite (Table 3.2).

These results show that 2D model yielded higher habitat quality than the 1D model for the SFBR. In general, 2D model should yield better simulated flow patterns over the floodplain and complex channel environment, where flow paths are multidimensional (Gillam et al., 2005).

Table 3.2: Differences in WUA, HHS from 1D and 2D models for high and low discharges (Q) and agreement between the maps using error matrix.

River	Reach	Low Q							High Q						
		WUA (1000 m^2)		Δ	Agreement (-)		HHS (-)		WUA (1000 m^2)		Δ	Agreement (-)		HHS (-)	
		1D	2D	%	K	OA	1D	2D	1D	2D	%	K	OA	1D	2D
SF Boise	St	10.96	10.57	-4	0.27	0.46	0.66	0.65	2.36	3.16	25	0.42	0.64	0.12	0.16
	Md	11.61	12.55	7	0.25	0.47	0.42	0.45	3.24	5.61	42	0.39	0.61	0.03	0.16

[Md] Meander reach [St] Straight reach [WUA] Weighted usable area [HHS] Hydraulic habitat suitability

Δ Difference in WUA between 1D and 2D models [K] Kappa coefficiet [OA] Overall accuracy

4 STREAM TEMPERATURE ESTIMATION

4.1 *Introduction*

Stream water temperature plays an important role in aquatic ecosystems and is an important cue for organism behavior (Rice *et al.*, 1983; Jobling, 1997; Rieman *et al.*, 2007; Isaak *et al.*, 2012), fish metabolism (Forseth and Jonsson, 1994; Railsback and Rose, 1999; Mesa *et al.*, 2013; Isaak *et al.*, 2015) and growth rates (Brett, 1979; Crozier et al., 2010; Xu et al., 2010). Stream water temperature controls dissolved oxygen concentrations, which may affect water quality and biogeochemically reactive solutes (Webb *et al.*, 2008; Marzadri *et al.*, 2011; Marzadri *et al.*, 2012; Tonina *et al.*, 2015) whereas high stream water temperatures may negatively affect industrial activity (Boogert and Dupont, 2005; Null *et al.*, 2012; Vliet *et al.*, 2012b; Vliet *et al.*, 2013). These studies indicate the value of accurate estimates of daily stream water temperatures for dam and water resource managers, ecologists, economists and decision makers.

Many stream temperature models have been developed. These can be divided into mechanistic models that use physical processes (Carron and Rajaram, 2001; Ficklin et al., 2012; Vliet et al., 2012a) and statistical models that rely on covariates that indirectly represent physical processes (Hockey *et al.*, 1982; Mohseni *et al.*, 1998; Gu *et al.*, 1999; Bogan *et al.*, 2003; Neumann *et al.*, 2003; Ahmadi-Nedushan *et al.*, 2007). Process-based models require a large number of input variables (e.g., wind speed, net radiation, relative humidity, stream hydraulic cross sections), which may not be available in many locations, limiting opportunities for prediction. Process models may also be more computationally intensive because they solve a large number of equations to quantify energy balance and heat transport within the watershed.

Conversely, statistical models are simpler to apply and have lower data requirements (Benyahya et al., 2007) but sacrifice interpretability. Regression approaches rely on correlations between stream water temperature and environmental covariates that vary spatially or temporally. When used with air temperature data series measured contemporaneously with stream temperature, predictions can be made at various times-steps (e.g., daily, weekly, monthly). However, air-water temperature relationships become weaker at finer temporal

resolutions (Webb *et al.*, 2003; Ahmadi-Nedushan *et al.*, 2007), due to the large heat capacity of water, which does not respond to heat exchanges as quickly as air temperature. At short time-steps, temporal autocorrelation may also cause parameter estimation bias because measurements are not independent (Webb et al., 2003). Statistical autoregressive (AR) models account for the autocorrelation structure within stream water temperature time series by considering stream water temperatures of previous time steps and the correlation with meteorological variables of interest (e.g., air temperature). Stochastic models have two components, (1) the long-term annual component (seasonal variation) and (2) the departure from annual component (short-term variation; residual). In these models, a fixed function, e.g. a sinusoidal function, is fitted to stream water temperature time series, which in turn may cause non-stationarity in the residual from year to year (Caissie *et al.*, 2001; Benyahya *et al.*, 2007). Non-parametric approaches, such as artificial neural networks (ANN) train the models with relatively long time series of input data. This prevents their applicability in locations with short time series. These models capture complex non-linear relationship between independent and dependent variables solely based on data and without assuming *a priori* statistical distributions and relationships among variables (Bélanger et al., 2005; Benyahya et al., 2007). Their lack of a general theoretical framework and dependence on training data make them less reliable in predicting stream water temperatures outside the range of their training conditions (i.e. dry or wet) (Risley *et al.*, 2003; Benyahya *et al.*, 2007).

The Mohseni et al. (1998) statistical model that predicts stream temperatures at a site from air temperatures at a remote climate station is widely used in riverine studies because of its simplicity and good performance (reported average RMSE of 1.64 mm (Mohseni et al., 1998)). It is often fit at a weekly time-step but can be run at any interval resolvable within the temperature time-series. A non-linear regression function captures hysteresis effects associated with differential stream-atmosphere heat transfer rates that vary seasonally (Mohseni et al., 1998). The model was initially developed using only air temperature as a covariate but stream discharge is now routinely incorporated and usually improves model performance (Vliet *et al.*, 2011; Isaak *et al.*, 2012; Luce *et al.*, 2014), especially in regions with snow-dominated hydrologic regimes where spring and early summer snowmelt cause strong seasonal pulses of cold water.

Stream temperature has been a key factor that has profound influence on aquatic habitat. Unfortunately, there is no long-term stream temperature data available in SFBR, specifically in tributaries. To evaluate the impact of Anderson Ranch Dam on stream temperature, estimation of tributary stream temperature should be performed by other methods. We developed the method (model) to predict stream water temperature that utilizes long and high quality records of measured data including minimum and maximum air temperature and discharge.

The main objective of this section was to develop and test a new parsimonious statistical model to predict stream water temperature at the daily temporal resolution under a wide range of climatic conditions in unregulated streams and for current, historical and future conditions. The model was designed to overcome one of the limitations of existing statistical models by including the effect of discharge on stream water temperature. However, it can be parameterized solely with air temperature data when discharge data are unavailable. It is based on a piecewise Bayesian approach and accounts for the autocorrelation structure within the stream water temperature time series. We tested model performance in different climatic regions and compared it to that of the widely-used Mohseni et al. (1998) model in a mountain river basin and selected locations throughout the U.S. with different climatic regimes. The main goal of this stream water temperature model is to predict precise daily stream water temperature and to apply it to ungauged tributaries of the SFBR system.

4.2 *Study area and data*

Model development was done in the Boise River Basin of central Idaho, USA (Figure 4.1) because of the availability of extensive stream temperature datasets (http://www.fs.fed.us/rm/boise/AWAE/projects/NorWeST.html); and climate monitoring stations. The terrain of the basin is mountainous ranging from about 1,000 to 3,000 m, which creates complex meteorological conditions with strong temporal and spatial variability and provides a challenging test for water temperature model performance. The Boise River Basin also has strongly seasonal weather patterns, with large snowpack accumulations occurring during winter and annual floods occurring during late spring when snow melts.

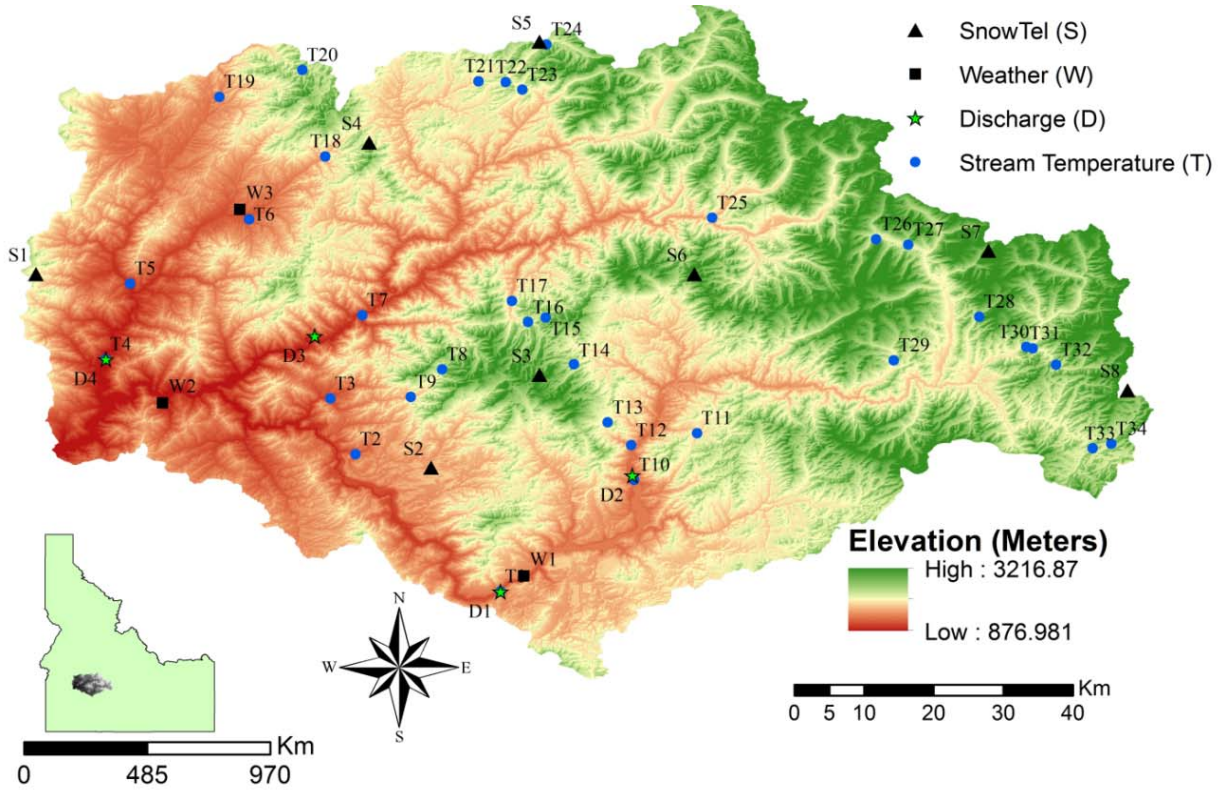

Figure 4.1. Study area and spatial distribution of the metrological, hydrological and temperature gauge stations.

Eight additional stream temperature stations were selected in different parts of the U.S. to test and validate the generality of the model (Figure 4.2). Those climate regions include (Sohrabi et al., 2015): Semi-Arid Steppe (CT1), Marine West Coast (also known as Oceanic Climate) which is also the predominant climate across most parts of Europe (CT2), Mediterranean (CT3), Mid-Latitude Desert (CT4), Highland or Alpine (CT5), Humid Continental with cool summer (CT6), Humid Continental with warm summer (CT7) and Humid Subtropical (CT8). These eight stations are distributed over a wide range of elevations, from 29 to 2,700 meters above mean sea level (Table 4.1). Each station recorded mean daily stream temperature and discharge.

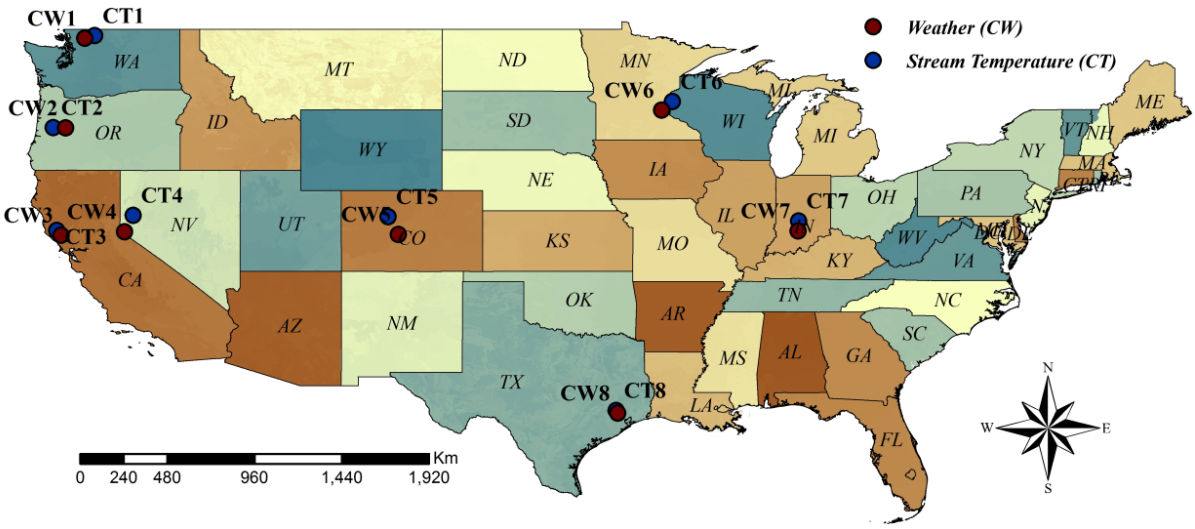

Figure 4.2. Location of weather and stream temperature stations at eight different climate regions in United States.

Table 4.1. Detailed information of stream temperature stations

Station NO.	Stream	Latitude	Longitude	T*	Elevation (m)
CT1	Skagit River at Newhalem, WA	48.67	-121.25	CW1	59
CT2	Long Tom River near Alvadore, OR	44.12	-123.30	CW2	205
CT3	Russian River near Hopland, CA	39.03	-123.13	CW3	609
CT4	Truckee River near Nixon, NV	39.78	-119.34	CW4	1435
CT5	Eagle River near Wolcott, CO	39.70	-106.73	CW5	2682
CT6	ST. Croix River at ST. Coix Falls, WI	45.41	-92.65	CW6	295
CT7	White River near Centerton, IN	39.50	-86.40	CW7	228
CT8	Spring Creek near Spring, TX	30.11	-95.44	CW8	29
T1	Dixie creek	43.34	-115.48	W1	1171
T2	Smith Creek	43.52	-115.67	S2	1171
T3	Little Rattlesnake Creek	43.59	-115.70	W3	1134
T4	Mores Creek	43.64	-115.48	W3	1134
T5	Grimes Creek	43.74	-115.96	W4	1032
T6	Bannock Cr	43.82	-115.80	W4	1216
T7	MF Boise River	43.70	-115.66	W4	1048
T8	Rattlesnake Creek	43.63	-115.56	S3	2000
T9	Rattlesnake Creek	43.59	-115.60	S2	1527
T10	South Fork Boise River	43.48	-115.31	S3	1281
T11	Grouse Creek	43.54	-115.23	S3	1660
T12	Dog	43.53	-115.31	S3	1371
T13	Dog Creek	43.56	-115.34	S3	1838
T14	Trinity Creek	43.63	-115.39	S3	2034
T15	Scotch Creek	43.69	-115.42	S3	2063
T16	EF Roaring River	43.69	-115.44	S3	1831
T17	Roaring River	43.72	-115.47	S3	1547
T18	Mores Creek	43.90	-115.71	S4	1499
T19	GRIMES CR	43.98	-115.84	W4	1362
T20	Grimes Creek	44.01	-115.74	S4	2002
T21	Pikes Fork	44.00	-115.51	S5	1701
T22	Crooked River	44.00	-115.47	S5	1806
T23	Bear Creek	43.99	-115.45	S5	1790
T24	Crooked River	44.05	-115.42	S5	1942
T25	Queens River	43.82	-115.21	S7	1507
T26	SF Ross Fork	43.79	-115.00	S8	2025
T27	Gold Run Cr	43.79	-114.95	S8	1997
T28	Paradise Ck	43.69	-114.86	S8	2056
T29	Skeleton Cr	43.64	-114.97	S8	1853
T30	BIG SMOKY	43.66	-114.80	S9	1799
T31	Big Peak Creek	43.65	-114.79	S9	1854
T32	Big Peak Creek	43.63	-114.76	S9	1959
T33	Little Smoky Creek	43.52	-114.72	S9	1945
T34	Little Smoky Creek	43.53	-114.69	S9	2015

T* shows weather or Snowtel stations which were used to estimate stream water temperature for each stream water temperature station. Letter C, T, S and W stand for Climate Region, Stream Water Temperature station, SNOTEL and Weather stations, respectively, for example CW1 indicates the weather station located at first climate region.

4.3 *Method*

4.3.1 Data collection

We obtained mean daily water temperature data in the Boise River Basin at 34 stations for the period of August 2010 to August 2012. Miniature digital temperature sensors were placed in solar shields and epoxied to the downstream side of large boulders below the low-flow summer water surface as described in Isaak et al. (2013). One additional water temperature record was obtained at T4 station, which had data from November 1969 to July 1972 at a USGS flow gauge. The water temperature records were matched with contemporaneous meteorological and hydrological data from 3 weather stations, 8 SNOTEL stations and 4 stream discharge gauging stations (Figure 4.1). Table 4.1, A.1, A.2 and A.3 report detailed information of stream water temperature, weather, SNOTEL (www.wcc.nrcs.usda.gov) and discharge stations (USGS website: www.usgs.gov), respectively. Because there was not a weather or SNOTEL station for each reach with a temperature sensor, we matched the nearest weather or SNOTEL station to each stream water temperature gauge (therefore, recorded mean daily air temperature of some weather and SNOTEL stations were matched with multiple water temperature sensors). The observed mean daily discharges at D1, D3 and D4 gauges were used for estimation of stream water temperature at T1, T7 and T4, respectively. Station D2 had discharge and stream water temperature measurements from April 1963 to September 1965 and from April 1978 to October 1979 (Table A.3). We used the observed data for these two periods at D2 to test the capability of our model to reconstruct historical stream water temperatures in periods with different hydrological conditions from those of the calibration period. After October 1979, only discharge was recorded at D2. At this gauge, the observed discharge was used for estimation of stream water temperature at T10, which is close to D2, for the period of August 2010 to August 2012.

At the eight stations selected to test the performance of the model in different climates, daily discharge measurements with less than 4% missing values were available for all stations except CT2. The discharges in this station (CT2) were influenced by upstream irrigation diversions and were not used. The stations CT1, CT2, CT3 and CT6 located downstream of a dam were used to test the model at regulated streams.

4.3.2 Model development

We developed a piecewise model, called the Stream Water Temperature Model (SWTM), which accounts for both linear and non-linear relationships between dependent and independent variables. The model uses mean daily air temperature (T_a) and discharge (Q) as meteorological and hydrological drivers, respectively to estimate mean daily stream water temperature (T_s). It accounts for antecedent conditions by considering the stream water temperature of the previous time step (day). We fit the model using Bayesian methods (Lunn *et al.*, 2000a; Gelman and Hill, 2007).

Stream water temperature is correlated with air temperature and discharge (Mohseni *et al.*, 1998; Luce *et al.*, 2014). Air temperature is commonly used as a surrogate for heat flux exchanges in stream water temperature models. The linear relationship between air and steam water temperatures becomes non-linear as air temperature approaches freezing conditions (0˚C) (Figure 4.3) (Mohseni et al., 1998; Neumann et al., 2003; Webb et al., 2003). Discharge is a proper proxy for snowmelt and rain, which have notable influences on stream water temperature (Hockey *et al.*, 1982; Gu *et al.*, 1999; Webb *et al.*, 2003). Webb et al. (2003) identified a linear relationship between discharge and stream water temperature at any time scale (e.g. daily or weekly).

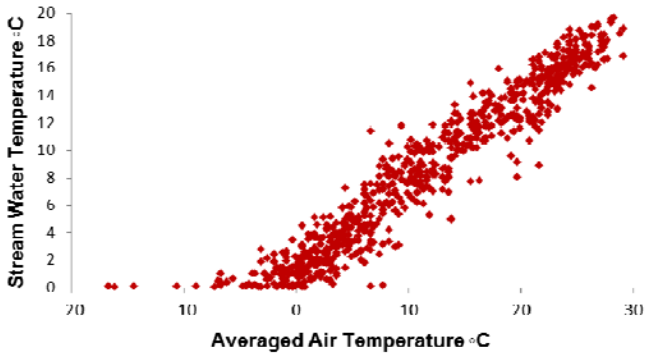

Figure 4.3. Linear and non-linear relationship between daily stream water and air temperatures at station T10.

A robust stream temperature model at a daily resolution should account for two important properties: the thermal inertia of the water and non-linearity near the freezing point. The former depends on the heat capacity of a system, which is the amount of heat required to increase the

temperature by 1˚C (IUPAC, 2014). Because heat capacity of water is large and larger than that of the air, stream water temperature does not respond to heat exchanges as quickly as air temperature. Consequently, stream water temperature changes slowly unless there are sources of water of a different temperature from that of the stream or changes in canopy cover. The correlation distance increases with discharge, as more heat or heat loss is required to warm or cool the water. This spatial longitudinal correlation is particularly true at fine temporal resolution i.e. hourly and daily (Webb *et al.*, 2003; Ahmadi-Nedushan *et al.*, 2007). The SWTM model considers the thermal inertia with an autoregressive component. We tested lag times varying between 0 and 7 days. We found that the highest autocorrelation was associated with a one-day lag (Figure 4.4) and therefore specified a 1-day lag in the model.

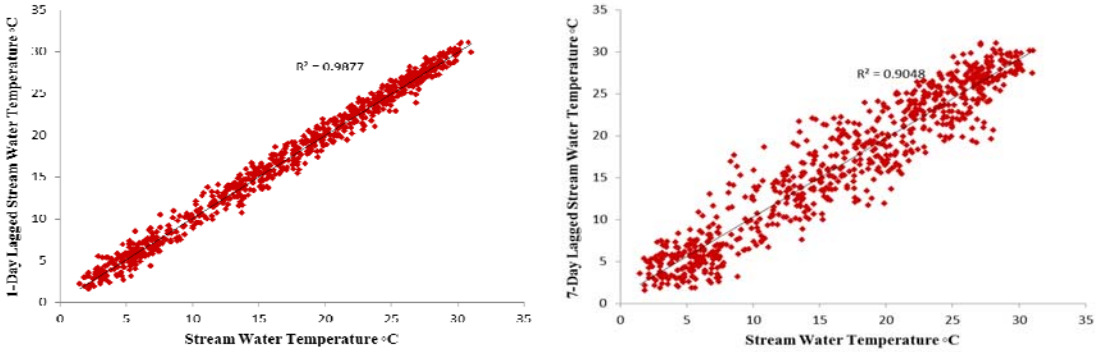

Figure 4.4. One-day and seven-day lagged autocorrelation of daily stream water temperature at station CT7.

To account for non-linearity near the freezing point, we divided the data series temporally into three parts: days T_a <1˚C (group 1), days in the October to May period that T_a >1˚C (group 2), and the June-September period (group 3). A linear model is applied for data in group 2 and 3, whereas a non-linear model is used for data in group 1. In both the linear and non-linear models, it is assumed that stream water temperature has a Gaussian (normal) distribution (Eq. 3.1), because daily T_s and T_a are strongly correlated and daily T_a follows a Gaussian distribution (Robeson, 2002).

$$T_s = Normal\,(\mu(t), \tau) \tag{4.1}$$

Where μ (mean) and τ (standard deviation) are location and scale parameters, respectively. The standard deviation τ is time independent, whereas μ is time dependent and defined in two different ways for the linear (Eq. 3.2) and non-linear (Eq. 3.3) models:

$$\mu(t) = a_1 \times T_a(t) + a_2 \times \mu(t-1) + a_3 \times Q(t) + b \tag{4.2}$$

$$\mu(t) = \exp[a_1 \times T_a(t)] + |a_2| \times \mu(t-1) + a_3 \times Q(t) + |b| \tag{4.3}$$

where a_1, a_2 and a_3 are coefficients related to air temperature, stream water temperature at the previous time step and discharge, respectively, *t* is time and *b* is intercept in both linear and non-linear models. For streams that have temperatures near the freezing point, a negative value could be estimated for a_2 or *b*; we prevent this by using absolute values of a_2 and *b* in the model (Eq. 3.3), to result in posterior distributions with a positive mean for these parameters. The second variable ($\mu(t-1)$) in Eq. 3.2 and 3.3 carries over the estimated stream water temperature from the prior time step.

With a large sample size the choice of prior distribution has a negligible impact on posterior inference (Gelman, 2002). We used minimally informative prior distributions. It is assumed that coefficients and intercepts in Eq. 3.2 and 3.3 followed a Gaussian distribution (Gelman, 2006; Kwon et al., 2008):

$$a_1, a_2, a_3 \text{ and } b \approx Normal\,(0, 10^{-4}) \tag{4.4}$$

The scale parameter τ must have positive values. We assumed the scale parameter followed a Gamma distribution to constrain the scale parameter to positive values (Spiegelhalter et al., 2003).

$$\tau \approx Gamma\,(10^{-3}, 10^{-3}) \tag{4.5}$$

We fitted these parameters using WinBUGS software, called from R with the R2WinBUGS package (Sturtz et al., 2005). WinBugs (Lunn et al., 2000b) applies Markov Chain Monte Carlo (MCMC), using Gibbs sampling and the Metropolis–Hastings algorithm to infer

posterior distributions. MCMC is a numerical method that generates dependent samples that follow a given probability distribution. The role of MCMC is to generate large enough dependent samples that the characteristics of a posterior distribution can be precisely summarized (Tierney, 1994; Campbell *et al.*, 1999). At each iteration, a parameter is updated by sampling from its full conditional distribution, which depends on the data, the prior and on the current values of the other parameters (Gilks et al., 1995). The R2WinBUGS package is used to call WinBUGS from R to facilitate the preparation and manipulation of the data in WinBUGS (Sturtz et al., 2005). We ran three chains for 2,000 iterations each, following a 1,000-iteration burn-in period. We evaluated convergence using the Gelman-Rubin statistic.

4.3.3 Model evaluation

The model was calibrated with the first two thirds of the data and then validated with the remaining one third. Accuracy of fit and error of the model were evaluated with the Nash-Sutcliffe coefficient (NSC) and root mean square error (RMSE), respectively. NSC is calculated as follows (Nash and Sutcliffe, 1970):

$$\boldsymbol{NSC = 1 - \frac{\sum_{i=1}^{n}(Ts_{sim,i} - Ts_{obs,i})^2}{\sum_{i=1}^{n}(Ts_{obs,i} - \overline{Ts}_{obs})^2}} \quad (4.1)$$

where, Ts_{sim} and Ts_{obs} are simulated and observed stream water temperatures, $\overline{Ts}_{obs}$ is the mean of the observed stream water temperatures and n is the number of data. The RMSE is computed based on the below equation:

$$\boldsymbol{RMSE = \sqrt{\frac{\sum_{i=1}^{n}(Ts_{sim,i} - Ts_{obs,i})^2}{p-m}}} \quad (4.2)$$

where, m is the number of parameters in the model. The effect of m in equation (3.7) is negligible when p is large as in this study.

4.3.4 Stream temperature prediction for Tributaries without observed stream temperature:

South Fork Boise River tributaries Dixie, Cow, Granite and Pierce Creeks have stream water temperature gauge stations. To estimate stream water temperature of ungauged tributaries, it was assumed that those tributaries stream water temperatures are similar to each other and follow similar patterns of gauged tributaries near closed to them. Observed water temperatures at Dixie, Cow, Granite and Pierce Creeks explain that this is a justifiable assumption (Figure 4.5). Therefore, calculated posterior distributions from these four tributaries are assumed be applicable to any ungauged tributaries closed to them. To evaluate this method, posterior distributions computed for Dixie Creek were used to estimate stream water temperature at Pierce Creek. As shown in Figure 4.5, the highest discrepancy in stream water temperature of these four tributaries is related to Dixie Creek and Pierce Creek. Therefore, if stream water temperature at Pierce Creek is well predicted by posterior distributions computed from Dixie Creek, this prediction method can be applied for other tributaries as well.

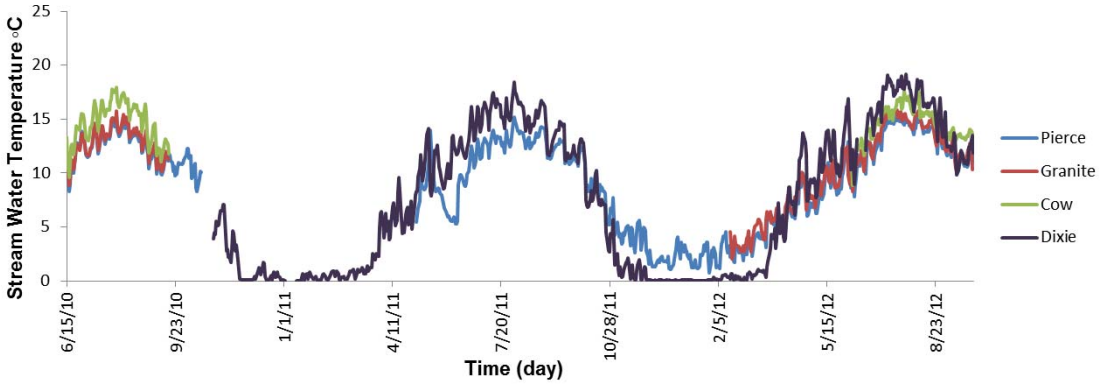

Figure 4.5: Observed stream water temperature at Dixie, Cow, Granite and Pierce creeks.

4.3.5 Role of discharge

Discharge measurements were available only at 11 (T1, T4, T7, T10, CT1, CT3, CT4, CT5, CT6, CT7 and CT8) of the 42 stations considered in the study. At these stations, mean daily stream water temperatures were estimated using both air temperature and discharge as inputs (Ta-Q model) and also using Ta model. Comparison between Ta-Q and Ta models allowed us to quantify the effect of discharge on model performance. Out of these 11 stations, 3

stations are regulated (CT1, CT3 and CT6), 2 stations (CT7 and CT8) are located at rain-dominated basins and 6 stations (T1, T4, T7, T10, CT4 and CT5) are located at snow-dominated basins.

4.3.6 Effect of inclusion of the autoregressive component

The most important effect of the autoregressive component is to prevent unrealistically rapid changes in the estimated stream water temperatures due to sudden changes in air temperatures. The effect of the autoregressive component was evaluated by comparing estimated stream water temperatures from Ta model with and without the autoregressive component.

4.3.7 Historical reconstruction

We tested the capability of the model to predict historical stream water temperatures for periods that may also have different hydrological conditions (e.g. dry or wet) from those of the calibration period. We performed this analysis using data from station D2, because at this station stream water temperature and discharge were available for two different hydrological conditions. The April 1963- September 1965 period coincides with an exceptionally wet period, whereas the April 1978- October 1979 period is representative of an averaged year with precipitation close to the long-term mean (Sohrabi *et al.*, 2013; Sohrabi *et al.*, 2015). We calibrated the Ta-Q model for the 1978-1979 period and compared its predictions with the 1963-1965 temperature records.

4.3.8 Comparison to the Modified Mohseni Model

SWTM performance for both Ta and Ta-Q versions was compared to that of the Mohseni model. We used the modified Mohseni model (2011) that uses mean daily air temperature and discharge to estimate mean daily stream temperature. Ta-Q model was used at the 11 sites that recorded discharge, and Ta model was used for the remaining sites with only air temperature measurements.

4.4 *Results*

4.4.1 Model evaluation

The NSC and RMSE values indicated that the Ta model performed well at unregulated streams but substantially worse at regulated streams. The 2-year RMSE and 2-year NSC, including both calibration and validation periods, ranged from 0.87 ˚C (at T15) to 2.5 ˚C (at CT5) and from 0.63 (at CT1 and CT3) to 0.97 (at CT6, CT7 and CT8; Figure 4.6), respectively. The largest RMSE was related to site CT5, which was located in a snow-dominated basin. Large errors were observed from May through August, the period when the contribution of snow melt to discharge substantially affects stream water temperatures. Across all sites the highest errors occurred in May (Figure 4.8), the month during which snowmelt makes the largest contribution to stream discharge (unlike the Ta-Q model, the Ta model does not account for the effect of discharge). The second highest RMSE (2.1 ˚C) was related to CT2 (Figure 4.6 and Figure 4.7 a), which is 0.32 km downstream from a dam. Site CT6, located 0.48 km downstream from a dam, had the highest NSC and a RMSE of 1.59 ˚C (Figure 4.6 and Figure 4.7 b). The RMSE was relatively low (1.1- 1.19 ˚C) during July and August (Figure 4.8), indicating good model performance during the warmest part of the year, which is particularly important for many aquatic habitat and water quality applications.

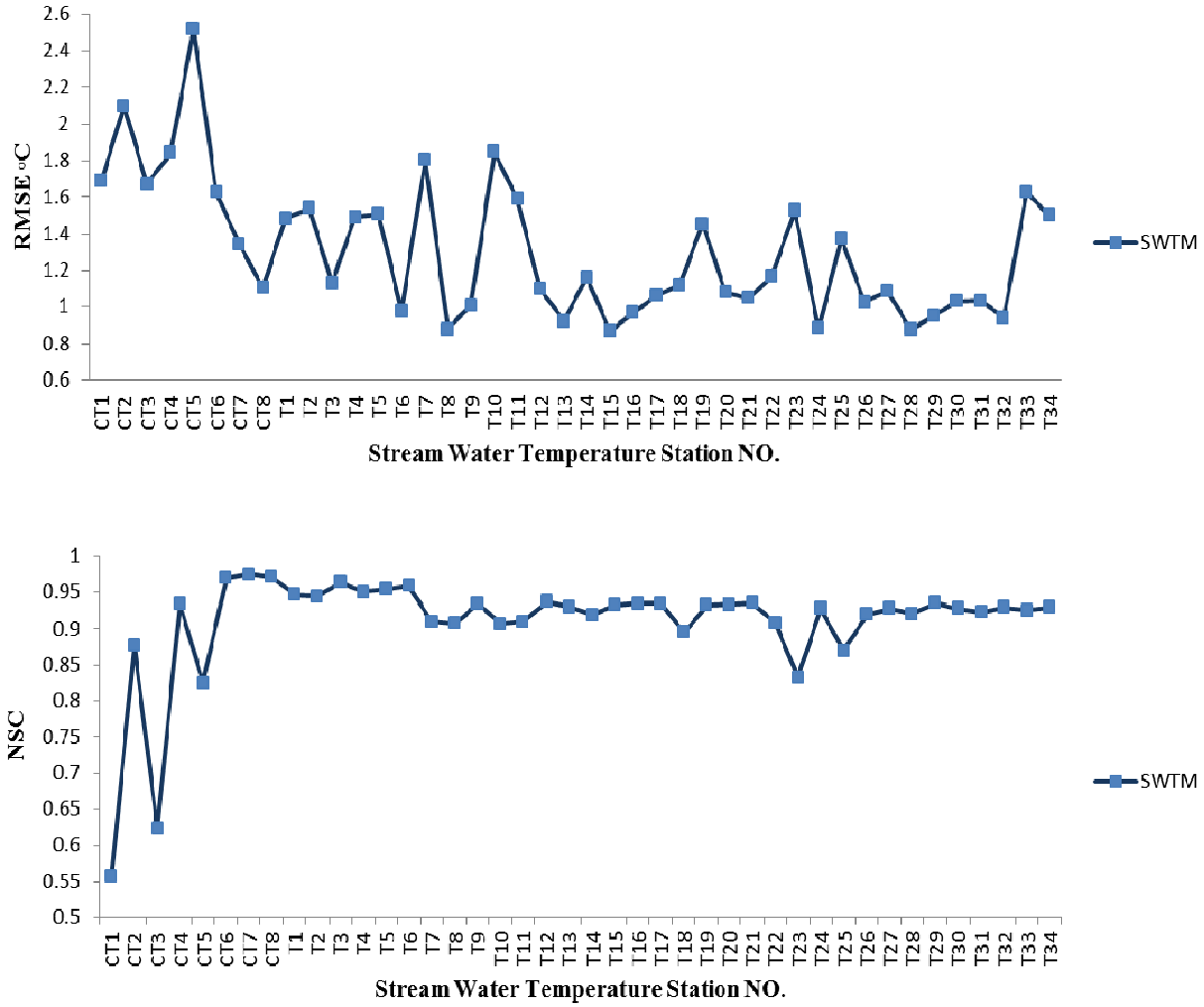

Figure 4.6. RMSE and NSC, including both calibration and validation periods, of Ta model.

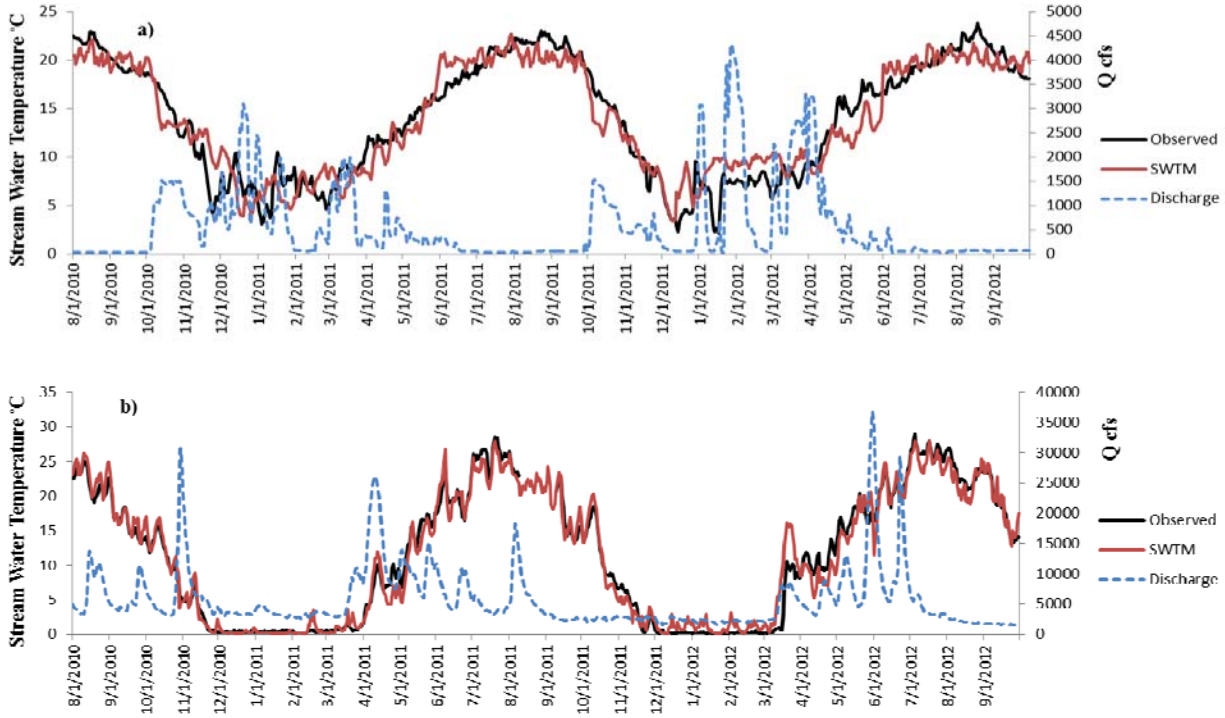

Figure 4.7. Simulated and observed daily stream water temperatures and discharge at CT2 (a) and CT6 (b) stations.

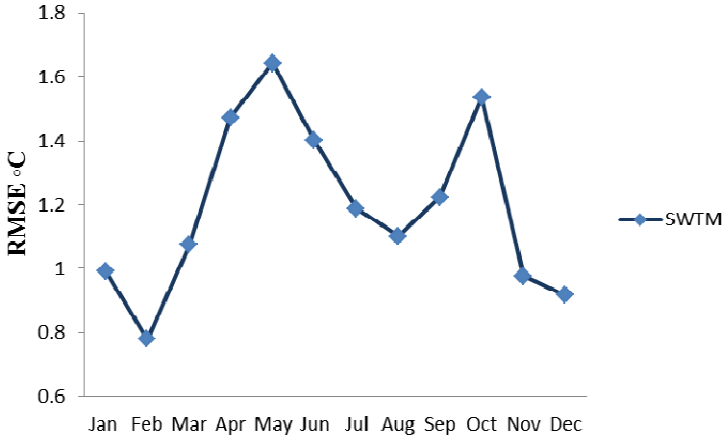

Figure 4.8. Average RMSE of Ta model for each month.

4.4.2 Stream temperature prediction

Four stream water temperature gauge stations at Boise River including one station located at North Fork (Grimes Creek), one station at Middle Fork (MF) and two stations at South Fork (SF) (one located downstream of Anderson Ranch Dam, Dixie Creek, and one located upstream of Anderson Ranch Dam) (Table 4.2) were used.

Table 4.2: Detailed information of water temperature gauge stations.

Station NO.	Stream	Latitude	Longitude	Study Period	Elevation (m)
T1	Dixie creek	43.34	-115.48	11/10 through 09/12	1171
T2	Grimes Creek	43.74	-115.96	08/10 through 08/12	1032
T3	MF Boise River	*43.70*	-115.66	08/10 through 08/12	1048
T4	SF Boise River	43.48	-115.31	08/10 through 08/12	1281

Figure 4.9 shows RMSE and NSC of the SWTM and Mohseni et al. model. The SWTM has considerable better performance in comparison to Mohseni et al. (1998) model. Furthermore, the developed model estimates stream water temperature at daily resolution, while temporal resolution of Mohseni et al. (1998) model is weekly.

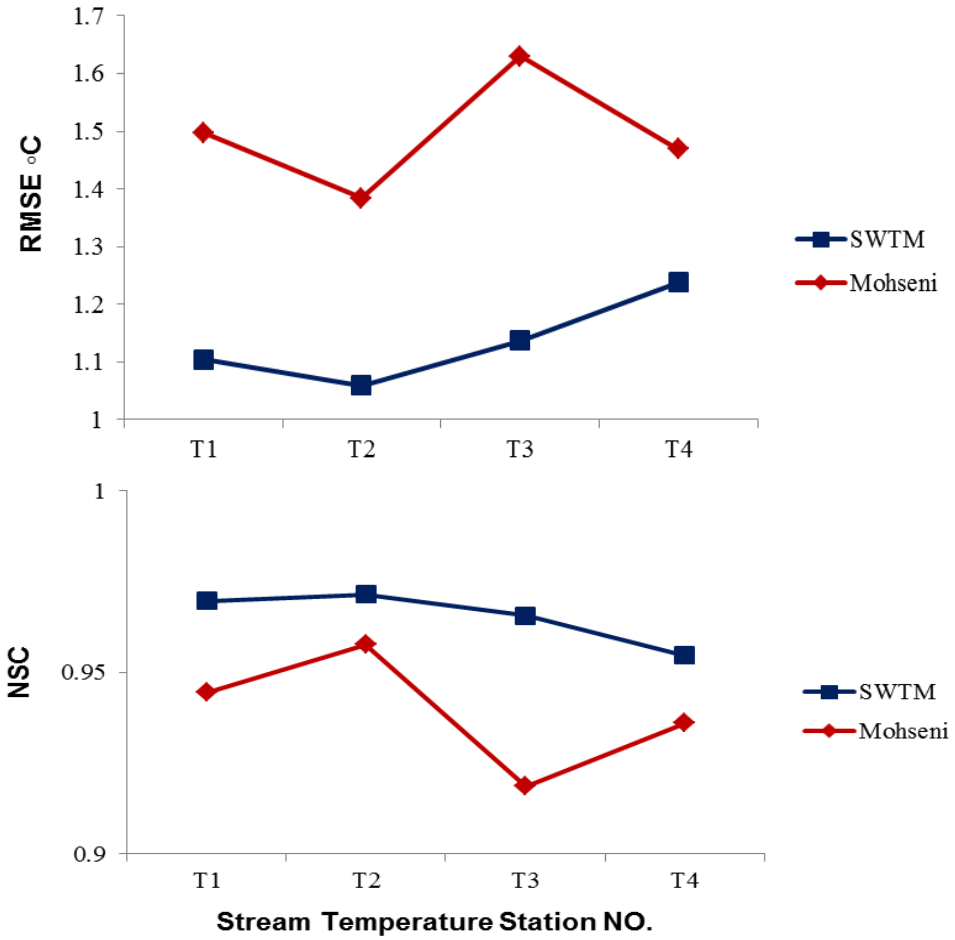

Figure 4.9: RMSE and NSC at four stations at Boise River Basin.

Figure 4.10 shows prediction of stream water temperature at Pierce Creek by using posterior distributions calculated from Dixie Creek. RMSE of the prediction is 2˚C, which explains acceptable daily prediction of stream water temperature at Pierce Creek.

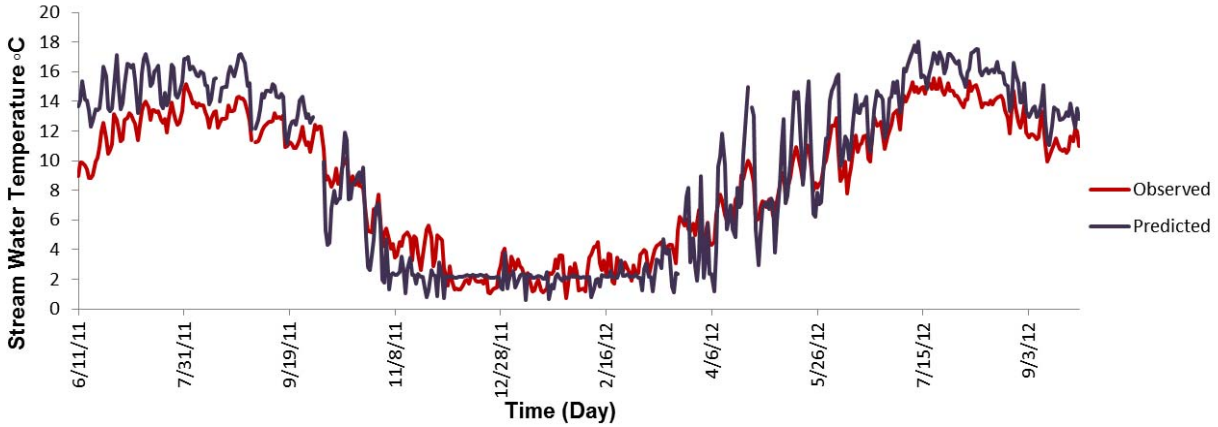

Figure 4.10: Predicted water stream temperature at Pierce Creek by using posterior distributions calculated from Dixie Creek.

4.4.3 Role of discharge

Stream discharge as an additional input variable had negligible influence on model performance for streams in rain-dominated basins and those with regulated flows. However, it significantly enhanced model performance for most snow-dominated streams (except T1; Figure 4.11) for the months between April through August, the period when discharge is dominated by snowmelt (Figure 4.12). The largest difference (RMSE) in performance between Ta and Ta-Q models was in June (1.5˚C), when snowmelt had the highest contribution to discharge (Figure 4.13). Performance of the Ta model was slightly better than that of Ta-Q model in March. For other months beside outside of the April to August period, the Ta-Q model was only modestly better (< 0.1˚C in RMSE) than the Ta model.

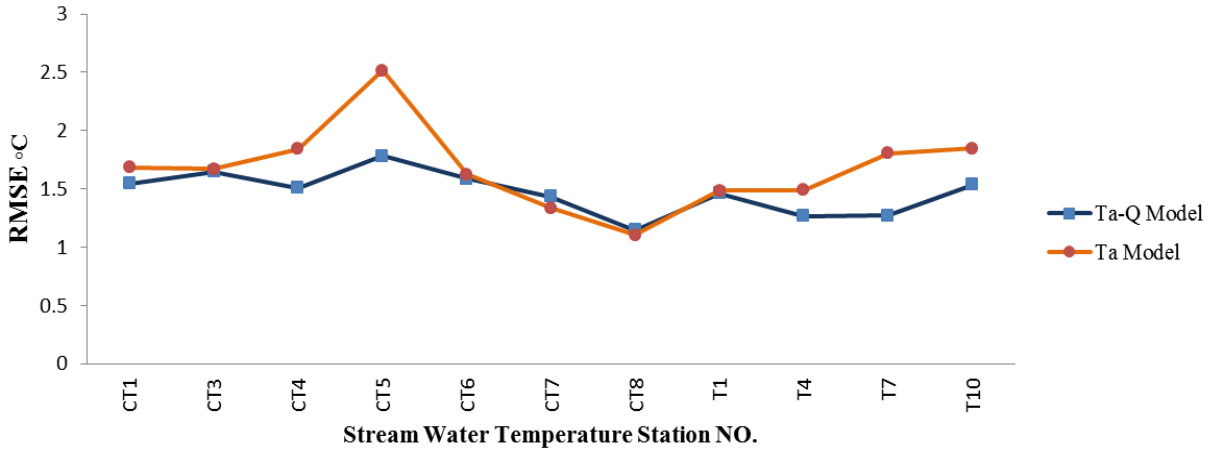

Figure 4.11. Changes in the RMSE of SWTM by adding discharge.

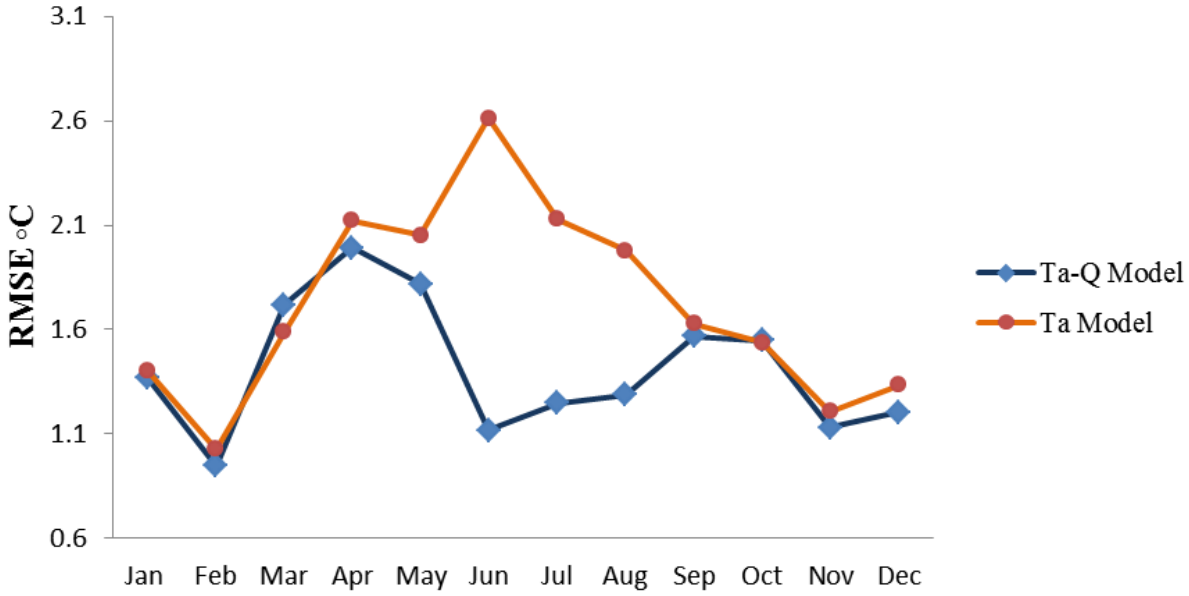

Figure 4.12. Changes in the RMSE of SWTM by adding discharge as a predictor at a monthly scale.

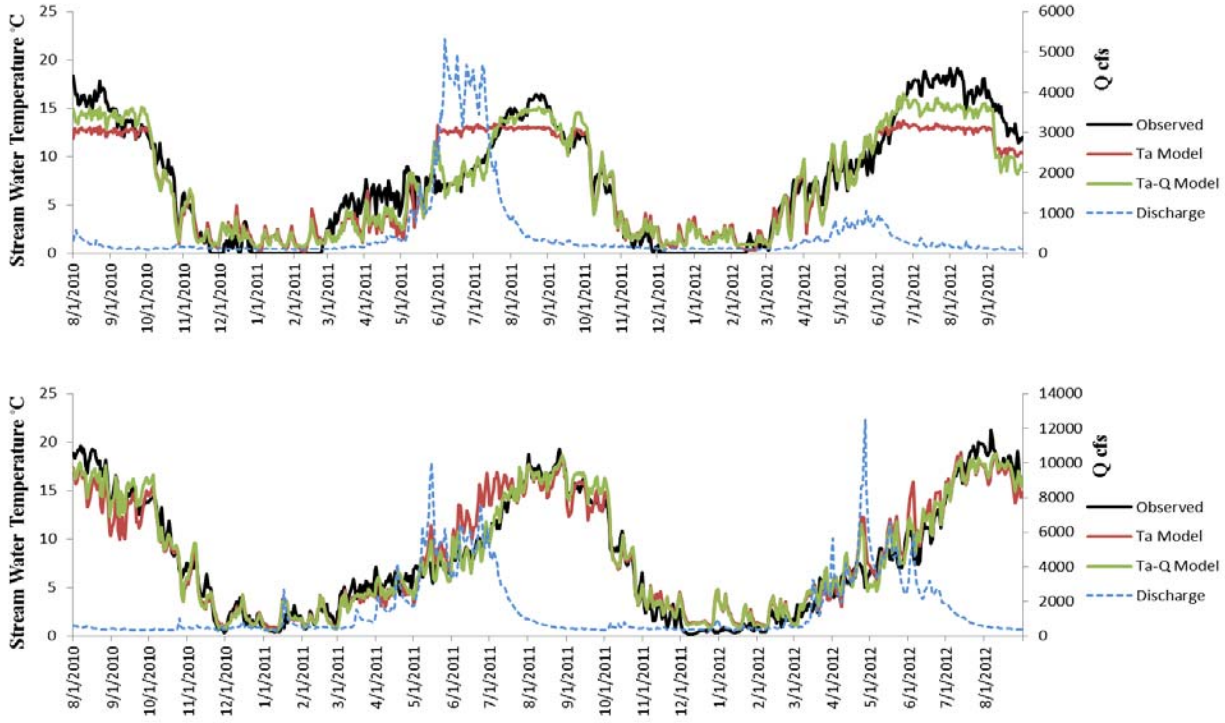

Figure 4.13. Time series of simulated and observed daily stream water temperatures at CT5 (the top figure) and T7 (the bottom figure) stations, respectively.

4.4.4 Effect of inclusion of the autoregressive component

Our analysis shows that the autoregressive component may have different effects on model performance when daily stream water temperatures are modeled at short (weekly) or long (yearly) time scale analysis. The autoregressive component has an important effect on predicting daily stream water temperatures within short temporal windows (weekly time scale analysis) as shown from fall to spring when sudden changes in temperature occur on a single day (Figure 4.14; the top figure) regardless of watershed size. However, at large time scales (monthly or yearly time scale) the autoregressive component increases model performance only in streams with a drainage area >100 km^2; its effect is negligible in streams <50 km^2 drainage area. On average RMSE was increased by 0.21˚C in large streams due to neglecting the autoregressive component, whereas on average only a 0.06˚C increase in RMSE was observed in small streams. The largest increase in RMSE (increase of 1.14˚C) was observed at CT7 site, which was the largest unregulated stream among the study sites (Figure 4.14; the bottom figure).

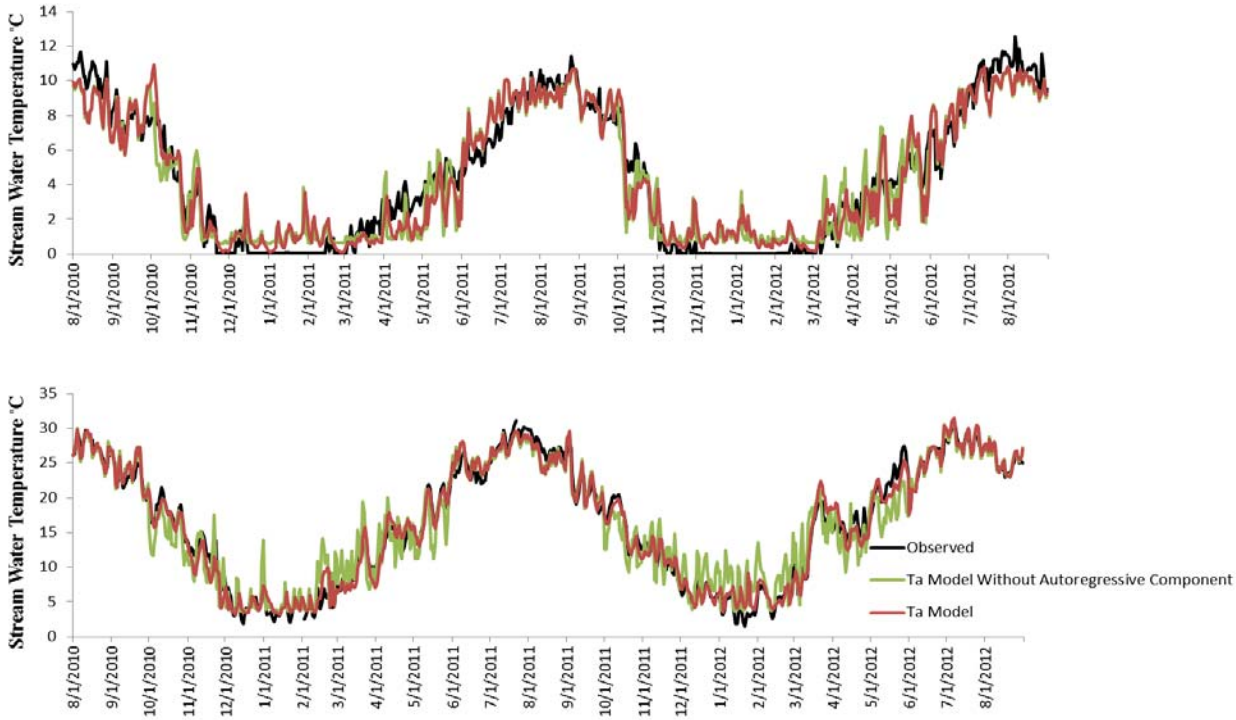

Figure 4.14. Effect of disregarding autoregressive component at T22 (the top figure) and CT7 (the bottom figure). Red line indicates estimated stream water temperatures from Ta model. Green line shows estimated stream water temperatures from Ta model without autoregressive component.

4.4.5 Historical reconstruction

SWTM predicted stream water temperature reasonably well (RMSE of 1.55°C) for the 2-year validation period at station D2, in spite of different climatic and hydrological conditions between the calibration and validation periods (Figure 4.15). SWTM extensively underestimated stream water temperature for only five days (mid-June 1965) (Figure 4.15). During those five days, air temperatures dropped from 21.5°C to 11.5°C and discharges increased significantly due to an exceptional summer rainfall event (40 mm in 5 days).

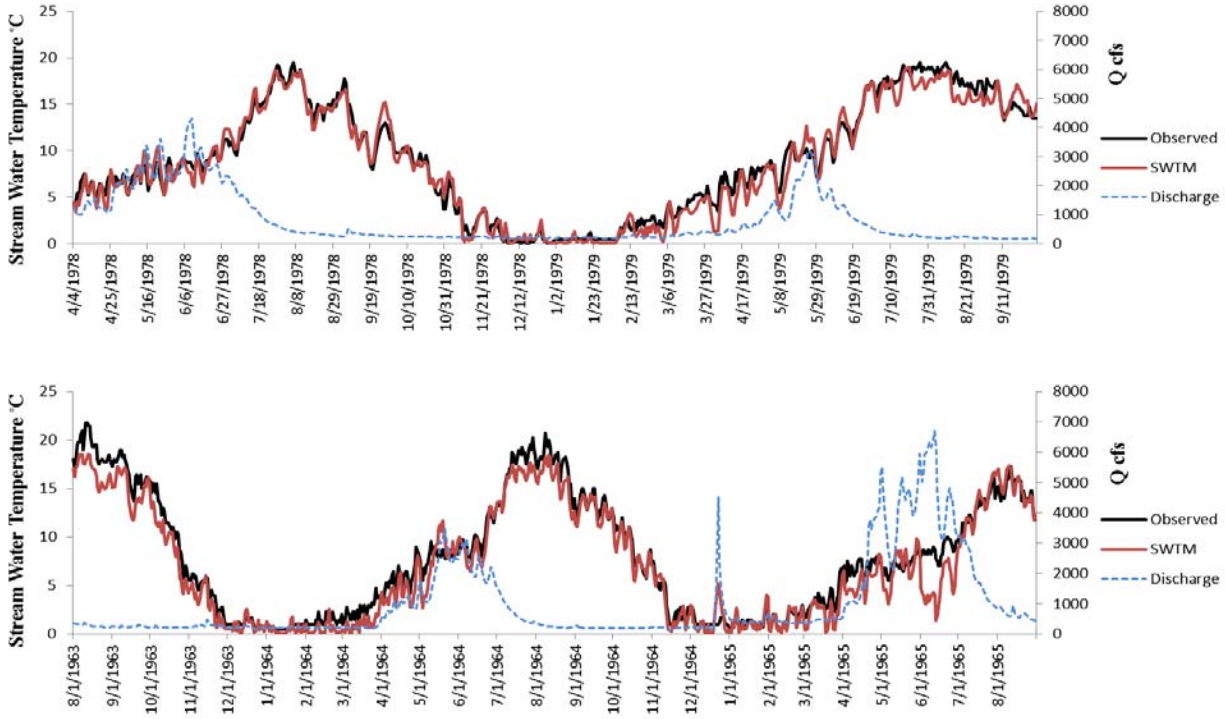

Figure 4.15. Hindcast of daily stream water temperature (Ta-Q model) for the period with different hydrological conditions from the calibration period at station D2. The top figure indicates calibration period (average year) and the bottom figure shows validation period (wet year).

4.4.6 Comparison to the modified Mohseni model

Performance of SWTM exceeded that of the modified Mohseni model (Figure 4.16). Average RMSE and NSC of SWTM were 1.25 ˚C and 0.91, respectively, whereas average RMSE and NSC of the modified Mohseni model were 1.68 ˚C and 0.86, respectively. Performance differences were most pronounced at stations with discharge measurements (T1, T4, T7, T10, CT4, CT5, CT7 and CT8). For these stations, SWTM had an average RMSE of 1.43 ˚C, compared to 2.24 ˚C, for the modified Mohseni model. The largest difference was observed at CT5 (Figure 4.17), in which RMSE and NSC of SWTM was 1.43 ˚C lower and 0.2 larger, respectively, than that of the modified Mohseni model. SWTM also performed better than the Mohseni model on regulated streams (Figure 4.16), with RMSE of 1.72 ˚C compare to 2.31 ˚C for the modified Mohseni model.

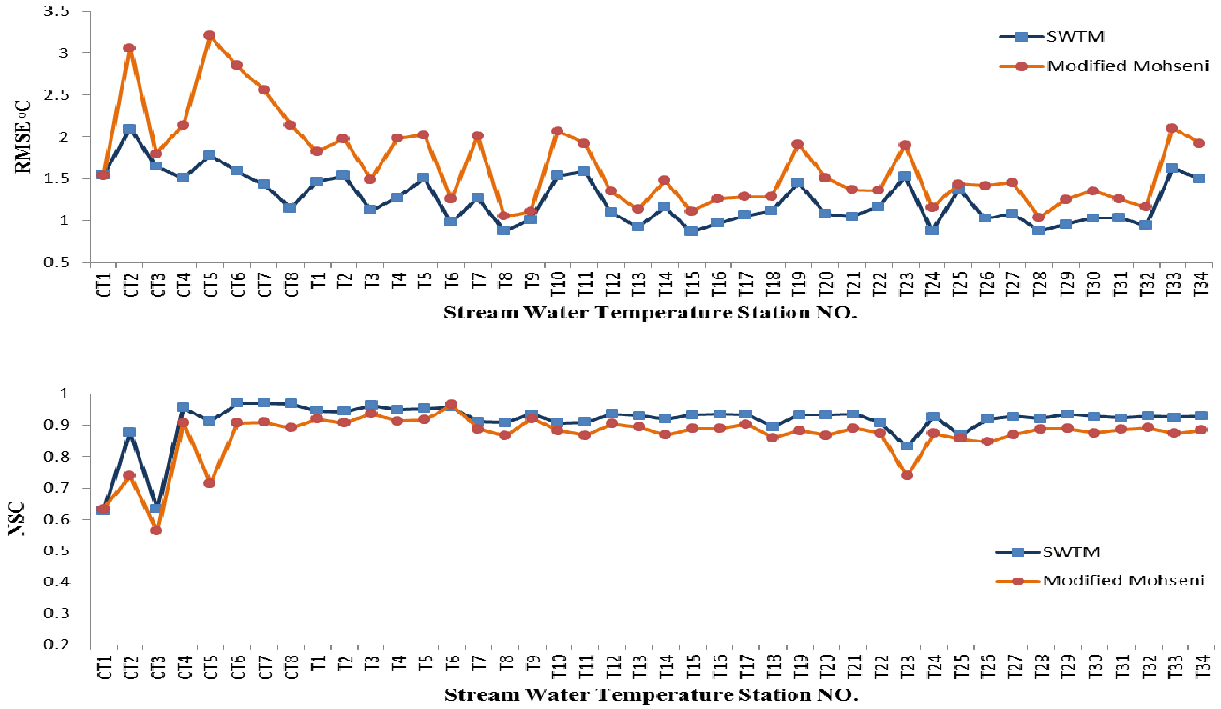

Figure 4.16. Comparison of daily stream water temperature predicted with the modified Mohseni and SWTM.

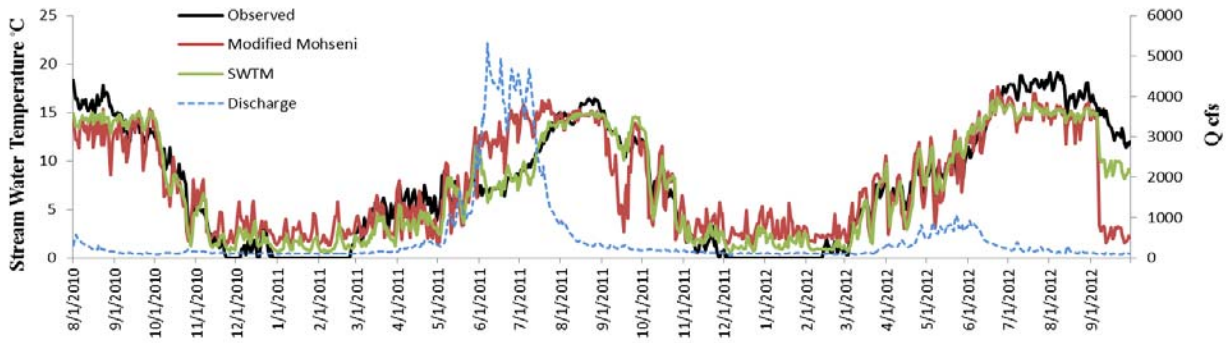

Figure 4.17. Comparison between generated daily stream temperatures from SWTM and the modified Mohseni model at CT5, a snow dominated basin.

4.5 *Discussion*

The performance of SWTM was good with average RMSE and NSC of 1.25°C and 0.91, respectively, over the study sites. Comparing these RMSE and NSC values to those of reported in the literature indicates robust performance of SWTM. Ficklin et al. (2012) reported average NSC of 0.82 and mean error of 0.66°C, and Vliet et al. (2011) reported average RMSE and NSC of 2.26°C and 0.85, respectively, for estimation of mean daily stream temperatures. Mohseni et

al. (1998) demonstrated average RMSE and NSC of 1.64°C and 0.93, respectively, for estimation of weekly stream temperature.

Available statistical stream temperature models have been rarely tested under a wide range of climate conditions. Most statistical models, such as those presented in the works of Caissie et al. (2001), Webb et al. (2003), Ahmadi-Nedushan et al. (2007) and Caldwell et al. (2013), were tested at one watershed and within one climate zone. Conversely, the Mohseni model was tested for regulated and unregulated streams under a wide range of climate and hydrologic conditions. However, it performed poorly in regions where the difference between maximum and minimum weekly averaged stream water temperature was low (Mohseni *et al.*, 1998; Benyahya *et al.*, 2007), as for instance our study site CT3, where the Mohseni model had a NSC value of 0.56, compared to SWTM with NSC of 0.63. Its performance was also low in snow dominated watersheds, where discharge variation had a pronounced effect on summer stream water temperature (Luce et al., 2014).

Our results indicate robust performance of SWTM across a range of climate and hydrologic conditions. Because SWTM tracks changes in the independent variables rather than depending on the difference between maximum and minimum values of stream water temperature, its performance is similar in different climate and hydrologic conditions. On the other hand, seasonality influences the hysteresis between air and water temperatures (Webb and Nobilis, 1997; Langan *et al.*, 2001; Benyahya *et al.*, 2007). Our model is separately fitted for cold and warm seasons to minimize the effect of seasonality. The autoregressive structure is another important feature of SWTM, because it prevents fluctuations in daily air temperatures from overly influencing daily stream water temperature estimations. Similar to Webb et al. (2003), our results indicated that inclusion of the autoregressive component is critical in large streams. These streams can absorb large amounts of heat with negligible change in their temperature because their large water volume provides high thermal capacity inertia. This causes hysteresis in the air-water temperature relationship and lowers the correlation between air and water temperatures.

Similarly to previous studies (Bogan *et al.*, 2003; Neumann *et al.*, 2003; Webb *et al.*, 2003; Ahmadi-Nedushan *et al.*, 2007), our analyses show that air temperature is the primary predictor for estimating stream water temperature for most hydrological settings. Consistent with the findings of Webb et al. (2003), our model shows that discharge is a secondary factor in predicting stream water temperatures in rain-dominated basins and those with regulated flows. Ahmadi-Nedushan et al. (2007) reported that discharge has a secondary impact in snow-dominated streams as well. However, our analyses indicate that stream discharge is a major hydrologic driver for unregulated streams in snow-dominated basins with a large drainage area, particularly during the spring-summer period from April through August. Ahmadi-Nedushan et al. (2007) used flow-derived variables, i.e. minimum and maximum flow of 3-, 5- and 7-day periods, rather than discharge measurements as independent variables. The disagreement between results of this work and those of Ahmadi-Nedushan et al. (2007) might be due to the difference in accounting for flow information. Our results indicate that the largest difference between the performance of Ta and Ta-Q models occurs in June. In this month, air temperature substantially increases but stream discharge also increases due to snowmelt. The latter contribution prevents stream water temperatures from increasing rapidly following the air temperature trend, which causes the Ta model to over-predict stream water temperature. An increase in a stream discharge increases thermal capacity and decreases travel time which in turn leads to less sensitivity of water temperature to air temperature, which is a surrogate for net heat exchanges at the air-water interface (Webb et al., 2003). In addition, when the source of discharge is cold water from snow melt, it causes hysteresis in the air-water temperature relationship (Mohseni *et al.*, 1998; Mantua *et al.*, 2010). The results suggest that the performance of Ta-Q over Ta decreases with smaller contributing drainage area, because discharge typically decreases with drainage area.

Statistical stream water temperature models such as SWTM may have some limitations when applied to time series far from the calibration period. For example, SWTM does not consider impacts of possible changes in vegetation on stream water temperatures. Shading influences sensible and latent heat fluxes, particularly in summer (Bogan et al., 2003). Furthermore, in groundwater dominated streams, particularly when there is considerable hyporheic exchange close to a stream temperature sensor, differences in hydrological conditions

of calibration and validation periods, i.e. dry or wet conditions, may results in large errors due to changes in magnitude of the interactions between surface and subsurface waters (Bogan et al., 2003). These two limitations can be solved by using equilibrium temperature as a predictor instead of air temperature. Equilibrium temperature is defined as the temperature that a water body can have when the integral of the heat fluxes across the air-water interface is zero (Bogan et al., 2003). Equilibrium temperature can be calculated using weather data including air temperature, dew point temperature, precipitation, solar radiation, sky cover, and wind speed. Bogan et al. (2003) found a linear relationship between equilibrium temperature above 0°C and stream water temperature. In streams where stream water temperatures follow heat exchanges at the air-water interface and are minimally affected by shading and groundwater exchanges, stream water temperature should be approximately equal to equilibrium temperature (roughly a 1:1 relationship (Bogan et al., 2003)). However, in streams where water temperatures are substantially influenced by groundwater exchanges or shading, for example, equilibrium temperatures are considerably lower or higher than stream water temperatures during winter and summer, respectively. In these streams, the relationship between equilibrium temperature and stream water temperature substantially deviates from the 1:1 relationship, but equilibrium temperatures can be adjusted to consider impact of shading and groundwater. To account for effect of shading and groundwater, which are not considered in equilibrium temperature calculation, on stream water temperature, a slope and intercept are calculated for the linear relationship between equilibrium temperature and stream water temperature to minimize their difference. (Bogan et al., 2003).

Model accuracy decreases in predicting stream water temperatures downstream of large reservoirs. The lower performance is mostly due to the reservoir releases, particularly from the hypolimnion, rather than variations in heat flux at air-water interface (Sinokrot *et al.*, 1995; Lowney, 2000; Risley *et al.*, 2010; Null *et al.*, 2013). The downstream distance at which the influence of the reservoir becomes negligible depends on reservoir depth and size, outlet vertical location and discharge (Sinokrot *et al.*, 1995; Mohseni *et al.*, 1998). Sinokrot et al. (1995) reported that the impact of reservoir releases from the hypolimnion can persist as far as 48 km downstream from the dam depending on the magnitude of releases. However, water releases may also form a consistent temporally-gradually varying stream temperature pattern (Lowney, 2000),

which SWTM proved capable of capturing at CT6. Dam releases are high between mid-spring to mid-summer (Figure 6b) at CT6, mimicking the effect of high discharge of unregulated streams due to snow melt in snow dominated regions during the period of mid-spring to mid-summer on stream water temperature.

4.6 *Conclusions*

We found that the SWTM model provided daily stream water temperature predictions of good accuracy, with average RMSE and NSC of 1.25°C and 0.92, respectively. Monthly RMSE of SWTM and time series of simulated daily stream water temperatures indicate that SWTM is capable of predicting well during the warmest periods, which are critical for aquatic habitats (RMSE of August is 1.1°C). Our results indicate that discharge improves model performance in snow-dominated basins with large drainage areas similar to the South Fork Boise River. Similar to other statistical models, performance of SWTM may be influenced by regulated discharges. It assumes static influence of both riparian vegetation shading and groundwater contribution.

SWTM can be a useful tool to either reconstruct historical daily stream water temperatures or to project daily stream water temperatures under different climate change scenarios. Therefore, we used this model to predict tributary stream temperature of South Fork Boise River, which may influence water temperature of the main stem river. We used SWTM simulated stream temperature as incoming water temperature boundary condition in the hydrodynamic model of main stem South Fork Boise River to simulate spatially distributed water temperature. In situations where riparian vegetation or/and groundwater influence is expected to change, air temperature should be replaced with equilibrium temperature.

5 HYDROLOGICAL MODEL

5.1 *Introduction*

Discharge is one of the most important hydrologic variable as it indicates changes in hydrological, geological and climatological cycles over a watershed (Dingman and Bjerklie, 2006; Choo *et al.*, 2015). Accurate estimation of discharge is necessary for flood forecasting, water resource planning and management, reservoir operation, river restoration and ecological studies (Smith and Pavelsky, 2008; Smith et al., 2014). Availability of discharge estimations can improve prediction accuracy of stream water temperature (Vliet *et al.*, 2011; Luce *et al.*, 2014; Piccolroaz *et al.*, 2016), which is of high importance in ecological studies, restoration of rivers and aquatic habitat. Stream water temperature plays an important role in aquatic ecosystems and is an important cue for organism behavior (Rice *et al.*, 1983; Jobling, 1997; Rieman *et al.*, 2007; Isaak *et al.*, 2012), fish metabolism (Forseth and Jonsson, 1994; Railsback and Rose, 1999; Mesa *et al.*, 2013; Isaak *et al.*, 2015) and growth rates (Brett, 1979; Crozier et al., 2010; Xu et al., 2010). These indicate the value of accurate estimates of daily discharge and stream water temperatures for dam and water resource managers, ecologists, economists and decision makers.

Hydrologic models are sensitive to distribution of precipitation data (Ajami et al., 2004; Wang et al., 2015), this sensitivity varies from one watershed to another as catchments respond differently to a precipitation event (Segond *et al.*, 2007; Viglione *et al.*, 2010b; Choo *et al.*, 2015). Accurate discharge estimations for watersheds with complex topography and rugged terrain, which causes pronounced precipitation spatial disparity, have been suggested to depend strongly on accuracy and detailed spatial information of precipitation (Ahl et al., 2008; Viglione et al., 2010a). Several previous studies showed that the use of detailed spatial information of precipitation increases discharge prediction accuracy in such watersheds (Haddeland *et al.*, 2002; Ajami *et al.*, 2004; Smith *et al.*, 2004; Lobligeois *et al.*, 2014). Boyle et al. (2001) concluded that detailed spatial information of precipitation improves estimation of peak rather than base flow.

In addition to detailed spatial information of precipitation, distribution, timing and magnitude of surface water input (SWI), which is combination of snow melt, rain on snow and rain on bare ground, are necessary for hydrologic modeling in mountainous watersheds (Liston

and Elder, 2006; Ahl *et al.*, 2008; Weill *et al.*, 2013; Kormos *et al.*, 2014). In such watersheds, precipitation is accumulated as snow in winter and the accumulated water is released in spring and early summer. In these watersheds, not only precipitation, but also snow accumulation and ablation are highly heterogeneous due to changes of elevation, slope, aspect and vegetation over small distances (Elder *et al.*, 1991; Trujillo *et al.*, 2012; Marks *et al.*, 2013; Winstral *et al.*, 2013). This adds more complexity to hydrologic modeling of mountainous watersheds, where accurate estimation of snow accumulation and ablation is required for modeling in addition to hydro-meteorological and geological processes that are calculated for rain dominated watersheds (Winstral *et al.*, 2014; Toffolon and Piccolroaz, 2015; Chen *et al.*, 2016; Piccolroaz *et al.*, 2016).

Advances in numerical modeling and computational power of computers have increased application of integrated hydrologic modeling frameworks in mountainous watersheds, in which snow, streamflow and stream temperature models are coupled. Such frameworks help to link changes in meteorological variables with physical hydrologic processes (Null *et al.*, 2010; Merenlender and Matella, 2013). In this section, an integrated hydrologic modeling framework was developed to understand changes in response of hydrological processes with regard to changes in meteorological variables. Specifically, we focused on calibration and validation of integrated models.

5.2 *Method*

To route runoff from the watershed to tributary confluences and estimate daily mean streamflow, a process-based snow model, ISNOBAL, was coupled with Penn State Integrated Hydrology Model (PIHM). To do this distributed SWI generated from ISNOBAL was used instead of precipitation and the temperature index snowmelt tool in PIHM was switched off in the source code.

5.2.1 Description of snow Model: ISNOBAL

Snobal is a physics-based snow model that conserves both mass and energy at a point (Marks, 1988). Spatial (image) version of Snobal, ISNOBAL, developed by Marks et al. (1999), uses the same set of equations as Snobal to calculate mass and energy flux exchanges at each

grid cell. The model uses a two-layer representation of the snow cover with fixed-thickness top layer, the interface between air and snow, and the bottom layer having the rest of the snowpack. Calculation of water exchanges, such as evaporation, condensation and sublimation, are conducted in the top layer. However, computation of energy exchanges are performed at both layers at each time step for each grid cell with the following energy balance equation, (Marks *et al.*, 1999; Garen and Marks, 2005) :

$$\Delta Q = R_n + H + L_v E + G + M \tag{5.1}$$

where ΔQ (W m^{-2}) is the snow cover energy that depends on changes in net radiation (R_n), sensible heat (H), latent heat ($L_v E$), conduction (G) and advection (M) energies (all units of W m^{-2}). L_v (W m^{-2} kg^{-1}) indicates specific latent heat of water and E (kg) represents mass of water that has phase change. An increase in the snow cover energy causes a decrease in the cold content, which is energy required to bring the snow cover temperature to 0 °C. Melt is calculated at both layers and occurs once the cold content reaches 0 °C. Estimated melt in the model consists of both melt and rain on snow and it drains out when total liquid water content in snowpack is higher than a specified threshold. Melt that drains out is surface water input (SWI).

5.2.2 Forcing data and spatial distribution method

ISNOBAL was run for the entire Boise River Basin (BRB; upstream of Lucky Peak dam) for the selected climatic years: 2007 (dry), 2010 (average) and 2006 (wet). Thus, forcing data were collected and spatially distributed at spatial resolution of 50 m for entire BRB. Snow Water Input (SWI) was then extracted for the watershed of interest.

Forcing data: There are 18 stations in or near BRB that measure meteorological variables on hourly basis (Figure 5.1 and Table 5.1). Ten of these stations are operated by Natural Resources Conservation Service (NRCS; SNOTEL sites). The rest of the stations are either operated by Bureau of Land Management (BLM) and U.S. Department of Agriculture (USDA) Forrest Service (FS; 5 stations) or Bureau of reclamation (BR; 3 stations). Hourly precipitation (p) and temperature (t) are available at all the stations. Relative humidity (rh), solar radiation (sr) and wind (w) are measured in station numbers 5, 6 and 9, respectively (Table 5.1).

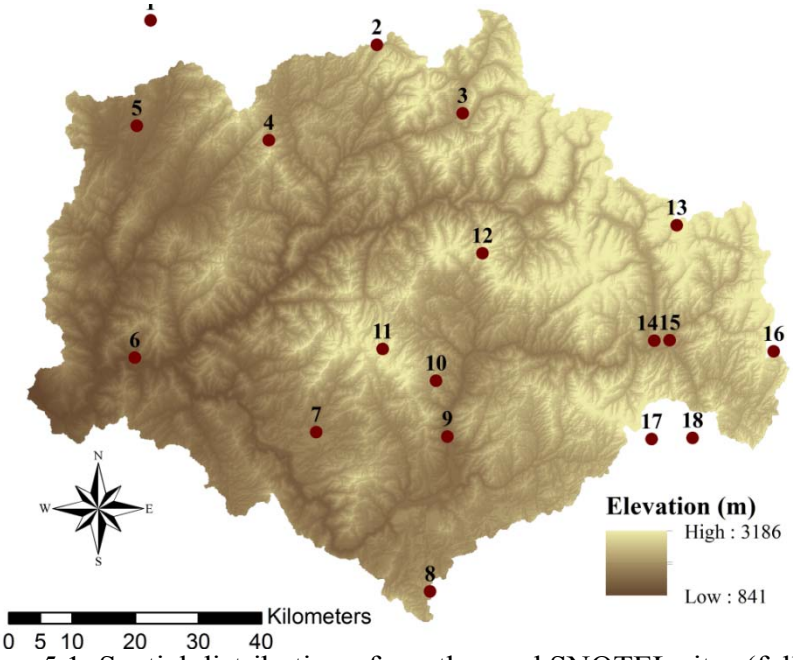

Figure 5.1: Spatial distribution of weather and SNOTEL sites (full circle).

Table 5.1: Detailed information of the stations.

NO.	Station Name	Latitude (Decimal ◦)	Longitude (Decimal ◦)	Elevation (m)	Variables Measured	Operated by
1	Little Anderson	44.09	-115.88	1389	p, t, rh, sr, w	BLM & FS
2	Jackson Peak	44.05	-115.44	2155	p, t, w, SWE	NRCS
3	Graham Guard STA.	43.95	-115.27	1734	p, t, w, SWE	NRCS
4	Mores Creek Summit	43.93	-115.67	1859	p, t, SWE	NRCS
5	Town Creek	43.94	-115.91	1415	p, t, rh, sr, w	BLM & FS
6	Arrowrock Dam	43.61	-115.92	998	p, t	BR
7	Prairie	43.5	-115.57	1463	p, t, SWE	NRCS
8	Camas Creek Divide	43.27	-115.35	1740	p, t, SWE	NRCS
9	South Fork Boise	43.49	-115.31	1286	p, t	BR
10	Wagontown	43.57	-115.33	1881	p, t, rh, sr, w	BLM & FS
11	Trinity Mountain	43.63	-115.44	2368	p, t, SWE	NRCS
12	Atlanta Summit	43.76	-115.24	2310	p, t, sr, w, SWE	NRCS
13	Vienna Mine	43.8	-114.85	2731	p, t, w, SWE	NRCS
14	Fleck Summit	43.62	-114.9	2164	p, t, rh, sr, w	BLM & FS
15	Big Smokey Ranger	43.62	-114.87	1706	p, t	BR
16	Dollarhide Summit	43.6	-114.67	2566	p, t, SWE	NRCS
17	Soldier Mountain Peak	43.48	-114.91	2904	p, t, rh, w	BLM & FS
18	Soldier R.S.	43.48	-114.83	1749	p, t, SWE	NRCS

Variable abbreviations: p, precipitation; t, air temperature; rh, relative humidity; sr, solar radiation; w, wind speed and direction; swe, snow water equivalent.
Abbreviations for institutes operate the stations: BLM & FS, Bureau of Land Management and U.S. Department of Agriculture (USDA) Forrest Service, respectively; NRCS, Natural Resources Conservation Service; BR, Bureau of reclamation.

Spatial distribution: ISNOBAL requires spatially distributed meteorological inputs, which are precipitation, air temperature, vapor pressure, solar and thermal radiation and wind speed. We distributed these inputs at 50 m spatial resolution. Spatially distributed data was obtained by interpolation using detrended elevation (vertical) and distance (horizontal) Kriging method (Garen and Marks, 2005). More details about the interpolation methodology for different meteorological variables are described below.

Air temperature-elevation trends were constrained to be zero or negative values, because air temperature decreases with increase in elevation. However, relative humidity-elevation trends were not constrained. The distributed relative humidity and air temperature were then used to compute dew point temperature and vapor pressure, which in turn was used to identify the precipitation phase and calculate latent heat flux exchanges from the snow cover, respectively (Garen and Marks, 2005).

Wind speed and direction were distributed using a detrended elevation and distance based Kriging method. Wind speed of a grid cell, then, was adjusted based on a wind factor calculated from two terrain parameters, maximum upwind slope (s_x) and upwind slope break (s_b). Detailed description of the wind distribution approach can be found in the literature (Winstral et al., 2002; Winstral and Marks, 2002; Winstral et al., 2009; Winstral et al., 2013), however, here the approach is explained in brief. Values of s_x and s_b were calculated for each cell, and for each wind direction. The s_x values are the maximum slope between the cell of interest and all cells in the upwind direction up to a user defined search distance (d_{max}). At topographically exposed cells, where s_x is negative, wind speed is increased due to vertical flow constriction (Winstral and Marks, 2002). In contrast, at topographically sheltered grid cells, where s_x is positive, wind speed is decreased due to expansion of flow (Winstral and Marks, 2002). The s_b parameter calculates upwind breaks in slope to identify flow separation zones, where there is no contact between airflow and the ground and downwind lee eddy is formed, which substantially reduces wind

speed (Winstral et al., 2013). The value of s_b is the difference between two s_x values, the local s_x minus outlying s_x, which are calculated using two different search distances. Local s_x is calculated using d_{max}, whereas outlying s_x is calculated using a distance quite larger than d_{max}. 100 and 1,000 m were used for local s_x and outlying s_x d_{max} values, respectively, which were suggested and used in the literature (Winstral et al., 2002; Winstral and Marks, 2002; Winstral et al., 2009; Winstral et al., 2013).

Precipitation was distributed analogous to wind speeds. Precipitation was first distributed using a detrended elevation and distance based Kriging method with precipitation-elevation trends that were constrained to be zero or positive, because precipitation increases with elevation (Garen and Marks, 2005). Next, at each grid cell, wind-induced snow redistribution was calculated using a snow drift factor that was computed based on s_b and wind speed (Winstral et al., 2002; Winstral et al., 2013; Winstral et al., 2014). Snow erosion occurred at cells where wind speed was high and s_b was negative. The transported snow particles from eroded cells were, then, deposited at cells where wind speed was substantially low, such as cells with large s_b. This precipitation distribution approach has been previously used in several studies (Winstral and Marks, 2002; Winstral et al., 2013; Winstral et al., 2014).

Solar radiation was distributed and corrected to account for variations in solar angle, shading, vegetation, and albedo (Link and Marks, 1999; Susong et al., 1999). Snow albedo was adjusted with snow age to consider the influence of dust and organic debris exposure (Garen and Marks, 2005). Distributed thermal radiation was first calculated for clear sky based on temperature, vapor pressure, elevation and sky view factor. Calculated thermal radiation was then adjusted for cloud cover and vegetation (Link and Marks, 1999).

5.2.3 Pre-calibration analyses

To understand the watershed characteristics, spatially averaged melt was first compared to measured discharge. Distributed melt data then divided into three elevation bands and four aspect bands (Tonina et al., 2008). These three elevation bands are shown in Table 5.2. The bands e1 and e3 include regions with elevation below and above one standard deviation from the mean elevation of the watershed, respectively. The band e2 consists of regions with elevations within

one standard deviation from the mean elevation of the watershed. Aspect bands are the 4 directions: North, East, South and West (Table 5.2 and Table 5.2: Elevation bands

	Elevation (m)		
Bands	e1	e2	e3
Featherville	< 1754	≥ 1754 and ≤ 2470	> 2470
Dixie	< 1450	≥ 1450 and ≤ 1550	> 1550
Pierce	< 1700	≥ 1700 and ≤ 1900	> 1900

Table 5.3). These analyses provide useful information about the watershed characteristics, such as timing and magnitude of groundwater contribution, which are very important for calibration.

Table 5.2: Elevation bands

	Elevation (m)		
Bands	e1	e2	e3
Featherville	< 1754	≥ 1754 and ≤ 2470	> 2470
Dixie	< 1450	≥ 1450 and ≤ 1550	> 1550
Pierce	< 1700	≥ 1700 and ≤ 1900	> 1900

Table 5.3: Aspect bands

Bands	Aspect (◦)
Northern (N)	≥ 315 or < 45
Western (W)	≥ 225 to < 315
Eastern (E)	≥ 45 to < 135
Southern (S)	≥ 135 to < 225

In water year (WY) 2013, October through May, there are four flood events including one rain on snow event and three melt events. Comparison of melt spatially averaged over the watershed of interest and streamflow provides insights on watershed responds to melt. Figure 5.2 indicates that several severe melt events occurred during fall and early winter, when discharge

changed slightly. In the spring, even a mild melt event led to a significant increase in discharge. This suggests that the watershed's groundwater is almost completely depleted during summers and fills during falls and winters. Therefore, during springs the watershed is saturated and despite of increase in evapotranspiration most of melt turns to runoff.

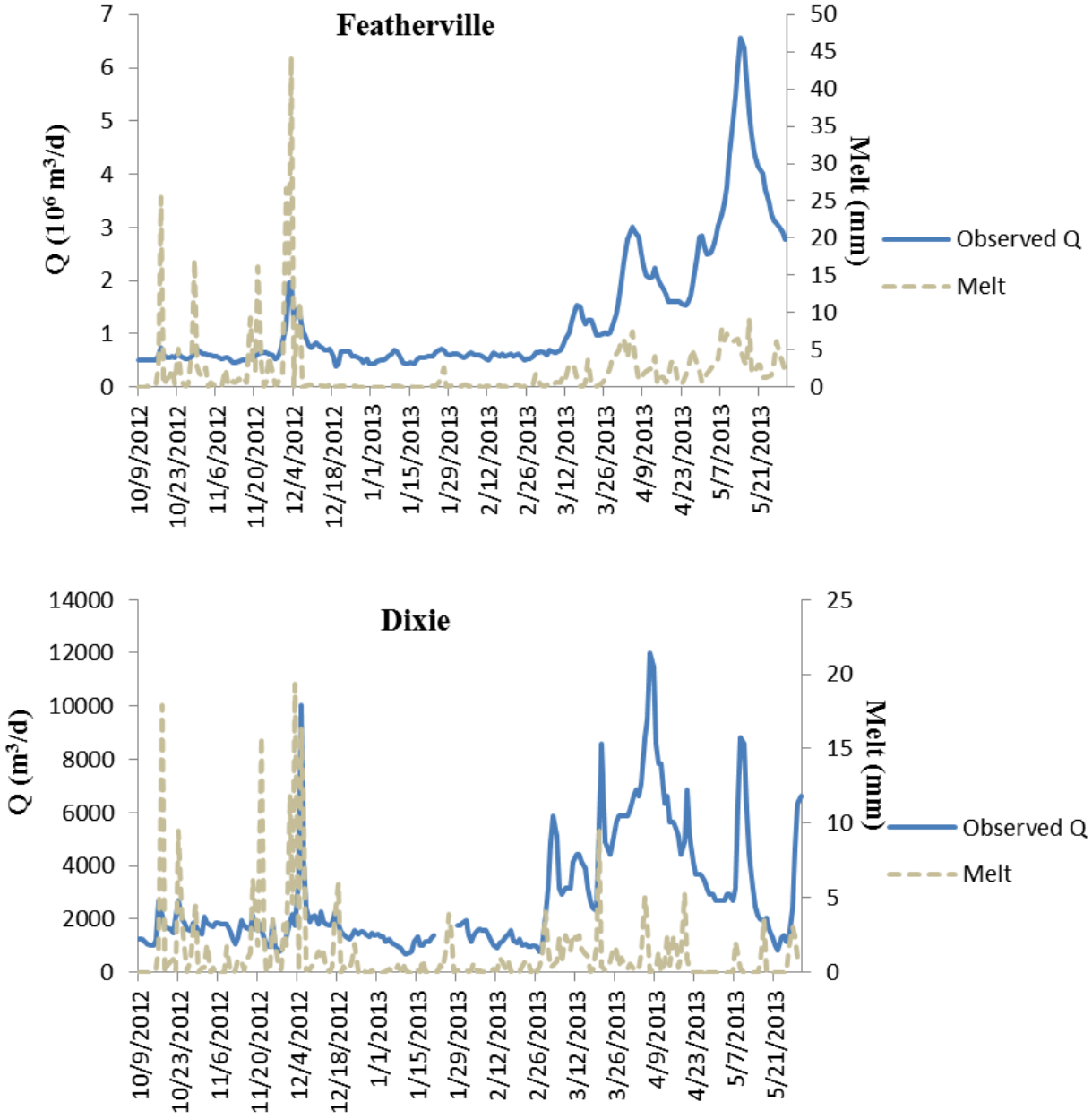

Figure 5.2: Comparison of spatially averaged melt and discharge at Featherville and Dixie gauge stations.

Moreover, this analysis shows that groundwater contribution is significant (approximately 50%) in generating April and May peaks, particularly the largest peak in Featherville. Melt related to elevation and aspect bands indicate effect of elevation and solar angle on melt (Figure 5.3). There is no significant difference in melt at different bands, except for melt events. In Featherville watershed, the largest discrepancy in melt between different bands occurred in May. However, difference between melt between different bands is in months of March and April for Dixie and Pierce watersheds, the largest, respectively. In Dixie and Pierce the highest melt occurred at N-e3 band, whereas it is related to N-e3 and E-e3 bands in Featherville.

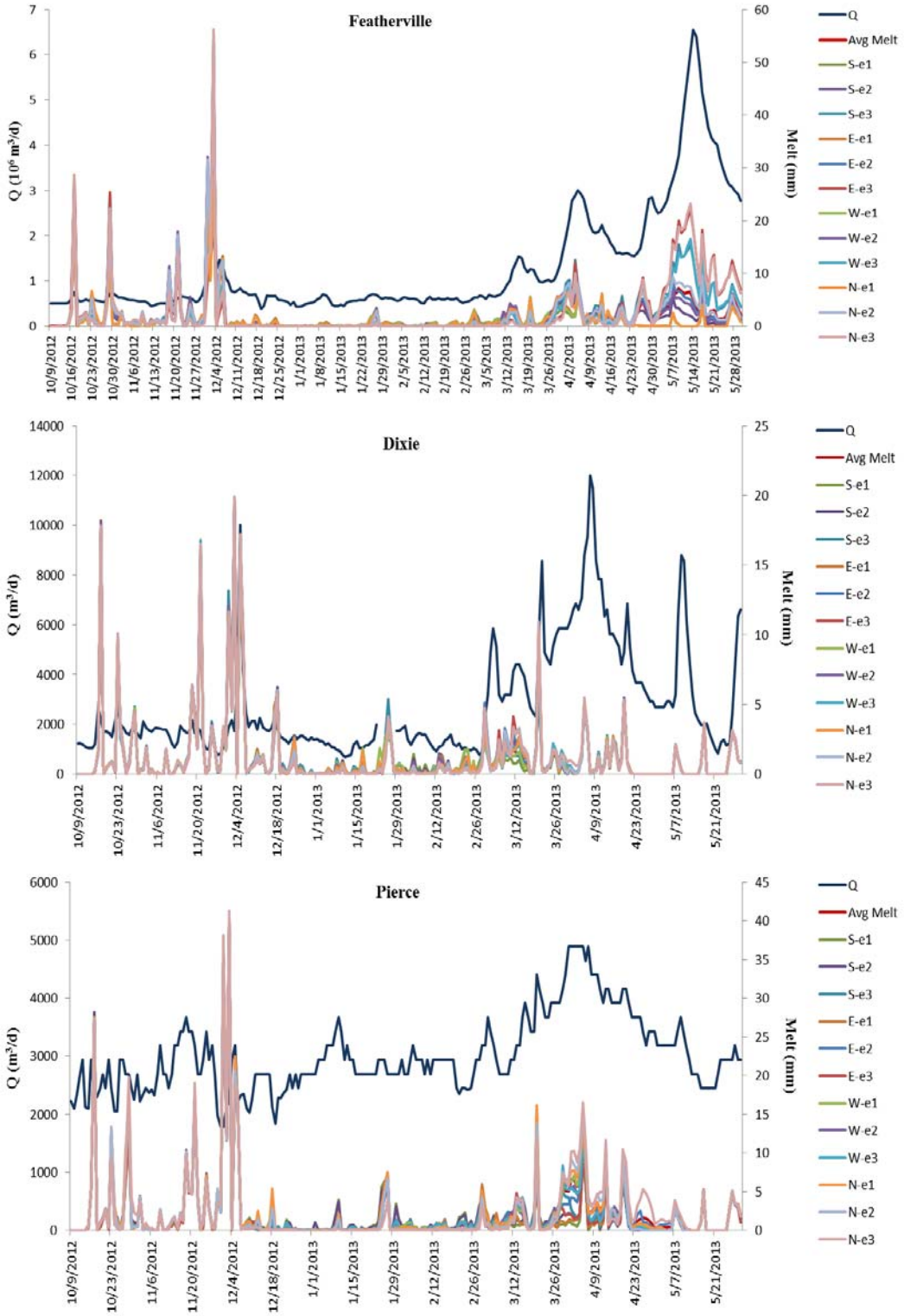

Figure 5.3: Melt partitioned with elevation and aspect bands. Note that Avg Melt shows spatially average melt over the watershed. The first letter of aspect-elevation name indicates the aspect band and letter "e" followed by a number the elevation band. For instance, S-e1 indicates melt in southern aspect and first elevation band.

The highest discharge peak occurred in May for Featherville, and in April for both Dixie and Pierce stations. There are irrigation diversions in Dixie starting in mid-April, thus no longer representative of unregulated discharge. Most of distributed melt is observed at April and May peaks (Figure 5.4). Most of snow is melted by the end of April for the area downstream of Anderson Ranch Dam. Therefore, high flows in the SFBR tributaries downstream from Anderson Ranch Dam are expected to occur in April. However, the peak discharge at the Featherville gauge occurs later due to higher elevation watershed in comparison to downstream of Anderson Ranch Dam.

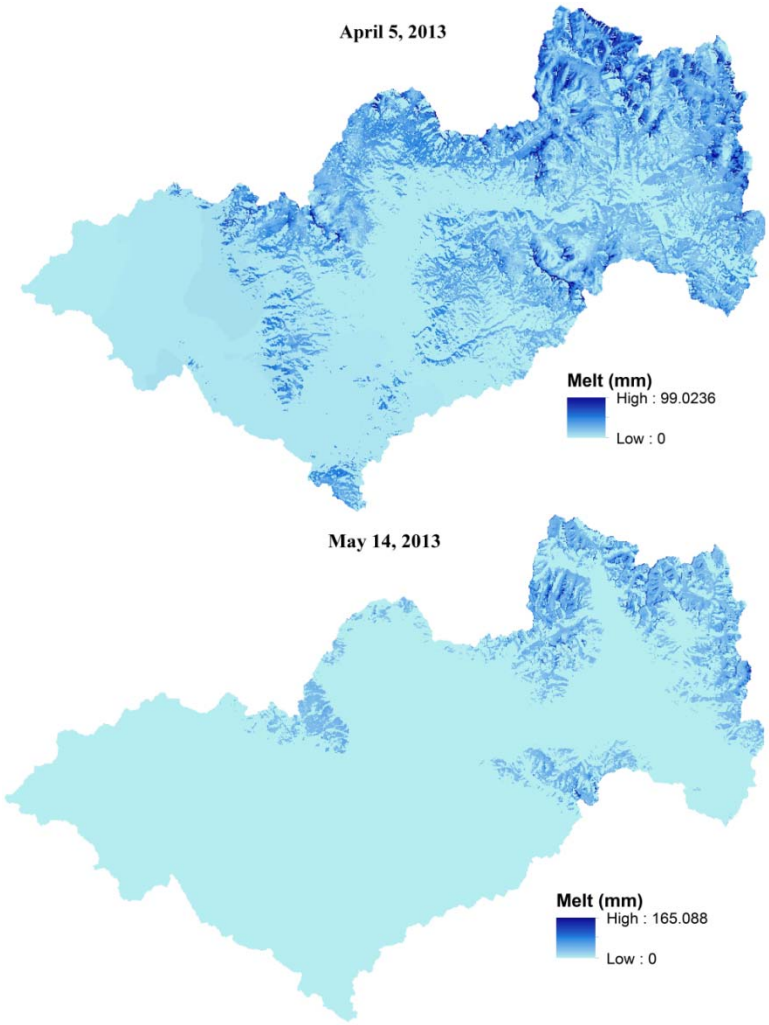

Figure 5.4: Spatial distribution of SWI for the April and May peak discharges over SFB watershed.

5.2.4 PIHM inputs

Forcing data: Forcing data for PIHM are air temperature, relative humidity, solar net radiation, wind speed, vapor pressure and SWI. SWI includes rain and snow melt generated using ISNOBAL at daily time steps. We used a spatial resolution of 250 m because of the large extend to the watershed. We were interested in daily discharge, thus streamflow was simulated at a daily basis.

River elements and meshes: Surface and subsurface soil, land cover, river elements, meshes and attribute for PIHM are generated in PIHMgis. PIHM employs D8 algorithm for routing and watershed identification (Tarboton, 1997). Based on a user defined number of grids river threshold, PIHMgis identifies rivers in a DEM. PIHMgis recognizes a grid as a river, if the number of grids that drain into the grid of interest is equal or greater than the river threshold. The river threshold is the minimum drainage area required to form a first order stream. The resulting river polyline can be unrealistically sinuous and thus it is simplified based on a user defined threshold, called simplification threshold. Larger simplification threshold filters more bends and leads to a river with smaller sinuosity.

PIHM runtime is highly dependent to number of cells forming the mesh or grid. The number of cells depends on the number of river elements and restriction options used for generating the mesh. The number of river elements depends strongly on river and simplification thresholds. For instance, larger river and simplification thresholds lead to small number of cells. However, unreasonable large river and simplification thresholds lead to the following inaccuracy and issue in streamflow simulation. Selecting a very large river threshold generates a river network that covers a very small area of the watershed. Therefore, during a rain or melt event, river network collects significantly smaller runoff than in the real river network and most of the rain or melt enters to the groundwater domain. Choosing a very large simplification threshold causes shift in river network from the original location. Thus, some of river elements might have higher elevation than that of cells located right and left sides of river element. Restriction options are available for generating meshes, such as minimum angle and maximum area of cells, which

allow generation of large cells at homogenous areas and small cells at locations with significant contribution in streamflow simulation (i.e., close to river elements).

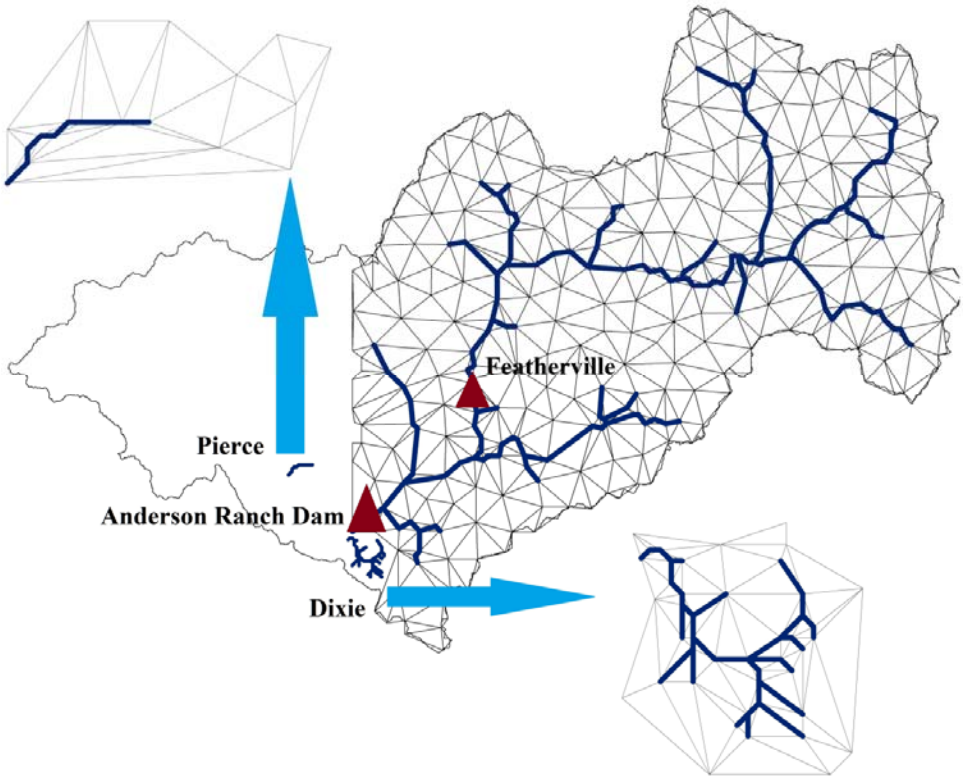

Figure 5.5: Generated river elements and meshes for the sub-basins of Pierce, Dixie, and South Fork of Boise River upstream of the Featherville gauge.

Drainage area of SFB is approximately 3,382 km^2 and drainage areas of tributaries located downstream of Anderson Ranch Dam is less than 26 km^2 (except three tributaries). If we want to generate a river network that includes SFB and all of its tributaries, we have to set a very small river threshold. Very small river threshold (e.g., 12), generates realistic river network density for small tributaries, such as Dixie, but that lead to a very dense river network and consequently very small cells in large watersheds, like the SFB above Featherville (Featherville). We tested a small river threshold for Featherville, which resulted in many very small cells. These cells drain water very slowly, that led to ponding in small cells and at some time steps numerical model could not converge. Due to different scope of SFB and its tributaries, we decided to run PIHM separately for each tributary. We calibrated PIHM for Featherville and calibration factors were validated for Dixie and Pierce.

For Featherville and Dixie watersheds, the river elements are generated to cover the main river and its main tributaries, whereas for Pierce watershed generated river elements cover the main river (Figure 5.5). We generated fine cells close to the river and large cells at the locations that have homogenous characteristics. 237, 77 and 26 meshes and 75, 34 and 8 river elements were generated for Featherville, Dixie and Pierce watersheds, respectively (Figure 5.5).

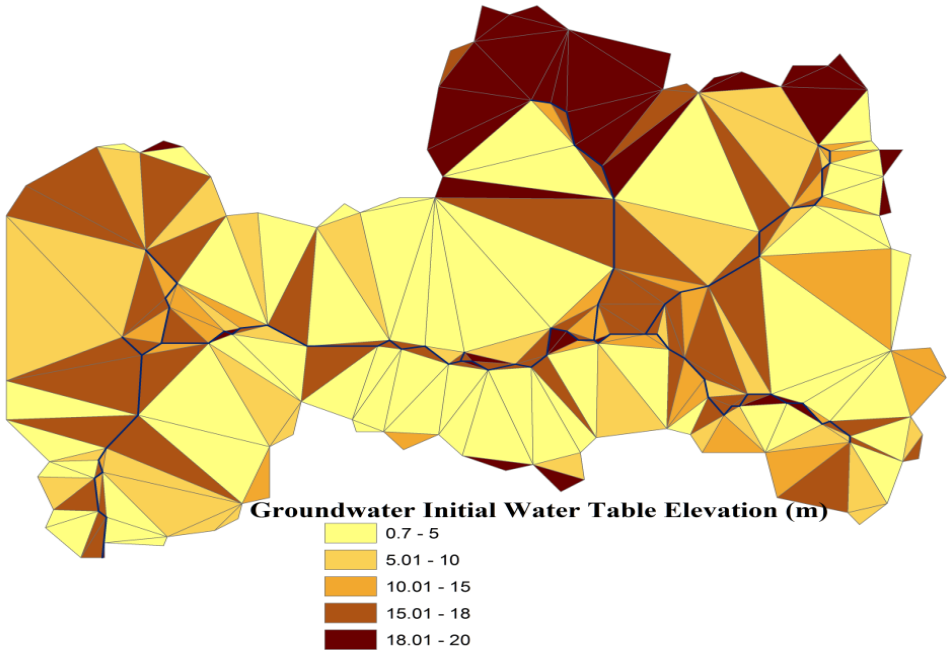

Figure 5.6: Groundwater initial water table elevation for PIHM at Featherville.

Groundwater initial condition: Groundwater initial level and its distribution are very important, because they control timing and magnitude of groundwater contribution to streamflow. To identify groundwater initial level over the watershed, we used Kumar et al. (2013) approach. PIHM groundwater model is run for ten years with zero SWI and fully saturated watershed. We assumed that a spatially constant groundwater depth in SFB watershed of 20 meters. Therefore, to have an almost fully saturated watershed, groundwater initial level for all meshes is set to 19.9 meters. The purpose of this approach is to estimate groundwater level when streamflow is merely generated by groundwater and the basin is not fed by SWI for a long time. Eventually, groundwater level at the end of the 10-year simulation is set for initial groundwater condition. After generation of PIHM inputs, groundwater model of PIHM was run for these three watersheds to estimate groundwater initial condition. Figure 5.6 shows estimated

initial groundwater level at Featherville watershed. As shown in this figure, cells that are close to the river elements have higher groundwater level, which is realistic.

5.2.5 Sensitivity analyses

Sensitivity analysis was performed to understand the influence of each parameter on streamflow. Calibration factor of one parameter was increased or decreased in each PIHM run while keeping the other parameters unchanged. PIHM has 27 parameters that require calibration. Thus, PIHM was run 54 times.

5.2.6 Initial calibration and evaluation of the model

Measured discharge is available at three locations, Featherville, Dixie and Pierce. For the purpose of the modeling effort Featherville is considered the headwater of the SFB with drainage area of approximately 1,600 km^2. Dixie and Pierce are SFB's tributaries located downstream of Anderson Ranch Dam with drainage area of 26 and 13 km^2, respectively. We calibrated PIHM for Featherville streamflow and validated these calibration factors by simulating streamflow of Dixie and Pierce. Calibration and validation were conducted using forcing data for October 2012 through May 2013 period, hereafter WY2013 (water year 2013).

A Nash-Sutcliffe coefficient (NSC) (equation 3.6) and percent BIAS (PBIAS) were used to evaluate the hydrologic model performance. PBIAS indicates percent of underestimation (positive value of PBIAS) or overestimation (negative value of PBIAS) of the simulated data (Moriasi et al., 2007), is calculated as follows:

$$\mathbf{PBIAS} = \left[\frac{\sum_{i=1}^{n}(Q_i^{obs} - Q_i^{sim}) * 100}{\sum_{i=1}^{n} Q_i^{obs}}\right] \quad (5.1)$$

where Q_i^{obs} and Q_i^{sim} are observed and simulated streamflow at time step i, respectively.

5.2.7 Final calibration and evaluation of the model

In the previous section, the model was calibrated merely for October through May. The model has not been calibrated for June through September, when water loss, such as

evapotranspiration, is significant and precipitation is slight. Therefore, calibration for this period is needed for estimation of a basin's recession curve.

Recession curve of a basin's hydrograph represents an important characteristic of that basin. A basin's recession curve describes period of time required for the basin to reach base flow after the maximum streamflow occurs. Main parameters that control recession curve are geology (under surface soil layer) horizontal hydraulic conductivity (gH), macro-pore horizontal hydraulic conductivity (mH) and macro-pore depth (mD). In addition to these parameters, Transpiration (E1) and Evaporation from ground (E2) required to be calibrated. Calibration of E1 and E2 are critical for summer streamflow.

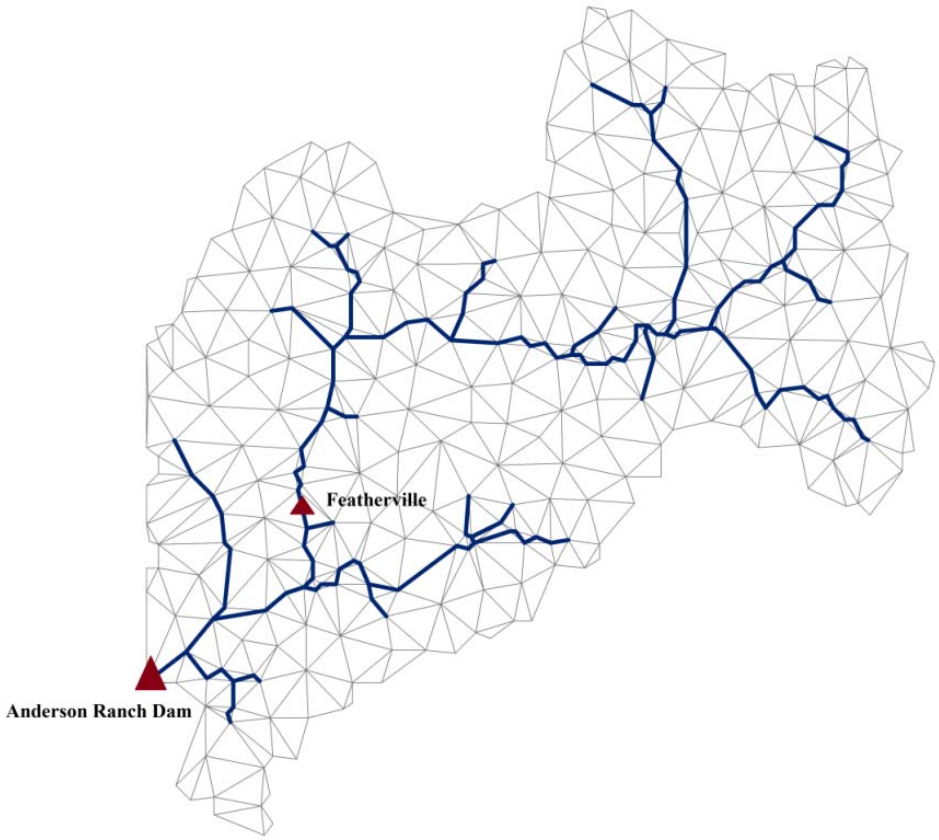

Figure 5.7: River elements and mesh cells for upstream of Anderson Ranch Dam.

For final calibration PIHM's inputs, as described in section 5.2.4, was prepared for upstream of Anderson Ranch Dam. To set up PIHM to simulate streamflow for upstream of Anderson Ranch Dam watershed 152 river elements and 592 mesh cells were generated (Figure

5.7). There are two streamflow gauges in Anderson Ranch Dam watershed, one gauge is located at the dam, hereafter Anderson, and the other is Featherville (Figure 5.7). The model was calibrated for water year 2006 (wy2006; October through September) at Anderson Ranch Dam. Validation of the model was then performed for wy2006, wy2007, wy2010 and wy2013 at Featherville, for wy2007, wy2010 and wy2013 at Anderson Ranch Dam and for wy2013 at Dixie and Pierce.

5.3 *Result and discussion*

5.3.1 Sensitivity analysis

Results of sensitivity analysis and of pre-calibration analyses showed that the watershed is sensitive to parameters related to groundwater. Among all the parameters related to groundwater, the watershed is very sensitive to four parameters, which are soil (top layer) vertical hydraulic conductivity (infiltration rate; sV), macro-pore vertical hydraulic conductivity (mV), porosity (p) and Beta (Figure 5.8). Lower value of this parameter produces more runoff from a SWI event. Increasing mV leads to increase vertical travel time and contribution magnitude of groundwater. The value of p strongly regulates soil water storage. Decreasing porosity leads to increase in discharge peaks, where there is groundwater contribution. Beta is Van Genuchten parameter that is related to soil water retention curve. Beta is the shape parameter of soil water retention curve.

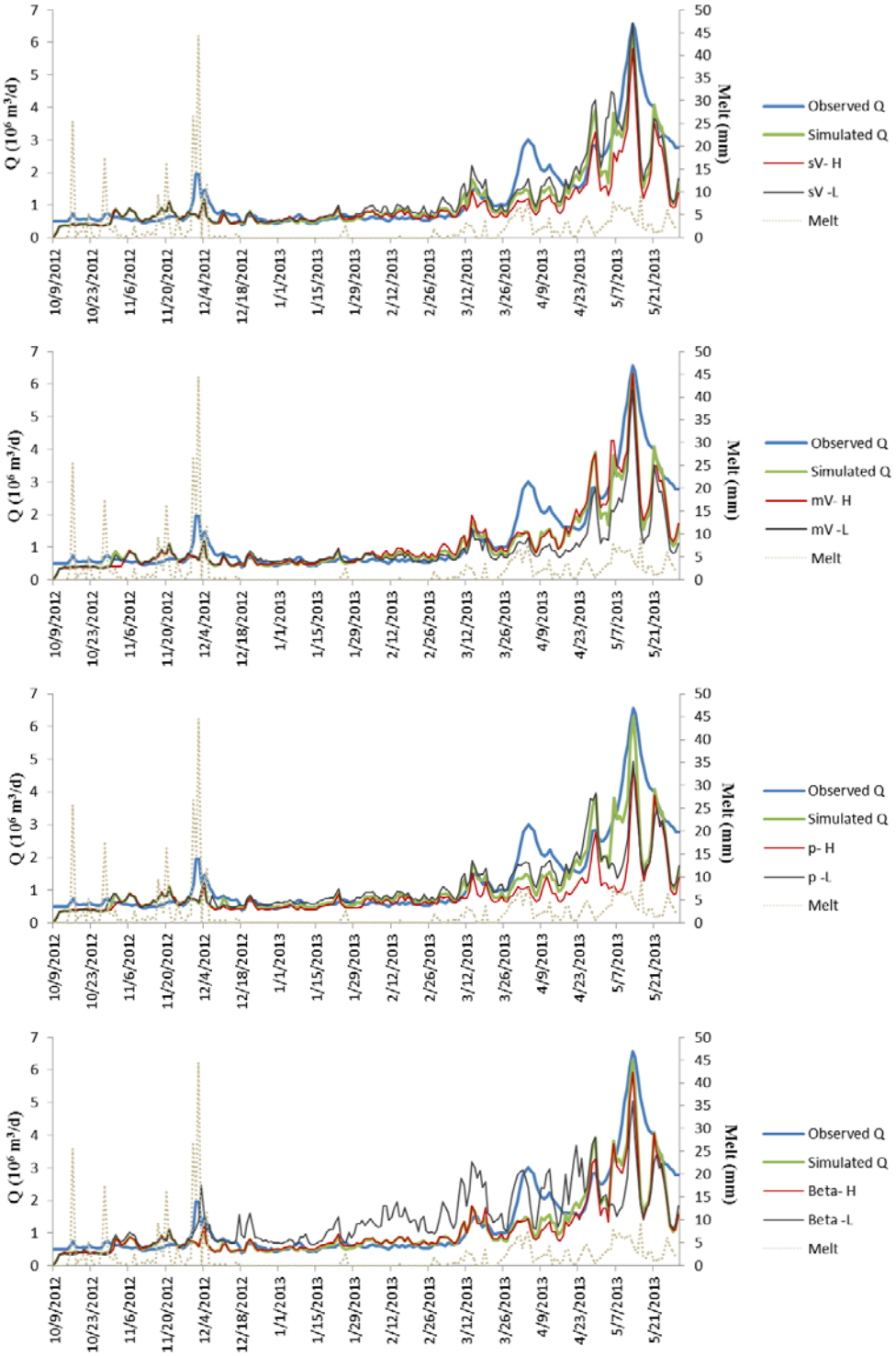

Figure 5.8: Sensitivity analysis results for soil vertical hydraulic conductivity (sV), macro-pore vertical hydraulic conductivity (mV), porosity (p) and Beta. Simulated Q is discharge simulation without any change in calibration factors. Letters H and L show increase and decrease in a parameter, respectively.

5.3.2 Initial calibration and evaluation of the model

PIHM is calibrated for Featherville watershed for WY2013. The calibrated model is well capable of catching all the discharge peaks derived from rain on snow or melt events (Figure 5.9). Discharge of Dixie and Pierce simulated using Featherville calibration factors to validate these factors. To evaluate performance of hydrologic models, Moriasi et al. (2007) classified NSC and PBIAS values into four classes including very good, good, satisfactory and weak.

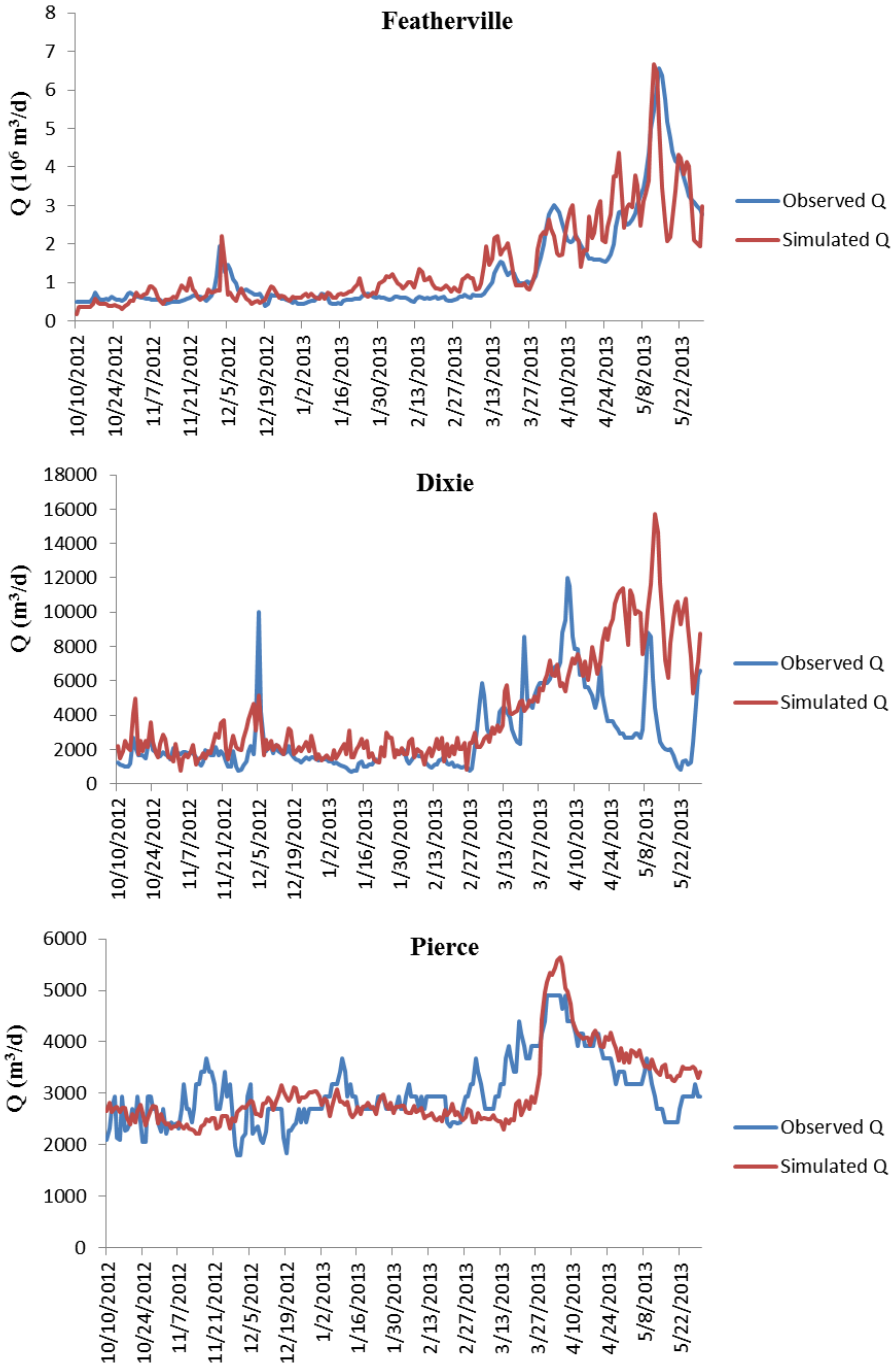

Figure 5.9: Comparison between simulated and measured discharges at Featherville, Dixie and Pierce gauge stations.

NSC values for calibration (Featherville) and validation (Dixie and Pierce) are 0.74, 0.66 and 0.32, and PBIAS values are -6%, -11% and 0%, respectively (Table 5.4). Except NSC of

Pierce, discharge simulations show NSC and PBIAS values that represent the model performances are good or very good at these watersheds.

Table 5.4: NSC and PBIAS values

Watersheds	NSC	PBIAS (%)
Featherville	0.74	-6
Dixie	0.66	-11
Pierce	0.32	0

Dixie and Pierce have very similar soil type, vegetation and SWI pattern, but these watersheds respond differently to melt, particularly in fall and winter. For instance, in December severe rain on snow event, there is no peak in Pierce discharge, whereas SWI magnitude in Pierce watershed is almost twice as that of Dixie, representing all the SWI in Pierce watershed infiltrates to ground and Pierce discharge mostly generated by groundwater.

5.3.3 Final calibration and evaluation of the model

Figure 5.10 shows capability of the calibrated model to capture peak flows at Featherville. In addition, the calibrated model well estimated recession curve of the basin's hydrograph. However, the calibrated model underestimated the highest peak of wy2006 (wet year). Quantification of the model performance indicates that the model was well calibrated (Table 5.5). Goodness of fit of simulated stream flow represented by NSC values higher than 0.75 at all the water years, except in wy2013 which was not simulated for the entire year. PBIAS values indicate that simulation errors are not significant.

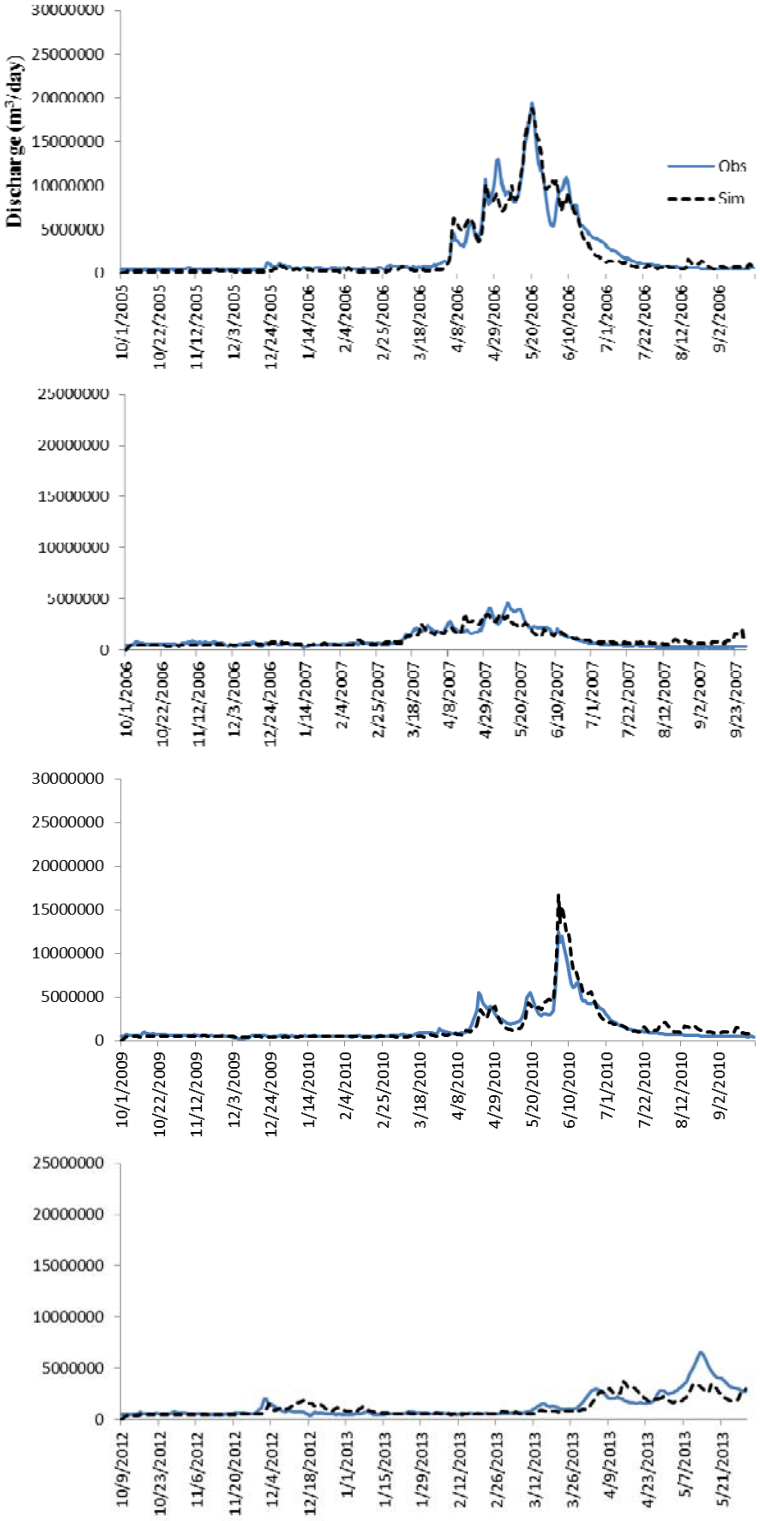

Figure 5.10: Simulated and observed stream flow at Featherville.

Table 5.5: NSC and PBIAS values for Featherville

	WY2006	WY2007	WY2010	WY2013
NSC	0.92	0.77	0.81	0.63
PBIAS (%)	6.1	-4.0	-8.0	12

Similar to the results of Featherville, simulated stream flow at Anderson followed measured stream flow pattern (Figure 5.11). NSC and PBIAS values also indicate that simulated stream flow fits observed stream flow (Table 5.6).

Table 5.6: NSC and PBIAS values for Anderson.

	WY2006	WY2007	WY2010	WY2013
NSC	0.94	0.75	0.76	0.62
PBIAS (%)	8.8	-1	-7.3	7

According to these results, performance of the model is very good for both calibration and validation periods at Featherville and Anderson. Moriasi et al. (2007) arranged results of 128 works that simulated stream flow using various hydrologic model at a daily resolution at different watersheds. According to these 128 studies, median NSC value for validation period is 0.67.

In addition, comparing our results to those works that applied PIHM indicates that the performance of the model is very good at Featherville and Anderson. Kumar et al. (2013) simulated daily stream flow using coupled ISNOBAL and PIHM for wy2006 and wy2007 over Reynolds Mountain East with drainage area of 0.4 km^2. They reported NSC values of 0.73 and 0.60 for calibration (wy2006) and validation (wy2007) periods, respectively. Yu et al. (2013) simulated streamflow using PIHM over two watersheds including Young Womans Creek watershed (YWC) and Little Juniata River watershed (LJR) with drainage area of 230 and 843 km^2, respectively. They reported NSC values of 0.66 and 0.54 for calibration and validation periods, respectively, for LJR. At YWC, NSC values of 0.80 and 0.65 were reported for calibration and validation periods, respectively.

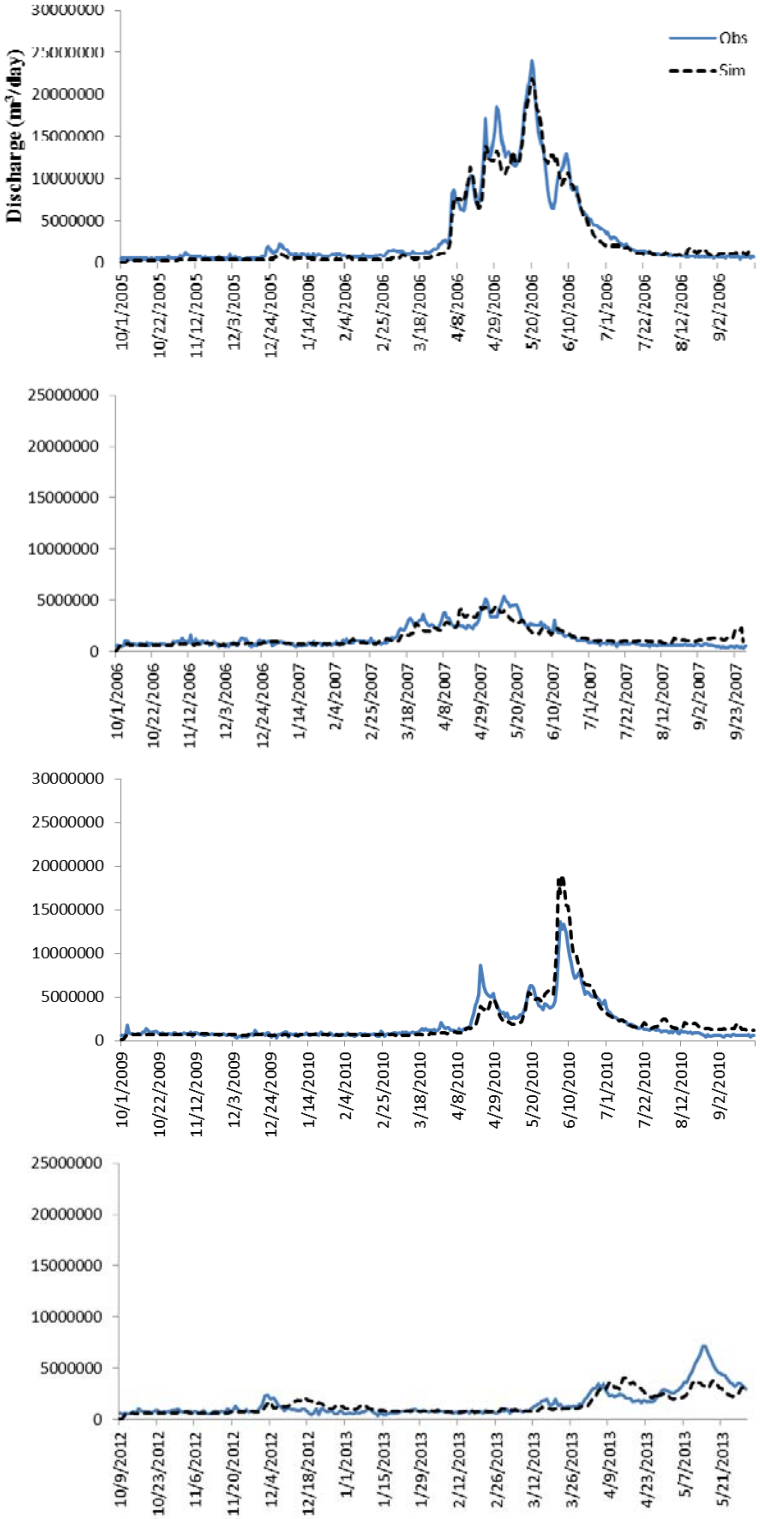

Figure 5.11: Simulated and observed stream flow at Anderson.

At Dixie and Pierce, stream flow was simulated using the same calibration factors used to simulate stream flow for Anderson Ranch Dam watershed. Figure 5.12 compares simulated and observed streamflow for wy2013 at Dixie and Pierce. This comparison indicates that the simulated stream flow follows the measured stream flow patterns at Dixie, whereas the performance of the model is poor at Pierce. The performance of the model at Dixie with NSC of 0.63 is similar to that of Anderson and Featherville. However, the performance of the model is poor at Pierce with NSC of -0.31 (Table 5.7). NSC represents goodness of fit when observed versus simulated data is plotted. Negative values of NSC indicate that average of observed stream flow is better estimation than simulated stream flow.

Low model performance at Pierce may suggest that calibration factors that were adjusted for a large watershed like that upstream Anderson Ranch Dam are not applicable to simulate stream flow for a small watershed like Pierce, but worked for a larger watershed such as Dixie. There might be several reasons: (1) input data do not capture the grain-scale variability of small watersheds like Pierce, (2) difficulty in measure discharge in such small streams and (3) stream network not well captured by the model. We observed that measured stream flow at Pierce do not well correlate with Featherville or Dixie (Figure 5.13). This implies that Featherville watershed's respond to SWI is differently than that of Pierce watershed.

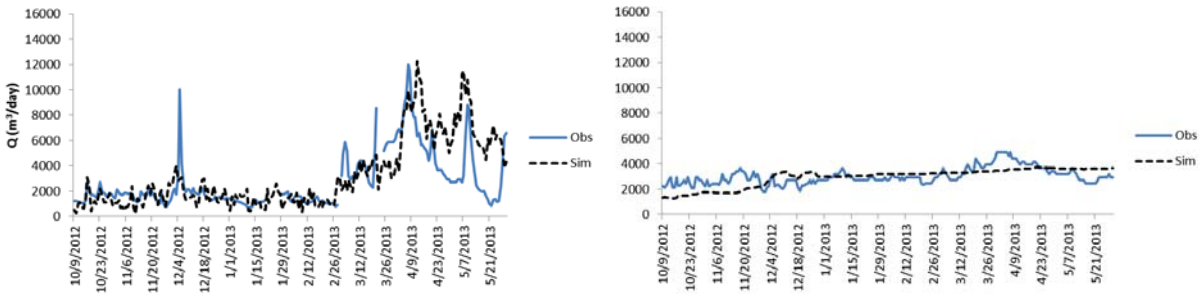

Figure 5.12: Simulated and observed streamflow at Dixie (the left graph) and Pierce (the right graph) for wy2013.

Table 5.7: NSC and PBIAS values for wy2013 for Dixie and Pierce.

	NSC	PBIAS (%)
Dixie	0.63	9
Pierce	-0.31	2

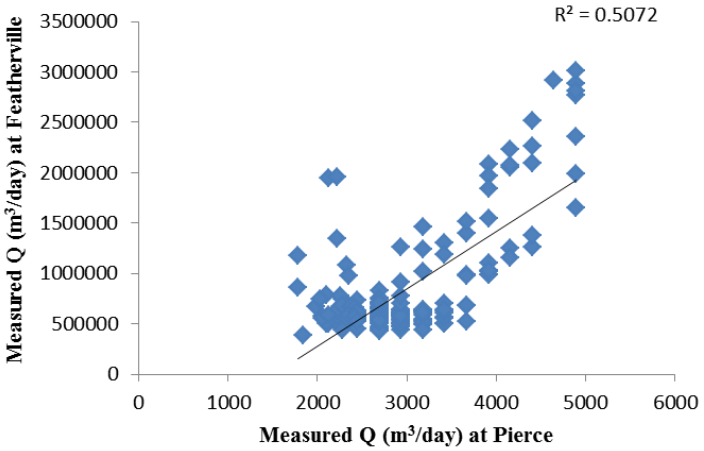

Figure 5.13: Correlation between measured stream flow of Pierce and Featherville for wy2013.

5.4 *Conclusion*

The calibrated integrated model was able to capture flow patterns at Featherville and Anderson Dam locations for both calibration and validation periods. However, model results were relatively poor specifically Pierce Creek, which is a small watershed compared to Featherville and Dixie Creek. Consequently, a regression analysis based on drainage-area water approach (Chapter 5) was developed to predict discharges of ungauged small watershed tributaries of the South Fork Boise River. These predicted hydrographs were used as boundary conditions for both 1D and 2D hydrodynamic flow model (Chapter 5 and 6).

6 ONE-DIMENSIONAL HYDRAULIC MODEL

6.1 *Introduction*

Ecohydraulics defines ecosystem status based on physical environment of the system their interaction with biological requirements (Newson and Newson, 2000) and examines the effects of physical properties of the system (e.g., hydrologic, hydraulic and geomorphologic) on the ecosystems (Bovee, 1982; Lancaster and Downes, 2010). Hydraulic properties (e.g., water depth, velocity, shear stress, etc) are one of the important parameters for the riverine habitat characteristics (Bovee, 1982; Kondolf et al., 2000; Pasternack et al., 2004).

Aquatic habitat modeling integrates flow hydraulic properties such as flow depth velocity, and shear stress with biological requirements, to quantify habitat availability. In general, habitat models utilize flow properties simulated by one-dimensional (1D) and two-dimensional (2D) hydrodynamic models because measurements of depth and velocity in the natural channel are rare and specifically velocity fields are complex and irregular (Whiting, 1997).

A one-dimensional model utilizes cross sections of a river to compute water surface elevation (WSE) and average flow velocity across a section of a given river flow solving the cross-sectional integrated equations of continuity and momentum conservation known as the De-Saint Venant equations. More recently, two-dimensional finite difference and finite element models were developed to simulate flood inundation patterns in channel and floodplains utilizing channel bathymetry and floodplain topography solving the vertically integrated continuity and momentum equations in two horizontal dimensions, also known as shallow water equations.

The 1D model is capable of reproducing flooding phenomenon in a homogeneous river channel, but it does not predict spatially complex flow patterns (Mason et al., 2003). Whereas 2D models are capable of differentiating among various hydraulic conditions in heterogeneous channels and overland flow, incorporating spatially varied topography and friction (Horritt, 2000). Past studies has shown that 1D and 2D models can provide comparable cross-sectional averaged flow properties when the topography varies uniformly but significantly different in heterogeneous topography, which causes large flow propriety gradients (Brown and Pasternack,

2009). Both 1D and 2D models may introduce noticeable error (Kondolf et al., 2000; Pasternack et al., 2006) and the accuracy of the results is directly proportional to the accuracy of the bathymetric data available.

6.2 *Method*

6.2.1 1D hydraulic model development

As mentioned above, one of the primary objective of this study is to analyze the effects of Anderson Ranch Dam operation on thermal and hydraulic regimes of South Fork Boise River (SFBR) spatially and temporarily. In order to meet the goals of the project, we develop a one-dimensional (1D) river model coupled with a heat transport module that can simulate different flows and heat transfer, which vary with respect to space and time. Although, flow patterns in a natural river system are three-dimensional (longitudinal, transversal and vertical) (Henderson, 1966), a 1D model may provide adequate mean flow velocity and water surface elevation in stream reaches where flow characteristics vary primarily in the longitudinal direction and less extensively in the transverse and vertical.

Although, several public domain and commercial software packages capable of performing one-dimensional unsteady simulations are available, we chose the DHI (Danish Hydraulic Institute) MIKE11 software, because of its integrated nature and opportunity to link one-dimensional and two-dimensional simulations, to couple with heat transfer, water quality and sediment transport modules.

The MIKE11 model uses the one-dimensional unsteady flow De-Saint Venant equations based on the following assumptions:

- Flow is one-dimensional and velocity is uniform within a cross-section.
- Water is incompressible and homogeneous, i.e., density is constant.
- The bottom slope is too small such that the angle between the streambed and the horizontal place is small.
- Flow is mainly subcritical.

- Streamline curvature is small with negligible vertical accelerations, such that the pressure is hydrostatically distributed along the water column.

The equations that describe one-dimensional unsteady flow are:

$$\frac{\partial A}{\partial t} + \frac{\partial Q}{\partial x} = q \tag{6.1}$$

$$\frac{\partial Q}{\partial t} + \frac{\partial(\alpha \frac{Q^2}{A})}{\partial x} + gA\left(\frac{\partial h}{\partial x}\right) + \frac{gQ|Q|}{C^2 AR} = 0 \tag{6.2}$$

Where, Q= discharge; A= flow area; q= lateral inflow; h= stage above datum; C= Chezy resistance coefficient; R= Hydraulic radius; α = momentum distribution coefficient

6.2.2 River Network

Initially, we utilized the raw thalweg created from River Bathymetric Toolkit (RBT) (McKean et al., 2009b) for SFBR River network as an input for MIKE 11 model. However, we needed to smooth the raw thalweg manually to keep it within the streambed boundary based on visual judgment and laying river network over an aerial image of the SFBR. The total network length of the study reach is about 42 km and it runs from Anderson Ranch Gauge Station (USGS 13190500) to the Neal Bridge Gauge Station (USGS 13192200). We did not create an additional network around islands and side channels to make 1D model as simple as possible and because of lack of visibility of these structures on the surveyed topography and aerial images. The extents of these areas (side channel and islands) are relatively small compared to entire study area. However, these structures should be covered by relatively high-resolution cross section (1 m in transverse and 30 m in longitudinal directions) input as channel bathymetry in the model. Nevertheless, we developed a fully 2D model to cover side channel and islands because of importance of 2D model for fish habitat modeling.

6.2.3 Channel cross-section

We utilized high-resolution river bathymetry surveyed with the aquatic-terrestrial Experimental Advanced Airborne Research LiDAR (EAARL) system in 2007 to extract channel

cross-sections. Cross sections (300 m wide) were extracted from the 1 m DEM using MIKE11 GIS tool (DHI, 2011c) at 30 m interval longitudinally and 1 m transverse directions along the centerline/thalweg of the SFBR. Later, cross-sections were trimmed (cut) at an inundation extent of flow magnitude of 248 m^3/s, which is about 200-year Recurrence Interval (RI) at the Featherville gauge station located upstream from the study reach. This 30 m cross-section spacing and 1 m transverse direction provides a greater density of topographic and bathymetric information of the system than is typically implemented in a 1D model. Thus, this provides exceptional level of confidence in the river topography inputted into the 1D model, and the hydrodynamics derived from the model.

6.2.4 Upstream and downstream boundary conditions

Boundary conditions are required at the upstream and downstream model limits, and at the locations of additional fixed constraints on river flow in the model. The hydrologic data from Anderson Ranch and Neal Bridge USGS Gauge stations are upstream (discharge) and downstream (stage), respectively for the model calibration, validation and application for different climatic scenarios. The measured discharge and stage time series are available from Anderson Ranch (1944-up to date) and Neal Bridge (1978-up to date). Depending on the analysis, the model can simulate unsteady and steady state flow utilizing time series and constant (e.g., for model calibration and validation) upstream and downstream boundary conditions, respectively.

6.2.5 Tributary inflows

Additional hydrologic inputs from tributaries and other sources (e.g., seepage flow) are required between upstream and downstream boundary of the model to simulate channel hydraulics accurately. These lateral inputs occur at point locations (e.g., tributary inputs) or as dispersed (uniform) contributions (e.g., seepage or overland flow from slopes that discharge directly into the main stem river). We added tributaries input as point inflows for twelve streams between Anderson Ranch and Neal Bridge USGS gauge station (Table 6.1), which has watershed area higher than 9 km^2.

Table 6.1: Tributaries and their locations included in the MIKE11 model.

No.	Creek Name	Side	$^{\varphi}$Area	Chinage (m)	$^{\Delta}$R
1	Dixie	L	26	3045	0.8
2	Cow	L	7	12775	0.1
3	Cayuse	L	9	14370	0.1
4	Granite	R	9	14815	0.8
5	Pierce	R	13	18160	1.3
6	Mennecke	L	10	20525	0.2
7	Bock	L	10	22410	0.2
8	Rock	R	76	23410	3.7
9	Dead Horse	R	13	27200	1.7
10	Smith	R	134	40685	6.0
11	Big Fiddler	L	10	42625	1.0
12	Long Gulch	R	25	43110	0.8

$^{\Delta}$Ratio between yearly average tributary flow and main stem flow at Anderson Ranch gage station(%) ^{R}Right side of tributary ^{L}Left side of tributary $^{\varphi}$Watershed area (km^2)

Measured temperature and discharge time series are available for some of these tributaries for the period after 2011.

6.2.6 Mass balance analysis of discharge within the study reach

Regression equations are generally used for estimating stream flows at ungauged sites from gauged reaches (Burke, 2006; RiesIII, 2007). Here, graphical correlation and regression methods among streams with similar geographic and climatic characteristics have been used to predict discharge from streams with measured data to those with periods without measurement data and for ungauged tributaries of the South Fork Boise River. USGS National Stream Statics computer program uses the weighting procedure to estimate flood frequency of an ungauged drainage area based on regression equation developed for stream gauged station and drainage areas associated with them (RiesIII, 2007). Both drainage basins have to be on the same stream and a drainage area of stream gauge station should be between 0.5 and 1.5 times of the drainage area of an ungauged station. This method estimates flood-frequency of an ungauged site based on area-weighted flood frequency of the gauged station considering flow per unit area.

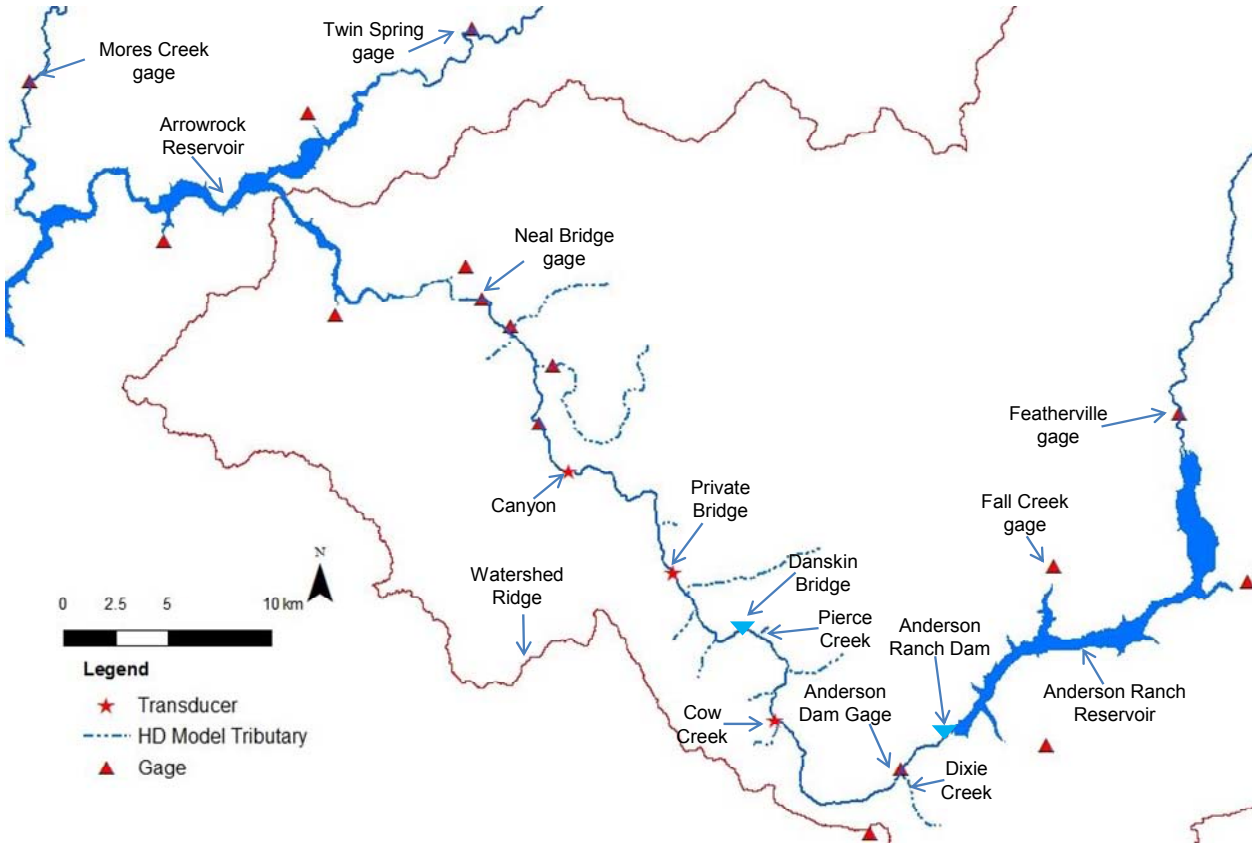

Figure 6.1: Gauge stations within Boise River Basin and transducers location to measure stages and water temperatures.

We used a graphical correlation and regression methods to predict stream flows for periods that have no measurement based on regression equation developed by correlating measurements at the another gauge station. Whereas, we adopted an area-weighted approach to estimate stream flows for a specific drainage area based on regression equation developed for two other gauged drainage basins. Finally, we estimated daily averaged discharges for the tributaries within the hydraulic model domain (Table 6.1).

Table 6.2: The regression equation used to predict tributary discharges

Regression equation	Tributary									
	Cow*	Cayuse	Granite	Mennecke*	Bock	Rock	Dead Horse	Smith*	Big Fiddler	Long Gulch
Fall Vs Mores						X		X		
Dixie* Vs Mores										X
Pierce Vs Mores	X	X	X	X	X		X		X	

*Temperature mesurement available

Daily or more frequent observations of main stem South Fork Boise River and tributaries discharge and stage measurements are available through USGS managed gauge stations. The

discharge data are available from two gauge stations in each main stem Boise River and tributaries. Daily discharges are available for Anderson Ranch Dam and discharges and stages for the Neal Bridge gauge station for the main stem South Fork Boise River. These stage and discharge time series were utilized as input to the hydrodynamic models and for model calibration. Twelve tributaries of the South Fork Boise River between Anderson Ranch Dam and Neal Bridge gauge stations have been included in the numerical model. Most of these tributaries have no discharge measurements except for a short period for Dixie and Pierce creeks. Therefore, discharges of Dixie and Pierce Creeks for the ungauged periods were predicted by graphical correlation with discharge measurements for Mores Creek (Boise River Basin) (Figure 6.1), which has long-term discharge measurements. We developed three regression equations correlating measured discharges of Fall, Dixie, and Pierce creeks with Mores Creek (Figure 6.2). Then, we estimated discharges of the remaining ten tributaries using these regression equations (Table 6.2) and drainage area associated with each tributary (Table 6.1).

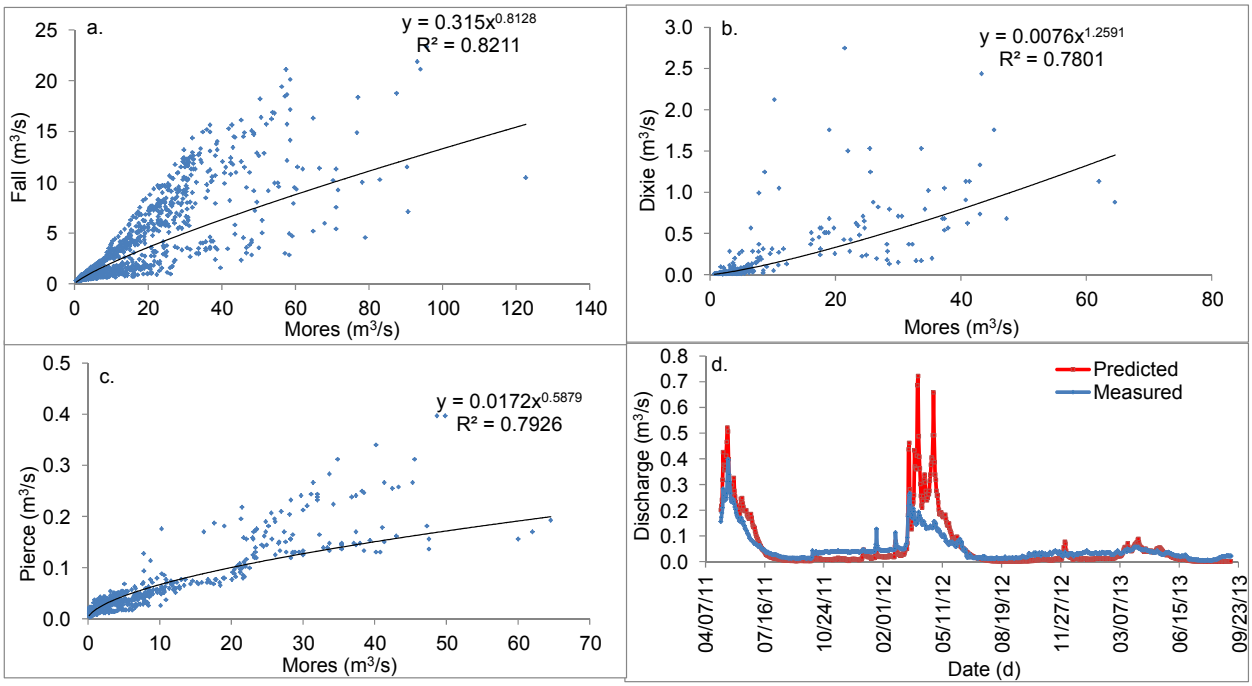

Figure 6.2: Regression equations developed by correlating discharges of Fall, Dixie and Pierce creeks to Mores Creek (a, b, c). Measured and predicted discharges from regression equation based correlation between Dixie and Mores Creeks at the Pierce Creek and weighted-area approach (d).

We performed mass balance analysis of discharges within the study reach considering estimated discharges from tributaries and measured discharges at the main stem river. This is an assessment that confirms discharge input and output from the model area are equal or within the permissible error range of 10% (Turnipseed and Sauer, 2010). Our analysis showed that the error between input and output from the study areas is within 10% for 857 days out of 935 (05/03/2011-11/22/2013). Thus, estimated discharges for the tributaries are within the permissible error range and hence used for hydrodynamic hydraulic and temperature modeling. Some of the errors were originated from discharge ramping from the Anderson Ranch Dam (Figure 6.3).

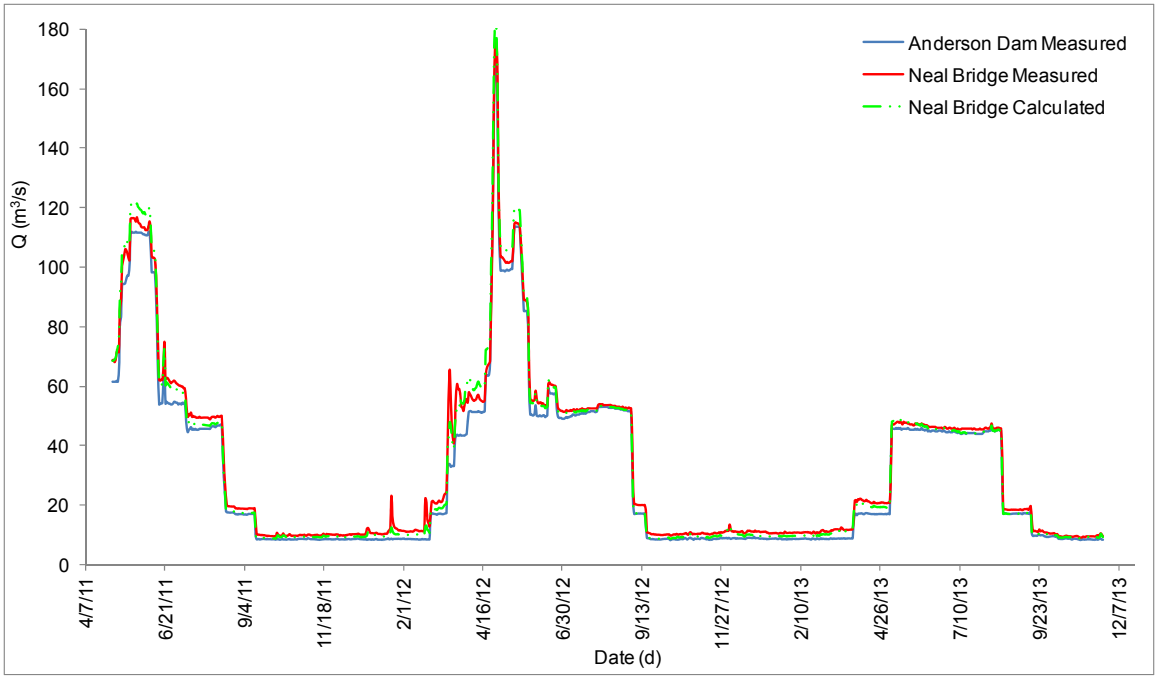

Figure 6.3: Measured and estimated discharges at the Neal Bridge gauge station.

6.2.7 Boundary resistance

Boundary resistance is an important parameter of the model setup, which can be adjusted during the model calibration process in order to make model predicted variables (e.g., water surface elevation) comparable to the measured. It represents resistance to flow exerted by the bed and banks of a channel. The boundary resistance is related to factors such as bed and bank irregularity, particle size distribution in the channel, cross section variation, vegetation density, obstruction, degree of channel meandering, etc (Henderson, 1966). The Manning's equation is

most commonly utilized in the modeling processes and it is used to select the resistance coefficient *n*, which is an empirically-based coefficient. Selection of Manning's *n* for a specific river system should be based on model calibration, where simulated hydraulic parameters (e.g., flow and water surface profiles) are compared against measured in order to provide the most accurate results from the model.

In this study, we selected an initial Manning's *n* coefficient, which varies longitudinally, based on professional judgment and estimation using reference values from similar sites or systems (Arcement and Schneider, 1989). Later, we adjusted these values during the calibration process. One of the advantages of the MIKE 11 software is that it provides flexibility in describing boundary resistance by enabling either application of a single Manning's *n* value uniformly to an entire cross section, or application of unique values to three separate zones "triple zone" within each cross section (DHI, 2011a). We utilized "triple zone" approach, where the three zones approximately correspond to a low-, medium- and high-flow zones.

6.2.8 Stream temperature model development

Hourly time series data, which captures sufficient day to night variations of temperature in detail, are used for model run and validation. The time series should be long enough such that it covers seasonal variations during fall, winter, spring and summer. Thus, for better outcome of temperature modeling, hourly resolution meteorological data are required to simulate heat exchanges between atmosphere and stream. These metrological data are global solar radiation, air temperature and relative humidity. The amount of sunlight (hour/day) or solar radiation is specifically important for temperature model calibration even more than air temperature (Johnson, 2003). Heat is transported through the system similar to a mass solute transport via advection-dispersion processes (DHI, 2011a). The net heat exchange among the stream water, the atmosphere and the bed sediment depends on several process and parameters.

We used DHI software MIKE 11 to simulate stream temperature in the South Fork Boise River. MIKE 11 simulates heat transport with one-dimensional advection-dispersion heat transport equation. The model considers solar, atmospheric, evaporation, convection, and water radiation for the atmospheric heat balance. However, heat exchange from groundwater and

runoff sources is not included in the MIKE 11, but process can be included in the modeling by using DHI software ECO Lab.

US Bureau of Reclamation (USBR) installed TidBiT temperature sensors and pressure transducers to measure stream water temperatures at different locations along the main stem Boise River and at a few tributaries (Figure 6.1and Table 2.3). Stream temperatures measured at these locations were used as a boundary condition in the temperature model and for model calibration processes. For tributaries without measurement, we use water temperature predicted by Stream Water Temperature Model (SWTM) (Chapter 3) based on predicted discharges (Section 6.2.6).

Metrological data relative humidity (1-hour interval) and air temperature (15-minute interval) were used from Boise airport and Arrowrock Dam weather stations, respectively. There are no metrological stations that measure solar radiation near the study site, therefore solar radiation data (1-hour interval) measured in Bearskin Creek Weather Station was used for this study.

The geography and geology of the study reach in the South Fork Boise River is similar to the lower Deadwood River located in Central Idaho. Drainage basins of both of these rivers are located in Idaho Batholith and rivers flow through the mountainous terrain. Like in the lower Deadwood River system, the canyon-like nature of South Fork Boise River prevents most sunlight (for the geographic area) to reach the river. Thus, this supported a shift in the timing and amount of incoming solar radiation. During morning hours, there is a significant delay in sunlight reaching the river in the canyon. Thus, the modeled time zone was shifted back by 4 hours to consider this constrain, which was found to represent the hour at which sun first reaches the river bottom. As with the lower Deadwood River, the canyon walls of the South Fork Boise River were found to be approximately 35 degrees from the center of the river. Thus, we did not consider any incoming solar radiation in calculations of number of sunlight hour per day below 35 degrees from the horizon.

The daily maximum incident solar radiation from the Bearskin Creek Weather Station was calculated and utilized to calculate available sunlight per day. Furthermore, calculated sunlight

per day was compared to the calculated number of theoretically available sunlight hours. We used the data from a NOAA web product to build a relationship to calculate the total hours of sunlight theoretically available at 35 degrees above the horizon line throughout the year. We found that a third degree polynomial relationship accurately represents sunlight hours per day based on Bearskin Creek maximum daily solar radiations. With this methodology, a time series for South Fork Boise River sunlight hours per day was calculated to use as an input data for the MIKE11 temperature model.

6.2.9 Hydraulic model calibration and validation

Model calibration provides confidence in application of the models to different time periods, discharges and other hypothetical scenarios. We calibrated the model adjusting initially estimated empirical Manning's coefficient *n*, so that simulated flow characteristics closely follow observed flow characteristics. We compared simulated water surface elevation (WSE) to two measured WSEs (for low and medium flows) in the SFBR. Due to low discharges from the dam we were not able to calibrate the model for high flow discharges. The WSE measurements were carried out for two discharges released from Anderson Ranch Dam i.e., low flow (8.5 m^3/s) and medium flow (45.6 m^3/s). We also confirmed dam release discharge by measured discharge at the Cow Creek Bridge, where discharges are 8.9 (low flow on 27th March, 2013) and 46.0 m^3/s (high flow on 23rd May, 2013). The WSE were surveyed using real-time kinematic global positioning system (RTK Leica-GPS System500). The used RTK equipment provides an accuracy of centimeter horizontally and vertically (Jackson, 1999). Measured water surface elevations are limited to the upper 22 km of the river from upstream model boundary due to limited accessibility in the lower canyon section.

For the model calibration, we simulated constant discharges (e.g., 8.5 and 45.6 m^3/s) for 36 hours, which is a period longer than that required by the system to reach a steady state condition. We did not consider any tributary discharges for the calibration because their contributions are small during the summer survey period. Thus, they will not change water surface elevation significantly. We compared simulated WSEs from the end of simulation period to measured WSEs to quantify the deviation using root mean square error (RMSE) approach. Based on

estimated uncertainty (Section 1.3.2) in the elevation of LiDAR surveyed topography, we lowered the measured WSEs by 0.39 m before comparing with the simulated WSEs during model calibration. RMSE is described by the following relationships:

$$RMSE = \sqrt{\frac{\sum_{i=1}^{n} (P_{obs} - P_{sim})^2}{p}} \tag{6.3}$$

where, *RMSE*= root mean square error; P_{obs}= value of parameter in observed data series; P_{sim}= value of parameter in simulated data series, *p*= number of data points. We established a target RMSE below 0.15 m to guide the calibration process, which is about the suggested vertical accuracy of the EAARL technique surveyed LiDAR data reported by (McKean et al., 2009b) in another system. Thus, we adjusted the Manning's roughness coefficient *n* until the WSE RMSE is less than 0.15 m or until additional adjustments did not improve error estimates. In general, we adjusted roughness values at upstream and downstream locations, where WSE measurements were available. Initially, we assigned a Manning's *n* value of 0.055 throughout the model domain based on our professional judgment at similar system and estimation using reference values (Arcement and Schneider, 1989). Later, we adjusted the value (increase or decrease) based on estimated differences at WSE measured locations. After several iterations, the Manning's roughness *n* values were finalized for low discharge (8.5 m^3/s) within the entire model domain. The calibrated *n* values vary from 0.05 to 0.11. These estimated values are consistent with similar system in other watershed (e.g., Soong et al., 2012). Similarly, we fixed Manning's roughness *n* values for the medium discharge (45.6 m^3/s) after several iterations. These values vary from 0.033 to 0.072, which are approximately 75% of the Manning's roughness *n* values finalized for the low discharge. Our calibrated Manning's roughness trend is expected because in general, the effect of roughness parameters (e.g., bed and bank irregularity, particle size distribution in the channel, cross section variation, vegetation density, obstruction, degree of channel meandering, etc.) decreases with increased discharges (Soong *et al.*, 2012; Conner and Tonina, 2013).

For model validation, we simulated discharges from 3/22/2013 to 11/22/2013 including tributary discharges and compared with water surface elevation (WSE) time series for three

transducer locations at Cow Creek Bridge, Private Bridge near Danskin Bridge and Canyon section (Figure 6.1). This analysis provided differences in simulated and observed water wave-travel along the river due to boundary resistance assigned during model calibration process. We did not surveyed relative elevation of the transducer located at the Canyon section due to accessibly, thus assigned average elevation of channel bathymetry within 3 m radius assuming transducer is laid over the channel bottom, which is true for all transducers.

6.2.10 Stream temperature model calibration

To calibrate the MIKE11 model for temperature, modeled temperatures were compared to the temperature observed from the temperature logger and transducers at Cow Creek Bridge, Danskin Bridge, Private Bridge and Canyon section of the main stem of the South Fork Boise River. Model parameters including calculated daily sunlight hour per day of the temperature model were modified to match the diel temperature fluctuations observed in the river.

During the calibration, it was found that, sunlight hours do not affect the heat exchange between atmosphere and the river system between October 1st and April 1st, therefore solar radiation influence was limited and set to zero for this time period in the model. Furthermore, an hour deduction from calculated sunlight hour per day yielded better result for the South Fork Boise River.

6.3 *Calibration result and discussion*

6.3.1 Hydraulic model

The results of the model calibration for low (8.5 m^3/s) and medium discharges (45.6 m^3/s) are shown in Figure 6.4 and Figure 6.5. These results from the model calibration show acceptable agreement between the simulated and the measured WSEs for both discharges. The RMSE are 0.13 m and 0.11 m for low and medium discharges, respectively, which are less than the targeted value of 0.15 m. The RMSE is smaller (0.11 m) for medium discharge than the low discharge (0.13 m) as found in other studies (e.g., Bruxer and Thompson, 2008).

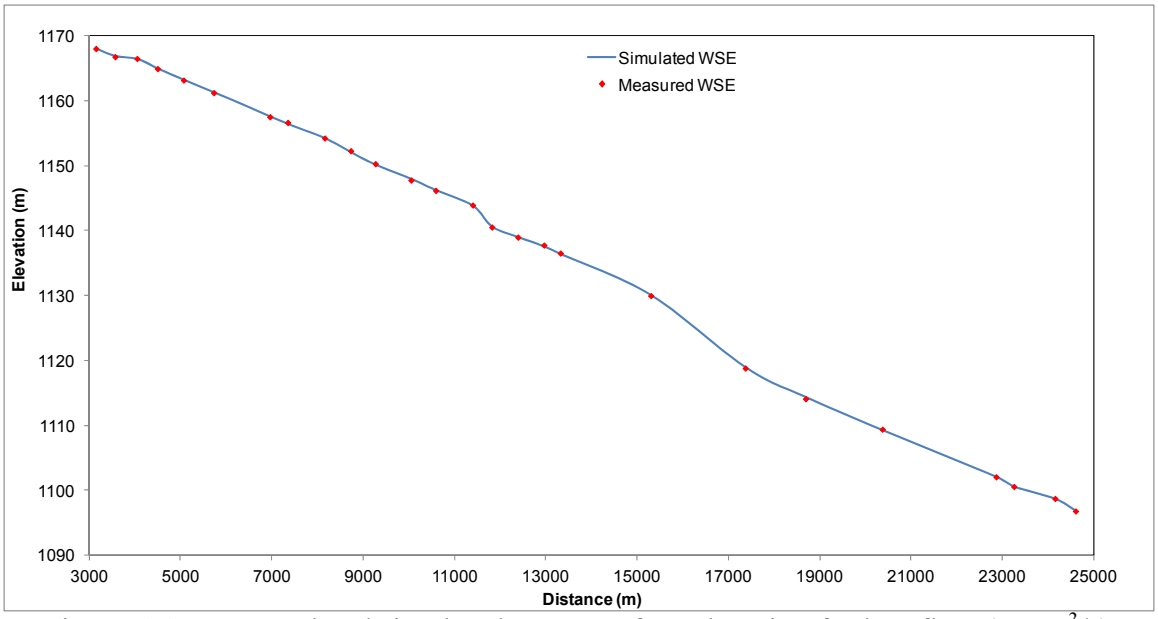

Figure 6.4: Measured and simulated water surface elevation for low flow (8.5 m^3/s)

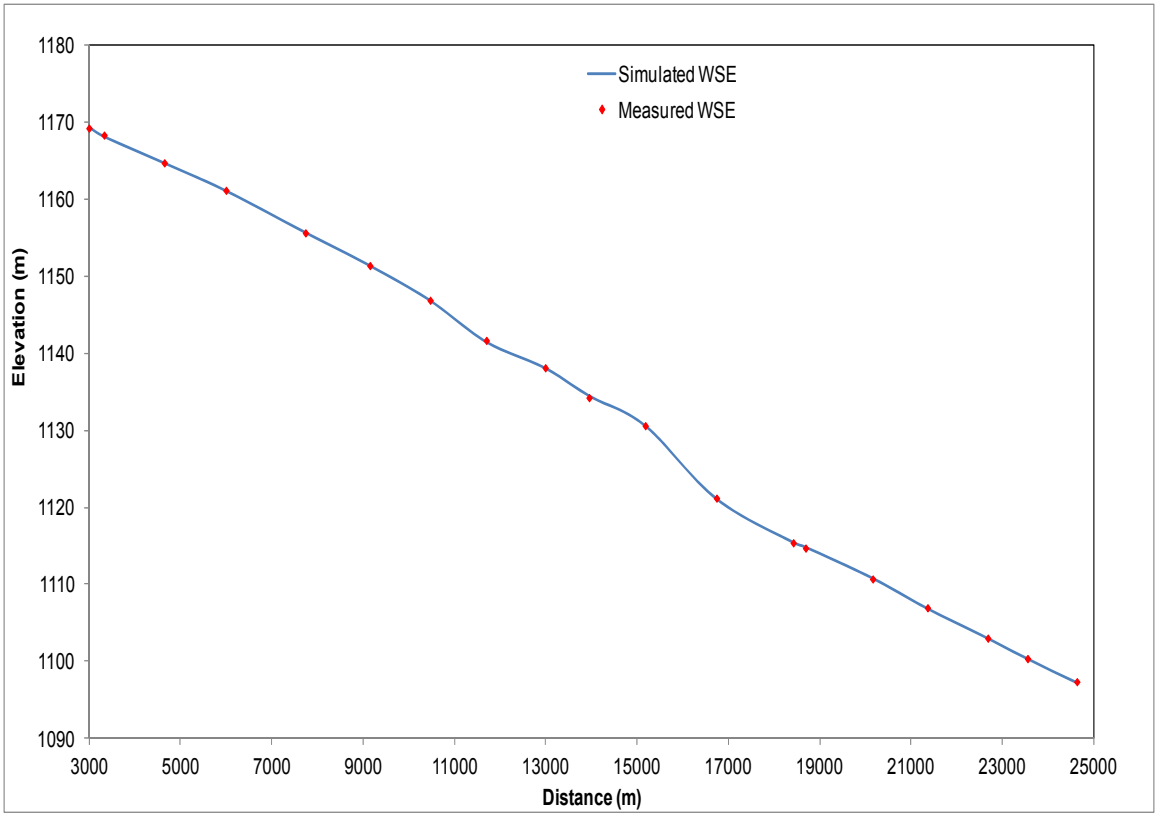

Figure 6.5: Measured and simulated water surface elevation for medium flow (45.6 m3/s)

There are abrupt changes in Manning's roughness *n* values for both discharges (i.e., low and medium), which may be due to sudden changes in river gradients. For example, the

Manning's roughness *n* changes from 0.055 to 0.11 and then back to 0.055 at chainage 11,400, 12,930 and 15,270 m, respectively. The difference between measured and simulated WSEs do not fall within an acceptable range of accuracy (0.15 m) at some measured locations. Extreme values of difference is +0.23 m to -0.30 m for the low discharge. Positive value indicates higher measured value, whereas opposite with negative values. However, the range is narrow +0.19 m to -0.25 m for the medium flow.

These deviations are most likely due to a combination of linear interpolation between simulated values in order to calculate WSE at the measured point and also may have reflected local hydraulic conditions that 1D model is not able to simulate (e.g., variation of WSE along cross-section). Some of the field measured WSE points are located near the right channel bank, where WSE varies from one bank to another. We also calculated possible uncertainties in the LiDAR surveyed topographic elevations, which are comparable with Skinner (2011). These errors may be more pronounced at those areas causing the larger observed discrepancy between predicted and observed WSEs.

Model validation analysis showed a reasonable correlation between simulated and observed water wave-travel along the river reach. The RMSE errors in WSE were 0.14, 0.09 and 0.04 m for Cow Creek Bridge, Private Bridge and Canyon, section, respectively, which is less than the targeted value of 0.15 m. Most importantly, the model is able to replicate comparable water surface elevation change due to ramping discharge from the Anderson Ranch Dam at all three locations (Figure 6.6, Figure 6.7 and Figure 6.8). However, we believe that there is a problem in observed WSE at the Private Bridge. The observed WSE should be near constant within a period of constant discharge release from the dam. Thus, the validation confirms that boundary roughness assigned along the river during model calibration processes replicates the field condition.

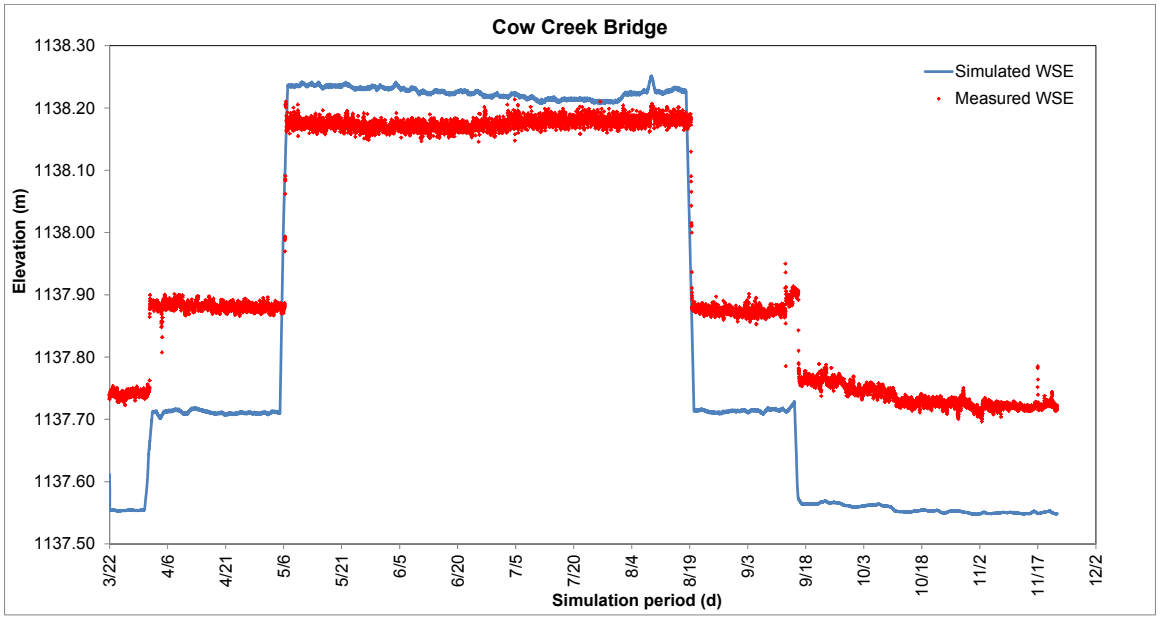

Figure 6.6: Simulated and observed WSE at the Cow Creek Bridge

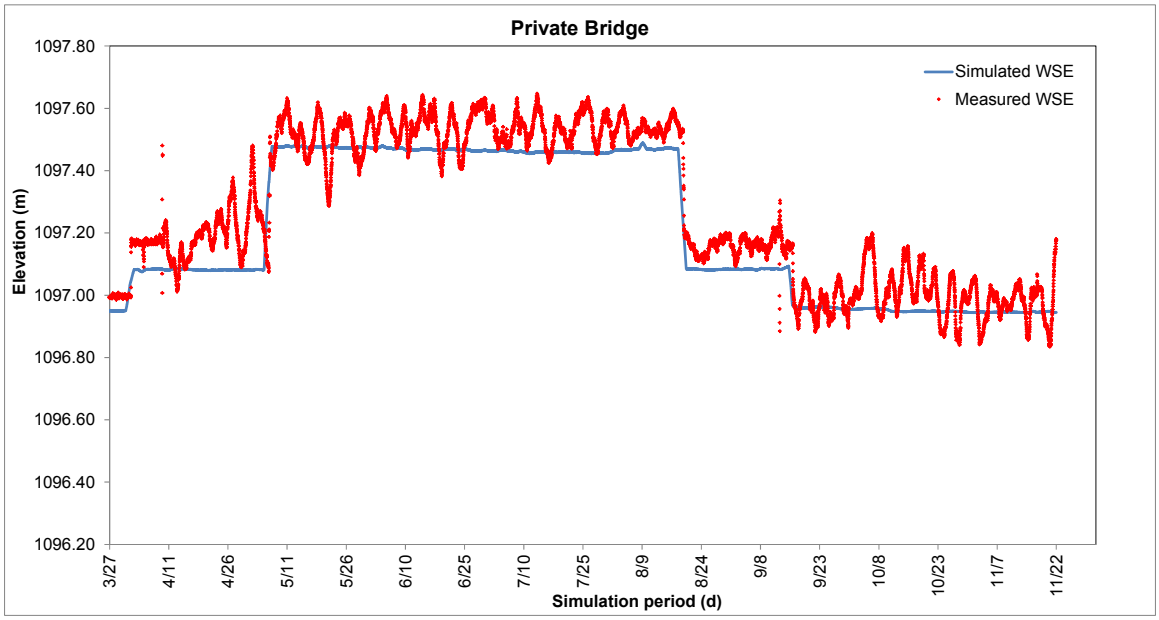

Figure 6.7: Simulated and observed WSE at the Private Bridge

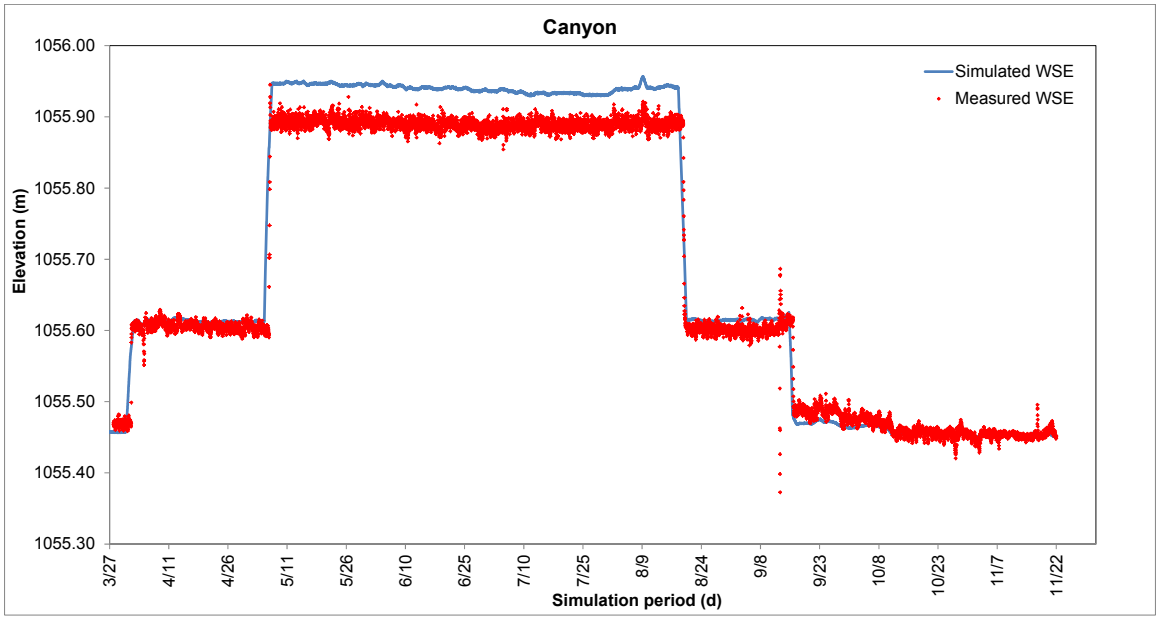

Figure 6.8: Simulated and observed WSE at the Canyon section.

6.3.2 Stream temperature model

MIKE11 temperature model performance after calibration was analyzed by comparing field observed and model simulated temperatures at Cow Creek Bridge, Danskin Bridge, Private Bridge and Canyon section of the main stem for the period between 3/22/2013 to 11/22/2013 (Figure 6.1). Figures below showed observed and simulated temperatures with 30-minute time step (Figure 6.9, Figure 6.10, Figure 6.11, and Figure 6.12).

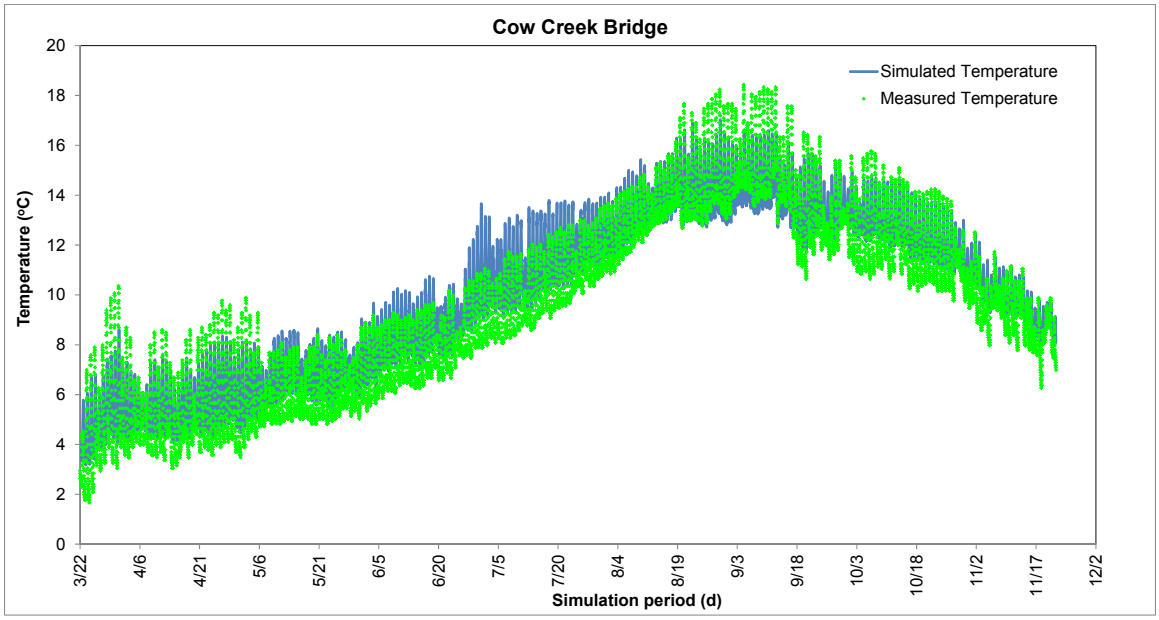

Figure 6.9: Observed and simulated temperatures at the Cow Creek Bridge.

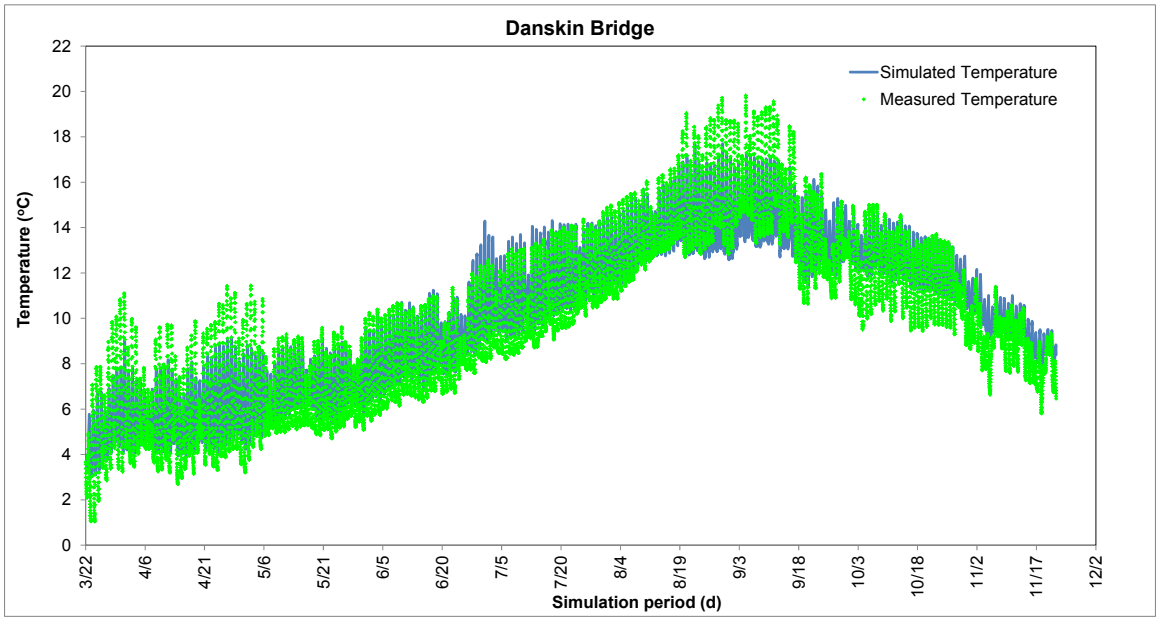

Figure 6.10: Observed and simulated temperatures at the Danskin Bridge.

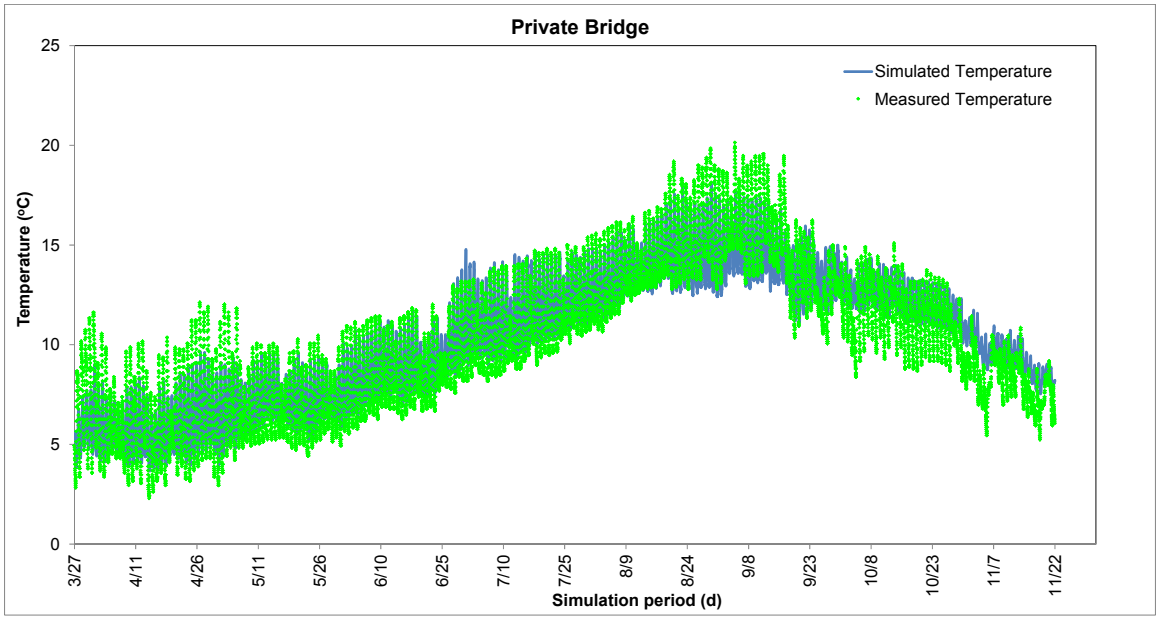

Figure 6.11: Observed and simulated temperatures at the Private Bridge.

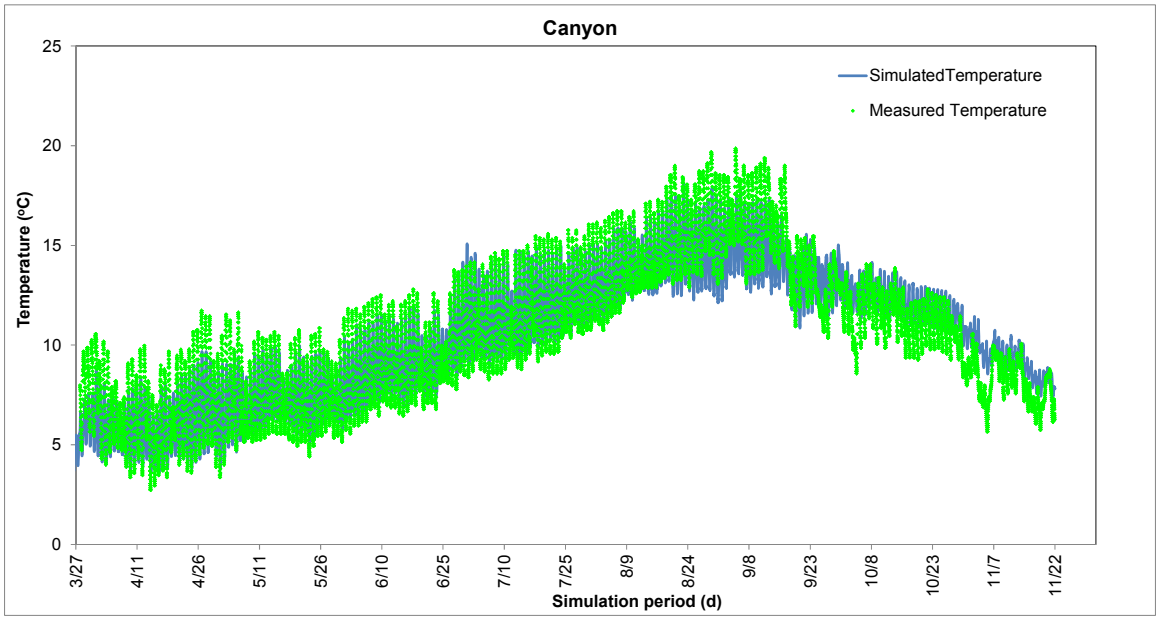

Figure 6.12: Observed and simulated temperatures at the Canyon section.

The RMSE error between simulated and observed 30-min time step temperatures were 1.15, 1.34, 1.61 and 1.49 for Cow Creek Bridge, Private Bridge and Canyon section, respectively. Whereas, the RMSE for daily averaged simulated and observed temperatures were 0.66, 0.70, 0.86 and 0.95 °C, respectively. The results showed simulated temperatures overlaid with the observed temperatures throughout the simulation period. The model is able to replicate change in temperature quite well throughout the simulation period at all four locations. The

model somehow over predicted the stream temperature during some summer days (Figure 6.9). This result could be influenced by the calculated temperature model boundary condition. The measured temperature is not available at the model boundary, which is at the Anderson Ranch Dam gauge station. The measured temperature is available at the dam outlet, which is about 2.8 km upstream from the model boundary. Thus, we calculated water temperature for the model boundary by linear interpolation between measured temperature at the dam and Cow Creek Bridge.

7 TWO-DIMENSIONAL HYDRAULIC MODEL

7.1 *Introduction*

Two-dimensional (2D) models are developed to simulate flood inundation patterns in complex topography (Horritt, 2000; Horritt and Bates, 2002; MacWilliams et al., 2004) and for ecohydraulics analyses (Lane and Bates, 1998; Crowder and Diplas, 2000). Two-dimensional (2D) models represent spatial and temporal variations of flow properties in longitudinal and transversal directions. Past studies have shown that one-dimensional (1D) and two-dimensional (2D) models may provide comparable cross-sectional averaged properties when the topography mostly varies longitudinally, but they diverge when complex transversal topographical features are present, causing change in flow gradients (Brown and Pasternack, 2009; Benjankar *et al.*, 2014b). One of the reasons for the application of a 2D model over the traditional 1D or quasi 2D models is its capability to provide a more robust result in stream with complex bathymetry (Gillam et al., 2005).

Furthermore, the application of 2D modeling in ecohydraulics analyses has been supported by advances in data-acquisition methods such as Green LiDAR (McKean et al., 2009b) and development of efficient and robust numerical codes (e.g. FaSTMECH and MIKE21) and the availability of fast and affordable computers (Hardy, 1998).

For 2D flow modeling, the grid resolution should be high enough to capture complex flow pattern (e.g., eddy) and morphodynamic features such as pool, riffle, run, etc. For instance, large boulders or cobbles are a key topographical and morphodynamic features and they have ecological importance. Previous studies (e.g., Lane and Richards, 1998; Benjankar *et al.*, 2014b) have shown that flow predictions will be affected by the topographic interpolation.

A 2D model solves the depth-average Reynolds Averaged Navier-Stokes (RANS) equations, also known as shallow water equations. 2D models derived flow properties are averaged on the transversal or vertical directions. The vertically averaged RANS equations derived from the three-dimensional shallow water equations, which assume negligible vertical accelerations are used to compute water surface elevations and horizontal velocity components. Vertically averaged models are most common in studying stream hydraulics where transversal

and longitudinal spatial distributions of water depths, shear stresses and vertically (depth) averaged velocities are important.

One of the disadvantages of 2D models is its longer computational time than 1D modeling. However, this is becoming less important as computer hardware capability improves. 2D models are typically used at the geomorphic unit and reach scales (10-50 channel widths) because they require detailed topographical surveys with a resolution finer than the important topographical features such as pool and riffles and have high computational requirements. It has been applied with high resolution (e.g., 10^{-1} channel widths or 1–10 m^2) on several kilometers of reaches (Barton et al., 2005; Pasternack and Senter, 2011). In ecohydraulics, 2D hydraulic modeling is becoming more common because it can be sufficient for most applications in ecohydraulics. For example, it can be applied at the 1 m^2 scale, which is comparable with the fish microhabitat scale (Leclerc et al., 1995; Pasternack and Senter, 2011). Some of the advantages of a general 2D model compared to a 1D are outlined below:

- The flow in a wide floodplain is mostly a two-dimensional process.
- The 2D model can incorporate a full representation of the actual area terrain to be modeled, instead of a series of interconnected cross-sections.
- The 2D model can determine flow path as a function of topography and applied boundary conditions.
- Manning's roughness coefficients can be specified in terms of a detailed roughness map that is the function of grain size and vegetation covers.
- The 2D model is also able to simulate local flow properties such as velocity, inundation depth, duration, and shear stress with have important riverine ecological functions.

Field data required for 2D modeling are detailed topography of the study area, water surface elevations along the reach and hydrographs at specific locations or stage-discharge relationship at the downstream end of the model, grain size distribution and vertically averaged velocity distributions. DEM construction from topography is the primary foundation for all modeling efforts; therefore, it should be as accurate as possible. Accuracy and reliability of DEM is simply a function of the accuracy and reliability of data sources, (i.e., LiDAR, field survey, and photogrammetry, etc). Recent development of remote sensing technology in the form of light detection and ranging (LiDAR) provides a considerable advancement in elevation accuracy over

conventional topographic mapping sources (Brown, 2005; McKean et al., 2009b). It is also equally important to understand that potential errors associated with interpolation of grid surfaces from point and contour data, and converting from high resolution to low resolution. DEM is a very critical factor for producing a sound and reliable model results.

The boundaries of the model should be in a simple reach avoiding recirculating eddies, which may create model instability. Typically, the upstream boundary conditions consist of a constant discharge or a hydrograph and profile of vertically averaged velocities. The downstream boundary conditions are constant water surface elevations or time series a stage–discharge relationship. If tributaries are contributing discharge in the model domain, boundary condition should be provided as point boundary conditions.

Initial conditions specify the initial values of hydraulics for unsteady and steady state simulations at each grid within the numerical domain of the model at the beginning of a simulation. It can be spatially varied or constant value throughout the model domain. Water surface elevation is the most important variable, which can be specified based on field measured values, predicted from a 1D simulation or linearly interpolated between an upstream and downstream elevation or 2D model simulated values before model calibration. The values of the other dependent variables, such as flow velocity and depth, are then derived from the continuity or the uniform flow equation (Tonina and Jorde, 2013). Furthermore, the model can be started as a "hot-start" option, which defines the model variables from a previous simulation results within the entire domain.

Parameterization is the process to assign model parameters such as turbulence parameters and the streambed roughness required to predict flow hydraulics, which are specific for the study reach. In 2D models, a spatially varied roughness parameter is one of the main parameters to calibrate a 2D model. Streambed roughness expresses the resistance within a grid and it accounts for local losses due to grain size, turbulence and land cover. The roughness is the most important parameter for model prediction, which can be estimated from field study, theoretical analysis, by model calibration or a combination of these methods. Typically, modelers use a combination of field measurements and theoretical analysis for estimating model parameters (Lane, 1998; Crowder and Diplas, 2000) followed by an assessment of model performance rather than optimizing parameters through calibration alone.

Calibration is a process of estimating model parameters such as lateral eddy viscosity and streambed roughness in order to minimize differences between predicted and measured values. Typically, water surface elevation and/or velocity distribution at selected locations are compared during model calibration processes. The calibration processes may be affected by equifinality, where different parameter combinations may result to the same observed data (Beven and Freer, 2001; Pasternack et al., 2004). Furthermore, optimizing parameters during calibration may reduce model predictive capability under different boundary conditions. Therefore, to use field measured information and theoretical analysis of model parameter (e.g., roughness) followed by a comparison between predicted and observed values may limit equifinality. The model parameter values should be adjusted or optimized within a realistic range. Following the model calibration, validation is done by comparing predicted and measured water surface elevations, flow depth or vertically averaged velocities for different discharge or time period, which was not used during the calibration process.

7.2 *Methodology*

7.2.1 2D hydraulic model setup

We developed 2D models utilizing high-resolution (2m grid size) DEMs, upstream discharge and downstream water surface elevation as boundary conditions for 23 km river reach of South Fork Boise River (SFBR), which is wider and open than downstream canyon reach (Figure 7.1). For the current study, 2 m grid size was selected considering objective of the study (fish habitat analysis), computational time and the extent of the study area. The original 1m grid size raster was resampled with the nearest neighborhood method to develop 2 m grid size raster, which is converted to DEM to use as model bathymetry. Resampling is the process of interpolating grid values when transforming raster dataset from one resolution to another.

Considering computation time required for the simulation, the model reach is divided into Upper (13 km) and Lower (10 km) reaches (Figure 7.1). Therefore, two separate models were developed to represent the entire 23 km study reach. In order to minimize the effect of boundary conditions, the upper and lower model extents overlapped by 120 m. Furthermore, we disregarded the areas that are 60 m from upstream and downstream boundaries of each model.

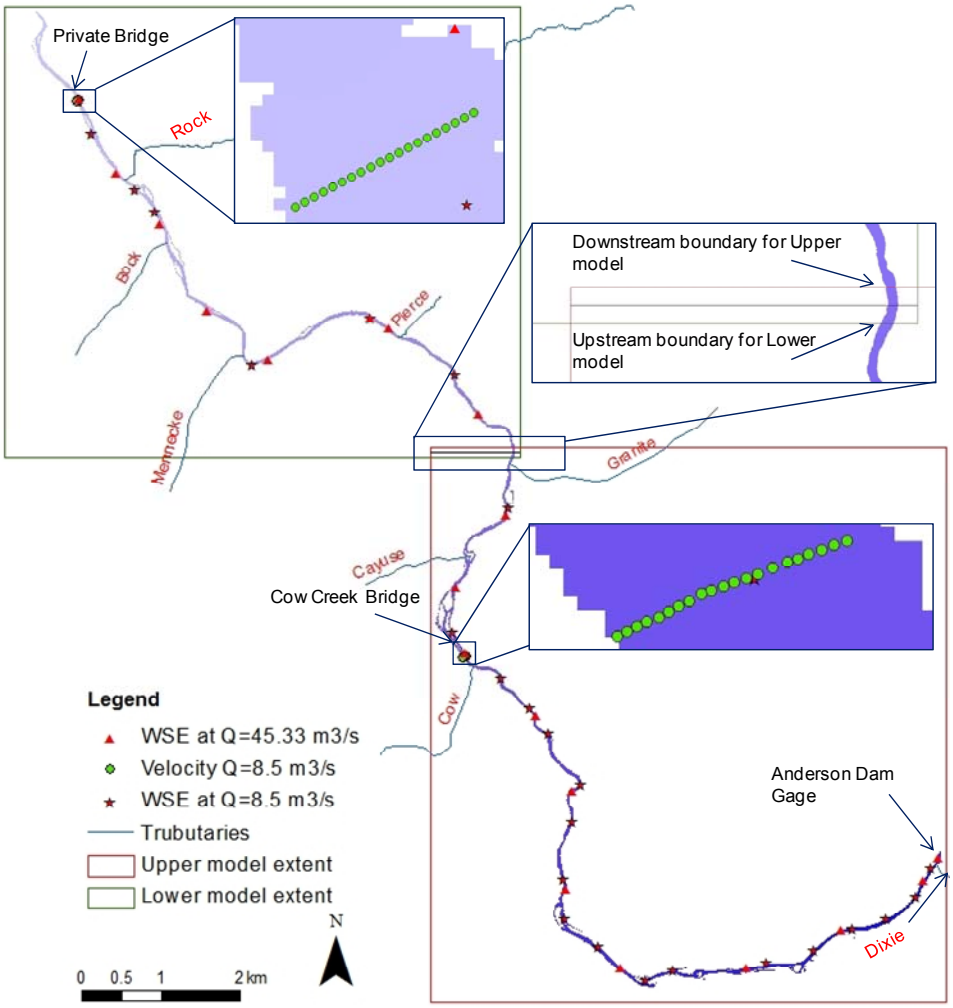

Figure 7.1: Upper and lower 2D model extents, water surface elevation and velocity measured locations along the channel.

We used MIKE 21 software as the 2D model. MIKE21 is a 2D free-surface flow modeling system used to simulate two-dimensional hydraulics and hydraulics-related phenomena such as water surface elevations, depth-averaged flow velocities and bottom shear stresses in estuaries, coastal areas, and floodplains (DHI, 2007). The MIKE 21 flow model simulates unsteady hydraulic properties with the defined bathymetry and other parameters, such as resistance and eddy coefficients, using a finite difference algorithm (DHI, 2011b). It solves the time-dependent, vertically-integrated RANS equations of mass and momentum conservation in two-horizontal directions.

We simulated flow properties depth, water surface elevation and velocity for two constant low (8.5 m^3/s) and medium (45.33 m^3/s) discharges. The flows are upstream boundary conditions

for both Upper and Lower models. The downstream boundary conditions were water surface elevation for corresponding discharges simulated from the 1D model. We did not consider tributary input during model calibration because contributions from them were negligible compared to Anderson Ranch Dam releases (Section 6.2.6). The simulation period for each discharge was 12 and 10 hours for Upper and Lower models, respectively. The simulation time period was estimated based on time required by the flow to travel from the upstream to downstream model boundary for a discharge 4.25 m^3/s over an initially dry channel bed. We assigned simulated water surface elevation discharge for 4.25 m^3/s as an initial condition for other simulations.

7.2.2 2D hydraulic model calibration

We assigned constant Manning's coefficient *n* of 0.025 $m^{1/3}/s$ for the entire channel bed inundated at a discharge of 4.25 m^3/s and a higher Manning's coefficient *n* of 0.03 $m^{1/3}/s$ on the remaining part of the stream bathymetry, which includes the banks, and on floodplain. Currently, the minimum flow in the SFBR is 8.5 m^3/s. Our pre-analysis showed that there is negligible difference in inundation extent between the discharges of 4.25 and 8.5 m^3/s in the current channel bathymetry.

We surveyed water surface elevations for low (8.5 m^3/s) and medium (45.33 m^3/s) discharges along the SFBR (Figure 7.1). Detail about water surface elevation measurements are described in Section 6.2.9. We measured flow velocities twice during low flow at Cow Creek and Private Bridge. The velocity measurement points were approximately 2 m apart across channel and approximately at the same location in both days. We compared the time-averaged measured velocity with simulated velocities.

We calibrated the model adjusting the Manning's coefficient *n*, to minimize the differences between measured and predicted velocities and water surface elevations. We adjusted Manning's coefficient *n* within a realistic range for this type of stream.

Model simulated 2 m resolution velocities were converted to Triangulated Irregular Network (TIN) format and converted into 1 m ArcGIS compatible Raster format to avoid error

associated with the grid size. The simulated velocities were extracted at the field measured locations from 1 m Raster using ArcGIS tool. We calculated the root mean square error (RMSE), the coefficient of determination (R^2) and average error (AE) to evaluate difference between measured and predicted water surface elevations and velocity.

7.3 *Calibration Result and Discussion*

After several iterations, we selected the Manning's coefficient *n* value of 0.025 and 0.03 $m^{1/3}/s$ for channel and outside the channel extent, respectively for both low and medium discharges. The results of model calibration for both discharges are shown in Figure 7.2 and Table 7.1. The RMSE and AE were 0.2 m and -0.01 m, respectively for low flow, whereas 0.17 m and -0.09 m, respectively for medium flow. These results from the model calibration show acceptable agreement between the simulated and the measured WSEs for both discharges.

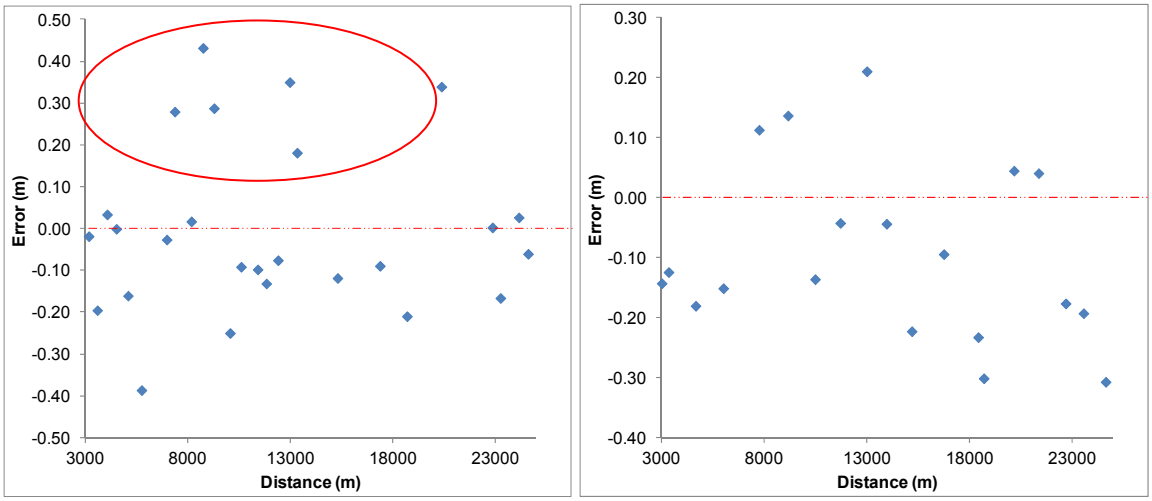

Figure 7.2: Difference between measured and predicted water surface elevations for discharges of 8.5 (left) and 45.6 m^3/s (right). +ve and –ve values indicate higher and lower measured values, respectively.

The RMSE for velocities at Cow Creek and Private Bridges were 0.07 m/s and 0.10 m/s, respectively at low discharge (Figure 7.3 and Table 7.1). Overall combined RMSE and AE were 0.09 m/s and -0.01 m/s, respectively. The correlation coefficient was 0.77 (Table 7.1). The model calibration results showed acceptable agreement between the simulated and the measured velocity for both Cow Creek and Private bridges.

Table 7.1: Root mean square error (RMSE) and average error (AE) for water surface elevation and velocity. +ve and –ve values indicate higher and lower measured values, respectively

SN	Discharge (m^3/s)	WSE (m)		Velocity (m/s)						
		All		CCB		PB		Combined		
		RMSE	AE	RMSE	AE	RMSE	AE	RMSE	AE	*R^2
1	8.5	0.20	-0.01	0.07	0.04	0.10	-0.05	0.09	-0.01	0.77
2	45.33	0.17	-0.09	-	-	-	-	-	-	-

[All]Including all measured points [RMSE]Root Mean Square Error [AE]Average Error

[Partial]Excluding specific measured points [PB]Private Bridge [CCB]Cow Creek Bridge

*Combinding all velocity measured points at Cow Creek and Private Bridges and setting Intercept=0

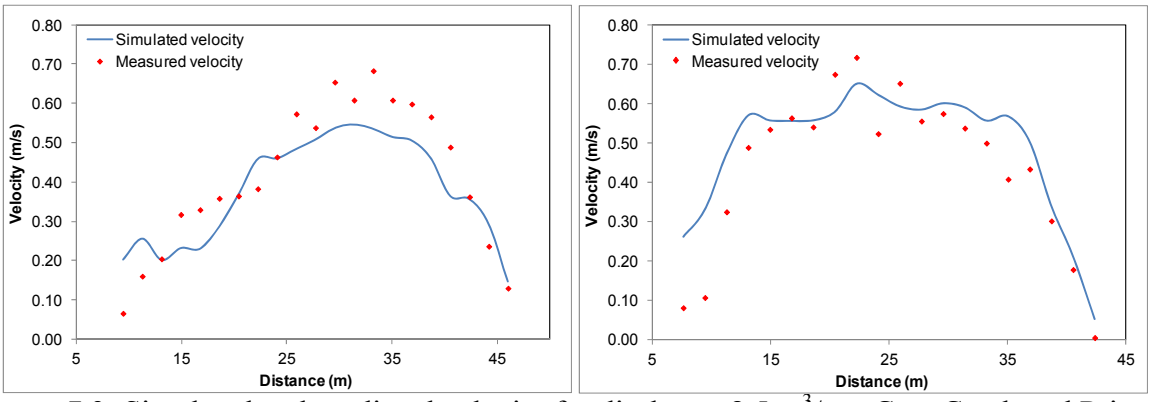

Figure 7.3: Simulated and predicted velocity for discharge 8.5 m^3/s at Cow Creek and Private Bridge, respectively. The progressive distance is from the right to left bank.

We did not optimize Manning's coefficient *n* for the specific flow or measured location. This approach may help to improve the accuracy of the model at other discharges. For example, we could increase Manning's coefficient *n* at specific locations (within red oval in Figure 7.2) in order to increase simulated water surface elevation, which would result in lower RMSE at low discharge. One of those locations was close to Cow Creek Bridge velocity measurements. The agreement between simulated and measured velocity is satisfactory in this area, which indicates Manning's coefficient n (0.025) is reasonable and within a realistic range. The average error between measured and predicted velocity was +0.4 m/s, which reveals higher Manning's coefficient *n* in the model than in the field. If we have increased roughness coefficient to improve RMSE for water surface elevation, that would have negatively affected the velocity distribution and accuracy. Most importantly, LiDAR surveyed topography was about 0.63 m (average) lower than surveyed topography near this area (Table 2.1 in Section 1.3.2). Although, we raised entire SFBR topography by 0.39 m, the value was probably not enough for Cow Creek Bridge area, which resulted in noticeable lower water surface elevation than measured.

Therefore, based on different factors such as uncertainty in measurement and bathymetry, Manning's roughness coefficient *n* adjusted during model calibration processes is reasonable (Tonina and Jorde, 2013). These Manning's roughness coefficient *n* of 0.025 and 0.03 for channel and outside channel extent will be used for all other simulations.

8 FISH HABITAT MODEL

8.1 *Introduction*

River-damming and reservoir operations, which have economic benefits and reduce flood hazards, are one of main human influences on freshwater ecosystem worldwide (Poff et al., 1997; Pringle, 2003). They have affected hydrological processes by altering stream water flow, nutrient concentration, water temperature, sediment transport and direct impact on riverine ecosystem as a habitat loss and aquatic biodiversity decline. Changes in flow regime, whose hydrograph depends also on watershed hydrology, affect channel connectivity to floodplain, side-channel and backwater habitats that are important to a variety of terrestrial and aquatic ecosystems. Floodplain contain off-channel habitats that include sloughs, wetlands, side channels, and other seasonally-flooded lands, which are productive for juvenile fishes (Schlosser, 1991; Martens and Connolly, 2014) and can serve as refugia, during high flows in the main channel (Bell et al., 2001).

On top of human influences, warming climate is projected to accelerate (IPCC, 2013) and to increase precipitation variability and extreme events: both droughts and floods. Climatic variability will impact the thermal regime of aquatic systems as well as shift in aquatic habitat distribution for different species (Perry *et al.*, 2005; see, Battin *et al.*, 2007). Researchers have already found increased precipitation variability and decreased snowpack that have been linked to warming, altered stream hydrology and increased channel disturbance from post-fire landslides and debris flows in the Pacific North West of the United States (Isaak et al., 2010). These impacts may force to change water resources development, operation, and management in the future. Interaction among flow releases, timing and dam operation on stream thermal regime, which is a key element for aquatic habitat quality (Torgersen *et al.*, 1999; Lessard and Hayes, 2003; Johnson *et al.*, 2004; Danehy *et al.*, 2005; Loinaz *et al.*, 2013; Carey and Zimmerman, 2014; Hébert *et al.*, 2015)**,** has also been overlooked and a major gap in current environmental flow assessments (Olden and Naiman, 2010).

Riverine ecosystems depend on maintaining and recovering hydraulic habitat that includes structural components associated physical landscape, processes related by flow dynamics and

understanding of species habitat requirements for survival and reproduction (Merenlender and Matella, 2013). Physical processes driven by channel flow determine the health of riverine ecosystem and habitat availability or suitability; therefore recovering hydraulic habitats are focused on recovering more natural flows and channel morphology (Tetzlaff et al., 2007). Instream flow incremental methodology (IFIM) provide the framework for aquatic habitat modeling to study aquatic ecosystem (Bovee, 1982), where habitat is quantified in terms of Suitability Index (SI) and Weighted Usable Area (WUA) as a function of discharges, but habitats also changes spatially and temporarily with discharges. One of the criticisms of IFIM approach is, it overly focused on reach scale based on physical habitat (e.g., depth, velocity, substrate, cover, etc.) but there are many variables such as water quality, flow regime (temporal distribution), and competition and predation between species (Hudson et al., 2003; Leclerc et al., 2003). These models have been frequently used to analyze fish habitat as a function of discharge (e.g., Tiffan *et al.*, 2002; Muhlfeld *et al.*, 2012) to study habitat improvements due to river restoration activities (e.g., Lacey and Millar, 2004; Pasternack et al., 2004) and to establish environmental in-stream flows releases from reservoir (Bovee et al., 1998). However other methods such as bio-energetic or carry capacity biological model could be used as well.

Stream water temperature is crucial physical characteristics of aquatic systems because it affects water quality parameters as well as biological processes of aquatic species such as ecology, evolution and distribution (Carey and Zimmerman, 2014). Severity of impacts of hydrological alteration on stream water temperature depends on many factors such as discharge magnitude, local hydraulics, size and purpose of dam and noticeably it varies temporarily and spatially (Poff and Hart, 2002; Hudson *et al.*, 2003; Lessard and Hayes, 2003). For example, fish species may not use a favorable habitat physically considering water depth, velocity and substrate, if water temperature is exceeds a threshold critical value (Torgersen et al., 1999). Despite water temperature being an important variable for salmonid habitat, most of current studies lacked consideration for aquatic habitat (Lessard and Hayes, 2003; Johnson *et al.*, 2004; Danehy *et al.*, 2005; Loinaz *et al.*, 2013; Hébert *et al.*, 2015). Furthermore, apart from few studies (e.g., Hightower et al., 2012; Li et al., 2015) most of habitat models have not considered stream water temperature, while analyzing available habitat (e.g., Tiffan *et al.*, 2002; Muhlfeld *et al.*, 2012). Studies have considered water temperature separately instead of integrating with

physical variables water depth, velocity, substrate to calculate combined habitat suitability (Maret et al., 2006; Sinokrot and Gulliver, 2010).

Hydrological, thermal and water quality regimes of streams and rivers depend on large-scale hydrological and atmospheric cycles in unregulated systems and also by dam operation in regulated system. These effects then cascade on habitat quality, which can be quantified with different methods from the in-stream flow incremental methodology (IFIM) (Bovee, 1982), carrying capacity (Cramer and Ackerman, 2009) or bioenergetic methods (Chipps and Wahl, 2008). Despite the needs to have tools for simulate different scenarios to quantify the complex interaction among biotic and abiotic systems, based on our knowledge only few models integrating large scale processes such as hydrological modeling with fine scale processes such as aquatic meso- and micro-habitat were proposed so far to analyze status or impacts of human activities or climate change on riverine ecosystem (e.g., Loinaz *et al.*, 2013; Merenlender and Matella, 2013; Kail *et al.*, 2015). Merenlender and Matella (2013) integrated modeling of stream flow and aquatic habitat but did not account for watershed hydrological and water quality modeling. Loinaz et al. (2013) simulated watershed hydrology, stream water temperature and interaction between surface and ground water but did not link them to habitat quality. Recently, Kail et al. (2015) simulated watershed hydrology and water quality using SWAT, river hydraulics and change in channel morphology by 2D hydrodynamic model, whose outputs fed a spatially distributed habitat model in order to predict presence or absence of aquatic species. This last integrated model is what we defined an "ecohydraulics virtual watershed" because it captures large-scale physical processes and quantifies their effects on local biotic processes.

The calibrated and validated models presented in the previous sections are used as a cascade of models to quantify rearing habitat quality and distribution of the native endangered Bull Trout, a cold water fish species

8.2 *Methodology*

We developed an integrated modeling framework, which links physical and ecologic processes to analyze aquatic habitat distribution. Physical model includes hydrologic (Chapter 4), hydraulic and temperature modeling (Chapter 5 and 6), whereas fish habitat represents their

biological processes and behavior. Watershed hydrological model is used to predict hydrology and water quality information used as boundary conditions for hydraulic models. The predicted local flow hydraulics and water quality values were used as inputs of an instream flow incremental methodology (IFIM), the selected ecological model, to predict spatial and temporal aquatic habitat quality distribution (Bovee, 1982).

8.2.1 Preference curves

Bull Trout is a coldwater species and their life-cycle are sensitive to temperature change (Fraley and Shepard, 1989; Rieman and Mclntyre, 1993). Thermal requirement for Bull Trout may vary with geographical area (Hillman and Essig, 1998; Poole *et al.*, 2001; Selong *et al.*, 2001; Anglin *et al.*, 2004). Although it has been hypothesized that Bull Trout optimal survival and reproduction temperature occurs within a narrow range (<15^{o}C) of cold temperatures, Hillman and Essig (1998) has shown that they can adopt their life-cycle to wide range of temperature thresholds (Howell *et al.*, 2010).

We used daily maximum temperature (DMT) as a metric for temperature suitability index (SI_t) for each day based on literature information. Previous researchers concluded DMT above a critical threshold is a fundamental parameter for determining distribution of majority of aquatic species (Olden and Naiman, 2010). Based on a literature review (Bonneau and Scarnecchia, 1996; Poole *et al.*, 2001; Selong *et al.*, 2001; McMahon *et al.*, 2007; Maret and Schultz, 2013), we identified SI_t for <16^{o}C and >22°C are 1 and 0, respectively, whereas for 16-22°C, it is linearly interpolated (Figure 8.1, left). We then verified the water temperature preference curve by comparing stream water temperatures at Bull Trout locations in the South Fork Boise River. Because DMTs do not change considerably spatially (from upstream to downstream) for the specific day in our study site, we used a single SI_t for entire study area (see, Maret et al., 2006) (Figure 8.2).

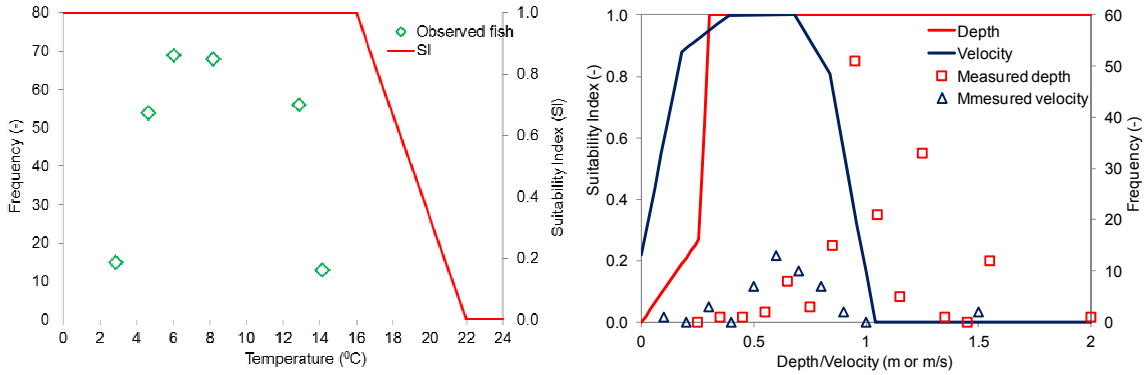

Figure 8.1: Temperature preference curve and green diamonds represents measured water temperatures at fish locations (left).Water depth and velocity preference curves for Bull Trout rearing habitat, red squares and blue triangles are measured depths and velocities at fish locations (right).

This approach might introduce some uncertainties, when DMTs are different between upstream and downstream areas and between 16°C to 22°C (Figure 8.2).

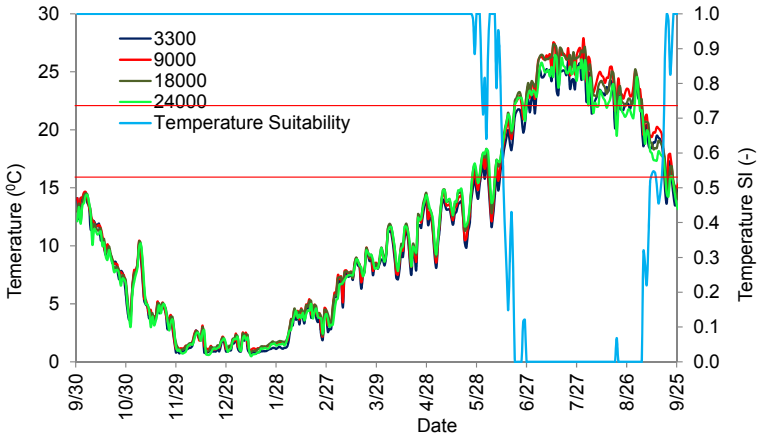

Figure 8.2: Maximum daily temperature from upstream (XS3300) to downstream (XS24000) for the entire simulated water year (WY 2013)

We adopted depths and velocities rearing habitat preference curves from previous studies (Lewis River workshops, 2000; WDFD, 2004). Although, these preference curves are developed for streams of Washington State, observed water depths and velocities at Bull Trout observed locations in the SFBR system fitted fairly well (Figure 8.1, right).

8.2.2 Fish habitat model development

We developed a fish habitat model in ArcGIS to quantify habitat quality using simulated water depth, velocity, and temperature with univariate rearing habitat preference criteria for Bull Trout. We used geometric product of the individual cell suitability indices, *CSI*, to determine the overall habitat suitability index (*HSI*) (Moir *et al.*, 2005; Tonina *et al.*, 2011; Benjankar *et al.*, 2014b). The model quantifies spatially distributed *CSI*, an indicator of habitat quality at the cell scale (2 m grid size), and weighted useable area (WUA), an indicator for quality at the river segment scale (10^2 channel width) (Bovee, 1978). We specifically selected rearing habitat because the study reach is known as a rearing habitat (which refers to the USFWS classification of the reach as Foraging, Migration, Overwintering habitat) for sub-adult and adult Bull Trout year around.

We calculated suitability index for each *i*-th grid cell ($SI_{i,j}$) and *j*-th variable, considering water depth ($SI_{i,d}$),velocity ($SI_{i,v}$) and temperature ($SI_{i,t}$) and preference criteria for those variables using eq. 7.1, which simplifies to eq. 7.2 when SI_t is constant over the entire study area for the specific day, as in our case:

$$SI_{\mathrm{i}} = \sqrt[3]{SI_{d,i} * SI_{v,i} * SI_{t,i}} \quad (7.1)$$

$$SI_{\mathrm{i}} = \sqrt[3]{SI_{t,i}} * \sqrt[3]{SI_{d,i} * SI_{v,i}} \quad (7.2)$$

We have fish observation data during river discharges of 8 and 16 m^3/s, which were used to validate the fish habitat model. The model predicted high quality habitat, where fish were observed with a good correlations between predicted habitat and fish observations (Figure 8.3).

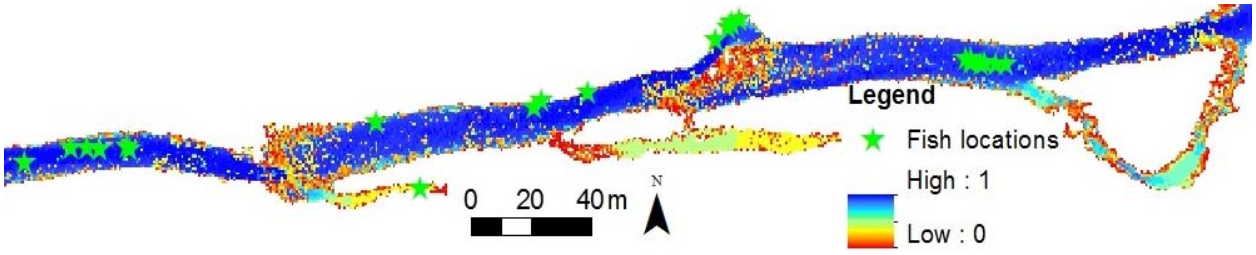

Figure 8.3: Observed fish distribution over spatially distributed habitat quality

8.2.3 Habitat function of discharge

We simulated distributed water depth and depth-averaged velocity with the 2D hydraulic model for the following discharges 4, 8, 17, 28, 45, 57, 68, 85, 102, 142, 184 and 227 m^3/s and then calculated area-weighted median depth and velocity to analyze relationship between discharges and hydraulics. These discharges cover the entire flow regime during both regulated (dam releases) and unregulated (without dam and reservoir) flows. The discharge of 8 m^3/s is the present minimum flow release through the Anderson Ranch Dam, whereas 227 m^3/s (2006) is a maximum discharge measured at the USGS Featherville gauge station (natural) during the period between 1946 and 2012. We also considered a hypothetical minimum release of 4 m^3/s to study the potential impact of dam management during a drought event on aquatic habitat. We used fish habitat model to simulate habitat suitability index (HSI) and change in WUA (Q-WUA curve) based on hydraulics for all discharges.

8.2.4 Habitat time series

We simulated habitat time series for an entire water year (i.e., 2013) based on stream flow at the Anderson Ranch gauge station. Habitat time series, which is an extension of the IFIM approach, can be used to indicate temporal status of habitat (Muhlfeld *et al.*, 2012; Li *et al.*, 2015). Fundamental behind habitat time series is that habitat is a function of stream flow and thus varies temporally. One of the advantages of this approach is that it allows for comparisons of flow management regimens. Mean daily discharges were used to interpolate daily weighted usable areas (WUA) from the Q-WUA curve. Finally, we calculated daily WUA using eq. 7.3 from interpolated hydraulic habitat (SI_h, product between SI_v and SI_d) and temperature (SI_t) suitability indices for the specific day, where (SI_t) and (SI_h) varies daily based on DMT and mean daily discharges, respectively.

$$\mathrm{WUA(t)} = \sum_{i=1}^{N}\left(\prod_{j}^{m} \mathrm{SI_{i,j}}\right)^{1/m} \mathrm{A_i} \qquad (7.3)$$

with N is the total number of cells, m is number of variables and its dimensional form HSI:

$$\mathrm{HSI(t)} = \frac{\mathrm{WUA(t)}}{\sum_{i=1}^{N} \mathrm{A_i}} \qquad (7.4)$$

8.2.5 Habitat prediction

We compared habitat time series considering with- and without-water temperature variable to analyze effect of temperature on habitat for unregulated and regulated scenarios for the year 2013. Regulated and unregulated scenarios define temperature and flow regimes with- and without-Anderson Dam operation impacts. For the without-temperature case, we assigned water temperature suitability Index (SI_t) as 1 for each day assuming water temperature suitability is optimal (eq. 7.1).

Whereas, for habitat distribution, we separated the simulated HSI and WUA between in-channel habitat, that within the bankfull channel (here after in-channel), and lateral habitat, that is beyond the bankfull wetted area extension (here after lateral-channel). The later includes side channels, back water areas and inundated floodplain. We delineated the spatial extent of bankfull channel using the River Bathymetry Toolkit (RBT) that characterizes in-stream and floodplain geomorphology to support aquatic habitat analyses (McKean et al., 2009b). We defined low and high flows those below and above bankfull flow (68 m^3/s), respectively.

8.3 *Results:*

8.3.1 Hydraulics

Inundated areas increased slowly up to the bankfull discharge, thereafter rapidly, indicating the in-channel is entirely inundated and the flow reaches lateral-channels and floodplains (Figure 8.4). The inundation area for the maximum flow (227 m^3/s) was twice (1.14 km^2) that of bankfull discharge. The median (50%) water depth increased with higher discharges, except for 227 m^3/s (Figure 8.4), for which median depth decreased. Furthermore, ranges of minimum (5%) and maximum (95%) depths increased with discharge.

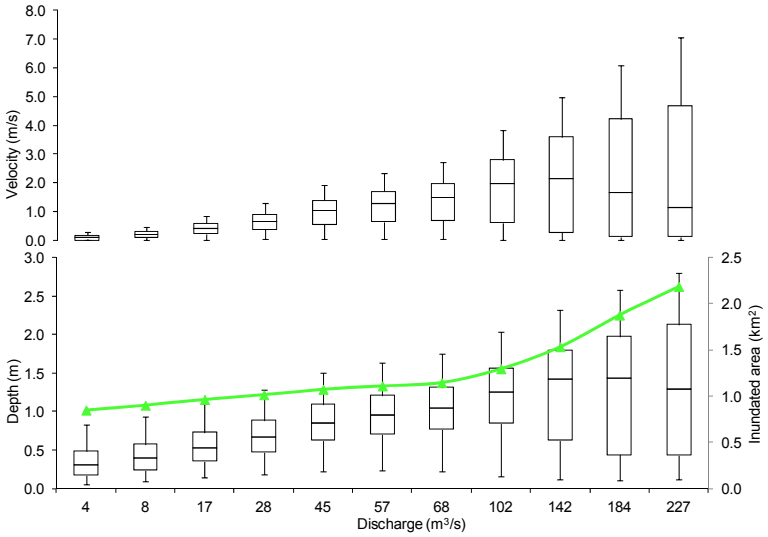

Figure 8.4: Box plots for minimum (5%), first quartile (25%), median (50%), third quartile (75%) and maximum (95%) of water depths (bottom) and velocities (top) for different discharges. Green line indicates inundated area (extent) for different discharges.

Swift flow velocities (larger than 1 m/s) were observed in the in-channel zone, whereas slower in lateral-channel zone (lower than 1 m/s) (Figure 8.4 and 7.5) for discharges higher than bankfull. Area-weighted median velocity increased with higher discharges, except for 184 and 227 m^3/s, where it decreased. This indicated the in-channel connected with side-channels and floodplain increasing inundation areas extensively for these two large flows, where velocities are relatively slower than in the in-channel zone. As with water depths, range of minimum and maximum velocities increased with higher discharges (Figure 8.4).

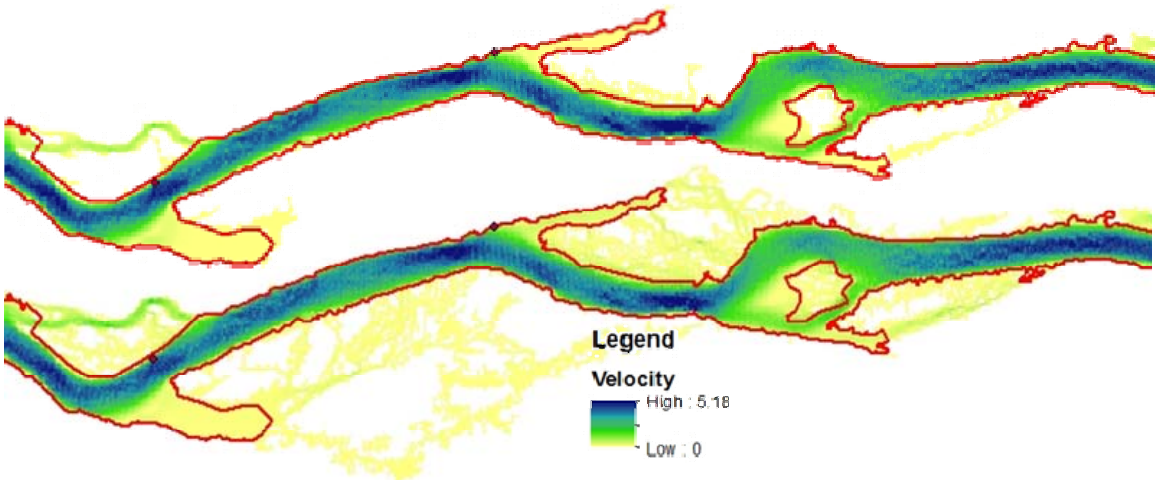

Figure 8.5: Spatial distribution of velocities and inundated areas for discharges 68 m^3/s (top panel) and 102 m^3/s (bottom panel). Red lines indicates bankfull channel boundary.

8.3.2 Habitat

The magnitude of habitat quality changed spatially with higher discharges (Figure 8.6). The in-channel habitat connecting with lateral-channels (side channels and floodplain) during high flows improved Bull Trout rearing habitat (Figure 8.4, 7.5 and 7.6). Optimal rearing Bull Trout habitats were available at discharge 17 m^3/s based on both WUA and HSI, whose values decreased for discharges less than 17 m^3/s primarily due to reduction in flow depths (Figure 8.5 and 7.6) and for discharges higher than 17 m^3/s up to the bankfull but increased for higher flows (Figure 8.6). However, increases in WUAs were considerable compare to HSI (0.21 to 0.33), due to increase in wetted areas (Figure 8.4, 7.5 and 7.6) rather than habitat quality at high flows.

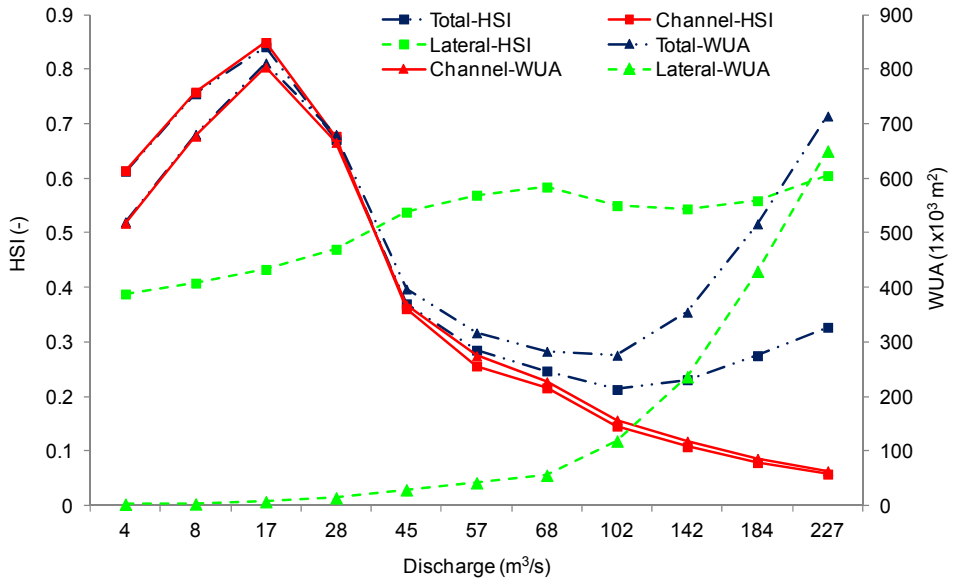

Figure 8.6: WUA and HSI quantified with water depth and velocity only (without temperature) as a function of discharges calculated for channel, off-channel and combined spatial extents.

8.3.3 Temperature effect

During July, August and September, WUA were noticeably lower for the with- than without-temperature cases due to daily maximum water temperature (DMT) larger than the threshold value for optimal temperature (16°C) (Figure 8.7). DMTs were less than 16°C in other months (October to June), resulting with $SI_t = 1$, and consequently with similar habitat between with- and without-temperature. For the regulated scenario, DMTs were less than 16°C, such that

temperature did not affect habitat quality, because dam released cold water within the preference range for Bull Trout during summer months.

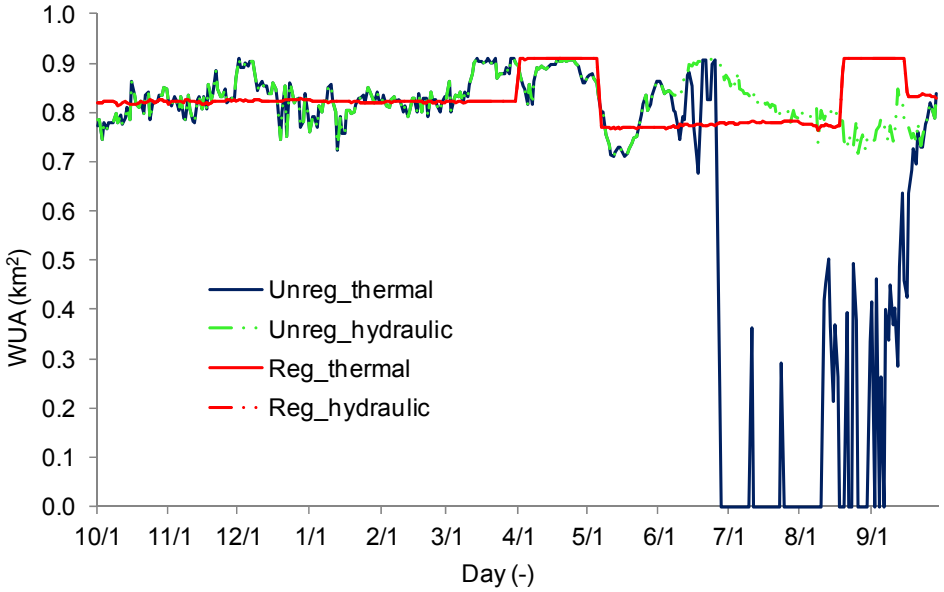

Figure 8.7: Dam regulated and unregulated (natural) weighted usable area (WUA) (left). Temperature in legend indicates inclusion of water temperature for WUA calculation.

8.3.4 Spatial habitat shift

Our analysis showed that the spatial distribution of rearing habitat is quite homogenous and mostly of high quality in the in-channel zone at low discharges (less than bankfull) (Figure 8.8). In-channel average HSI and WUA increase to a peak for 17 m^3/s and then decrease (Figure 8.6). Conversely, lateral-channel WUAs are low at low flows and increased exponentially for high discharges. This result revealed that good quality habitat shifts toward lateral-channel (former floodplain and side channels) as river discharge rises (Figure 8.6 and 7.8). Nevertheless, HSI increased slightly (0.39-0.61) for low to high discharges for lateral-channel.

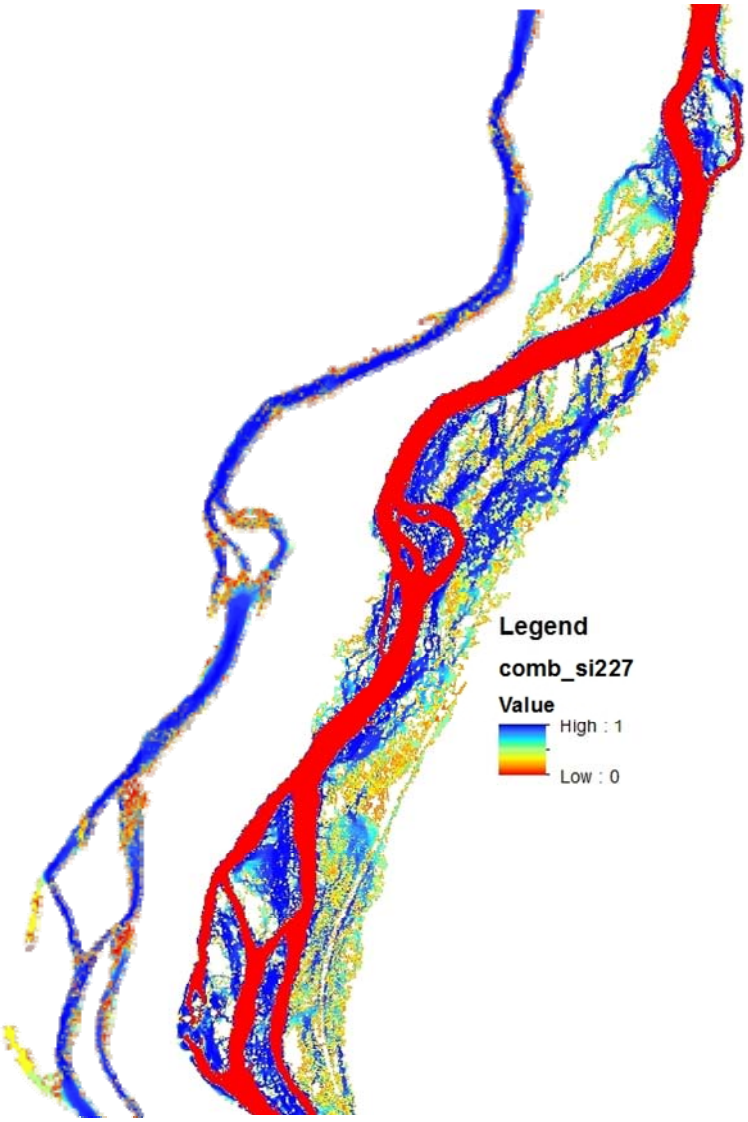

Figure 8.8: Spatial shift in high quality habitat for low (8 m3/s) and high flows (102 m3/s) (right).

8.4 *Discussions*

Bull Trout rearing habitat quality is sensitive to change in river discharges, as it shifts habitat distribution, stream water quality and floodplain connectivity. Minimum flow release through dam less than current minimum flow (8 m^3/s) will reduce the available Bull Trout rearing habitat. Interestingly the flow which (17 m^3/s) maximizes the in-channel habitat is also the minimum flow release during spring and summer months (April to September) to fulfill the

irrigation water demand during average climatic years. However, the dam may release higher discharges depending on water volume in the reservoir.

Summer releases are cold hypolimnetic releases from the reservoir resulting in stream temperature not being a critical parameter for Bull Trout using the SFBR below Anderson Ranch Dam. Migratory Bull Trout annually over-winter in Arrowrock Reservoir and the SFBR the majority of which migrate to their spawning locations in the Middle and North Forks of the Boise River before returning to the reservoir in November (Salow and Hostettler, 2004; U. S. Bureau of Reclamation (USBR), 2013). Our results showed that changes in discharge and water temperature patterns at Anderson Ranch Dam maintain suitable Bull Trout habitat throughout the year (Figure 8.7).

Conversely, stream water temperatures are a critical factor for Bull Trout rearing habitat in the unregulated scenario for the majority of summer months (July, August and September). Thus historically as shown by the unregulated case, Bull Trout may have not used this portion South Fork Boise River for summer rearing habitat due to high temperatures (>22^{o}C), suggesting that they may have migrated upstream or to tributaries (Figure 8.9).

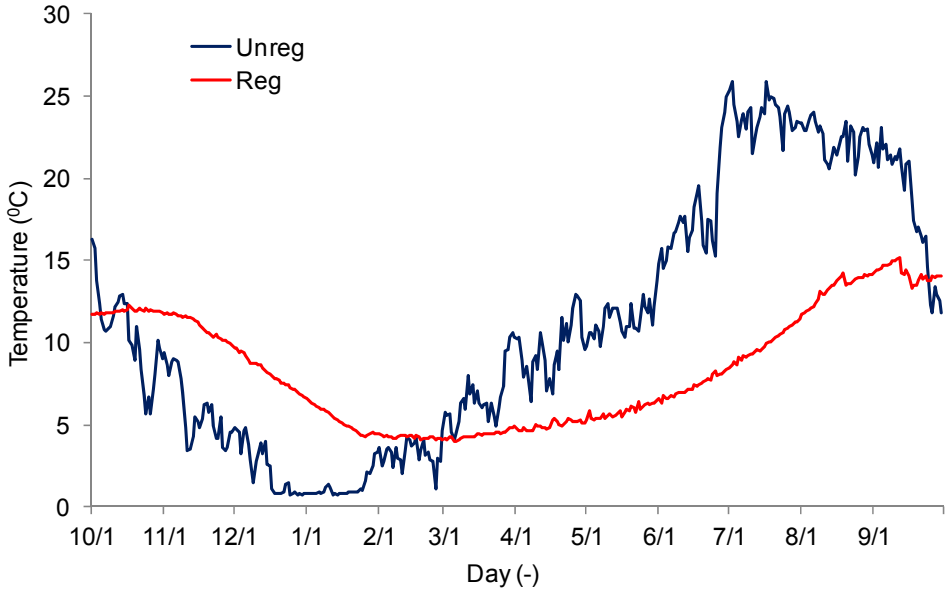

Figure 8.9: Water temperature patterns for the water year 2013 for unregulated and regulated scenarios.

This result confirms the importance of consideration of a water temperature variable, which depends on flow releases, timing and dam operation on stream thermal to analyze aquatic habitat, specifically for summer months (Salow and Hostettler, 2004; Olden and Naiman, 2010; U. S. Bureau of Reclamation (USBR), 2013). One of major finding of our study is that habitat analyses may over predict available habitat for salmonid based only on physical variables without considering water quality (temperature) (Figure 8.7).

Our results underscore the importance of the lateral-habitat as the main refugia for fish at high flows (Shirvell, 1994; Bell *et al.*, 2001) due to shift of good-quality habitat from in-channel to lateral-channel. Adult and sub-adult Bull Trout as well as other fish species such as Sculpins (*Myoxocephalus octodecemspinosus*), Dace (*Leuciscus leuciscus*), Kokanee (*Oncorhynchus nerka*), and Rainbow Trout (*Oncorhynchus mykiss*) resident in the SFBR system could use lateral-channels during high flows (USBR, 2013). Salmonids also use lateral-channel habitats to avoid predation and reduce competitions from other species (Shirvell, 1994) as well as for rearing during winter months (Solazzi et al., 2000). Consequently, conservation and restoration of lateral-channel habitat is necessary and requires periodic high discharges to maintain the connectivity with the main channel (Bowen et al., 2003; Gorski et al., 2014).

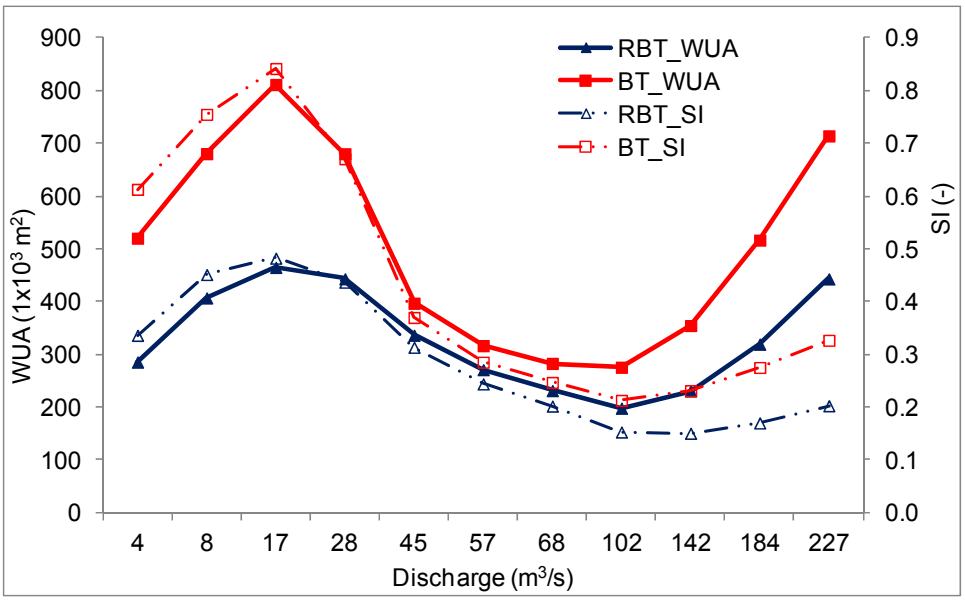

Figure 8.10: WUA and SI for Bull Trout (BT) and rainbow trout (RBT) rearing habitats as a function of discharges

There is a diversity of age classes of Sculpins, Dace, Kokanee, and Rainbow Trout in the SFBR system. Bull Trout prey on these sub-adult sized young nonnative species (USBR, 2013). Idaho Department of Fish and Game, IDFG, surveys of young-of-year Rainbow Trout show good recruitment within the Boise River system. Our study also shows that the Rainbow Trout rearing habitat is comparable to the Bull Trout habitat, although the former is less than the latter during low flows. (Figure 8.10). However, there is no competition documented between the species for this habitat (USBR, 2013). Both SI and WUA decreased with discharge until the main channel connects to former side channels and floodplain.

8.5 *Conclusions*

Contrarily to expectations, our results showed that Bull Trout habitat is not limited by present reservoir operations although operations do alter historic stream temperature and discharge regimes to some extent. Although, in-channel habitat quality decreases with increasing discharge within the channel, good habitat quality shifts to lateral-channels as high flows reconnects lateral-channel with the main channel. At high flows, fish may seek refugia to excessive flow velocity in the lateral-channel. These high flows are important because they shape the stream geometry, clean gravel from fine sediment, mobilize and transport sediments and connect floodplain to exchange nutrients.

9 IMPACTS OF DAM MANAGEMENT ON AQUATIC HABITAT

9.1 *Introduction*

Dam management affects hydrological processes, alters stream flow, sediment transport and water temperature, and potentially habitat loss and reduction of aquatic biodiversity (Poff *et al.*, 1997; Ward and Tockner, 2001; Bunn and Arthington, 2002). Typically, regulated flow decreases magnitude of peak flows and increase minimum base flows. Dam management impacts stream thermal regimes spatially and temporally beside hydrological alterations (Preece and Jones, 2002; Steel and Lange, 2007; Angilletta *et al.*, 2008). However, the magnitude of impacts depends on many factors such as size and purpose of dam, discharge released from dam and local hydraulics (Lessard and Hayes, 2003). Previous studies have documented that rapid reductions in river water surface elevation due to dam management cause stranding of fish species and mortality (Saltveit *et al.*, 2001 ; Bragg *et al.*, 2005; Irvine *et al.*, 2009; Nagrodski *et al.*, 2012). Nevertheless, fish stranding was not just related to the rate of change in water surface elevation, but depends on many factors such as fish species and their life stages, stream temperature, the time of the day versus night (Higgins and Bradford, 1996; Halleraker *et al.*, 2003; Dauwalter *et al.*, 2013).

Additionally, climate change may increase precipitation variability and extreme events, e.g., droughts and floods (IPCC, 2013), decrease snowpack, thereby altering stream hydrology and thermal regime (Isaak et al., 2010). Furthermore, changing climate may impact the thermal regime of river systems as well as shift in aquatic habitat for different species (Perry *et al.*, 2005; see, Battin *et al.*, 2007). These effects may force to change water resources operation and management in future.

Flow alteration by dam management can limit and even prevent lateral hydraulic connectivity, causing disconnection with floodplain, side-channel and backwater habitats from the main channel. Lateral-habitat is a very important refugia for fish and a key part of aquatic ecosystems (Schlosser, 1991; Martens and Connolly, 2014). It can have lower velocity than the main stem and different stream temperature such that it can be both a thermal and hydraulic refugia for fish (Schlosser *et al.*, 2000; Carey and Zimmerman, 2014). However, studies have

shown that reservoir management could provide an opportunity to manipulate flow release and their temperature, to accommodate aquatic species requirements (Yates *et al.*, 2008; Sinokrot and Gulliver, 2010; Null *et al.*, 2013). For instance, water releases from deep thermally-stratified reservoirs have colder water than unregulated flows during summer periods and may be beneficial for cold-water species such as Bull Trout. It has been also suggested that dam management could help mitigate some of the impacts caused by human and climate change on stream flows and temperature downstream (Yates *et al.*, 2008; Null *et al.*, 2013).

Previous studies have mainly focused on analyzing human impacts in the main-channel habitat, but large flows for example greater than 10-year recurrence interval form new habitats by connecting secondary channels and oxbows, which is known as off-channel habitat (Richter and Thomas, 2007). Off-channel habitats can serve as refugia, during high flows in the main channel (Bell et al., 2001). The interaction among flow and timing of reservoir released flows on stream ecosystem and thermal regime has been overlooked in river flow management (Olden and Naiman, 2010). Many studies have used process-based hydrodynamic and fish habitat models to quantify the impacts of reservoir management, however most of them do not consider stream water temperature, while analyzing available habitat (e.g., Tiffan *et al.*, 2002; Lacey and Millar, 2004; Pasternack *et al.*, 2004; Muhlfeld *et al.*, 2012).

We apply the process-based integrated model developed in the previous Chapter 4, 5, 6 and 7 to quantify impacts of dam operation on aquatic habitats for dry, average and wet climatic conditions This Chapter focuses on: i) Impact of dam operation on fish habitat; ii) Analyzed if flow regulation can offset impact on habitat?; iii) impact of dam operation on spatial shift of habitat.

9.2 *Methodology*

9.2.1 Climatic conditions

In collaboration with USBR, we identified a set of discharge scenarios for dry, average and wet climatic conditions to understand the impacts of the reservoir operation on Bull Trout habitat (Table 9.1). We selected three functional climatic conditions to represent typical wet, average and dry climatic years based on measured flows at USGS gauge SFBR near Featherville, ID,

which is located upstream of Anderson Ranch Reservoir. Frequency analysis was performed for the measured flows to estimate recurrence interval (RI) floods. Typical wet, average and dry years were identified based on annual natural flow characteristics of the basin. We selected dry (2007), average (2010) and wet (2006) years based on flow magnitude of less than 1.5-year RI, between 1.5 and 5-year RI and greater than 5-year RI, respectively in both annual maximum and mean floods and based on drought indices calculated for the region (Sohrabi et al., 2015).

Table 9.1: Hydrologic scenarios of dry, average and wet climatic conditions for habitat analysis.

Scenario Number	Background Conditions from BiOp	Winter Reservoir Release	River Modeling Time frame	Hydrology
Dry (2007)				
1	Historical	Historical	10/1/06-09/30/07	Historical Actual
2		Modified	10/1/06-09/30/07	Modified
3	Natural Flows	Natural Flows	10/1/06-09/30/07	Natural Hydrograph
Average (2010)				
4	Historical	Historical	10/1/09-09/30/10	Historical Actual
5		*150 cfs	10/1/09-09/30/10	Modified
6	Natural Flows	Natural Flows	10/1/09-09/30/10	Natural Hydrograph
Wet (2006)				
7	Historical	Historical	10/1/05-09/30/06	Historical Actual
8		*150 cfs	10/1/05-09/30/06	Modified
9	Natural Flows	Natural Flows	10/1/05-09/30/06	Natural Hydrograph

Historic: Hydrographs recorded at Anderson Ranch Dam for water years 2006, 2007 and 2010.
Modified: Hydrographs recorded at Anderson Ranch Dam modified by replacing the 300 cfs with 150 cfs, all the other discharges remain the same for water years 2006, 2007 and 2010.
Naural Flows: Natural flows estimated without Anderson Ranch Dam operation and storage for water years 2006, 2007 and 2010.

9.2.2 Impacts of dam management

We developed a biological model in ArcGIS using 2D simulated hydraulic variables water depth and velocity, water temperature and univariate rearing habitat preference criteria for Bull Trout (Chapter 7). Geometric product of the individual suitability indices, *SI*, of physical parameters water depth, velocities and temperature were used to determine the overall suitability index (*CSI*) for each cell.

First, we developed discharge-WUA (Q-WUA) curve from a range of discharges 4, 8, 17, 28, 45, 57, 68, 85, 102, 142, 184 and 227 m^3/s. We separated the calculated WUA between the channel habitat, that within the bankfull channel (here after in-channel), and lateral habitat, that beyond the bankfull wetted area extension (here after lateral-channel).

We developed habitat time series for different climatic conditions dry (2007), average (2010) and wet (2006) under dam regulated and un-regulated scenarios based on Q-WUA curve and mean daily discharges, which is an indicator for long-term impacts of dam operation impacts on fish habitat (Chapter 7). Furthermore, we analyzed potential impact of low flow release through dam (4 m^3/s) lower than current minimum flow 8 m^3/s as an option for future water management to compensate for drought conditions. For this analysis, we modified the regulated hydrograph through dam for all climatic conditions by assigning 4 m^3/s discharge for when flows are 8.5 m^3/s (Figure 9.1). Specifically, we reduced dam released discharges during winter and spring months for all three climatic conditions. However, we assumed similar water temperature time series released from dam as for the unregulated scenario. This assumption is justifiable because flow is released through bottom of the reservoir and water temperature should not be significantly different between 8 and 4 m^3/s.

We addressed the impact of dam operation on aquatic habitat and if dam management offsets those impacts by comparing WUA calculated by water depth, velocity and stream temperature and WUA only based on hydraulic variables water depth and velocity (here after hydraulic-quantified) between regulated and unregulated scenarios. Comparisons between these two habitats quantify the impacts of water temperature on aquatic habitats. We compared in-channel and later-channel habitats between regulated and unregulated scenarios to address impacts of dam operation on shift of habitat quality spatially.

9.3 *Results and Discussions*

Anderson Ranch Dam has altered hydrology and thermal regimes, causing minimum base-flow to increase and peak-flow to decrease distinctly (Figure 9.1). Winter water temperatures increased but water temperature diminished in the summer months. Unregulated flow hydrographs of SFBR system peak from late March to May with cold waters as a result of snowmelt and have warm low flows in the dry summer period (Figure 9.1) (DEQ, 2008).

Anderson Ranch Dam management has smoothened the peak of hydrograph by storing water for later use (e.g., energy production and irrigation) and flood management downstream, which resulted in relatively higher and stable flow during summer, fall and winter months (e.g., Yarnell *et al.*, 2010; Muhlfeld *et al.*, 2012).

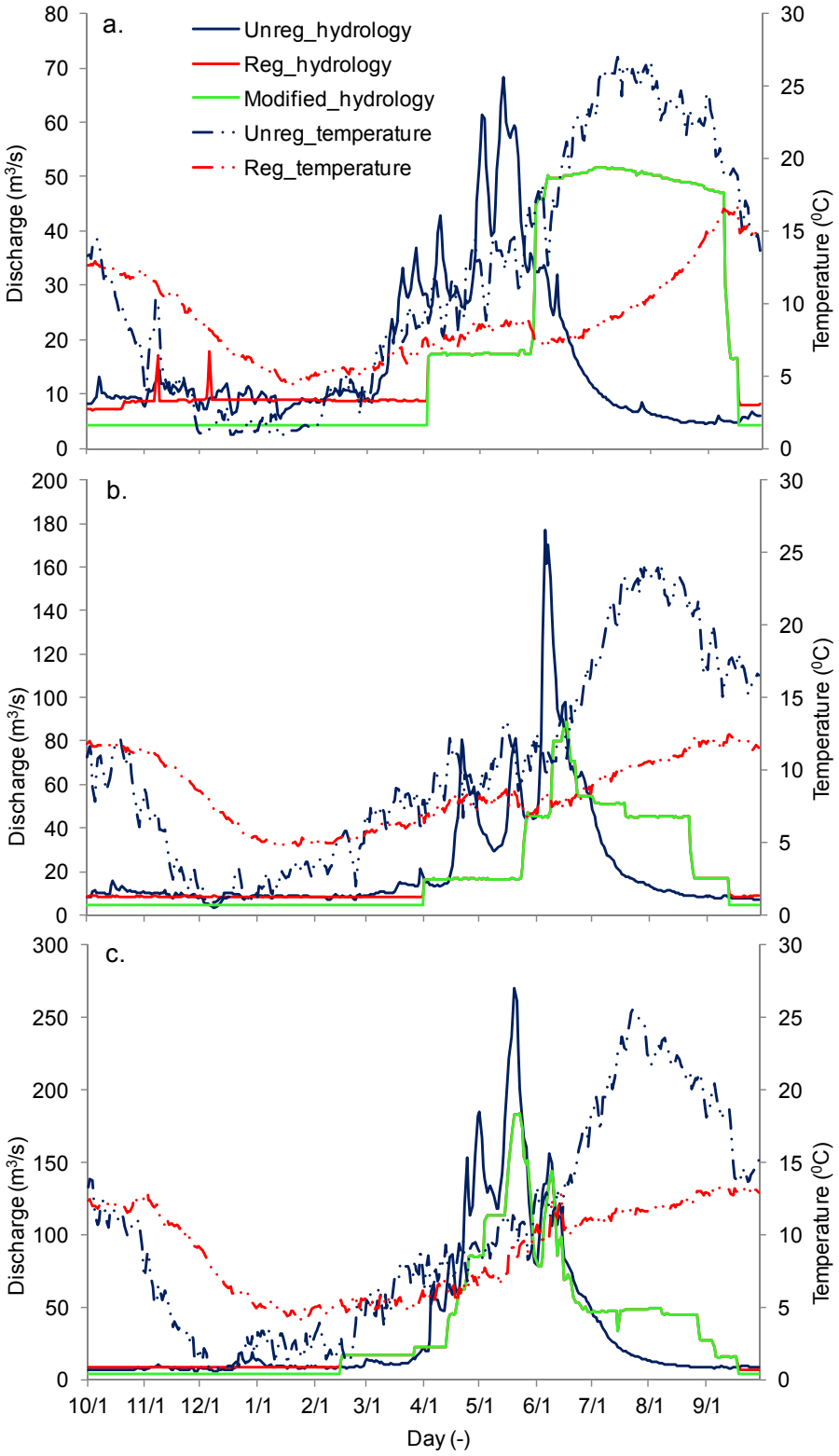

Figure 9.1: Regulated, modified and unregulated hydrology and daily averaged water temperature at the Anderson Dam for a. dry (2007), b. average (2010), and c. wet (2006) climatic years

9.3.1 Dam impacts

9.3.1.1 Habitat

Habitat quality time series analyses showed habitats were consistent in winter (December, January and February) and early-spring months (March) as a result of steady regulated higher low-flows and colder stream temperature less than 16^{o}C, which benefits Bull Trout rearing habitat downstream of Anderson Ranch Dam (Figure 9.1 and 8.2). Habitat increased during later stages of spring months due to medium low-flows (higher than the winter) release from the dam. The increase in habitat quality with discharge for low discharges is shown by the noticeably higher quality of habitat for wet than for dry and average climatic conditions (Figure 9.2). Later, habitat decreased in summer and early spring months as a result of high flow release to fulfill irrigation demand downstream. Habitat distributions were consistent throughout all climatic years for the regulated scenario. Patterns of habitats for the unregulated scenario were similar to the regulated in fall and winter months for all climatic conditions (Figure 9.2).

Habitat quality was noticeably higher for wet than dry and average years for spring months. However, habitat quality was considerably lower in summer months for the unregulated scenario than for the regulated scenario and other seasons (spring, fall and winter). For flows higher than bankfull, river velocities were higher than 1 m/s in the SFBR system for both regulated and unregulated scenarios, which reduced habitat (Chapter 7). Furthermore, habitats induced by regulated flows were comparable to the unregulated scenario year around, and regulated habitat had higher quality during warm summer months than the unregulated scenario regardless of climatic conditions. The better summer habitat quality for the regulated than unregulated case is due to lower high flows and stream water temperature for the former than latter scenario (Figure 9.2). Other studies have shown that smoothing flow is beneficial to river ecosystem maintaining suitable habitat for native fish and invertebrate communities (e.g., Muhlfeld et al., 2012).

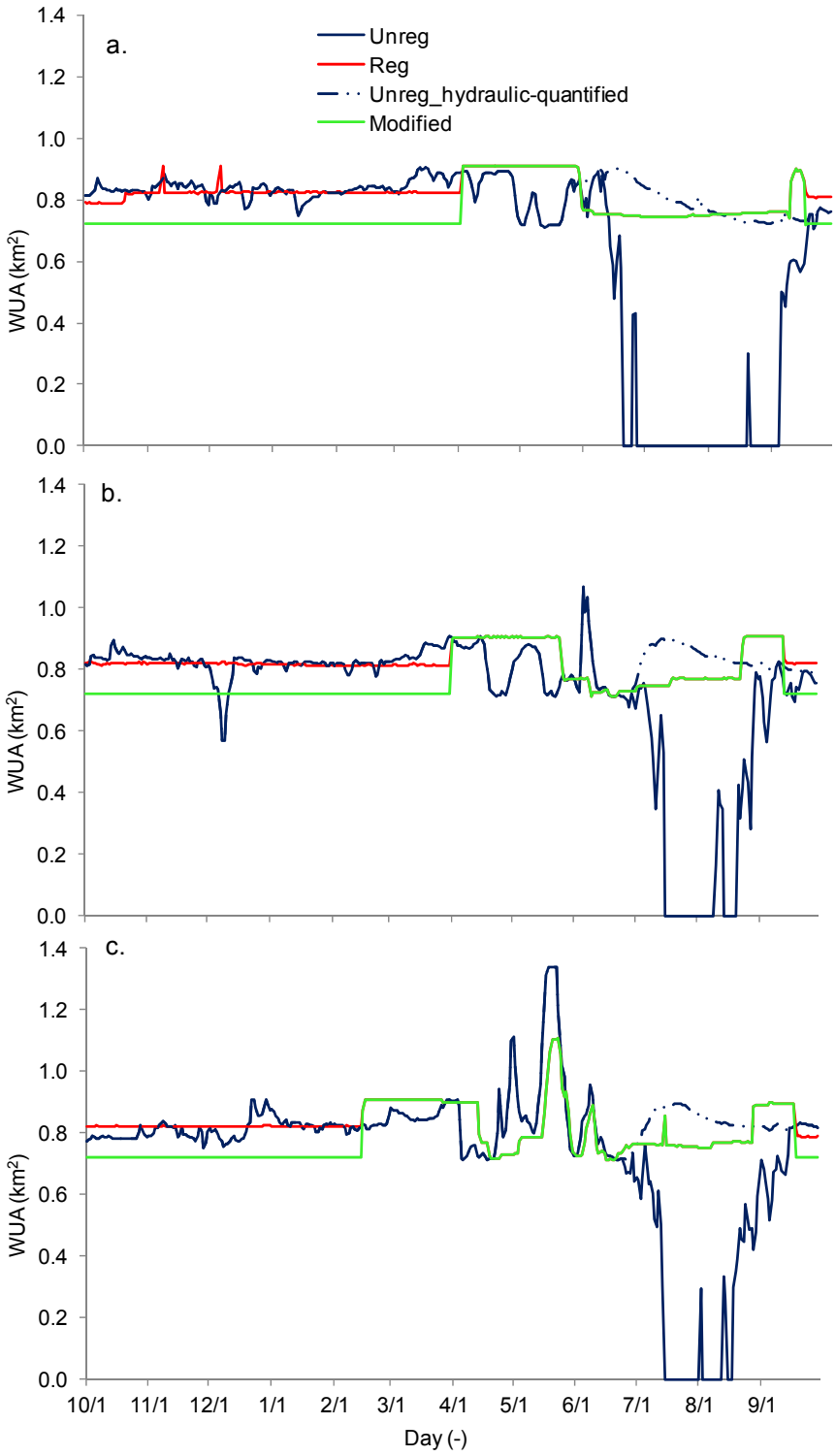

Figure 9.2: Total (channel and lateral channel) WUA with all three hydraulic variables water depth, velocity and temperature for regulated, modified and unregulated flows for a. dry (2007), b. average (2010), and c. wet (2006) climatic years. Hydraulic-quantified WUA is based on water depth and velocity only.

Habitat qualities for modified low flow were noticeably lower than for the regulated scenario (Figure 9.2). The results were consistent with other studies where degradation of habitat occurred due to low flow in the channel as a result of dam management or flow diversion (e.g., Yarnell *et al.*, 2010; Muhlfeld *et al.*, 2012). Median water depths were less than 0.25 m due to modified low flows, which is one of the main reasons for reduction of habitat in the SFBR system (Chapter 7, Figure 7.4). In general, modified low flows resulted in lower inundated areas (extent), which also contributed in lower habitat, but it is minor compared to impact of water depths (Figure 7.4). There were no impacts of water temperatures in habitat for modified low flow because they were less than 16^{o}C during winter and spring months. Therefore, our results indicated that modification (lowering) of dam release flows less than current minimum flow of 8 m^3/s would degrade Bull Trout rearing habitat in the SFBR system. However, further research is required to conclude if lowered habitat can have negative impacts on sustainability (carrying capacity) of current Bull Trout population in the SFBR system.

The temperature effect on habitat quality remained consistent in all three climatic years for the regulated scenarios, because stream water temperatures were less than 16^{o}C for each year (Figure 9.1 and 8.2). Hydraulic-defined habitat quality, that quantified using velocity and depth supposing temperature is not a limiting factor, were different from those accounting for temperature mainly in summer months for the unregulated scenario because of effect of water temperature, which were greater than 16^{o}C. Hydraulic-defined habitat quality was much greater than combined (hydraulic and temperature) habitat quality in summer months for the unregulated scenario. There were no differences between hydraulic and combined habitats in regulated scenario because water temperatures were less than 16^{o}C for all three climatic conditions.

This result underlines the importance of the stream temperature as a critical variable for aquatic species habitat (Hillman and Essig, 1998; Poole *et al.*, 2001; Selong *et al.*, 2001; Anglin *et al.*, 2004). The dam releases cold water less than 16^{o}C from the bottom of the reservoir and increases historic minimum low flows, which suit Bull Trout (Connor et al., 2003; Null et al., 2013). Bull Trout use the South Fork Boise River downstream year-round as both overwintering and summer rearing habitat during post-dam era (Salow and Hostettler, 2004). Historically, there were no migration barriers (e.g., Lucky Peak, Arrowrock, Anderson Ranch or Kirby dams) in the

Boise River system, therefore Bull Trout could freely move toward headstream tributary habitats to avoid stressing water temperatures in the main stem river. Water temperature of the SFBR systems for the unregulated scenario are much higher (>22^{o}C) than the current regulated water temperature (USBR, 2013) and late summer flows are considerably low, therefore we speculate that there were virtually no habitats during summer months. Our data suggested that Anderson Ranch Dam management has not deteriorated Bull Trout rearing habitat downstream. Our results are consistent with other studies that dam management alters physical characteristics and water quality (temperature), however they were within preferable range for Bull Trout resulting better habitat in regulated scenario than for the unregulated (Poff *et al.*, 1997; Muhlfeld *et al.*, 2012).

9.3.1.2 Spatial habitat shift

Regulated flows have reduced and limited the connection between main-channel and lateral-channel habitats, with the latter a vital zone for many aquatic species (Bunn and Arthington, 2002; Martens and Connolly, 2014). The reduction in connectivity is more pronounced for the average and wet climatic than dry conditions. Lateral-channel habits were significantly higher in the unregulated than regulated scenario for the average and wet conditions (Figure 9.3) because of higher stream flows in these conditions than the dry climatic scenario. During high flows, they function as refugia (Shirvell, 1994; Bell *et al.*, 2001; Tiffan *et al.*, 2010) for fish as high-quality habitat shift from in-channel to lateral-channel due to high (> 1 m/s) flow velocity in the main-channel (Figure 9.4). This is supported by the observation that adult and subadult Bull Trout and other fish species such as Sculpins, Dace, Kokanee, and Rainbow Trout use lateral-channels during high flows in the SFBR system (USBR, 2013). Our study strengthen the importance of connectivity between main-channel and lateral-channel habitats especially during high flows as previous studied also observed (Bowen et al., 2003; Gorski et al., 2014). This suggests that restoration efforts should focus on re-establishing high flows that connect main-channel with lateral-channel habitats because they are important ecological indicators for aquatic ecosystem (Bednarek and Hart, 2005; Sabaton et al., 2008).

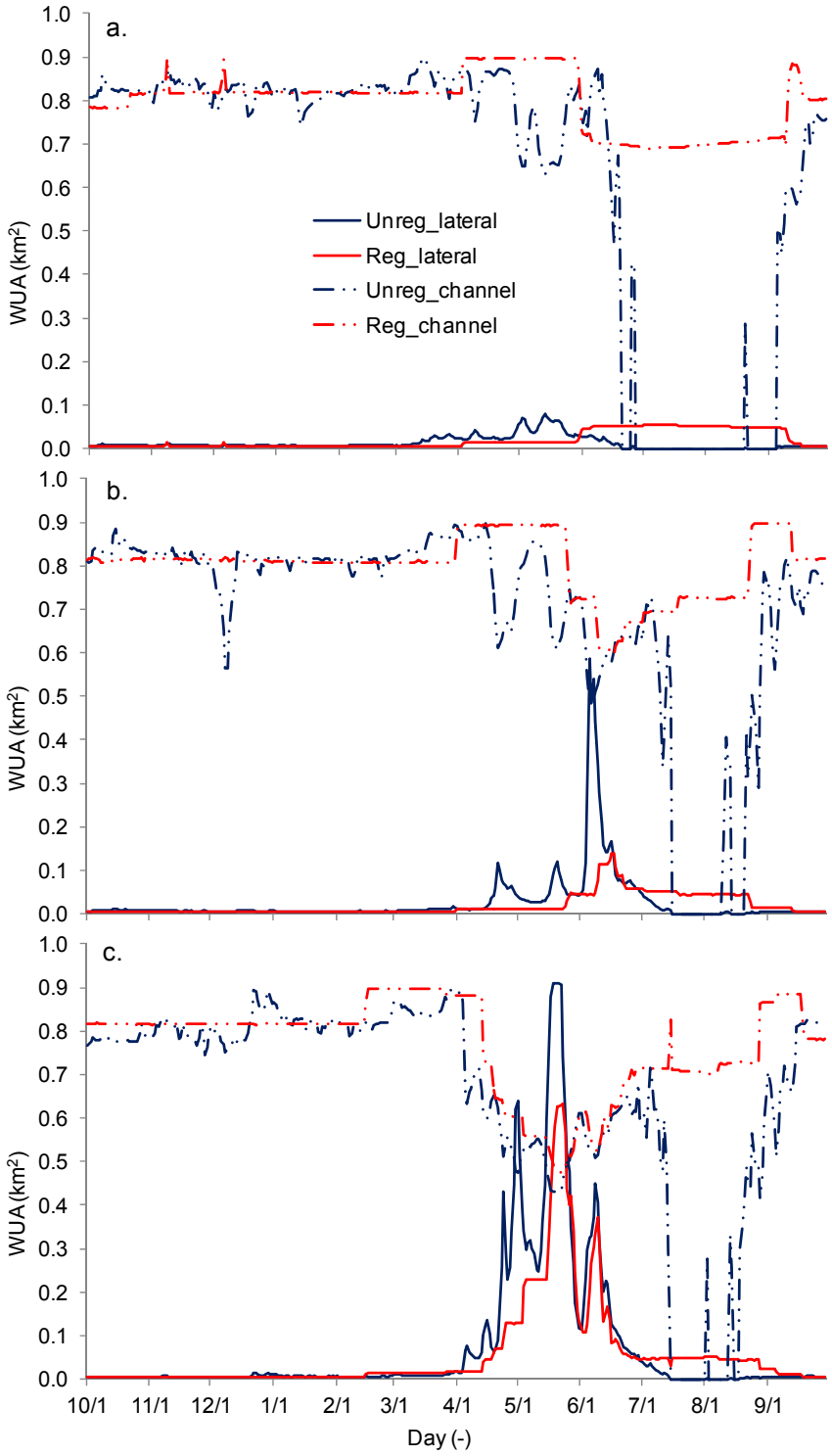

Figure 9.3: Channel and lateral channel WUA for regulated and unregulated flows for a. dry (2007), b. average (2010), and c. wet (2006) climatic years.

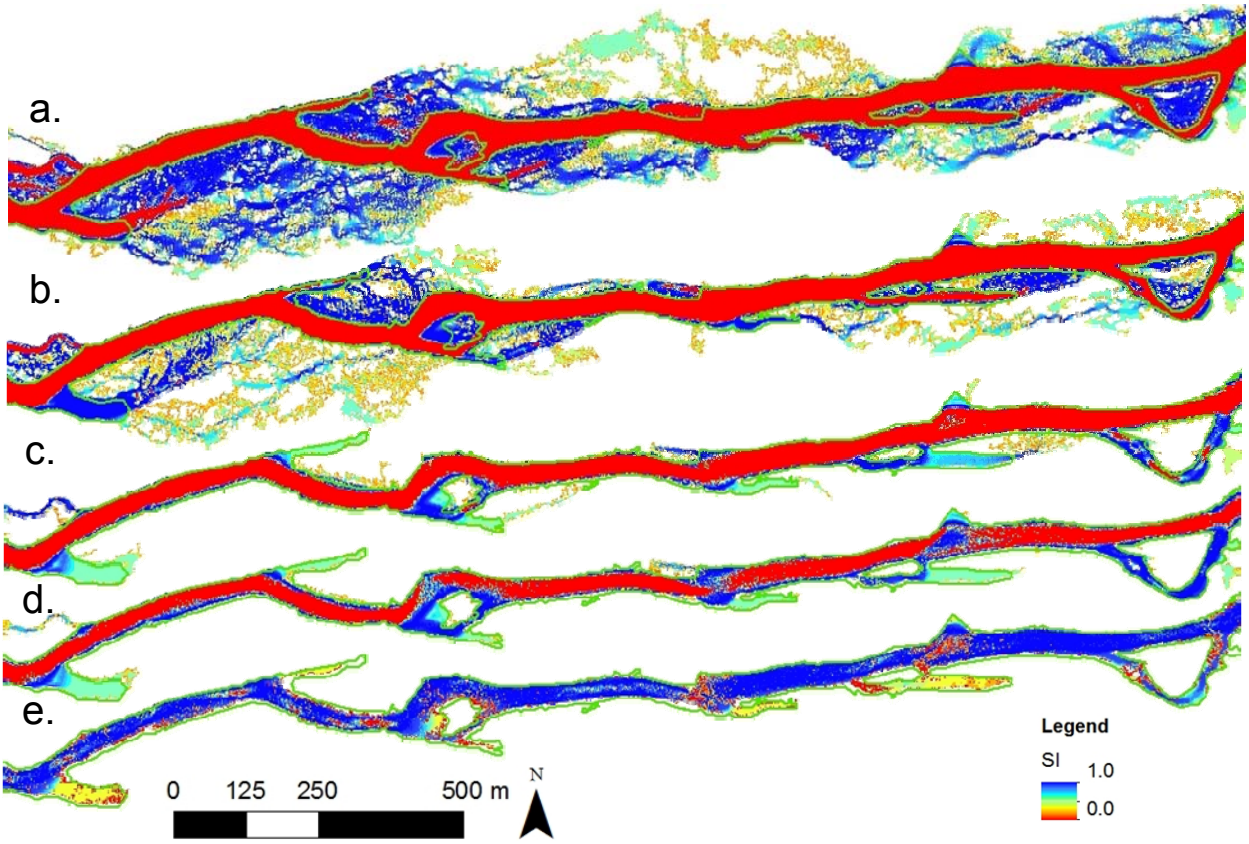

Figure 9.4: Spatially distributed habitat quality in main- and lateral-channel for a. 227, b. 142, c. 68, d. 45, and e. 17 m^3/s. Green line is boundary for bankfull extent.

9.3.2 Can dam management offset degraded habitat?

Water temperatures were higher than 16^oC for the majority of summer days in the unregulated scenario, consequently decreasing habitat quality (Figure 9.1 and 8.2). Conversely, the regulated water temperature is within the range suitable for Bull Trout rearing habitat. This contributed to maximize the habitat and maintain the quantity and quality for the summer months. Hydraulic-quantified habitat qualities were much greater than combined (hydraulic and temperature) habitat quality that indicates temperature played major role to degrade habitat quality for summer months in unregulated scenario.

Warmer water temperature may become a major issue in future climates for aquatic habitat due to climate warming (Null et al., 2013). In our study, dam management reduced water temperature (less than 16^oC) for summer months and increased the minimum low flows (< 8 m^3/s) in winter and spring months, which improved habitat quality from the unregulated scenario

in all climatic conditions. Attention should focus on managing water temperature to maintain and enhance aquatic ecosystems. Our study showed that dam management may offset impacts of low flows and high water temperature on aquatic habitat by increasing historic low flows and decreasing water temperature specifically during dry climatic cases. We also suggest that dam management could mitigate some of climate change impacts on the stream water temperature, consequently for aquatic ecosystem as with other previous studies (see, Yates *et al.*, 2008; Null *et al.*, 2013). Reservoir management may provide suitable coldwater habitat for fish and wildlife by releasing water from the bottom of the reservoir when high stream water temperature are an issue. However, temperature of water releases depends on reservoir water temperature distribution. This is a function of reservoir water level, reservoir bathymetry, hydrodynamics and heat exchange. Therefore, research should include a reservoir model, such as Estuary, Lake and Coastal Ocean Model (ELCOM), to predict water temperature release through dam based on carry-over volume of water from previous year, reservoir level, atmospheric temperature and climatic condition (Vilhena et al., 2010).

9.4 *Conclusions*

Our results showed that regulated flows maximize the quantity of habitat as well as maintaining good habitat the entire year for adult Bull Trout in the SFBR system regardless of climatic conditions compared to the unregulated flows. Summer months were a critical period for fish habitat in the SFBR system for unregulated cases in all climatic conditions because summer temperatures were comparatively higher than those preferred by Bull Trout. Water temperature caused degradation of habitat quantity and quality in summer and early fall months for the unregulated scenario, which is further intensified by low flows in the river. In contrast, regulated flows maintain uniform habitat throughout the summer period for all three climatic conditions because Anderson Ranch Dam operation maintains water temperatures within the range of Bull Trout preference. This suggests that dam management has the potential to offset negative impacts on fish habitat quality from future climate change effects especially during dry climatic years. Nevertheless, our results showed that modification (reduction) of current minimum flow (8 m^3/s) would result lower habitat than for the regulated cases in the SFBR system.

Our results revealed that lateral-channel habitats are important part of river ecosystem, which are connected during high flows. High quality habitats shifted to lateral-channels from the main-channel, consequently sustaining the high quality habitat during high flows specifically in average and wet climatic conditions. Although our system was static, as we studied each climatic condition separately, future study could account for potential climatic scenarios time series. This would allow quantifying the risk of climate change on the ecosystems due to succession of dry and wet years.

10 ANALYSIS OF STRANDING POOL FORMATION

10.1 *Introduction*

The stranding of fish species due to rapid reductions in river water surface elevation is one of the ecological impacts associated with dam management (Bragg et al., 2005; Irvine et al., 2009). Stranding can occur by formation of isolated pool when water surface elevation drops in the river. Fish stranding has been reported during high to low flows below dams causing mortality of salmonids (Nagrodski et al., 2012) and invertebrates. Dauwalter et al. (2013) reviewed stranding data from the SFBR and after finding similarities with other systems including Bear River below Grace Dam (Idaho) concluded that the likelihood of fish stranding was not related to the rate of change in water surface elevation. The chance of fish stranding depends on many factors such as fish species and their life stages, rate of change in water surface elevation due to flow management, stream temperature, the time of the day (night Vs day), so it appears to be site specific (Higgins and Bradford, 1996; Halleraker *et al.*, 2003; Dauwalter *et al.*, 2013).

In this study, we focused on quantifying the impact of flow releases from the Anderson Ranch Dam on formation of stranding pools in the South Fork Boise River. We developed 2-dimensional (2D) model using high resolution (2-meter) channel bathymetry to delineate stranding pool formation for different discharge (i.e., 17, 28, 45, 57, 68, 102, 142, 184 and 227 m^3/s) releases from the dam. We compared predicted and observed stranding pool locations to verify our approach.

10.2 *Methodology*

We simulated stranding pools based on water depths and inundation extent for different flows, when flows recede from high (e.g., 227 m^3/s) to base flow (8 m^3/s). Stranding pools are inundated areas, which are disconnected from the main channel during discharge recession from a high to low flows. We defined stranding pools as polygons (areas) greater than 16 m^2 (4 cells) and were 2 m (one cell) away from other polygons and detached.

The goal of this study was to determine the extent of fish stranding pool formation during flow downramping. To verify the model results, we compared spatial location of predicted stranding pools to surveyed fish stranding pools formed during flow change from 51 m^3/s to 8 m^3/s below Anderson Ranch Dam in the South Fork Boise River (Dauwalter et al., 2013). Since, the field surveyed stranding pools were reported by a point with X-Y coordinates survey by handheld GPS device; it is difficult to compare two-dimensional polygons to the point location. The horizontal accuracy (1 to 30 m) of handheld GPS depends on features and their capabilities (UC Berkeley, 2015). We calculated the nearest distance of modeled stranding pool (polygon) for 57 m^3/s from a surveyed point, to analyze model performance on detecting stranding pools. Furthermore, we quantified the number of stranding pools and their areas for specified discharges. We developed a relationship between flow recession rate and stranding pool areas and fitted a regression line. This allowed calculating possible pool areas formation for each day based on flow recession rates and regression equation.

To analyze the role of dam management on stranding pool formation, we compared number of days (frequency) that have potential to form the specific areas of stranding pools between regulated and unregulated scenarios for dry, average and wet climatic years. Furthermore, we also compared number of days (frequency) that have specific flow recession rate of <8.5, 8.5-17, and >17 m^3/s/day between regulated and unregulated scenarios for high (>68 m^3/s) and low (>68 m^3/s) flows. These three flow recession rates are typically adopted to release flow through Anderson Ranch Dam.

10.3 ***Results and discussion***

Our results showed that the model delineated stranding pools for 57 m^3/s were matched with field surveyed stranding pools in 2012 (Figure 10.1). The model was able to delineate the pools close to surveyed stranding pools, where median distances were 10.46 m from field surveyed pool location. The size of stranding pools ranged from 16 to 1,082 m^2. The performances of model were deemed satisfactory considering objective of the study and probable uncertainties in coordinates of points surveyed using handheld GPS.

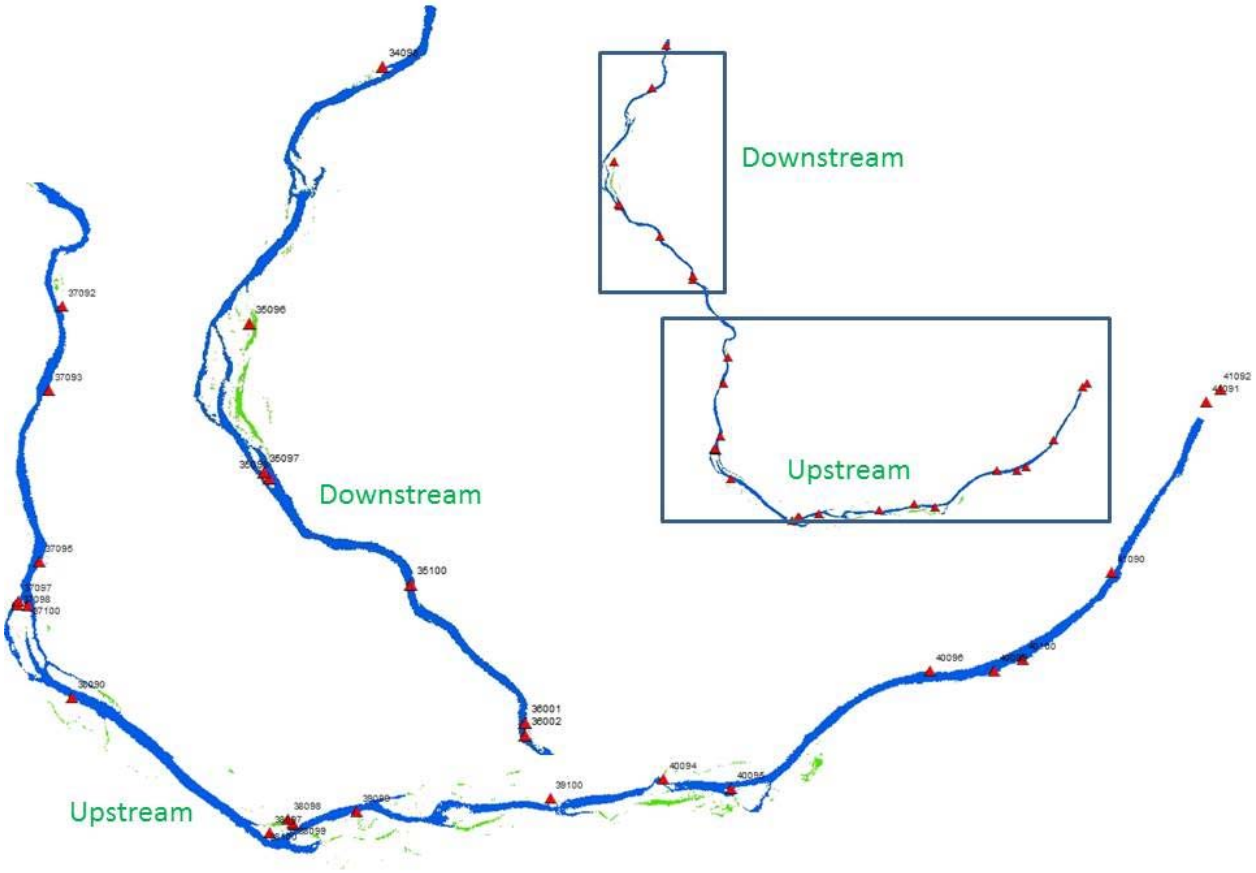

Figure 10.1: Preliminary map of model delineated stranding pools (green) for discharge 57 m^3/s and field surveyed stranding pools in 2012.

The number and areas of stranding pools increased with discharges (Figure 10.2). The number of pools increased slowly with discharge up to 68 m^3/s (from 34 to 280), whereas they increased noticeably for discharges higher than 68 m^3/s (from 280 to 2993). Pool area followed a similar trend as pool number (Figure 10.2), where pool area increased distinctly for discharges higher than 68 m^3/s. Inundations maps showed that the flow connects floodplain and side channels at discharges higher than 68 m^3/s and creates pools, which are disconnected later during flow recession to base flow. Our results showed that chance of development of stranding pools are higher for large (e.g., 227 m^3/s) discharges than those for small (17 m^3/s) (Figure 10.3).

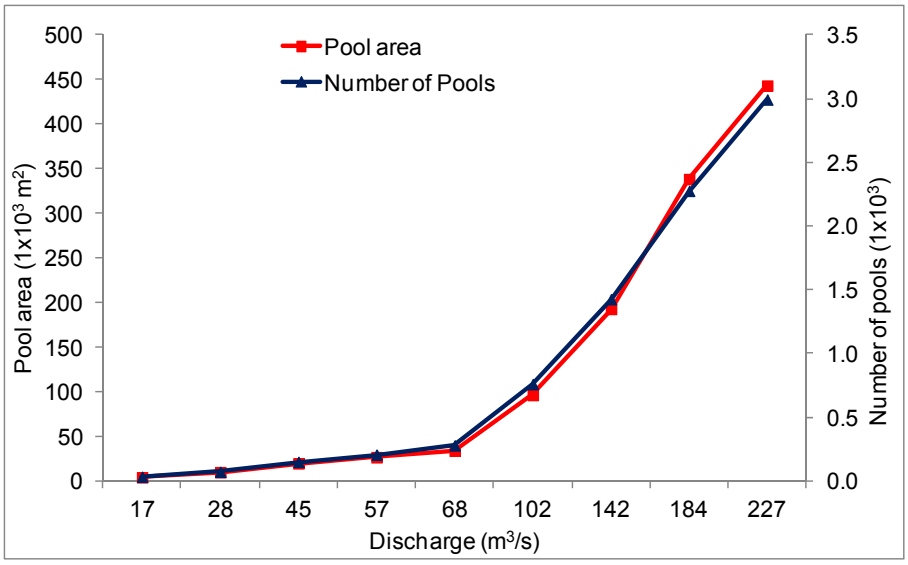

Figure 10.2: Model delineated number of stranding pools and area against discharge magnitude.

Rate of pool areas increased slowly (585 $m^2/m^3/s$) with discharge up to 68 m^3/s, whereas they increased noticeably (2666 $m^2/m^3/s$) for discharges higher than 68 m^3/s (Figure 10.3 and 9.4a). Field survey reported that more fish were stranded during the recession of flows from 51 to 25 m^3/s than for recession from 17 to 8 m^3/s (Dauwalter et al., 2013).

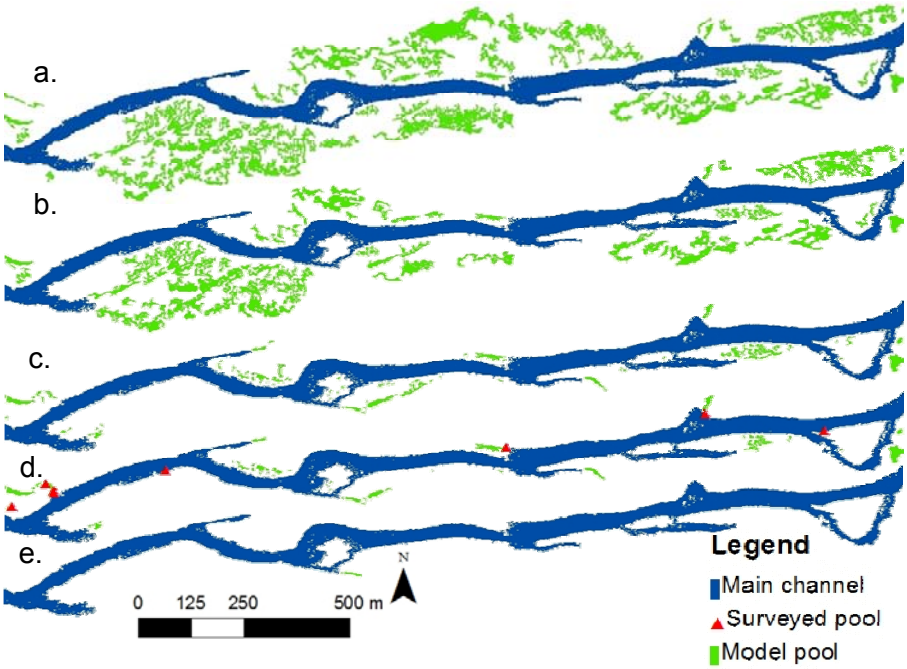

Figure 10.3: Spatially distributed stranding pools for a. 227*, b. 142*, c. 68, d. 57, and e. 17 m^3/s. *only pools more than 200 m^2 are shown.

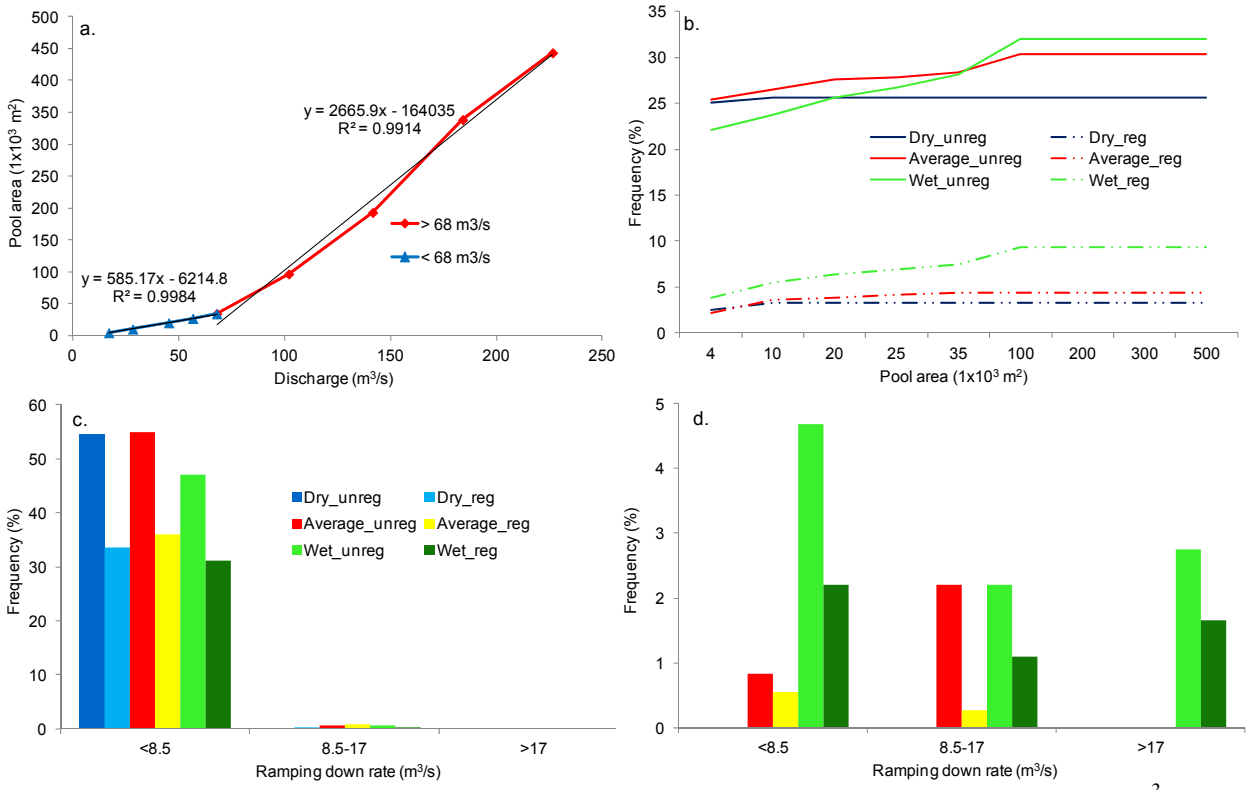

Figure 10.4: a. stranding pool (area) formation when flows recede from high (e.g., 250 m^3/s) to base flow (8 m^3/s), b. frequency of days (%) that specific areas of stranding pool formation between regulated and unregulated scenarios for dry, average and wet climatic conditions, c., frequency of days for down ramping rate of <8.5, 8.5-17, and >17 m^3/s/day during flow <68 m^3/s and d. flow >68 m^3/s.

10.3.1 Probabilities stranding pool formation

Number of days (frequency) corresponding to different stranding pool formation areas were higher for unregulated than for regulated scenarios in all climatic conditions (Figure 10.4b) indicating that there were higher probabilities of stranding pool formation in the unregulated than regulated case. Wet climatic years had higher frequency of stranding pools compared to average and dry climatic years because the higher flows caused frequent connection with lateral-channels, floodplains and backwater areas, which have greater potential to form stranding pools (Bradford, 1997; Brown, 2002). This suggests that fish stranding is potentially a natural phenomena driven by both natural (high degree of seasonal flow fluctuation) and anthropogenic activities (for the flow regulated case) (Junk *et al.*, 1989; Bradford, 1997; Brown, 2002). Studies have documented evidence of fish stranding within gravel depression, isolated flood channels and side channels after the spring floods in natural and regulated systems (e.g., Brown, 2002).

10.3.2 Flow recession rates

The majority of flow recession rates were <8.5 m^3/s/day for flows less than 68 m^3/s in both regulated and unregulated scenarios and all climatic cases, whereas the minority of flow recession rates falls into 8.5-17, and >17 m^3/s/day (Figure 10.4c). Percentage of all flow recession rates (<8.5, 8.5-17, and >17 m^3/s/day) were higher in the unregulated than regulated scenarios. The percentage of all flow recession rates were distinctly lower for flow >68 m^3/s than for < 68 m^3/s, but showed similar trend between unregulated and regulated scenarios and all climatic cases. This suggests that current dam management has recession rates comparable to those observed in the natural system. However, flow regulation has reduced the frequency of flow recession rates at both daily and seasonal temporal scales in comparison with unregulated scenario because dam released constant flows for longer periods (see, Chapter 8). Consequently the system is less variable than the natural system and may have reduced the risk of fish stranding (Bradford, 1997; Brown, 2002). Average water level recession rates were 0.4-0.8 cm/h for recession rate of flows 8.5-17 m^3/s/day based on model simulations, when flows were less than 68 m^3/s in our study site, which are distinctly lower than recommended maximum water level recession rate about 2.5-5 cm/h on another study to reduce probability of fish stranding in gravel bars of regulated river (Higgins and Bradford, 1996). This result showed flow recession rates adopted in SFBR for dam management may not increase fish stranding compared to unregulated case, however, many other factors such as water temperature, channel morphology and species and life stages play a role.

10.4 *Conclusion*

The model delineated stranding pools were close to field surveyed pools. Large discharges have higher chance of developing stranding pools than small discharges. Probabilities of formation of stranding pools were greater for unregulated flows than for regulated flows for all climatic cases. Dam management reduced flow magnitude and helped to reduce flow recession rates compared to unregulated cases.

11 HYPORHEIC FLUX MODEL

11.1 *Introduction*

Part of the stream water flows as subsurface flow within the streambed sediment (Tonina, 2012). These flows are known as hyporheic flows and cause an exchange of water between surface stream water and stream pore water within the streambed material. They have important ecological impact affecting the habitat of developing embryos which salmonids typically bury within the streambed hyporheic sediments (Tonina and Buffington, 2009). Here we measured hyporheic flows nearby a debris flow formed after a wildfire in the SFBR. The location was selected to detect changes in hyporheic flows as fine sediment delivered by the debris fan were eroded away during high summer irrigation flows. Additionally, dam operations coordinated a flood pulse to move most of the fines. Consequently, our measurements coordinated with this effort to monitor changes in hyporheic flows.

11.2 *Methods*

Hyporheic flows are quantified using the method based upon one-dimensional advection and diffusion of temperature (Luce et al., 2013; Tonina et al., 2014), where phase, ϕ, and amplitude, A, of cyclic temperature signals from paired temperature sensors in the surface water and within the streambed sediment are analyzed (equations 1-3):

$$\eta = \frac{-\ln\left(\frac{A_2}{A_1}\right)}{\phi_2 - \phi_1} = \frac{-\ln\left(A_r\right)}{\Delta\phi} \tag{11.1}$$

$$\kappa_e = \frac{\omega \Delta z^2}{\Delta\phi^2}\frac{\eta}{1+\eta^2} \tag{11.2}$$

$$\Delta z = \Delta\phi\sqrt{\frac{\kappa_e}{\omega}\left(\eta + \frac{1}{\eta}\right)} \tag{11.3}$$

where η is a dimensionless number relating the natural logarithm of the amplitude ratio, $A_r = \frac{A_2}{A_1}$, to the phase difference between paired temperature signals, $\Delta\phi$. $\omega = \frac{2\pi}{T}$, is the expected angular frequency and *T* is the period of the temperature signal being analyzed. Calculation of sediment thickness between temperature sensors, Δz, allows quantification of bed elevation changes over time. Effective thermal diffusivity, κ_e, is a thermal property of the sediment and pore-water matrix and is calculated from the temperature time series obtained during an intitial, steady state elevation of the bed where Δz is known and constant. This calculation of κ_e is different from previous methods (Constantz, 1998; Hatch et al., 2006; Keery et al., 2007; Lautz, 2012; Swanson and Cardenas, 2010), which require an estimated value of κ_e. Once known, κ_e should remain unchanged, thus the value is held constant, and Δz over time is calculated. Bed elevations are then calculated by summing Δz and respective temperature sensor constant elevations.

Seepage velocities, i.e., Darcy velocities, can be calculated at each location once κ_e is known. Luce et al. (2013) provide one option for calculating advective thermal velocity independent of depth:

$$v = \gamma \sqrt{\frac{\kappa_e \omega}{\eta}} \frac{1-\eta^2}{\sqrt{1+\eta^2}} \tag{11.4}$$

The equations and the signal analysis were coded in the open source statistical computing environment, R. Numerical analysis uses a discrete Fourier transform (DFT) to extract phase and amplitude from cyclical temperature time series. Bed elevation and velocity calculations use only measured temperature data and require no parameterizations.

11.3 *Temperature probes design*

UHMW (Ultra High Molecular Weight) plastic tube houses the same DS18B20 temperature sensors used in the laboratory. The 1 inch long sensors are placed at a 45 degree angle to allow a smaller diameter tube. Exact sensor locations along the probe are referenced using the unique serial address of each individual sensor. The three wires from each sensor are

connected in a star network, allowing one three wire sleeved bundle to exit the top of the probe with a connector for connection to a data logger. This connector provides the advantage to connect the probe to an attached data logger or to run longer wires and connect multiple probes to one central data logger. A 60 degree angled aluminum cone drive tip is inserted and pinned in the bottom of the probe and is larger in diameter at the probe/tip interface, allowing for driving and anchoring the probe. The anchor ensures the probe will not uplift or float out of the sediments during deployment and during scour events, assuming scour is not so deep to remove the probe entirely. An open source Arduino based microcontroller is used for data logging onto a micro SD card. It is powered with AA, alkaline batteries and is placed inside a waterproof housing, constructed with 1 ½ inch PVC fittings and pipes.

11.4 *Temperature probes installation*

Installation in the field can be challenging and involves driving the probe into the streambed using a 2 ½ inch diameter cast iron pipe and a large post hammer. The drive tip fits snuggly just inside and against the bottom end of the driver and is placed with the probe inserted in the pipe before driving the assembly vertically down into the stream bed with a post hammer. The driver is then carefully pulled up, leaving the installed probe in the bed. The data logger is then connected to the probe with the waterproof connector and placed on top of the probe using the threaded connection. Excess wire is placed within a storage cavity in the data logger housing during deployment.

Field temperature probes were deployed on August 6, 2014 in the South Fork Boise River (SFBR) (Figure 11.1). Several tributaries to the SFBR deposited major alluvial sediments into the river in 2013 following wildfires in the area. One of the largest debris fans was selected for scour and hyporheic flow monitoring due to the high probability of changes in streambed elevation due to the loose arrangement of the sediment and to quantify the impact of fine deposition in the flow and potential scour of those fines. The U.S. Bureau of Reclamation (USBR) manages the dam and planned a high flow release of 68 m^3s^{-1} (hereafter referred to as flood) for the period from August 18 through 27 to remove fine sediments delivered by the debris fans. Grain size distributions, derived from a Wörman pebble count survey, for the

streambed before and after the flushing flow (i.e. flood) are shown in Figure 11.2 for the selected debris fan.

Two of the aforementioned temperature probes were installed. In addition, two probes constructed of Hobo Tidbit sensors in PVC pipe, similar to the design presented in the work of Tonina et al. (2014), were used at intermediate locations of the two other probes. To collect water surface temperature, one additional, single Hobo Tidbit sensor was placed in the surface water where no scour or deposition was expected. Data from each temperature sensor was collected and recorded at 15 minute intervals. Probe locations and initial bed elevations relative to the probe and a control point were surveyed using an engineering level. The four locations are labeled 1, 2, 3, and 4, starting at the upstream end of the debris fan toward the downstream end, respectively. The probes were deployed until September 29, at which point the probes were no longer submerged. Final bed elevations relative to each probe were measured using a ruler prior to removal. To evaluate scour/deposition, each probe location is assigned an initial bed elevation of 0 cm, thus scour events are represented by negative values and deposition with positive values. Bed elevation change is tracked by measuring the distance from the top of the probe to the bed before and after the high flow event. Increase in the distance indicates scour occurred (negative bed elevation), and decrease in the distance indicates deposition occurred (positive bed elevation). No additional measurements were possible during the flood period due to safety.

Figure 11.1: Left: South Fork Boise River study site showing the debris flow that added sediment to the channel, with approximate thermal scour/ deposition chain installation locations 1, 2, 3, 4. (Photo used with permission from the USDA, Boise National Forest); Middle: Field temperature probe; Right: Temperature probe installed with data logger.

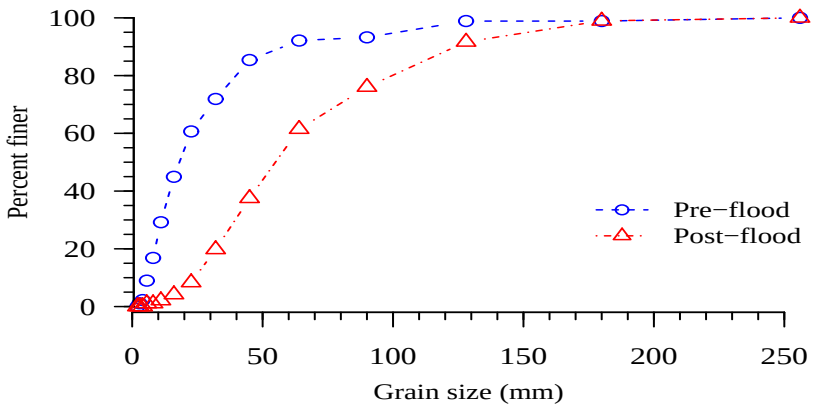

Figure 11.2: Pre-flood (blue) and post-flood (red) grain size distribution at South Fork Boise River locations 1 and 2. Locations 3 and 4 did not experience significant change in grain size distribution due to little scour or deposition and their grain size distribution remained similar to the pre-flood condition.

11.5 *Field Study Site*

For the period prior to the flood flow, amplitude of the temperature signals from sensor 4 and deeper were too low to obtain results for κ_e at any of the four locations. After flood and associated scour events at locations 1 and 2, the temperature signal from sensor 4 was strong enough to obtain results, but sensor 2 no longer provided results as it was in the surface water. The paired adjacent sensor results were used to verify sediment did not move in these locations. Locations 3 and 4 provide very similar results before and after scour suggesting no sediment movement at these elevations along the temperature probe. At locations 1 and 2, values for sensor 4 after scour are similar to those at sensor 3 before scour, indicating that sediment between sensors 3 and 4 did not move, while some sediment between sensors 2 and 3 was scoured.

Figure 11.3 shows the streambed elevation changes calculated from the temperature data at each of the four probe locations in the SFBR, along with the pre-flood measured bed, post-flood measured bed, and post-flood calculated average bed. The last is the mean of the calculated bed elevation during post-flood period of data relative to the initial bed elevation of 0 cm at each location. Bed elevations relative to each probe were measured after installation using an engineering level and after flow recession using a ruler. For each plot, the dam release hydrograph is shown on the secondary axis in blue.

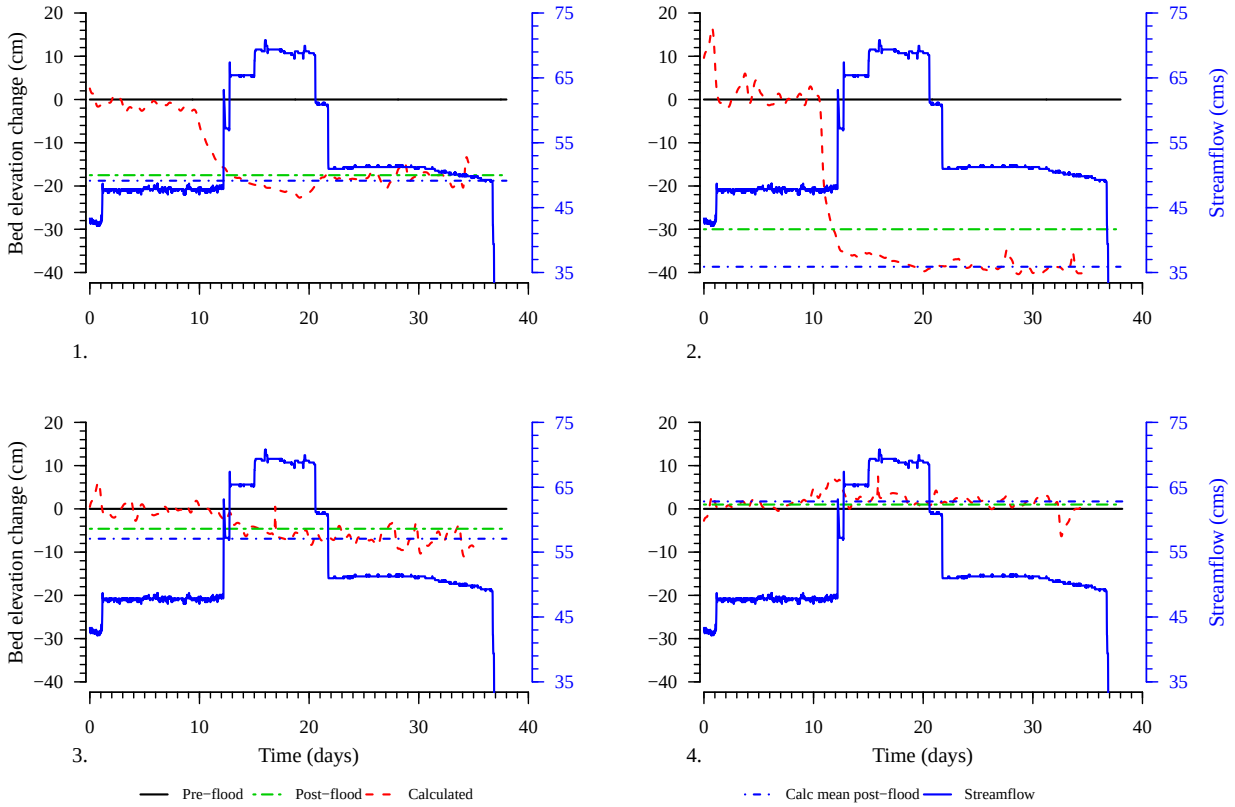

Figure 11.3: South Fork Boise River measured and calculated stream bed elevations at locations 1, 2, 3, and 4, plotted with the hydrograph released from Anderson Ranch Dam (secondary y-axis, blue line).

Stream sediment seepage velocities were calculated for each probe location (Figure 11.4). At locations 3 and 4, measured seepage velocities are near zero and have little noticeable change throughout the installation period. However, there is some noticeable increase in upwelling velocities (negative indicates upward velocity) at locations 1 and 2 during the high flow period and continuing after high flow subsided. Location 2 also appears to have some seepage velocity that is a function of streamflow.

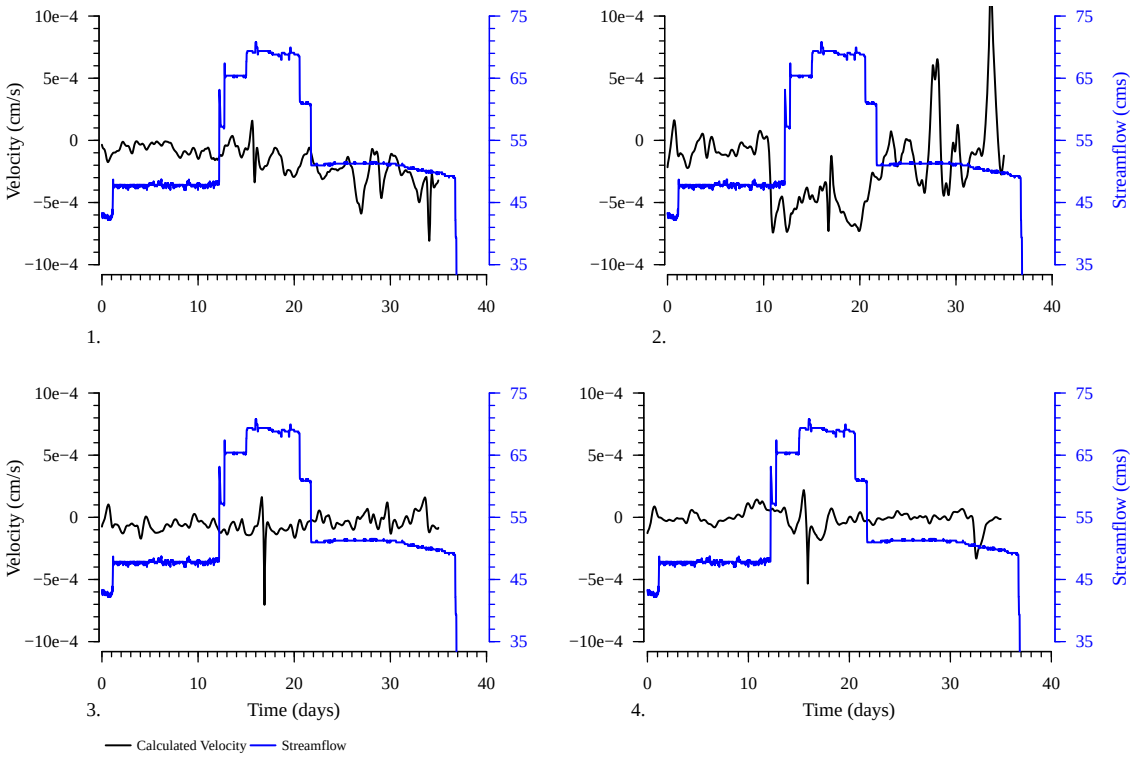

Figure 11.4: South Fork Boise River calculated sediment seepage velocities at field locations 1, 2, 3, and 4, plotted with the hydrograph released from Anderson Ranch Dam (secondary y-axis, blue line). Depth of temperature sensor increases with increasing sensor number

Locations 1 and 2 experienced significant bed scour, and changes in seepage velocities were measured after the scour event. Negative velocities indicate upward flow, which may be present at a location due to the stream receiving groundwater inputs in the area associated with steep, high ridges on either side of the river. It is possible that the small, cohesive particles present prior to scour caused low hydraulic conductivity of the bed material, limiting the stream recharge. During scour, fine particles where removed from the surficial layer, typically 2 median grain sizes thick. The reduction of fine material in the armored layer increased the hydraulic conductivity of the sediment and thus increased seepage flux within this thin and near surface layer. At location 2, significant upward seepage flux occurred during scour, which may be linked to hyporheic return flow through the riffle from the upstream pool. Probes 3 and 4 detected little or no change in velocity after the high flow event, which is expected due to minor streambed changes at these locations. Velocity data combined with water thermal regime are useful information to characterize benthic organism habitats. Solutes and particle drift depend on near bed and intra gravel velocity, and metabolic rate and growth depend on water temperatures. Dam

operations, which impact both thermal and flow regime of the surface water, affect the subsurface environment and the behavior of dwelling organisms, as observed by others (Bruno et al., 2009).

11.6 *Conclusion*

Hyporheic fluxes were measured in a small reach of the SFBR after wildfire-triggered debris fans entered the system. Because fine sediment covered most of the system this location was chosen to monitor if hyporheic flows were still present and if scour could increase the exchange by removing fine material.

Results show that hyporheic flows increased at the 2 locations where scour occurred. Flows were both upwelling and downwelling indicating changes of hyporheic flow cells with discharge and time possibly due to groundwater effects. Additional measurements are needed to understand how hyporheic flow changes along the SFBR and are important to monitor changes in hyporheic flows as fine sediments are removed from the system.

12 APPENDIX A: MAPPING OF SUCCESSFUL COTTONWOOD RECRUITMENT AND PLANTATION IN THE SOUTH FORK BOISE RIVER

12.1 *Introduction*

Reservoir operations cause regulated and predictable pattern of stream flows, which may limit, if not prevent, successful recruitment of native riparian cottonwood species (Auble and Scott, 1998; Lytle and Merritt, 2004; Braatne *et al.*, 2007). Riparian cottonwood are highly productive, protects banks from erosion, which may have detrimental impact on aquatic habitats, maintains favorable water temperature for fish by providing shade and are source of nutrients and woody debris for the channel (Naiman et al., 1993). The recruitment of cottonwood trees is strongly dependent on infrequent high flows that create moist bare emerged patches. It also requires specific flood recession pattern for seedlings to establish successfully (Figure 1) (Mahoney and Rood, 1998; Braatne *et al.*, 2007; Burke *et al.*, 2009; Benjankar *et al.*, 2014a).

Riverbanks of the South Fork Boise River downstream Anderson Ranch Dam have mostly old stands of cottonwood trees without new generation establishment. The 2013 wild fire damaged most of those cottonwood stands, which successively died. Current efforts focus on planting cottonwood seedlings to restore cottonwood forest. However, unfavorable flow recession, location and timing of planting may prevent successful growth resulting in loss of the investment.

This investigation developed a two-dimensional (2D) hydraulic model coupled with a cottonwood recruitment model to predict favorable areas for cottonwood seedling plantation (In this report, plantation refers to areas that are planted with propagated cottonwood seedlings for the purpose of enhancing natural recruitment) and evaluated the opportunity for successful natural cottonwood recruitment for current post-dam flow release case.

13 METHODOLOGY

13.1 *Study area*

We focused on the first 23 km reach of the South Fork Boise River, downstream of USGS Anderson Ranch Dam gauge station to Private Bridge near Danskin Bridge. The reach is braided

in several areas and has numerous side channels. Floodplain is 30 to 200 m wide and has some old cottonwood trees.

13.2 *Requirement for successful natural cottonwood recruitment*

The ecophysiologies of riparian cottonwoods and successful natural recruitment depend on riverine processes (Braatne et al., 1996). Successful cottonwood seedling recruitment is associated with channel and bank geomorphology, sediment transport and timing, magnitude and duration of large floods (Mahoney and Rood, 1998; Amlin and Rood, 2002). River hydrology is the driving force for these processes. In natural systems, water surface elevations recede following large floods and expose barren areas on floodplains and riparian zones, which are colonized by cottonwood seedlings. Successively, surface moisture conditions and water table decline rates govern seedling survival (Mahoney and Rood, 1991; Johnson, 1994). If the rate of water table recession exceeds the rate of root elongation, seedling mortality occurs due to drought stress (Braatne et al., 1996). This is one of the most common causes that prevents cottonwood recruitment in regulated reaches downstream reservoirs (Figure 13.1).

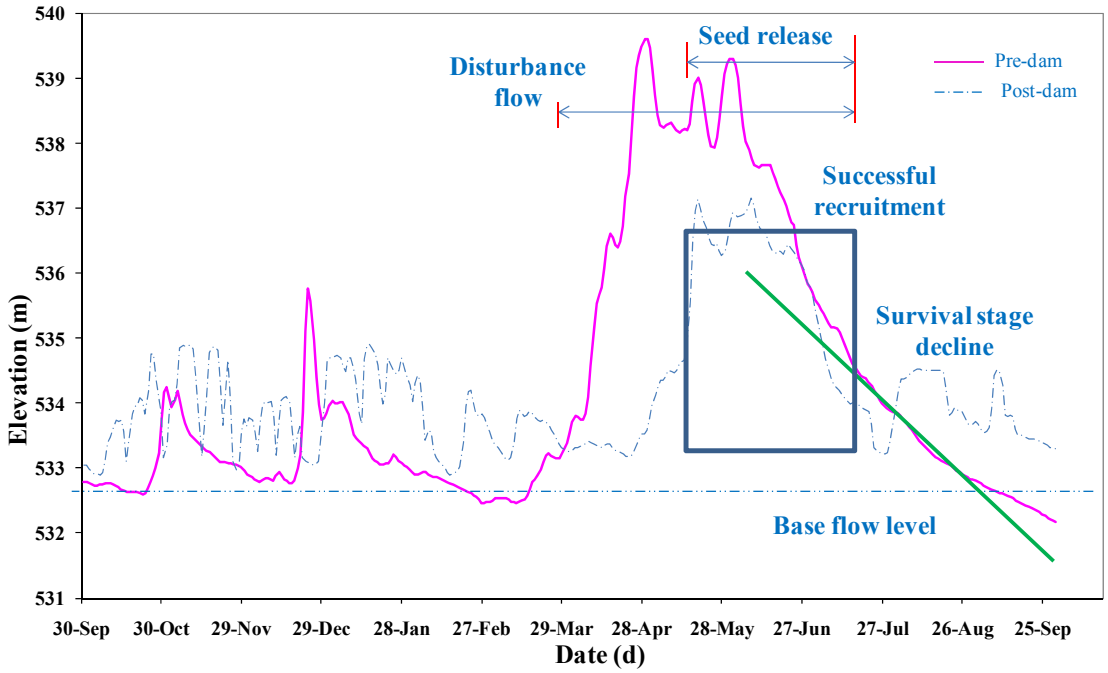

Figure 13.1**:** Required physical criteria for successful cottonwood requirement and typical hydrographs for pre-dam (unregulated) and post-dam (regulated) reaches (Benjankar et al., 2014a). Green line shows water surface optimal rate of change for cottonwood recruitment.

13.3 *Survey of cottonwood recruitment sites*

We surveyed cottonwood seedling recruitment areas in late summer 2016 (October) along the South Fork Boise River. We used hand-held GPS to survey cottonwood patches and delineated boundaries of cottonwood recruitment areas during the field visit. We observed sporadic cottonwood seedling recruitment in only few areas: at 5 main channel shoreline locations and 8 islands or exposed sediment bars. This is the typical case in regulated river systems (Figure 13.2a). We observed cottonwood recruitment within a narrow band (2 to 4 m) close to the channel (Figure 13.2b and c).

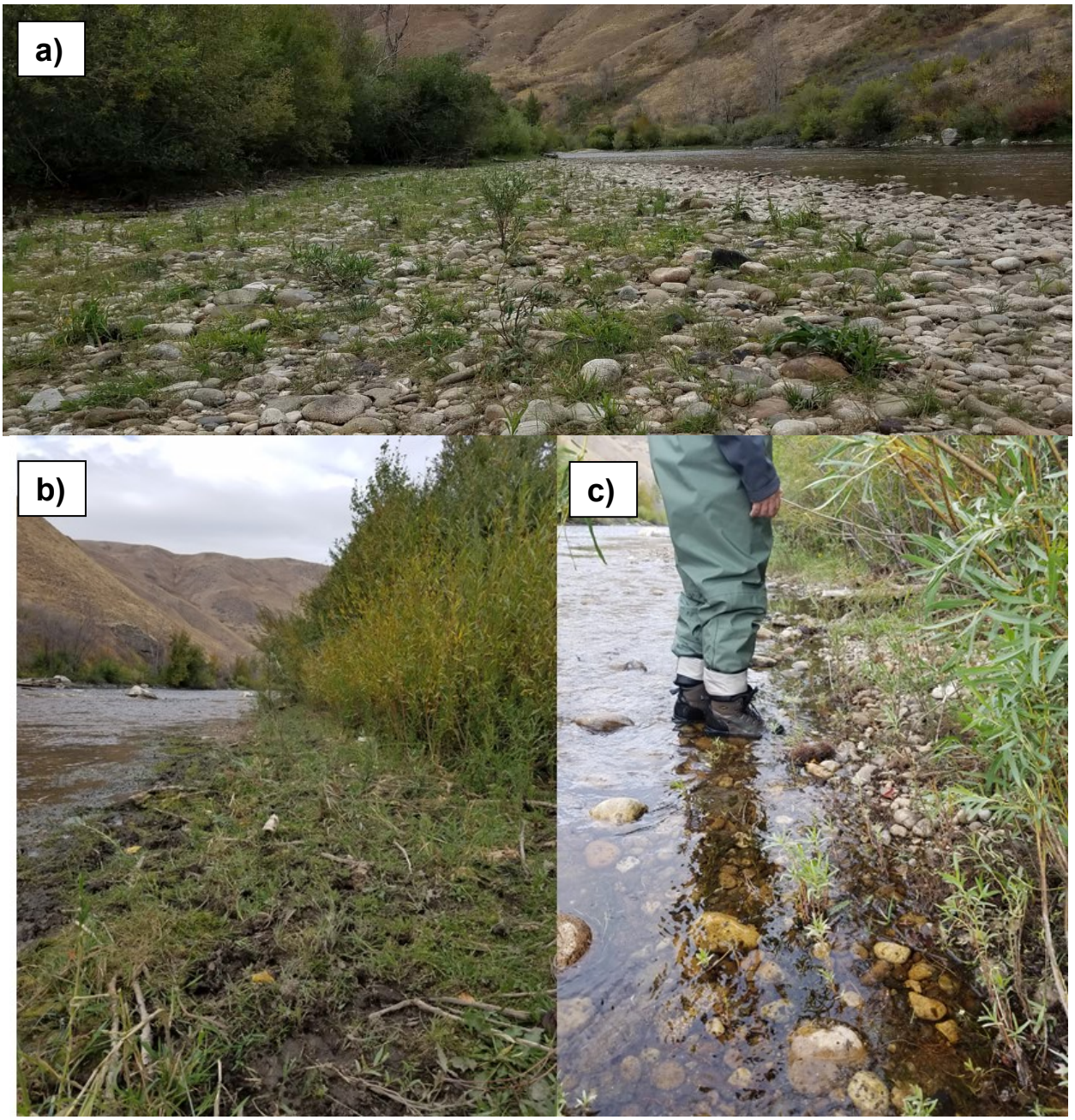

Figure 13.2: Example of field survey natural cottonwood recruitment area (a) and field surveyed cottonwood recruitment on a narrow band near channel (b and c).

13.4 *2D hydraulic and cottonwood model*

A 2D hydraulic model with grid size of 2m by 2m of the study area was developed and used to simulate water surface elevations and flow hydraulics for 300, 600, 1000, 1600, 2000, 2400, 3600, 5000, 6500 and 8000 cfs flow release from the Anderson Ranch Dam. We linearly interpolated water surface elevations for discharges between those simulated. This allows us to

identify the water surface elevation for any released flow between 300 and 8000 cfs. Required input parameters for the cottonwood model are seed dispersal period, shear stress, mortality coefficient, which is function of water surface recession rate, and elevation of topography reference to the mean water level in the channel (Figure 13.3). The cottonwood model predicts fully favorable, partially favorable, low favorable and not favorable areas for successful cottonwood recruitment, using rule-based Fuzzy approach (Figure 13.3) (Benjankar et al., 2014a).

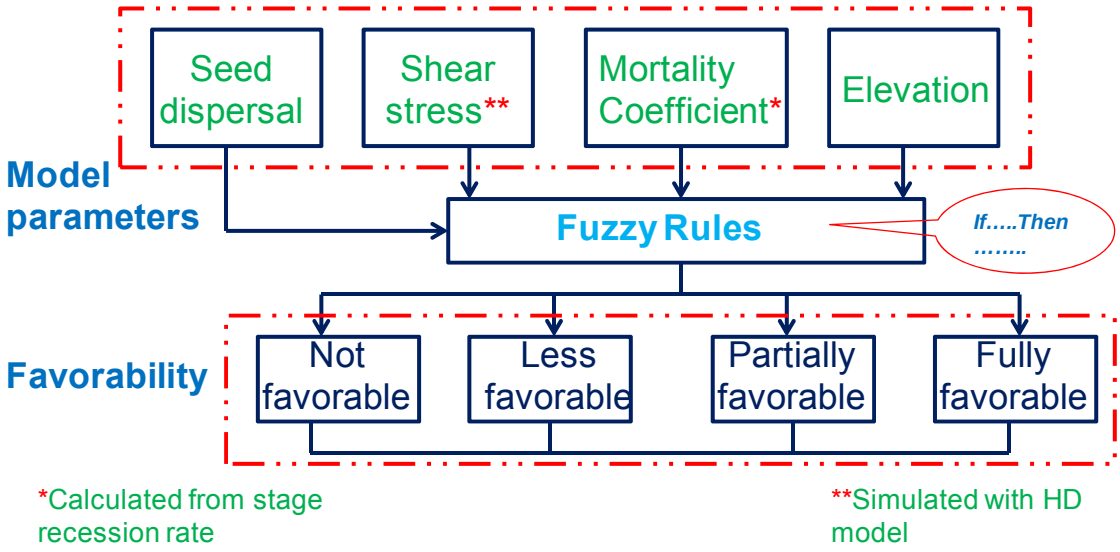

Figure 13.3: Input physical variables and output from the cottonwood model. Figure is modified from Benjankar, et al. (Benjankar et al., 2014a)

13.5 *Prediction of areas for seedling plantation*

For the scope of this project, we predicted only "Fully Favorable" (referred to as "favorable" for the remainder of this report) areas for cottonwood seedling plantation based on following assumptions:

- Cottonwood seedlings (1-year) have at least 50 cm root length and roots are fully buried into the ground during springtime.
- Shear stress is considered "Good" for entire area, because seedling will be planted.
- 3-day average water surface recession rate of ±1 to 10 cm per day is considered "Good" during May 20 to September 15
- Mortality coefficient <30 is considered "Good"

- Water surface elevation 25 to 120 cm above base flow level is considered “Good”

Favorable areas for cottonwood plantation were predicted based on the assumption that the ground water table is directly associated with water surface elevations in the channel. This is a reasonable assumption because of the confined characteristic of the canyon system. These assumptions are reasonable because seedling will be planted and not naturally germinating (Benjankar et al., 2014a).

13.6 *Result and discussion*

13.6.1 Survey of cottonwood recruitment sites

We observed sporadic cottonwood seedling recruitment in the South Fork Boise River along the 5 main channel shoreline locations and 8 islands or sediment bars surveyed. Hydraulic modeling showed that these areas are frequently flooded by medium- and high-regulated flows during spring and summer months. Thus, although seedlings were observed at these areas, subsequent spring and summer month floods may remove them because these areas were at low elevations relative to water surface elevation at minimum flow 8 m^3/s and near the channel. This field visit revealed that substrate at these areas were dominated by coarse gravels and cobbles. Large sediment sizes without fine materials indicate the river system has high stream power. We also noticed that most exposed gravel bars are notably armored indicating lack of fine sediment in the system. Riverbed armoring process is typical of regulated river systems like South Fork Boise River. Cottonwood seedling habitat requires moist sediment bars with elevations higher than low flow water levels (Mahoney and Rood, 1998). Consequently, these observations explain the unsuccessful natural cottonwood seedling recruitment in the South Fork Boise River. This is mainly due to lack of fine sediment on bars and unfavorable water surface elevation recession rates, which affect water table in the nearby areas of the channel.

13.6.2 Simulated favorable areas for cottonwood seedling plantation

The model simulated spatially distributed favorable areas for cottonwood seedling plantations (green areas in Figure 13.4,Figure 13.5, Figure 13.6 and Figure 13.7). Favorable areas were located at Site 1 (Figure 13.5), 2 (Figure 13.6), and 3 (Figure 13.7), which are located downstream from USGS Anderson Ranch gauge station, Cow Creek Bridge and Danskin Bridge,

respectively. These areas are primarily braided reaches with side channels and islands, which provide characteristics similar (but at a smaller scale) to developed floodplains. The predicted areas were similar to the field conditions where matured and old cottonwood trees were observed.

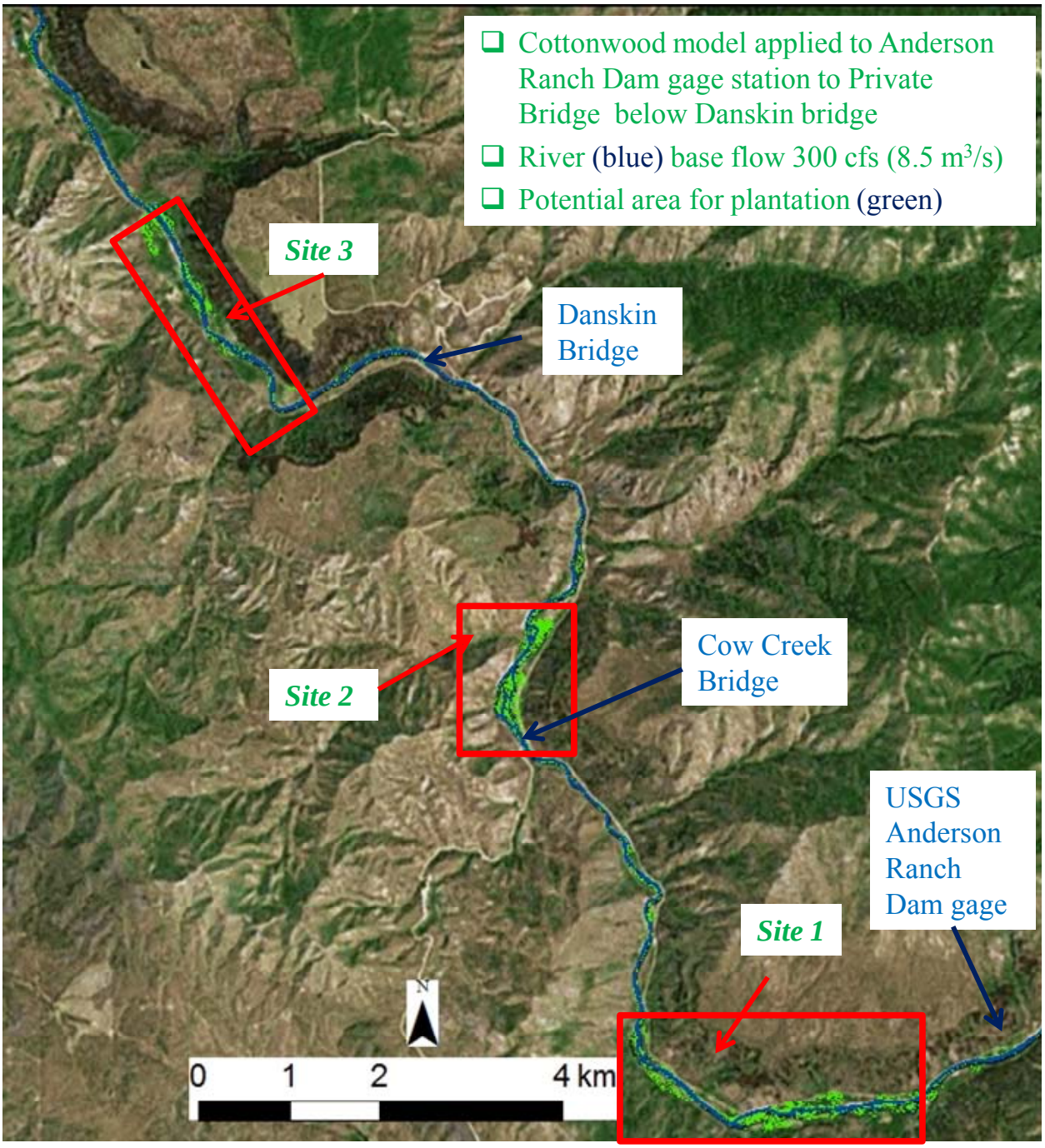

Figure 13.4: Favorable areas for cottonwood plantation.

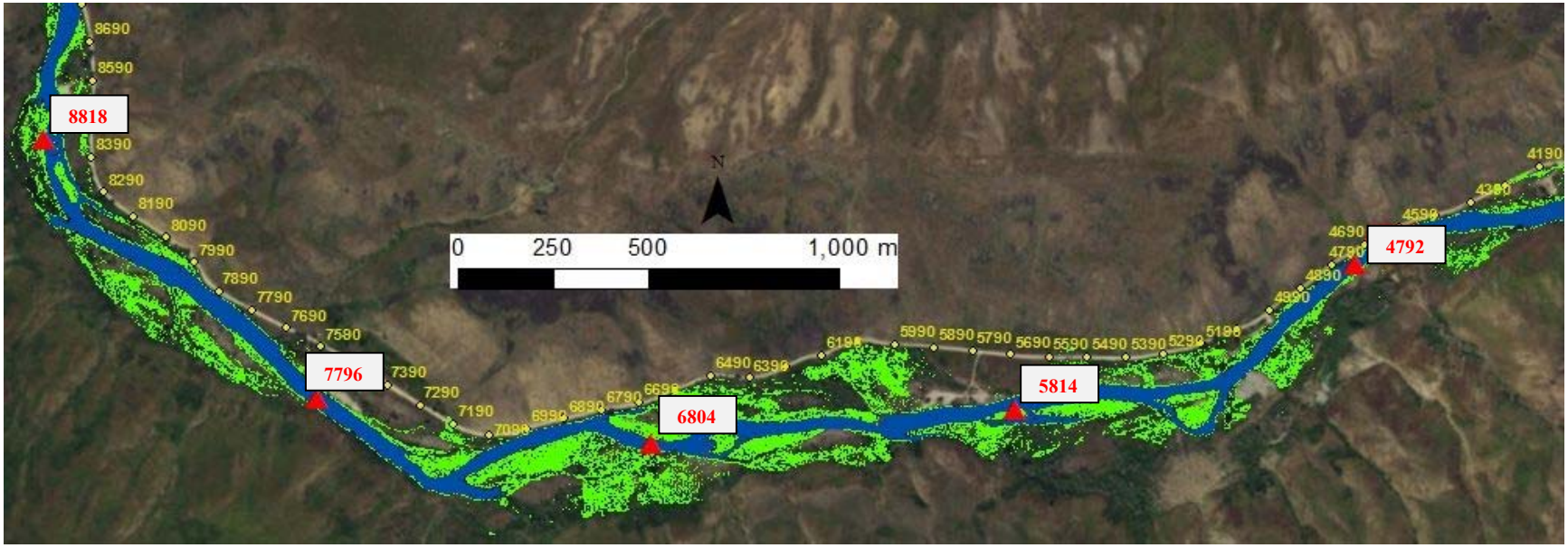

Figure 13.5: Detailed favorable areas (green) for cottonwood plantation at Site 1, downstream of Anderson Ranch Gauge Station (2790 m river distance from the Dam). Red triangles and yellow circles indicate river distance (m) from Anderson Ranch Dam and road distance based on Anderson Ranch Gauge Station, respectively.

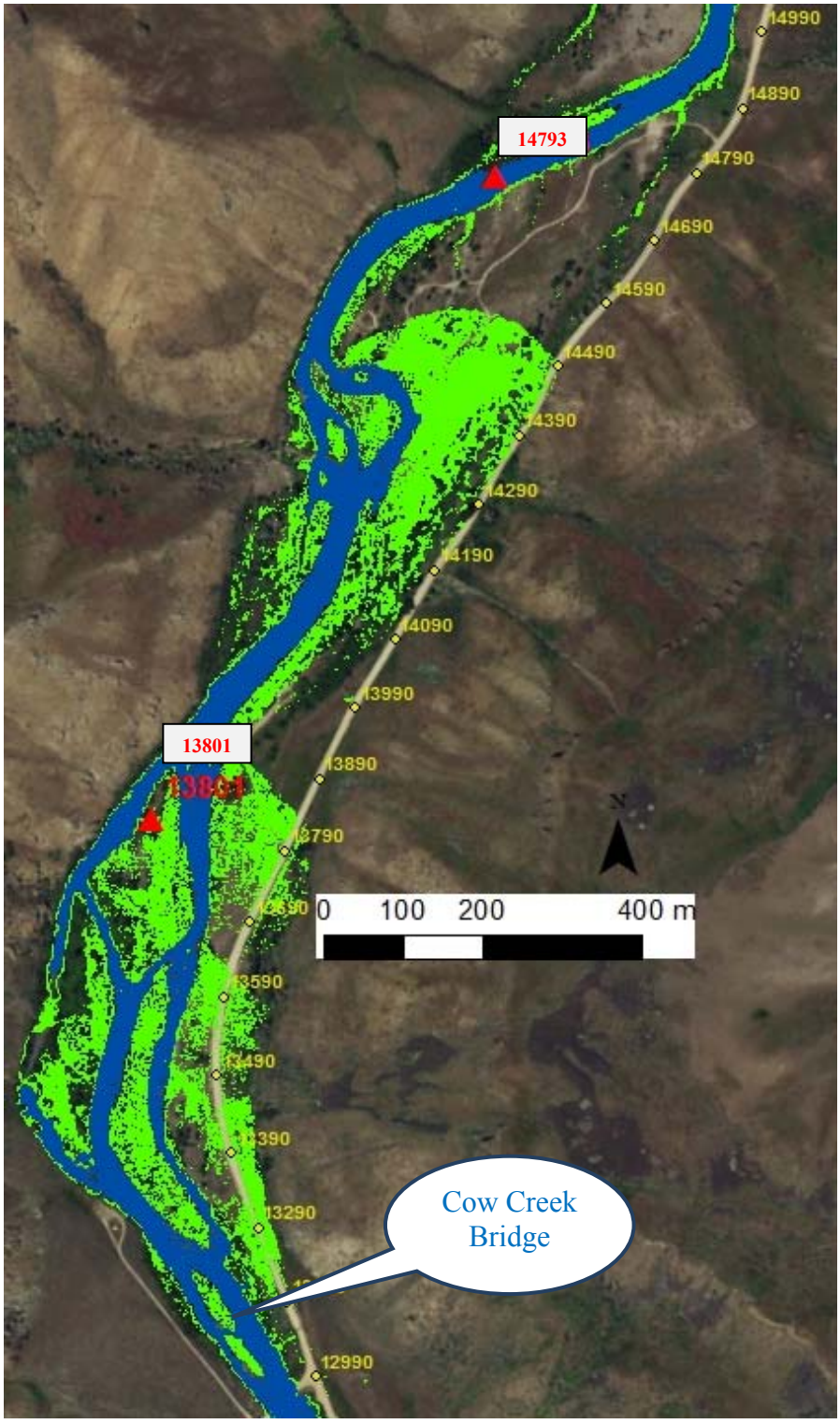

Figure 13.6: Detailed favorable areas (green) for cottonwood plantation at Site 2, downstream of Cow Creek Bridge (12990 m river distance from the Dam). Red triangles and yellow circles indicate river distance (m) from Anderson Ranch Dam and road distance based on Cow Creek Bridge, respectively.

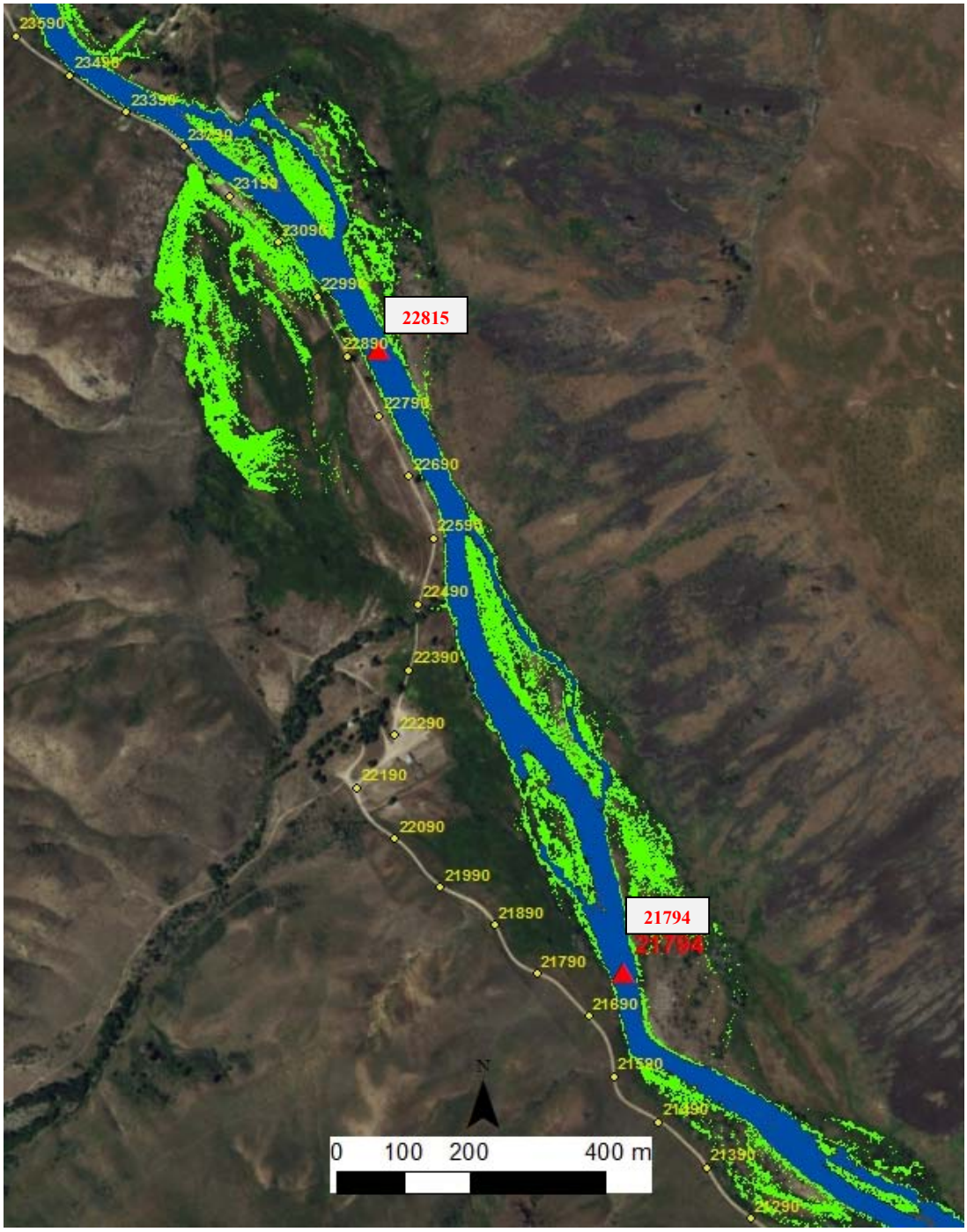

Figure 13.7: Detailed favorable areas (green) for cottonwood plantation at Site 2, downstream of Danskin Bridge (18690 m river distance from the Dam). Red triangles and yellow circles indicate river distance (m) from Anderson Ranch Dam and road distance based on Danskin Bridge, respectively.

Conversely from natural seedling recruitment, plantation has several favorable areas. Favorable areas may also include part of road, campground and tributaries, which should not be used for cottonwood plantation. Spring months may provide favorable conditions for cottonwood seedling plantations because of moist soil resulting from snow runoff and precipitation in the watershed. The Arc-GIS files are provided in a zip archive for easy printing of the favorable planting zones.

14 CONCLUSIONS

Field observation and numerical modeling show that natural cottonwood seedling recruitment is not successful in the South Fork Boise River mainly due to lack of fine sediment on emerged bars during the seedling dispersal period and unfavorable water surface elevation recession rates.

Conversely, planting of cottonwood seedlings (1-year) with 50 cm root length can be successful along the upper 23km portion of the South Fork Boise River downstream Anderson Ranch Reservoir. The numerical model developed in this work identified several locations, which are provided in Arc-GIS files. We suggest planting cottonwood seedlings in early Spring when sediment is moist and plants start to become active.

15 REFERENCES

Ahl, R.S., Woods, S.W. and Zuuring, H.R., 2008. Hydrologic calibration and validation of SWAT in a snow-dominated Rocky Mountain watershed, Montana, USA. *Journal of the American Water Resources Association*, **44**(6): 1411-1430.

Ahmadi-Nedushan, B., St-Hilaire, A., Ouarda, T.B.M.J., Bilodeau, L., Robichaud, E., Thiemonge, N. and Bobee, B., 2007. Predicting river water temperatures using stochastic models: case study of the Moisie River (Qu´ebec, Canada). *Hydrological Processes*, **21**: 21–34.

Ajami, N.K., Gupta, H., Wagener, T. and Sorooshian, S., 2004. Calibration of a semi-distributed hydrologic model for streamflow estimation along a river system. *Journal of Hydrology*, **298**: 112–135.

Amlin, N.M. and Rood, S.B., 2002. Comparative tolerances of riparian willows and cottonwoods to water-table decline. *Wetlands*, **22**(2): 338-346.

Angilletta, M.J., Steel, E.A., Bartz, K.K., Kingsolver, J.G., Scheuerell, M.D., Beckman, B.R. and Crozier, L.G., 2008. Big dams and salmon evolution: changes in thermal regimes and their potential evolutionary consequences. *Evolutionary Applications*, **1**: 286–299.

Anglin, D.R., Gallion, D.G., Barrows, M., Newlon, C., Sankovich, P., Kisaka, T.J. and Schaller, H., 2004. *Bull Trout Distribution, Movements and Habitat Usein the Walla Walla and Umatilla River Basins* U.S. Fish and Wildlife Service, Columbia River Fisheries Program Office, Vancouver, WA.

Arcement, G.J. and Schneider, V.R., 1989. *Guide for Selecting Manning's roughness coefficients for natural channels and floodplains*, USGS.

Auble, G.T. and Scott, M.L., 1998. Fluvial disturbance patches and cottonwood recruitment along the upper Missouri River, Montana. *Wetlands*, **18**(4): 546-556.

Barton, G.J., McDonald, R.R., Nelson, J.M. and Dinehart, R.L., 2005. *Simulation of flow and sediment mobility using a multidimensional flow model for the white sturgeon critical habitat reach, Kootenai near Bonners Ferry, Idaho*, U. S. Geological Survey, Reston, Virginia.

Battin, J., Wiley, M.W., Ruckelshaus, M.H., Palmer, R.N., Korb, E., Bartz, K.K. and Imaki, H., 2007. Projected impacts of climate change on salmon habitat restoration. *Proceedings of the National Academy of Sciences of the United States of America*, **104**(16): 6720-6725

Bednarek, A.T. and Hart, D.D., 2005. Modifying dam operations to restore rivers. Ecological responses to Tennessee River dam mitigation. *Ecological Applications*, **15**(997-1008).

Bélanger, M., El-Jabi, N., Caissie, D., Ashkar, F. and Ribi, J.M., 2005. Estimation de la température de l'eau en rivière en utilisant les réseaux de neurones et la régression linéaire multiple. *Journal of Water Science*, **18**(3): 403-421.

Bell, E., Duffy, W.G. and Roelofs, T.D., 2001. Fidelity and Survival of Juvenile Coho Salmon in Response to a Flood. *Transactions of the American Fisheries Society*, **130**(3): 450-458.

Benjankar, R., Burke, M., Yager, E., Tonina, D., Egger, G., Rood, S.B. and Merz, N., 2014a. Development of a spatially-distributed hydroecological model to simulate cottonwood seedling recruitment along rivers. *Journal of Environmental Management*, **145**: 277-288.

Benjankar, R., Tonina, D. and McKean, J., 2014b. One-dimensional and two-dimensional hydrodynamic modeling derived flow properties: Impacts on aquatic habitat quality predictions. *Earth Surface Processes and Landforms*, **40**(3): 340-356.

Benyahya, L., Caissie, D., St-Hilaire, A., Ouarda, T.B.M.J. and Bobée, B., 2007. A Review of Statistical Water Temperature Models. *Canadian Water Resources Journal*, **32**(3): 179–19.

Beven, K. and Freer, J., 2001. Equifinality, data assimilation, and uncertainty estimation in mechanistic modelling of complex environmental systems using the GLUE methodology. *Journal of Hydrology*, **249**(1-4), doi: 10.1016/S0022-1694(01)00421-8.

Bogan, T., Mohseni, O. and Stefan, H.G., 2003. Stream temperature-equilibrium temperature relationship. *Water Resources Research*, **39**(9): 1245 - 1257.

Bonneau, J.L. and Scarnecchia, D.L., 1996. Distribution of Juvenile Bull Trout in a Thermal Gradient of a Plunge Pool in Granite Creek, Idaho. *Transactions of the American Fisheries Society*, **125**(4): 628-630.

Boogert, A. and Dupont, D., 2005. The nature of supply side effects on electricity prices: The impact of water temperature. *Economics Letters*, **88**(1): 121-125.

Bovee, K.D., 1978. The Incremental Method of assessing habitat potential for cool water species, with management implications. *American Fisheries Society Special Publication*, **11**: 340-346.

Bovee, K.D., 1982. *A guide to stream habitat analysis using the instream flow incremental methodology. Instream Flow Information* Paper 12, US Fish and Wildlife Service, Fort Collins, Colorado.

Bovee, K.D., 1986. *Development and Evaluation of Habitat Suitability Criteria for Use in the Instream Flow Incremental Methodology. U.S. Fish Wildlife Service Biological Report 86 (7)*, Fort Collins, Colorado.

Bovee, K.D., Lamb, B.L., Bartholow, J.M., Stalnaker, C.B., Taylor, J. and Henriksen, J., 1998. *Stream habitat analysis using the instream flow incremental methodology*. Report USGS/BRD-1998-0004, U.S. Geological Survey, Biological Resources Division Information and Technology.

Bowen, Z.H., Bovee, K.D. and Waddle, T.J., 2003. Effects of Flow Regulation on Shallow-Water Habitat Dynamics and Floodplain Connectivity. *Transactions of the American Fisheries Society*, **132**: 809-823.

Boyle, D.P., Gupta, H.V., Sorooshian, S., Koren, V., Zhang, Z. and Smith, M., 2001. Toward improved streamflow forecasts: Value of semidistributed modeling. *Water Resources Research*, **37**(11): 2749-2759.

Braatne, J.H., Jamieson, R., Gill, K.M. and Rood, S.B., 2007. Instream flows and the decline of riparian cottonwoods along the Yakima River, Washington, USA. *River Research and Applications*, **23**(3): 247-267.

Braatne, J.H., Rood, S.B. and Heilman, P.E., 1996. *Life history, ecology and conservation of riparian cottonwoods in North America*. In: R.F. Stettler, G.A. Bradshaw, P.E. Heilman and T.M. Hinckley (Editors), Biology of Populus and Its Implications for Management and Conservation. NRC Research Press, Ottawa, Ontario, Canada.

Bradford, M.J., 1997. An experimental study of stranding of juvenile salmonids on gravel bars and in sidechannels during rapid flow decreases. *Regulated Rivers: Research & Management*, **13**(5): 395-401.

Bragg, O.M., Black, A.R., Duck, R.W. and Rowan, J.S., 2005. Approaching the physical-biological interface in rivers: a review of methods for ecological evaluation of flow regimes

Geography Depart. *Progress in Physical Geography* **29**: 506-531.

Brett, J.R., 1979. Environmental factors and growth. *Fish Physiology*, **VIII**: 599-675.

Brown, I., 2005. Modeling future landscape change on coastal floodplains using a rule-based GIS. *Environmental Modelling & Software*: 1-12.

Brown, R.A. and Pasternack, G.B., 2009. Comparison of methods for analysing salmon habitat rehabilitation designs for regulated rivers. *River Research and Applications*, **25**: 745-772.

Brown, T.G., 2002. *Floodplains, flooding, and salmon rearing habitats in British Columbia: a review*, Pacific Biological Station, Fisheries and Oceans Canada, Nanaimo, British Columbia, Canada.

Bruxer, J. and Thompson, A., 2008. *St. Clair River Hydrodynamic Modelling Using RMA2 Phase 2 Report*, Environment Canada, Canada.

Bunn, S.E. and Arthington, A.H., 2002. Basic Principles and Ecological Consequences of Altered Flow Regimes for Aquatic Biodiversity. *Environmental Management*, **30**(4): 492-507.

Burke, M., 2006. *Linking hydropower operation to modified fluvial processes downstream of Libby Dam, Kootenai River, USA and Canada*. MSc. Thesis, University of Idaho, Moscow, Idaho.

Burke, M., Jorde, K. and Buffington, J.M., 2009. Application of a hierarchical framework for assessing environmental impacts of dam operation: Changes in streamflow, bed mobility and recruitment of riparian trees in a western North American river. *Journal of Environmental Management*, **90**: 224-236.

Caissie, D., El-Jabi, N. and Satish, M.G., 2001. Modelling of maximum daily water temperatures in a small stream using air temperatures. *Journal of Hydrology*, **251**: 14-28.

Caldwell, R.J., Gangopadhyay, S., Bountry, J., Lai, Y. and Elsner, M.M., 2013. Statistical modeling of daily and subdaily stream temperatures: Application to the Methow River Basin, Washington. *Water Resources Research*, **49**: 4346–4361.

Campbell, E.P., Fox, D.R. and Bates, B.C., 1999. A Bayesian approach to parameter estimation and pooling in nonlinear flood event models *Water Resources Research*, **35**(1): 211-220.

Carey, M.P. and Zimmerman, C.E., 2014. Physiological and ecological effects of increasing temperature on fish production in lakes of Arctic Alaska. *Ecology and Evolution*, **4**(10): 1981-1993.

Carron, J.C. and Rajaram, H., 2001. Impact of variable reservoir releases on management of downstream temperatures. *Water Resources Research*, **37**(6): 1733-1743.

Chen, X., Kumar, M., Wang, R., Winstral, A. and Marks, D., 2016. Assessment of the timing of daily peak streamflow during the melt season in a snow-dominated watershed. *Journal of Hydrometeorology*, **17**: 2225–2244.

Chipps, S.R. and Wahl, D.H., 2008. Bioenergetics Modeling in the 21st Century: Reviewing New Insights and Revisiting Old Constraints. *Transactions of the American Fisheries Society*, **137**: 298-313.

Choo, T.H., Hong, S.H., Yoon, H.C., Yun, G.S. and Chae, S.K., 2015. The estimation of discharge in unsteady flow conditions, showing a characteristic loop form. *Environmental Earth Sciences*, **73**: 4451–4460.

Clayton, J.L., 1992. Mechanical and Hydrological Properties of Granitic Rock Associated with Weathering and Fracturing in the Idaho Batholith, Decomposed Granite Soils Conference, Boise, ID, pp. 40-50.

Congalton, R.G. and Green, K., 2008. *Assessing the accuracy of remotely sensed data: Principles and practices*. Lewis Publishers, Boca Raton, Florida, 137 pp.

Conner, J.T. and Tonina, D., 2013. Effect of cross-section interpolated bathymetry on 2D hydrodynamic results in a large river. *Earth Surface Processes and Landforms*, doi: 10.1002/esp.3458.

Connor, W.P., Burge, H.L., Yearsley, J.R. and Bjornn, T.C., 2003. Influence of Flow and Temperature on Survival of Wild Subyearling Fall Chinook Salmon in the Snake River. *North American Journal of Fisheries Management* **23**: 362-375.

Cramer, S.P. and Ackerman, N.K., 2009. Linking Stream Carrying Capacity for Salmonids to Habitat Features. *American Fisheries Society Symposium*, **71**: 225-254.

Crowder, D.W. and Diplas, P., 2000. Using two-dimensional hydrodynamic models at scales of ecological importance. *Journal of Hydrology*, **230**: 172-191.

Crowder, D.W. and Diplas, P., 2002. Vorticity and circulation: spatial metrics for evaluating flow complexity in stream habitats. *Canadian Journal of Fisheries and Aquatic Sciences*, **59**: 633-645, DOI: 10.1139/F02-037.

Crozier, L.G., Zabel, R.W., Hockersmith, E.E. and Achord, S., 2010. Interacting effects of density and temperature on body size in multiple populations of Chinook salmon. *Journal of Animal Ecology*, **79**: 342-349.

Danehy, R.J., Colson, C.G., Parrett, K.B. and Duke, S.D., 2005. Patterns and sources of thermal heterogeneity in small mountain streams within a forested setting. *Forest Ecology and Management*, **208** 287-302.

Danish Hydraulics Institute (DHI), 2007. MIKE21 flow model, hydrodynamic module, user guide, pp. 90.

Danish Hydraulics Institute (DHI), 2011a. MIKE11, reference manual: A modelling system for rivers and channels, pp. 536.

Danish Hydraulics Institute (DHI), 2011b. MIKE21 flow model, hydrodynamic module, user guide, pp. 116.

Danish Hydraulics Institute (DHI), 2011c. MIKE 11 GIS, pp. 90.

Dauwalter, D., Vidergar, D. and Kozfkay, J., 2013. *A pilot study of fish stranding on the South Fork Boise River, 2012*, Trout Unlimited, U.S. Bureau of Reclamation, Idaho Department of Fish and Game, Boise, ID.

Department of Environmental Quality (DEQ), 2008. *South Fork Boise River Subbasin Assessment, Total Maximum Daily Load, And Five-Year Review*, Department of Environmental Quality, Boise Regional Office and State Technical Services Office, Boise, Idaho.

Dingman, S.L. and Bjerklie, D.M., 2006. *Estimation of River Discharge. Encyclopedia of Hydrological Sciences. 5:61.*

.

Elder, K., Dozier, J. and Michaelse, J., 1991. Snow Accumulation and Distribution in an Alpine Watershed. *Water Resources Research*, **27**(7): 1541-155.

Ficklin, D.L., Luo, Y., Stewart, I.T. and Maurer, E.P., 2012. Development and application of a hydroclimatological stream temperature model within the Soil and Water Assessment Tool. *Water Resources Research*, **48** W01511.

Forseth, T. and Jonsson, B., 1994. The growth and food ration of piscivorous brown trout. *Functional Ecology*, **8**: 171-177.

Fraley, J.J. and Shepard, B.B., 1989. Life History, Ecology and Population Status of Migratory Bull Trout (salvelinusc onfluentus) in the Flathead Lake and River System, Montana. *Northwest Science*, **63**(4): 133-143.

Freeze, R.A. and Harlan, R.L., 1969. Blueprint for a physically-based, digitally-simulated hydrologic response model. *Journal of Hydrology*, **9**(3): 237-258.

Garen, D.C. and Marks, D., 1996. Spatially distributed snow modelling in mountainous regions: Boise River application, HydroGIS 96: Application of Geographic Information Systems in Hydrology and Water Resources Management. IAHS, Vienna, Austria, pp. 421-428.

Garen, D.C. and Marks, D., 2005. Spatially distributed energy balance snowmelt modelling in a mountainous river basin: estimation of meteorological inputs and verification of model results. *Journal of Hydrology*, **315**: 126-153.

Gelman, A., 2002. *Prior Distribution*, Encyclopedia of Environmetrics, pp. 1634 – 1637.

Gelman, A., 2006. Prior distributions for variance parameters in hierarchical models. *Bayesian Anal.*, **1**: 515–533.

Gelman, A. and Hill, J., 2007. *Data Analysis Using Regression and Multilevel/Hierarchical Models*. Cambridge University Press, 648 pp.

Gilks, W.R., Best, N.G. and Tan, K.K.C., 1995. Adaptive rejection metropolis sampling within Gibbs sampling. *Appl. Statist*, **44**(4): 455–472.

Gillam, P., Jempson, M. and Rogencamp, G., 2005. The importance of combined 2D/1D modelling of complex floodplains -Tatura case study, Fourth Victorian Flood Management Conference, Shepparton, Victoria, Australia.

Gorski, K., Collier, K.J., Hamilton, D.P. and Hicks, B.J., 2014. Effects of flow on lateral interactions of fish and shrimps with off-channel habitats in a large river-floodplain system. *Hydrobiologia*, **729**: 161-174.

Gu, R., McCutcheon, S. and Chen, C.-J., 1999. Development of weather-dependent flow requirements for river temperature control. *Environmental Management*, **24**(4): 529-540.

Haddeland, I., Matheussen, B.V. and Lettenmaier, D.P., 2002. Influence of spatial resolution on simulated streamflow in a macroscale hydrologic model. *Water Resources Research*, **38**(7): 1124.

Halleraker, J.H., Saltveit, S.J., Harby, A., Arnekleiv, J.V., Fjeldstad, H.-P. and Kohler., B., 2003. Factors influencing stranding of wild juvenile brown trout (Salmo trutta) during rapid and frequent flow decreases in an artificial stream. *River Research and Applications*, **19**: 589-603.

Hardy, T.B., 1998. The future of habitat modeling and instream flow assessment techniques. *Regulated Rivers: Research and Management*, **14**(2): 405-420.

Hébert, C., Caissie, D., Satish, M.G. and El-Jabi, N., 2015. Predicting Hourly Stream Temperatures Using the Equilibrium Temperature Model. *Journal of Water Resource and Protection*, **7**: 322-338.

Henderson, F.M., 1966. *Open Channel Flow*.

Higgins, P.S. and Bradford, M.J., 1996. Evaluation of a Large-Scale Fish Salvage to Reduce the Impacts of Controlled Flow Reduction in a Regulated River. *North American Journal of Fisheries Management*, **16**(3): 666-673.

Hightower, J.E., Harris, J.E., Raabe, J.K., Brownell, P. and Drew, C.A., 2012. A Bayesian Spawning Habitat Suitability Model for American Shad in Southeastern United States Rivers. *Journal of Fish and Wildlife Management*, **3**(2): 184-198.

Hillman, T.W. and Essig, D., 1998. *Review of Bull Trout Temperature Requirements:A Response To the EPABull Trout Temperature Rule*, BioAnalysts, Inc., Idaho DEQ and Idaho Division of Environmental Quality, Boise, Idaho.

Hockey, J.B., Owens, I.F. and Tapper, N.J., 1982. Empirical and theoretical models to isolate the effect of discharge on summer water temperature in the Hurunui River. *Journal of Hydrology*, **21**(1): 1-12.

Horritt, M.S., 2000. Calibration and validation of a 2-dimensional finite element flood flow model using satellite radar imagery. *Water Resources Research*, **36**(11): 3279-3291.

Horritt, M.S. and Bates, P.D., 2002. Evaluation of 1D and 2D numerical models for predicting river flood inundation. *Journal of Hydrology*, **268**: 87–99.

Howell, P., Dunham, J.B. and Sankovich, P., 2010. Relationships between water temperatures and upstream migration, cold water refuge use, and spawning of adult bull trout from the Lostine River, Oregon, USA. *Ecology of Freshwater Fish*, **19**: 96-106.

Hudson, H.R., Byrom, A.E. and Chadderton, W.L., 2003. A critique of IFIM—instream habitat simulation in the New Zealand context. *Science for Conservation*, **231**: 69.

Intergovernmental panel On climate change (IPCC), 2013. *Summary for Policymakers*. In: T.F. Stocker, D. Qin, G.-K. Plattner, M. Tignor, S. K. Allen, J. Boschung, A. Nauels, Y. Xia, V. Bex and P.M. Midgley (Editor), Climate Change 2013: The Physical Science Basis. Contribution of Working Group I to the Fifth Assessment Report of the Intergovernmental Panel on Climate Change Cambridge University Press, Cambridge, United Kingdom and New York, NY, USA., pp. 33.

Irvine, R.L., Oussoren, T., Baxter, J.S. and Schmidt, D.C., 2009. The Effects of Flow Reduction Rates on fish Stranding in British Columbia, Canada. *River Research and Applications*, **25**: 405-415.

Isaak, D.J., Horan, D.L. and Wollrab, S.P., 2013. *A simple protocol using underwater epoxy to install annual temperature monitoring sites in rivers and streams*, Department of Agriculture, Forest Service, Rocky Mountain Research Station, Fort Collins, CO: U.S.

Isaak, D.J., Luce, C.H., Rieman, B.E., Nagel, D.E., Peterson, E.E., Horan, D.L., Parkes, S. and Chandler, G.L., 2010. Effects of climate change and wildfire on stream temperatures and salmonid thermal habitat in a mountain river network. *Ecological Applications*, **20**(5): 1350-1371.

Isaak, D.J., Wollrab, S., Horan, D. and Chandler, G., 2012. Climate change effects on stream and river temperatures across the northwest U.S. from 1980–2009 and implications for salmonid fishes. *Climate Change*, **113**(2): 499-524.

Isaak, D.J., Young, M.K., Nagel, D.E., Horan, D.L. and Groce, M.C., 2015. The cold-water climate shield: Delineating refugia for preserving salmonoid fishes through the 21st century. *Global Change Biology*, **21**: 2540–2553.

IUPAC, 2014. *The Gold Book*, Compendium of Chemical Terminology version 2.3.3, pp. 610.

Jackson, P., 1999. *A high-performance, easy-to-use GPS surveying system*, Leica Geosystems AG, Heerbrugg, Switzerland.

Jobling, M., 1997. *Temperature and growth: modulation of growth rate via temperature change*, Global Warming: Implications for Freshwater and Marine Fish. Cambridge University Press, pp. 225-253.

Johnson, B.M., Saito, L., Anderson, M.A., Andre, M. and Fontane, D.G., 2004. Effects of Climate and Dam Operations on Reservoir Thermal Structure. *Journal of Water Resources Planning and Management*, **130**(2): 112-122.

Johnson, S., 2003. Stream temperature: scaling of observations and issues for modelling. *Hydrological Processes*, **17**(2): 497-499.

Johnson, W.C., 1994. Woodland Expansions in the Platte River, Nebraska: Patterns and Causes. *Ecological Monographs*, **64**(1): 45-84.

Junk, W.J., Bayley, P.B. and Sparks, R.E., 1989. The flood pulse concept in river-floodplain systems. In: D.P. Dodge (Editor), Proceedings of the international large river Symposium. Canadian Special Publication of Fisheries and Aquatic Sciences, Ottawa, Canada, pp. 110-127.

Kail, J., Guse, B., Radinger, J., Schröder, M., Kiesel, J., Kleinhans, M., Schuurman, F., Fohrer, N., Hering, D. and Wolter, C., 2015. A Modelling Framework to Assess the Effect of Pressures on River Abiotic Habitat Conditions and Biota. *PLoS ONE* **10**(6): 21.

Kondolf, G.M., Larsen, E.W. and Williams, J.G., 2000. Measuring and Modeling the Hydraulic Environment for Assessing Instream Flows. *North American Journal of Fisheries Management*, **20**: 1016-1028.

Kormos, P.R., Marks, D., McNamara, J.P., Marshall, H.P., Winstral, A. and Flores, A.N., 2014. Snow distribution, melt and surface water inputs to the soil in the mountain rain–snow transition zone. *Journal of Hydrology*, **519**: 190-204.

Kumar, M., Marks, D., Dozier, J., Reba, M. and Winstral, A., 2013. Evaluation of distributed hydrologic impacts of temperature-index and energy-based snow models. *Advances in Water Resources*, **56**: 77-89.

Kwon, H.-H., Brown, C. and Lall, U., 2008. Climate informed flood frequency analysis and prediction in Montana using hierarchical Bayesian modeling. *Geophysical Research Letters*, **35**: L05404.

Lacey, R.W.J. and Millar, R.G., 2004. Reach Scale Hydraulic Assessment of Instream Salmonid Habitat Restoration. *Journal of the American Water Resources Association (JAWRA)*, **40**(6): 1631-1644.

Lancaster, J. and Downes, B.J., 2010. Linking the hydraulic world of individual organisms to ecological processes: putting ecology into ecohydraulics. *River Research and Applications*, **26**: 385-403.

Lane, S.N., 1998. Hydraulic modelling in hydrology and geomorphology: A review of high resolution approaches. *Hydrological Processes*, **12**: 1131-1150.

Lane, S.N. and Bates, P.D., 1998. Special Issue: High Resolution Flow Modelling. *Hydrological Processes*, **12**(8): 1129-1396.

Lane, S.N. and Richards, K.S., 1998. High resolution, two-dimensional spatial modelling of flow processes in a multi-thread channel. *Hydrological Processes*, **12**(8): 1279-1298.

Langan, S.J., Johnston, L., Donaghy, M.J., Youngson, A.F., Hay, D.W. and Soulsby, C., 2001. Variation in river water temperatures in an upland stream over a 30-year period. *Science of The Total Environment*, **265**: 195-207.

Leclerc, M., Boudreault, A., Bechara, J.A. and Corfa, G., 1995. Two-dimensional hydrodynamic modeling: a neglected tool in the instream flow incremental methodology. *Transactions of the American Fisheries Society*, **124**(5): 645-662.

Leclerc, M., Saint-Hilaire, A. and Bechara, J., 2003. State-of-the-Art and Perspectives of Habitat Modelling for Determining Conservation Flows. *Canadian Water Resources Journal*, **28**(2): 135-151.

Lessard, J.L. and Hayes, D.B., 2003. Effects of elevated water temperature on fish and macroinvertebrate communities below small dams. *River Research and Applications*, **19**(7): 721-732.

Levin, P.S. and Schiewe, M.H., 2001. Preserving Salmon Biodiversity: The number of Pacific salmon has declined dramatically. But the loss of genetic diversity may be a bigger problem *American Scientist*, **89**(3): 220-227.

Lewis River workshops, 2000. *AQU 2 Appendix 1: Suitability Curves used in the Swift Bypass Reach IFIM study* Lewis River workshops.

Li, R., Chen, Q., Tonina, D. and Cai, D., 2015. Effects of upstream reservoir regulation on the hydrological regime and fish habitats of the Lijiang River, China. *Ecological Engineering*, **76**: 75-83.

Liang, X., Lettenmaier, D.P., Wood, E.F. and Burges, S.J., 1994. A simple hydrologically based model of land-surface water and energy fluxes for general-circulation models. *Journal of Geophysical Research-Atmospheres*, **99**: 14415-14428.

Link, T.E. and Marks, D., 1999. Distributed simulation of snowcover mass- and energybalance in the boreal forest. *Hydrological Processes*, **13**: 2439–52.

Liston, G.E. and Elder, K., 2006. A Distributed Snow-Evolution Modeling System (SnowModel). *Journal of Hydrometeorology*, **7**(6): 1259–1276.

Lobligeois, F., Andréassian, V., Perrin, C., Tabary, P. and Loumagne, C., 2014. When does higher spatial resolution rainfall information improve streamflow simulation? An evaluation using 3620 flood events. *Hydrol. Earth Syst. Sci.*, **18**: 575–594.

Loinaz, M.C., Davidsen, H.K., Butts, M. and Bauer-Gottwein, P., 2013. Integrated flow and temperature modeling at the catchment scale. *Journal of Hydrology*, **495** 238-251.

Lowney, C.L., 2000. Stream temperature variation in regulated rivers: Evidence for a spatial pattern in daily minimum and maximum magnitudes. *Water Resources Research*, **36**(10): 2947 - 2955.

Luce, C., Staab, B., Kramer, M., Wenger, S., Isaak, D. and McConnell, C., 2014. Sensitivity of summer stream temperatures to climate variability in the Pacific Northwest. *Water Resources Research*, **50**(4): 3428–3443.

Lunn, D.J., Thomas, A., Best, N. and Spiegelhalter, D., 2000a. WinBUGS-A Bayesian modelling framework: Concepts, structure, and extensibility. *Statatistical Computation*, **10**(4): 325–337.

Lunn, D.J., Thomas, A., Best, N. and Spiegelhalter, D., 2000b. WinBUGS -- a Bayesian modelling framework: concepts, structure, and extensibility. *Statistics and Computing*, **10**: 325--337.

Lytle, D.A. and Merritt, D.M., 2004. Hydrologic regimes and riparian forests: A structured population model for cottonwood. *Ecology*, **85**(9): 2493-2503.

MacWilliams, M.L., Street, R.L. and Kitanidis, P.K., 2004. Modeling floodplain flow on Lower Deer Creek, CA. In: C. Greco and D. Morte (Editors), River Flow 2004, Second International Conference on Fluvial Hydraulics. Balkema, Naples, Italy, pp. 1429-1439.

Mahoney, J.M. and Rood, S.B., 1991. A device for studying the influence of declining water table on poplar growth and survival. *Tree Physiology*, **8**: 305-3 14.

Mahoney, J.M. and Rood, S.B., 1998. Stream flow requirements for cottonwood seedling recruitment - An integrated model. *Wetlands*, **18**(4): 634-645.

Malcolm, I.A., Gibbins, C.N., Soulsby, C., Tetzlaff, D. and Moir, H.J., 2012. The influence of hydrology and hydraulics on salmonids between spawning and emergence: implications for the management of flows in regulated rivers. *Fisheries Management and Ecology*, **19**: 464–474.

Mantua, N., Tohver, I. and Hamlet, A., 2010. Climate change impacts on stream flow extremes and summertime stream temperature and their possible consequences for freshwater salmon habitat in Washington State. *Climate Change*, **102**: 187–223.

Maret, T.R., Hortness, J.E. and Ott, D.S., 2006. *Instream flow characterization of upper Salmon River Basin streams, central Idaho, 2005: U.S. Geological Survey Scientific Investigations Report 2006-5230*, U.S. Geological Survey Reston, Virginia.

Maret, T.R. and Schultz, J.E., 2013. *Bull Trout (Salvelinus confluentus) Movement in Relation to Water Temperature, Season, and Habitat Features in Arrowrock Reservoir, Idaho: U.S. Geological Survey Scientific Investigations Report 2013–5158*, U.S. Geological Survey and Bureau of Reclamation, Reston, Virginia.

Marks, D., 1988. *Climate, Energy Exchange, and Snowmelt in Emerald Lake Watershed, Sierra Nevada*. Ph.D. Thesis Thesis, University of California Santa Barbara, Santa Barbara, CA, 158 pp.

Marks, D., Domingo, J., Susong, D., Link, T. and D.Garen, 1999. A spatially distributed energy balance snowmelt model for application in mountain basins. *Hydrological Process* **13**: 1935-1959.

Marks, D., Winstral, A., Reba, M., Pomeroy, J. and Kumar, M., 2013. An evaluation of methods for determining during-storm precipitation phase and the rain/snow transition elevation at the surface in a mountain basin. *Journal of Advances in Water Resources*, **55**: 98-110.

Marotz, B., Becker, D., Hayden, J., Hoffman, G., Ireland, S., Paragamian, V., Rogers, R., Soults, S. and Wood, A., 2001. *Draft - Kootenai River sub-basin summary*, Northwest Power Planning Council.

Martens, K.D. and Connolly, P.J., 2014. Juvenile Anadromous Salmonid Production in Upper Columbia River Side Channels with Different Levels of Hydrological Connection

Transactions of the American Fisheries Society **143**: 757-767.

Marzadri, A., Tonina, D. and Bellin, A., 2011. A semianalytical three-dimensional process-based model for hyporheic nitrogen dynamics in gravel bed rivers. *Water Resources Research*, **47**: W11518.

Marzadri, A., Tonina, D. and Bellin, A., 2012. Morphodynamic controls on redox conditions and on nitrogen dynamics within the hyporheic zone: Application to gravel bed rivers with alternate-bar morphology. *Journal of Geophysical Research*, **117**.

Mason, D.C., Cobby, D.M., Horritt, M.S. and Bates, P.D., 2003. Floodplain friction parameterization in two-dimensional river flood models using vegetation heights derived from airborne scanning laser altimetry. *Hydrological Processes*, **17**: 1711-1732.

McKean, J.A., Isaak, D.J. and Wright, C.W., 2009a. Improving stream studies with a small-footprint Green Lidar. *EOS, Transactions of the American Geophysical Union*, **90**(39): 341-342.

McKean, J.A., Nagel, D., Tonina, D., Bailey, P., Wright, C.W., Bohn, C. and Nayegandhi, A., 2009b. Remote sensing of channels and riparian zones with a narrow-beam aquatic-terrestrial LIDAR. *Remote Sensing*, **1**: 1065-1096, doi:10.3390/rs1041065.

McMahon, T.E., Zale, A.V., Barrows, F.T. and Selong, J.H., 2007. Temperature and Competition between Bull Trout and Brook Trout: A Test of the Elevation Refuge Hypothesis. *Transactions of the American Fisheries Society*, **136**: 1313-1326.

Merenlender, A.M. and Matella, M.K., 2013. Maintaining and restoring hydrologic habitat connectivity in mediterranean streams: an integrated modeling framework. *Hydrobiologia*, **719**(1): 509-525

Mesa, M.G., Weiland, L.K., Christiansen, H.E. and Sauter, S.T., 2013. Development and Evaluation of a Bioenergetics Model for Bull Trout. *Transactions Of The American Fisheries Society*, **142**: 41-49.

Mohseni, O., Stefan, H.G. and Erickson, T.R., 1998. A nonlinear regression model for weekly stream temperatures. *Water Resources Research*, **34**(10): 2685–2692.

Moir, H.J., Gibbins, C.N., Soulsby, C. and Youngson, A.F., 2005. PHABSIM modelling of Atlantic salmon spawning habitat in an upland stream: testing the influence of habitat suitability indices on model output. *River Research and Applications*, **21**: 1021-1034.

Moore, V.K., Cadwallader, D.R. and Mate, S.M., 1979. *South Fork Boise River Creel Census and Fish Population Studies*, Idaho Department of Fish and Game.

Moriasi, D.N., Arnold, J.G., Liew, M.W.V., Bingner, R.L., Harmel, R.D. and Veith, T.L., 2007. Model evaluation guidelines for systematic quantification of accuracy in watershed simulations. *Transactions of the ASABE*, **50**(3): 885-900.

Muhlfeld, C.C., Jones, L., Kotter, D., Miller, W.J., Geise, D., Tohtz, J. and Marotz, B., 2012. Assessing the impacts of river regulation on native bull trout (Salvelinus confluentus) and westslope cutthroat trout (Oncorhynchus clarkii lewisi) habitats in the upper Flathead River, Montana, USA. *River Research and Applications*, **28**: 940-959.

Nagrodski, A., Raby, G.D., Hasler, C.T., Taylor, M.K. and Cooke, S.J., 2012. Fish stranding in freshwater systems: Sources, consequences, and mitigation. *Journal of Environmental Management*, **103**: 133-141.

Naiman, R.J., Decamps, H. and Pollock, M., 1993. The role of Riparian Corridors in Maintaining Regional Biodiversity. *Ecological Applications* **3**(2): 209-212.

Nash, J.E. and Sutcliffe, J.V., 1970. River flow forecasting through conceptual models part I- A discussion of principles. *Journal of Hydrology*, **10**(3): 282-290.

Neumann, D.W., Rajagopalan, B. and Zagona, E.A., 2003. Regression Model for Daily Maximum Stream Temperature. *Journal of Environmental Engineering*, **129**(7): 667-674.

Newson, M.D. and Newson, C.L., 2000. Geomorphology, ecology and river channel habitat: mesoscale approaches to basin-scale challenges. *Progress in Physical Geography*, **24**(2): 195-217.

Null, S.E., Deas, M.L. and Lund, J.R., 2010. Flow and water temperature simulation for habitat restoration in the Shasta River, California. *River Research and Applications*, **26**: 663-681.

Null, S.E., Ligare, S.T. and Viers, J.H., 2013. A Method to Consider Whether Dams Mitigate Climate Change Effects on Stream Temperatures. *Journal of the American Water Resources Association*, **49**(6): 1456-1472.

Null, S.E., Viers, J.H., Deas, M.L., Tanaka, S.K. and Mount, J.F., 2012. Stream temperature sensitivity to climate warming in California's Sierra Nevada: Impacts to coldwater habitat. *Climate Change*, **116**: 149–170.

Olden, J.D. and Naiman, R.J., 2010. Incorporating thermal regimes into environmental flows assessments: modifying dam operations to restore freshwater ecosystem integrity. *Freshwater Biology*, **55**: 86-107.

Palmer, M.A., Bernhardt, E.S., Allan, J.D., Lake, P.S., Alexander, G., Brooks, S., Carr, J., Clayton, S., Dahm, C.N., Shah, J.F., Galat, D.L., Loss, S.G., Goodwin, P., Hart, D.D., Hassett, B., Jenkinson, R., Kondolf, G.M., Lave, R., Meyer, J.L., O'Donnell, T.K., Pagano, L. and Sudduth, E., 2005. Standards for ecologically successful river restoration. *Journal of Applied Ecology*, **42**(2): 208-217.

Pasternack, G.B., Gilbert, A.T., Wheaton, J.M. and Buckland, E.M., 2006. Error propagation for velocity and shear stress prediction using 2D models for environmental management. *Journal of Hydrology*, **328**: 227-241.

Pasternack, G.B. and Senter, A., 2011. *21st Century instream flow assessment framework for mountain streams*, Public Interest Energy Research (PIER), California Energy Commission.

Pasternack, G.B., Wang, C.L. and Merz, J.E., 2004. Application of a 2D hydrodynamic model to design of reach-scale spawning gravel replenishment on the Mokelumne river, California. *River Research and Applications*, **20**(2): 205-225, doi: 10.1002/rra.748.

Perry, A.L., Low, P.J., Ellis, J.R. and Reynolds, J.D., 2005. Climate Change and Distribution Shifts in Marine Fishes. *Science*, **308**.

Piccolroaz, S., Calamita, E., Majone, B., Gallice, A., Siviglia, A. and Toffolon, M., 2016. Prediction of river water temperature: a comparison between a new family of hybrid models and statistical approaches. *Hydrological Processes*: DOI: 10.1002/hyp.10913.

Poff, N.L., Allan, J.D., Bain, M.B., Karr, J.R., Prestegaard, K.L., Richter, B.D., Sparks, R.E. and Stromberg, J.C., 1997. The natural flow regime. *Bioscience*, **47**(11): 769-784.

Poff, N.L. and Hart, D.D., 2002. How Dams Vary and Why It Matters for the Emerging Science of Dam Removal. *BioScience*, **52**(8): 659-668.

Poole, G., Dunham, J., Hicks, M., Keenan, D., Lockwood, J., Materna, E., McCullough, D., Mebane, C., Risley, J., Sauter, S., Spalding, S. and Sturdevant, D., 2001. *Scientific Issues Relating to Temperature Criteria for Salmon, Trout, and Char Native to the Pacific Northwest*, United States Environmental Protection Agency.

Preece, R.M. and Jones, H.A., 2002. The effect of Keepit Dam on the temperature regime of the Namoi River, Australia. *River Research and Applications*, **18**(4): 397-414.

Pringle, C.M., 2003. The need for a more predictive understanding of hydrologic connectivity. *Aquatic Conservation: Marine and Freshwater Ecosystems*, **13**: 467-471.

Railsback, S.F. and Rose, K.A., 1999. Bioenergetics Modeling of Stream Trout Growth: Temperature and Food Consumption Effects. *Transactions Of The American Fisheries Society*, **128**: 241-256.

Rice, J.A., Breck, J.E., Bartell, S.M. and Kitchell, J.F., 1983. Evaluating the constraints of temperature, activity, and consumption on growth of Largemouth Bass. *Environmental Biology of Fishes*, **9**(3/4): 263-275.

Richter, B.D. and Thomas, G.A., 2007. Restoring Environmental Flows by Modifying Dam Operations. *Ecology and Society*, **12**(1).

Rieman, B.E., Isaak, D.J., Adams, S., Horan, D., Nagel, D., Luce, C. and Myers, D., 2007. Anticipated climate warming effects on bull trout habitats and populations across the Interior Columbia River Basin. *Transactions of the American Fisheries Society*, **136**: 1552–1565.

Rieman, B.E. and Mclntyre, J.D., 1993. *Demographic and Habit Reauirements for conseriation of Bull Trout. General Technical Report-302*, U.S. Department of Agriculture, Forest Service, Intermountain Research Station, Ogden, UT.

RiesIII, K.G., 2007. *The National Streamflow Statistics Program: A Computer Program for Estimating Streamflow Statistics for Ungaged Sites: U.S. Geological Survey Techniques and Methods 4-A6*, U.S. Geological Survey, Reston, Virginia.

Risley, J.C., Constantz, J., Essaid, H. and Rounds, S., 2010. Effects of upstream dams versus groundwater pumping on stream temperature under varying climate conditions. *WATER RESOURCES RESEARCH*, **46**: W06517.

Risley, J.C., Roehl, E.A. and Conrads, P.A., 2003. *Estimating Water Temperatures in Small Steams in Western Oregon Using Neural Network Models*, U.S. Geological Survey Report 02-4218.

Robeson, S.M., 2002. Relationships between mean and standard deviation of air temperature: implications for global warming. **22**: 205-213.

Sabaton, C., Souchon, Y., Herve Capra, Gouraud, V., Lascaux, J.-M. and Tissot, L., 2008. Long-term brown trout populations responses to flow manipulation. *River Research and Applications*, **24**(5): 476-505.

Salow, T., 2005. *Arrowrock Dam Outlet Works Rehabilitation Endangered Species Monitoring and Mitigation Program: Compilation of 2003 monthly summary reports for radio telemetry investigations for bull trout (Salvelinus confluentus)*, U.S. Department of the Interior Bureau of Reclamation, Boise, Idaho.

Salow, T. and Hostettler, L., 2004. *Movement and mortality patterns of adult adfluvial Bull Trout (Salvelinus confluentus) in the Boise River basin, Idaho*, U.S. Bureau of Reclamation, Snake River Area Office, Boise, Idaho.

Saltveit, S.J., Halleraker, J.H., Arnekleiv, J.V. and Harby, A., 2001 Field experiments on stranding in juvenile atlantic salmon (Salmo salar) and brown trout (Salmo trutta) during rapid flow decreases caused by hydropeaking. *River Research and Applications*, **17**(4-5): 609-622

Schlosser, I.J., 1991. Stream Fish Ecology: A Landscape Perspective *BioScience* **41**(10): 704-712

Schlosser, I.J., Johnson, J.D., Knotek, W.L. and Lapinska, M., 2000. Climate Variability and Size-Structured Interactions among Juvenile Fish along a Lake-Stream Gradient. *Ecology*, **81**(4): 1046-1057.

Segond, M.-L., Wheater, H.S. and Onof, C., 2007. The significance of spatial rainfall representation for flood runoff estimation: A numerical evaluation based on the Lee catchment, UK. *Journal of Hydrology*, **347**: 116– 131.

Selong, J.H., McMahon, T.E., Zale, A.V. and Barrows, F.T., 2001. Effect of Temperature on Growth and Survival of Bull Trout, with Application of an Improved Method for Determining Thermal Tolerance in Fishes. *Transactions of the American Fisheries Society*, **130**(6): 1026-1037.

Shirvell, C.S., 1994. Effect of changes in streamflow on the microhabitat use and movements of sympatric juvenile coho salmon (Oncorhynchus kisutch) and chinook salmon (O. tshawytscha) in a natural stream. *Canadian Journal of Fisheries and Aquatic Sciences*, **51**: 1644-1652.

Sinokrot, B.A. and Gulliver, J.S., 2010. In-stream flow impact on river water temperatures. *Journal of Hydraulic Research* **38**(5): 339-349.

Sinokrot, B.A., Stefan, H.G., McCormick, J.H. and Eaton, J.G., 1995. Modeling of climate change effects on stream temperatures and fish habitats below dams and near groundwater inputs. *Climatic Change*, **30**: 181-200.

Skinner, K.D., 2011. *Evaluation of LiDAR-Acquired Bathymetric and Topograhic Data Accuracy in Various Hydrogeomorphic Settings in the Deadwood and South Fork Boise Rivers, West-Central Idaho, 2007: U.S. Geological Survey Scientific Investigations Report 2011–5051*, U.S. Geological Survey Reston, Virginia.

Smith, L.C. and Pavelsky, T.M., 2008. Estimation of river discharge, propagation speed, and hydraulic geometry from space: Lena River, Siberia. *Water Resources Research*, **44** W03427.

Smith, M.B., Koren, V.I., Zhang, Z., Reed, S.M., Pan, J.-J. and Moreda, F., 2004. Runoff response to spatial variability in precipitation: an analysis of observed data. *Journal of Hydrology*, **298** 267-286.

Smith, T., Marshall, L. and McGlynn, B., 2014. Calibrating hydrologic models in flow-corrected time. *Water Resources Research*, **50**: 748–753.

Sohrabi, M., Ryu, J., Abatzoglou, J. and Tracy, J., 2015. Development of Soil Moisture Drought Index to Characterize Droughts. *J. Hydrol. Eng.*, **DOI: 10.1061/(ASCE)HE.1943-5584.0001213**.

Sohrabi, M.M., Ryu, J., Abatzoglou, J. and Tracy, J., 2013. Climate extreme and its linkage to regional drought over Idaho. *Natural Hazards*, **65**(1): 653-681.

Sohrabi, M.M., Ryu, J.H., Abatzoglou, J. and Tracy, J., 2015 Development of Soil Moisture Drought Index to Characterize Droughts. *Journal of Hydrologic Engineering*, **20**(11): 1-15.

Solazzi, M.F., Nickelson, T.E., Johnson, S.L. and Rodgers, J.D., 2000. Effects of increasing winter rearing habitat on abundance of salmonids in two coastal Oregon streams. *Canadian Journal of Fisheries and Aquatic Sciences*, **57**: 906-914.

Solomon, D.J. and Sambrook, H.T., 2004. Effects of hot dry summers on the loss of Atlantic salmon, Salmo salar, from estuaries in South West England. *Fisheries Management and Ecology*, **11**: 353–363.

Soong, D.T., Prater, C.D., Halfar, T.M. and Wobig, L.A., 2012. *Manning's roughness coefficient for Illinois streams*, U.S. Geological Survey, Reston, Virginia.

Spiegelhalter, D.J., Thomas, A., Best, N.G., Gilks, W.R. and Lunn, D., 2003. *BUGS: Bayesian inference using Gibbs sampling*. MRC Biostatistics Unit. Cambridge.

Statzner, B., Gore, J.A. and Resh, V.H., 1988. Hydraulic stream ecology: observed patterns and potential applications. *Journal of the North American Benthological Society*, **7**(4): 307-360.

Steel, E.A. and Lange, I.A., 2007. Using wavelet analysis to detect changes in water temperature regimes at multiple scales: effects of multi-purpose dams in the Willamette River basin. *River Research and Applications*, **23**(4): 351-359.

Sturtz, S., Ligges, U. and Gelman, A., 2005. R2WinBUGS: A Package for Running WinBUGS from R. *Journal of Statistical Software*, **12**(3): 16.

Susong, D., Marks, D. and Garen, D.C., 1999. Methods for developing time-series climate surfaces to drive topographically distributed energy- and water-balance models. *Hydrol Proc*, **13**: 2003-2021.

Tarboton, D.G., 1997. A new method for the determination of flow directions and upslope areas in grid digital elevation models. *Water Resources Research* **33**(2): 309-319.

Tetzlaff, D., Soulsby, C., Bacon, P.J., Youngson, A.F., Gibbins, C. and Malcolm, I.A., 2007. Connectivity between landscapes and riverscapes-a unifying theme in integrating hydrology and ecology in catchment science? *Hydrological process*, **21**: 1385-1389.

Tierney, L., 1994. Markov Chains for exploring posterior distributions. *The Annals Of Statistics*, **22**(4): 1701-1728.

Tiffan, K.F., Garland, R.D. and Rondorf, D.W., 2002. Quantifying Flow-Dependent Changes in Subyearling Fall Chinook Salmon Rearing Habitat Using Two-Dimensional Spatially Explicit Modeling. *North American Journal of Fisheries Management*, **22**(3): 713-726.

Tiffan, K.F., Haskell, C.A. and Kock, T.J., 2010. Quantifying the behavioral response of spawning chum salmon to elevated discharges from Bonneville Dam, Columbia river, USA. *River Research and Applications*, **26**(2): 87-101.

Toffolon, M. and Piccolroaz, S., 2015. A hybrid model for river water temperature as a function of air temperature and discharge. *Environmental Research Letters*, **10**: 114011.

Tonina, D., 2012. *Surface water and streambed sediment interaction: The hyporheic exchange*. In: C. Gualtieri and D.T. Mihailović (Editors), Fluid mechanics of environmental interfaces. CRC Press, Taylor & Francis Group, London, UK, pp. 255-294.

Tonina, D. and Buffington, J.M., 2009. A three-dimensional model for analyzing the effects of salmon redds on hyporheic exchange and egg pocket habitat. *Canadian Journal of Fisheries and Aquatic Sciences*, **66**: 2157-2173, doi: 10.1139/F09-146.

Tonina, D. and Jorde, K., 2013. *Hydraulic modeling approaches for ecohydraulic studies: 3D, 2D, 1D and non-numerical models*. In: I. Maddock, P.J. Wood, A. Harby and P. Kemp (Editors), Ecohydraulics: An integrated approach. Wiley-Blackwell pp. 31-66.

Tonina, D., Luce, C.H. and Gariglio, F., 2014. Quantifying streambed deposition and scour from stream and hyporheic water temperature time series. *Water Resources Research*, **50**(1): 1-6, doi:10.1002/2013WR014567.

Tonina, D., Luce, C.H., Rieman, B., Buffington, J.M., Goodwin, P., Clayton, S.R., Ali, S.M., Barry, J.J. and Berenbrock, C., 2008. Hydrological response to timber harvest in northern Idaho: implications for channel scour and persistence of salmonids. *HYDROLOGICAL PROCESSES*, **DOI: 10.1002/hyp.6918**.

Tonina, D., Marzadri, A. and Bellin, A., 2015. Benthic uptake rate due to hyporheic exchange: The effects of streambed morphology for constant and sinusoidally varying nutrient loads. *Water*, **7 (2015)**: 398-419.

Tonina, D., McKean, J.A., Tang, C. and Goodwin, P., 2011. New tools for aquatic habitat modeling, 34th IAHR World Congress 2011. IAHR, Brisbane, Australia, pp. 3137-3144.

Torgersen, C.E., Price, D.M., Li, H.W. and McIntosh, B.A., 1999. Multiscale Thermal Refugia and Stream Habitat Associations of Chinook Salmon in Northeastern Oregon *Ecological Applications*, **9**(1): 301–319.

Trujillo, E., Molotch, N.P., Goulden, M.L., Kelly, A.E. and Bales, R.C., 2012. Elevation-dependent influence of snow accumulation on forest greening. *Nature Geoscience*, **5**(10): 705-709.

Turnipseed, D.P. and Sauer, V.B., 2010. *Discharge Measurements at Gaging Stations: U.S. Geological Survey Techniques and Methods 3–A8*, U.S. Geological Survey, Reston, Virginia.

U. S. Bureau of Reclamation (USBR), 2013. *Biological Assessment for Bull Trout Critical Habitat in the Upper Snake River Basin*, U.S. Department of the Interior Bureau of Reclamation, Boise, Idaho.

UC Berkeley, 2015. Handheld GPS Buyer's Guide: What you need to know when purchasing a GPS for field work.

Viglione, A., Chirico, G.B., Komma, J., Woods, R., Borga, M. and Blöschl, G., 2010a. Quantifying space-time dynamics of flood event types. *Journal of Hydrology*, **394**: 213–229.

Viglione, A., Chirico, G.B., Woods, R. and Blöschl, G., 2010b. Generalised synthesis of space–time variability in flood response: An analytical framework. *Journal of Hydrology*, **394**: 198–212.

Vilhena, L.C., Hillmer, I. and Imberger, J., 2010. The role of climate change in the occurrence of algal blooms: Lake Burragorang, Australia. *Limnology and Oceanography*, **55**: 1188-1200.

Vliet, M.T.H.V., Ludwig, F., Zwolsman, J.J.G., Weedon, G.P. and Kabat, P., 2011. Global river temperatures and sensitivity to atmospheric warming and changes in river flow. *Water Resources Research*, **47**: W02544.

Vliet, M.T.H.V., Vogele, S. and Rubbelke, D., 2013. Water constraints on European power supply under climate change: impacts on electricity prices. *Environmental Research Letters*, **8**(3): 10.

Vliet, M.T.H.V., Yearsley, J.R., Franssen, W.H.P., Ludwig, F., Haddeland, I., Lettenmaier, D.P. and Kabat, P., 2012a. Coupled daily streamflow and water temperature modelling in large river basins. *Hydrology and Earth System Sciences*, **9**: 8335–8374.

Vliet, M.T.H.V., Yearsley, J.R., Ludwig, F., Vogele, S., Lettenmaier, D.P. and Kabat, P., 2012b. Vulnerability of US and European electricity supply to climate change. *Nature Climate Change*, **2**: 676-681.

Wade, D.T., White, R.G. and Mate, S.M., 1978. *A study of fish and aquatic macroinvertebrate fauna in the South Fork Boise River below Anderson Ranch Dam*, College of Forestry Wildlife and Range Sciences, University of Idaho, Moscow, ID.

Wang, Y., He, B. and Takase, K., 2015. Effects of temporal resolution on hydrological model parameters and its impact on prediction of river discharge. *Hydrological Sciences Journal*, **54**(5): 886-900.

Ward, J.V. and Tockner, K., 2001. Biodiversity: Towards a unifying theme for river ecology. *Freshwater Biology*, **46**: 807-819.

Ward, J.V., Tockner, K., Uehlinger, U. and Malard, F., 2001. Understanding natural patterns and processes in river corridors as the basis for effective river restoration. *River Research and Applications*, **17**(4-5): 311–323

Washington Department of Fish and Wildlife (WDFW), 2004. *Instream Flow Study Guidelines: Technical and Habitat Suitability Issues including fish preference curves*, Washington Department of Fish and Wildlife, Olympia, WA

Watters, J.V., Lema, S.C. and Nevitt, G.A., 2003. Phenotype management: a new approach to habitat restoration

Biological Conservation, **112**: 435–445.

Webb, B.W., Clack, P.D. and Walling, D.E., 2003. Water–air temperature relationships in a Devon river system and the role of flow. *Hydrological Processes*, **17**: 3069–3084.

Webb, B.W., Hannah, D.M., Moore, R.D., Brown, L.E. and Nobilis, F., 2008. Recent advances in stream and river temperature research. *Hydrological Processes*, **22**(7): 902–918.

Webb, B.W. and Nobilis, F., 1997. Long-term respective on the nature of the air-water temperature relationship: A case study. *Hydrological Processes*, **11**(2): 137-147.

Weill, S., Altissimo, M., Cassiani, G., Deiana, R., Marani, M. and Putti, M., 2013. Saturated area dynamics and streamflow generation from coupled surface–subsurface simulations and field observations. *Advances in Water Resources*, **59**: 196-208.

Whiting, P.J., 1997. The Effect of Stage on Flow and Components of the Local Force Balance. *Earth Surface Processes and Landforms*, **22**(6): 517-530.

Winstral, A., Elder, K. and Davis, R.E., 2002. Spatial Snow Modeling of Wind-Redistributed Snow Using Terrain-Based Parameters. *Journal of Hydrometeorology*, **3**: 524–538.

Winstral, A. and Marks, D., 2002. Simulating wind fields and snow redistribution using terrain-based parameters to model snow accumulation and melt over a semi-arid mountain catchment. *Hydrological Processes*, **16**: 3585–3603.

Winstral, A., Marks, D. and Gurney, R., 2009. An efficient method for distributing wind speeds over heterogeneous terrain. *Hydrological Processes*, **23**: 2526–2535.

Winstral, A., Marks, D. and Gurney, R., 2013. Simulating wind-affected snow accumulations at catchment to basin scales. *Advances in Water Resources*, **55**: 64-79.

Winstral, A., Marks, D. and Gurney, R., 2014. Assessing the Sensitivities of a Distributed Snow Model to Forcing Data Resolution. *Journal of Hydrometeorology*, **15**: 1366–1383.

Xu, C., Letcher, B.H. and Nislow, K.H., 2010. Context-specific influence of water temperature on brook trout growth rates in the field. *Freshwater Biology*, **55**: 2253-2264.

Yarnell, S.M., Viers, J.H. and Mount, J.F., 2010. Ecology and Management of the Spring Snowmelt Recession. *BioScience*, **60**: 114-127.

Yates, D., Galbraith, H., Purkey, D., Huber-Lee, A., Sieber, J., West, J., Herrod-Julius, S. and Joyce, B., 2008. Climate warming, water storage, and Chinook salmon in California's Sacramento Valley. *Climatic Change*, **91**: 335-350.

Yu, X., Bhatt, G., Duffy, C. and Shi, Y., 2013. Parameterization for distributed watershed modeling using national data and evolutionary algorithm. *Computers &Geosciences*, **58**: 80-90.